Modeling microbial dynamics and nutrient cycles in ombrotrophic peatlands

Siya Shao
Department of Geography, McGill University, Montréal

September 2021

A thesis submitted to McGill University in partial fulfilment of the requirements of the degree of Doctor of Philosophy in Geography

Abstract

Peatlands store a vast amount of carbon (C) and have functioned as C sinks for millennia. The C sink function of peatlands may be at risk with increased nutrient deposition and climate change in the future. Models can make future projections for peatlands, but most peatland models do not include nutrient cycles, which are tightly couple to the C cycle. Furthermore, microbial activities have been found to play an essential role in regulating peatland biogeochemical cycles. Still, peatland models have not explicitly included any microbial controls, precluding our ability to examine the microbial feedbacks within the peatland ecosystem. This research explores the significance of microbe-mediated carbon-nutrient cycling in peatland ecosystem functions through a modelling approach. The McGill Wetland Model (MWM) was modified into MWMmic_NP by introducing a multi-layer cohort model to track the decrease in peat qualities with decomposition age; the growth and metabolism of saprotrophic microbes (SAP) as factors on the rates of peat decomposition; nitrogen and phosphorus cycles regulating the growth of plants and microbes; ericoid mycorrhiza fungi (ERM) exchanging nutrients for C from the host plant ericaceous shrubs; and the vertical and horizontal transport of the solutes in the peat pore water. MWMmic_NP was evaluated against the extensive whole-ecosystem measurements from the Mer Bleue Bog, eastern Canada, and the long-term fertilization experiments at the same site. MWMmic_NP was then used to examine the response of the bog to different scenarios of environmental changes.

MWMmic_NP was able to replicate the overall C-N-P cycles observed at the Mer Bleue bog. In particular, the model reproduced the observed dynamics of the newly added pools of SAP and dissolved organic matter, and captured the changes in stoichiometry profiles with peat depth. Furthermore, the model performed well in reproducing the response of the bog to nutrient additions. A diminished role of mycorrhiza fungi in nutrient uptake and subsequent lower C allocation from shrubs to ERM increased shrub growth. Possible environmental changes induced a transition from mosses to shrubs domination in the vegetation community and from ERM to SAP domination in microbial community composition in the bog, thus reducing carbon sequestration capacity. Water table drawdown and increased soil

temperature were the most important environmental factors for the weakening of the C sink. Reactions of SAP or ERM to changes in environmental conditions determined the response of the bog. This research contributes to a better understanding of the significance of microbe-mediated biogeochemical cycling in peatlands. ERM fungi may play a central role in maintaining the vegetation structure and C sink function of shrub-dominated ombrotrophic peatlands.

Résumé

Les tourbières accumulent une grande quantité de carbone (C) et ont fonctionné comme des réserves de C pendant des millénaires. L'accumulation de carbone dans les tourbières pourrait être menacée par une augmentation des dépôts de nutriments et des changements climatiques à l'avenir. Les modèles peuvent faire des projections à venir pour les tourbières, mais la plupart des modèles de tourbières n'incluent pas les cycles des éléments nutritifs, qui sont liés au cycle du C. De plus, il a été découvert que les activités microbiennes jouent un rôle essentiel dans la régulation des cycles biogéochimiques des tourbières. Pourtant, les modèles de tourbières n'ont inclus explicitement aucune dynamique microbienne, ce qui exclut notre capacité à examiner les rétroactions microbiennes au sein de l'écosystème des tourbières. Cette recherche explore l'importance du cycle carbone-nutriment médié par les microbes dans les fonctions des tourbières grâce à une approche de modélisation. Le modèle McGill Wetland Model (MWM) a été modifié en MWMmic_NP en introduisant un modèle de cohorte multicouche, pour suivre la diminution de la qualité de la tourbe avec l'âge de décomposition ; l'effet de la croissance et du métabolisme des microbes saprotrophes (SAP) sur les taux de décomposition de la tourbe ; cycles de l'azote et du phosphore régulant la croissance des plantes et des microbes ; les champignons mycorhizes éricoïdes (ERM) échangeant des nutriments contre le C de la plante hôte et les éricacées arbustives ; et le transport vertical et horizontal des solutés dans l'eau interstitielle de la tourbe. MWMmic_NP a été évalué par rapport aux mesures étendues de l'ensemble de l'écosystème de la tourbière Mer Bleue, dans l'est du Canada, et aux expériences de fertilisation à long terme. MWMmic_NP a ensuite été utilisé pour examiner la réponse de la tourbière à différents scénarios de changements environnementaux.

MWMmic_NP a pu reproduire l'ensemble des cycles C-N-P observés à la tourbière Mer Bleue. En particulier, le modèle reproduit la dynamique observée des pools de SAP nouvellement ajoutés, tandis que la matière dissoute a capturé les changements de profils stœchiométriques avec la profondeur de la tourbe. De plus, le modèle a bien réussi à reproduire la réponse de la tourbière aux ajouts de nutriments. Un rôle diminué des

champignons mycorhizes dans l'absorption des nutriments et l'allocation subséquente de C des arbustes à la GRE ont entraîné une croissance accrue des arbustes. Des changements environnementaux possibles ont induit une transition de la domination des mousses à celle des arbustes dans la communauté végétale et de la domination de l'ERM à la domination du SAP dans la composition de la communauté microbienne dans la tourbière, réduisant ainsi la capacité de séquestration du C. Le rabattement de la nappe phréatique et l'augmentation de la température du sol étaient les facteurs environnementaux les plus importants dans la réduction de C réserver. Les réactions du SAP ou de l'ERM aux changements des conditions environnementales ont déterminé la réponse de la tourbière. Cette recherche contribue à une meilleure compréhension de l'importance du cycle biogéochimique à médiation microbienne dans les tourbières. Les champignons ERM peuvent jouer un rôle central dans le maintien de la structure de la végétation et de la fonction de puits de carbone des tourbières ombrotrophes dominées par des arbustes.

Table of Contents

List of Figures

List of Tables

Acknowledgments

There are numerous people I would like to thank for their help along my PhD journey. First and foremost, I would like to thank my PhD supervisor, Dr. Nigel Roulet, for both his intellectual and financial support that make this journey possible. Nigel is a great mentor with generosity, hospitality, and passion in science. His guidance taught me to sharpen my critical thinking and think like a scientist, while his trust allowed to embrace novel approaches. I'm very grateful for the opportunity to be Nigel's student. I also want to thank my co-supervisor Dr. Jianghua Wu (Memorial University of Newfoundland) who provided instrumental support, advice, and feedbacks during my PhD, which broadened my understanding and help me grow as an individual.

I am grateful to many people that made my research possible. I am especially grateful to my committee member Dr. Tim Moore, for great scientific discussion, sense of humor and always being available to help. I also thank my committee members Dr. Graham MacDonald and Dr. Christian von Sperber for their valuable inputs on my research. Special thanks to Dr. Hongxing He, who provided invaluable feedbacks on my thesis and always challenged my way of thinking. I'm also thankful to Dr. Jinnan Gong for his great discussion to expand my horizon. Many thanks to Dr. Jill Bubier (Mount Holyoke College) for providing the vegetation and CO_2 chamber measurement data in Mer Bleue's fertilization experiments. I also thank Elyn Humphreys (Carleton University) and Mike Dalva for the providing the meteorological and eddy covariance data at the Mer Bleue. I'm grateful to Nathan Basiliko (Laurentian University) for providing the microbial data at the Mer Bleue. I'm also thankful to Dr. Tuula Larmola (Mount Holyoke College) for fruitful discussions on plant and mycorrhiza.

Special thanks to all the members of the peatland research group at McGill University, Tanja Živković, Hongxing He, Dan Dong, Tracy Rankin, Avni Malhotra, Martina Schlaipfer, Zheng Wang, Lorna Harris, Manuel Helbig, Bidya Sharma, Weifeng Wang, Lucy Lu, Silvie Harder, Andrew Pinsonneault for making the working environment not only intellectually stimulating but also warm and fun. I also want to thank all the great friends I meet in Montreal, especially Guanbo Wang, Pengfei Ou, Jixuan Li, Shimeng He, Yichen Zhang, Yihan Xin, Yue Cao, Bingqing

Guo and Hongzhi Zhu. They have accompanied me through good and bad times and made my PhD life colorful.

Finally, my deepest gratitude goes to my family. I sincerely thank my parents Jiajun Shao and Huarong Wang, for their unconditional love and support throughout my education and life. I would also like to thank my twin brother Siqi Shao, who, although shares a completely different life now, is always willing to show understanding and support through my tough times. I am blessed to have such a supportive family and I am dedicating this thesis to all of them.

Contribution to original knowledge

This thesis contributes to our understanding of the microbe-mediate nutrient cycles in ombrotrophic peatlands and its importance on maintaining the structure and C sink function of the peatlands. In particular, this thesis answers the calling of representing key regulating processes in peatland models: A peatland model that includes both N and P cycles, and dynamics of both saprotrophs and mycorrhiza fungi is developed for the first time. This is crucial for making accurate projections of the fate of the massive C storage in peatlands under environmental change. Apart from its implication for furthering peatland science, my findings on the significance of plant-microbe interactions can also be expanded to other ecosystem research.

Contribution of authors

There are three main chapters (Chapters 3 to 5) in this thesis that are written as manuscripts in a format suitable for publication in scientific journals. I have developed scientific questions, implemented new processes into the model, conducted the simulations, analyzed the results, and wrote manuscripts as a lead author. As my Ph.D. supervisor, Dr. Nigel Roulet offered the advice on developing scientific questions, model development and interpretation of results and provided detailed comments on each manuscript. My co-supervisor, Dr. Jianghua Wu also provided advice on development of my research questions, research planning and provided detailed feedbacks on each manuscript. The roles of other co-authors (for Chapters 3, 4 and 5) are described as follows:

Manuscript #1 (Chapter 3): "Integrating McGill Wetland Model (MWM) with Cohort Development and Microbial Controls" by Siya Shao, Jianghua Wu, Hongxing He and Nigel Roulet. Hongxing He provided detailed comments on the manuscript. Chapter 3 has been submitted to Science of Total Environmental for publication.

Manuscript #2 (Chapter 4): "A Mycorrhiza-mediated Carbon, Nitrogen and Phosphorus Cycling Model to Simulate Peatland's Response to Nutrient Fertilization" by Siya Shao, Jianghua Wu, Hongxing He, Nigel Roulet, Tim Moore, Jill Bubier and Tuula Larmola. Hongxing He provided detailed comments on the manuscript. Tim Moore, Jill Bubier and Tuula Larmola delivered valuable feedbacks on the interpretation of the results. Jill Bubier also provided the vegetation and CO_2 chamber measurement data in Mer Bleue's fertilization experiments.

Manuscript #3 (Chapter 5): "Effects of elevated nutrient deposition, rising atmospheric CO2 and climate change on ombrotrophic peatlands: a modeling analysis" by Siya Shao, Jianghua Wu, Hongxing He and Nigel Roulet. Hongxing He provided detailed comments on the manuscript.

Chapter 1. Introduction

1.1. Research context

Despite only occupying less than 3% of the world land area, northern peatlands store up to a third of the global soil organic carbon (SOC) (Yu et al., 2010; Dargie et al., 2017). This large C storage is a result of persistent C imbalance between plant production and microbial decomposition over thousands of years (Gorham, 1995; Turunen et al., 2002; Roulet et al., 2007). The low decomposition rates in northern peatlands can be attributed to several climate and biogeochemical controls including the waterlogged conditions, acidic pH, low peat temperature and nutrient scarcity (Limpens et al., 2008). However, these key environmental conditions for C accumulation are subject to significant alterations due to climate change and increased nutrient deposition. It is of great concern whether the northern peatlands will continue to function as C sinks in the future of environmental change.

A great many field-manipulative experiments have been conducted to address this question. It is found that climate change could pose severe threats to peatlands' large C storage either directly through increased decomposition (Dorrepaal et al., 2009; Bragazza et al., 2016), or indirectly through favoring the dominance of vascular plants over the 'peat engineer' *Sphagnum* mosses (Gavazov et al., 2018; McPartland et al., 2019; Norby et al., 2019). Increased nutrient availability could also result in enhanced growth of vascular plants at the expense of *Sphagnum* mosses (Bubier et al., 2007; Juutinen et al., 2010) and lead to reductions in C sequestration capacity (Bragazza et al., 2012; Larmola et al., 2013). Nevertheless, increase in plant production and peatland C accumulation with both increased nutrient deposition (Turunen et al., 2004) and warmer climate (Ward et al., 2013; Helbig et al. 2019) are also reported, showing the non-linearity of peatlands' response to environmental changes. Despite these endeavors, most field studies only focused on the impact of an individual environmental driver and few studies exist that assessed the effects of multiple drivers simultaneously (Weltzin et al., 2003; Dielemen et al., 2015; Luan et al., 2019).

Furthermore, the role of microbial dynamics in mediating the response of peatlands to

environmental change has been understudied yet increasingly recognized (Juan-Ovejero et al., 2020; Ritson et al., 2021). Peat decomposition is fundamentally regulated by microbial activities (Limpens et al., 2008). Climate change could induce physiological changes in microbes which could lead to both negative and positive feedbacks that determine the response of peat decomposition (Hagerty et al., 2014; Sihi et al., 2018). Moreover, microbes in peatlands also interact closely with plants in driving the ecosystem functioning (Robroek et al., 2015). One of the most important plant-microbe interactions is the mycorrhizal symbiosis, where the host plants transport C to the associated mycorrhiza fungi in exchange for nutrients (Smith and Read, 2010). Ericoid mycorrhizal (ERM) fungi, which are associated with ericaceous shrubs, are ubiquitous in ombrotrophic peatlands. In addition to providing nutrients to the shrubs, it is found that ERM fungi can also inhibit saprotrophic activities (Averil et al., 2014), produce recalcitrant necromass (Clemmensen et al., 2013) thus promote the ecosystem's SOC storage (Clemmensen et al., 2015). Recent evidence suggested similar impacts of ERM fungi on ombrotrophic peatlands' biogeochemical cycles (Wiedermann et al., 2017; Fernandez et al., 2019). Therefore, improving our knowledge on the significance of ERM fungi could further our understanding of the C sink function of ombrotrophic peatlands.

Process-based models allow the trajectory of a system to emerge from the multiple, simultaneous interactions among important internal processes, thus they can be used to examine the potential significance of microbial processes in peatlands and make long-term projections of the peatland's future. Despite the tremendous efforts being made in developing peatland-specialized models (St-Hilaire et al., 2010; Chaudhary et al., 2017; Qiu et al., 2018) and application of those models in projecting peatlands' response to environmental changes (Wu and Roulet, 2014; Qiu et al., 2020), integration of microbial-mediated processes into peatland models has not been conducted. Compounded by several other discrepancies, there still exist significant room for improvement in current peatland modeling efforts. To summarize them here: Firstly, the decreasing substrate quality with decomposition is poorly portrayed in peatland models, which may exaggerate the response of peat decomposition to disturbances. Secondly, few efforts have been made to incorporate nutrient cycles into peatland models. This hinders our ability to assess the effect of nutrient limitation on plant

growth and the impact of increased nutrient depositions. Thirdly, microbial controls on biogeochemical processes have yet to be incorporated explicitly in any peatland models, precluding us from examining important plant-microbe feedbacks within the peatlands. Fourthly, limited effort has been devoted to disentangling the contribution of individual drivers to the combined impacts of multiple disturbances.

1.2. Research objectives

In this thesis, I aimed to fill the four gaps in current peatland modeling efforts and sought to gain a better understanding of the controls of the ombrotrophic peatland biogeochemical cycles from a modeling perspective. My specific research objectives were to:

(1) Develop a peatland model that includes peat quality changes, microbial dynamics, and nutrient cycles.

(2) Investigate the importance of microbial physiological traits in regulating the response of peat decomposition to climate change.

(3) Assess the impact of nutrient dynamics on the C cycling of the ombrotrophic peatland.

(4) Examine the significance of plant-microbe interaction in the biogeochemical cycling of ombrotrophic peatlands.

(5) Evaluate the response of ombrotrophic peatlands to environmental changes with the consideration of the microbial dynamics and nutrient cycles.

1.3. Thesis structure

This thesis comprises six chapters including this introductory chapter. Chapter 2 presents a review of literature on peatland function, microbial importance in peatlands, response of peatlands to disturbances and peatland modeling efforts. The literature review will present knowledge on the significance of microbe-mediated nutrient cycles in regulating the response of peatlands and highlight the existing gaps in addressing this topic in current peatland modeling endeavors to set a framework for this thesis. The main body of my thesis is structured into three research chapters, which have been submitted or are being prepared for submission to peer-reviewed journals. The first manuscript, Chapter 3, presents the

development of new peatland model MWMmic that includes cohort development, solute transport, and metabolisms of saprotrophic microbes. The model is calibrated by and evaluated against extensive measurements done at the well-characterized Mer Bleue bog. The importance of substrate quality and microbial physiological traits in regulating the response of peat decomposition is investigated here. The second manuscript, Chapter 4, presents the development of new peatland model MWMmic_NP that incorporates nutrient cycles and metabolisms of ERM fungi. This new model is used to examine the response of ombrotrophic peatlands to increased nutrient deposition and evaluated against observations in the long-term fertilization experiment at the Mer Bleue bog. The significance of ERM in peatland biogeochemical cycles is also investigated here with a species-exclusion modeling experiment. The third manuscript, Chapter 5, assesses the response of Mer Bleue bog to different scenarios of environmental changes including climate change, increased nutrient deposition, and elevated CO_2 levels. The contribution of each driver to the combined impacts of multiple disturbances is disentangled. The significance of plant-microbe interaction in regulating the ombrotrophic peatland's resiliency is also examined here. Chapter 6 summarizes the main conclusions of this thesis and proposes future research directions.

Chapter 2. Literature review

2.1. Peatland description

Peat is a highly organic material that is composed of partially decomposed vegetation (Rydin and Jeglum, 2013). Peatlands are wetlands with a surface layer of peat that is at least 0.3-0.4 m thick, but often extends to several meters (Gorham, 1991; Frolking et al., 2011). This large accumulation of peat results from plant litter production exceeding the decomposition of organic matter (Moore et al., 1998), as decomposition in peatlands is dramatically constrained by anaerobic conditions due to the low oxygen diffusion in water. Based on the trophic status, peatlands can be broadly classified into two categories, ombrotrophic peatlands and minerotrophic peatlands, also referred to as bogs and fens (Clymo, 1984). Ombrotrophic peatlands receive all their water and nutrient from the atmosphere, are often acidic, nutrient-poor, and typically dominated by *Sphagnum* mosses and ericaceous woody shrubs. In contrast, minerotrophic peatlands receive inputs from outside their confines, from ground water or surface runoff, therefore tend to be more alkaline and nutrient-rich and have a higher portion of herbaceous vascular plant cover (Siegel and Glaser, 1987).

Globally, peatlands cover over 4 million km^2 (Xu et al., 2018). A major proportion of the peatlands (~80%) are distributed in the boreal and subarctic regions, mainly in Canada, the USA, Fennoscandinavia, and Russia (Lappalainen 1996). The remaining peatlands are found in tropical-subtropical climates (Joosten, 2004, Global Peatland Database). Despite covering less than 3% of the world land are, peatlands currently store ~644 Gt C, up to a third of the global soil organic carbon (Yu et al., 2010; Dargie et al., 2017), with northern peatlands estimated to contain ~500 Gt C (Yu, 2012; Scharlemann et al., 2014). This huge amount of carbon (C) is a legacy of peatlands being persistently accumulating C at an average rate of 0.02–0.03 $kgCm^{-2}$ yr^{-1} over thousands of years (Gorham, 1995; Turunen et al., 2002; Roulet et al., 2007). Therefore, the C sink function of peatlands has contributed to global cooling on the millennium scale (Frolking and Roulet, 2007). The significance of peatlands in global C cycle and climate regulation has prompted scientific research into the controls of peatland

biogeochemical cycles and how they respond to future environmental disturbances.

The low decomposition rates in peatlands could be attributed to several climate and biogeochemical controls (Limpens et al., 2008). The mechanism of 'enzyme-latch' induced by oxygen limitation in water-logged environment is proposed to be the determining factor (Freeman et al., 2001a, 2004), as the anaerobic conditions prevents the enzyme 'phenol oxidase' from eliminating phenolic compounds that inhibit biodegradation. Low temperature plays a significant role in suppressing microbial metabolism and enzymatic activities in northern peatlands (Freeman et al., 2001b; Pinsonneault et al., 2016b), especially in those that are situated in regions of sporadic to continuous permafrost (Tarnocai 2006; Smith et al. 2007). Nutrient scarcity, particularly in ombrotrophic peatlands, could contribute to low decomposition rates directly through inhibition of microbial activities (Basiliko et al., 2006; Pinsonneault et al., 2016a) and indirectly through favoring the growth of *Sphagnum* mosses over more nutrient-demanding vascular plants (Bubier et al., 2007). *Sphagnum* mosses, which are often considered as the "ecosystem engineer" of peatlands (Norby et al., 2019), not only produce litter that is resistant to microbial decomposition (Hájek et al., 2011) but are also thought to acidify the environment (Kilham et al., 1982; Vitt et al., 2000) which further suppresses the enzymatic activities (Williams et al. 2000). Given the tight coupling between the environmental conditions and peatland biogeochemical processes, disturbances like increased nutrient deposition and climate change could pose a threat to the C sink function of peatlands (Limpens et al., 2008). In this thesis, particular attention is given in northern high latitudes where disproportional climate changes are projected to occur (IPCC, 2018) and majority of the peatlands are distributed.

2.2. Microbial role in peatland biogeochemical cycling

In recent decades, the role of microbes in regulating soil organic matter (SOM) decomposition and persistence has been increasingly recognized across ecosystems (Conant et al., 2011; Schmidt et al., 2011; Cotrufo et al., 2013; Glassman et al., 2018). With a notably high organic C density, peatlands have long been known to contain large microbial populations of wide diversity (Xu et al., 2013; Andersen et al., 2013). In peatlands, not only

do microorganisms directly control the organic matter decomposition, but they also play important roles in nutrient mineralization and plant nutrient uptake, thus can feedback on plant productivity and overall peatland functioning (Andersen et al., 2013; Juan-Ovejero et al., 2020). Considering the central role of microbes in peatland biogeochemical cycling, detangling the controls of microbe-mediated processes is central to our understanding of the peatland biogeochemical cycling (Andersen et al., 2013).

SOM decomposition is fundamentally regulated by microbial activities, as it involves a series of processes in which microbes produce extracellular enzymes to break down complex biopolymers into simple monomers that microbes themselves can directly utilize (Limpens et al., 2008). Therefore, changes of microbial physiological properties induced by disturbances could have a profound impact on microbial activities and subsequent SOM decomposition (Allison et al., 2010). For example, higher temperature is often thought to decrease microbial carbon use efficiency (CUE) (Steinweg et al. 2008; Frey et al., 2013) and increase microbial turnover rates (Hagerty et al., 2014), both of which could result in decreasing in microbial biomass production and even promotion of soil organic carbon (SOC) with long-term warming (Allison et al., 2010; Li et al., 2019). Such microbial mechanisms are only limitedly explored in peatlands. Sihi et al. (2018) found decreased microbial CUE with warming in peat soil, but further suggested that microbial thermal acclimation with slow warming rate would lead to increased CUE and decomposition. Dieleman et al. (2016), on the contrary, reported larger peat respiration resulted from decreased CUE with increased phenolic compounds, as microbes emit a larger proportion of C as CO_2 with lower CUE. These studies highlight both the importance and complexity of the impact of microbial physiological changes on SOM transformation (Manzoni et al., 2012; Malik et al., 2020). There is a clear need for more research on microbial physiological traits in peatland ecosystems.

Besides direct controls on peat decomposition, microbes in peatlands also interact closely with plants in driving the ecosystem functioning (Robroek et al., 2015). The roots of vascular plants can produce exudates that stimulate microbial enzymatic activities and increase the peat decomposition, which is also known as the priming effect (Leroy et al., 2017; Jassey et al., 2018). Not only can the plant-derived metabolites destabilize the previously

'locked-up' C in the deep peat (Walker et al., 2016), but they can also enhance nutrient mineralization (Song et al., 2018) and promote the production of CH_4 over CO_2 (Wilson et al., 2021) which amplifies climate–peatland feedbacks. In a broad ecological sense, this surplus C is exported by plants in exchange for benefits provided by microbiomes, including nutrients, water, and protection against pathogens (Prescott et al., 2020), thus the plant-microbe interaction is generally perceived as a mutualistic relationship (Trivedi et al., 2020). Mycorrhiza, a ubiquitous symbiosis established between plant roots and soil fungi, is one of the most important plant-microbe mutualistic interactions (Genre et al., 2020). The role of mycorrhiza in regulating peatland biogeochemical cycles is getting more and more recognized (Juan-Ovejero et al., 2020), yet remains significantly understudied.

2.2.1. Mycorrhiza

Mycorrhizal fungi live in symbiosis with plants and form an interface with the plant root. This interface allows bilateral energy and nutrient transport between the plant and fungus (Smith and Read, 2010). Four main mycorrhizal types with distinct morphological traits have emerged throughout over 400 million years of co-evolution between plants and fungi: arbuscular mycorrhizas (AM), ectomycorrhizas (ECM), ericoid mycorrhizas (ERM) and much less studied orchid mycorrhizas (ORM) (van der Heijden et al., 2014). Different nutrient and C acquisition strategies were used by different mycorrhiza types: AM fungi primarily scavenge inorganic nutrients from soil solution while ECM and ERM fungi produce extracellular enzymes to extract nutrient from complex organic compounds (Smith and Read, 2010). AM fungi get almost all their C from the host plants whereas ECM & ERM fungi could potentially 'mine' C from SOM decomposition and adopt a dual lifestyle as a saprotroph (SAP) (Martino et al., 2018). These different traits considerably affect the impact of different mycorrhizal types on the system's biogeochemical cycles. ECM and ERM fungi were long proposed to hinder decomposition through effective competition with SAPs over nutrients and other resources, thus promoting SOM accumulation (Gadgil & Gadgil, 1975; Averill et al., 2014; Averill & Hawkes, 2016; Kyaschenko et al., 2017). Recent evidence, however, has challenged this prevailing view as certain ECM fungi are reported to take active part in decomposition

(Lindahl et al., 2021; Terrer et al., 2021). In contrast, ERM fungi are found to play a more significant role in SOM accumulation (Clemmensen et al., 2015) which could have confounded the interpretation of ECM effects (Ward et al., 2021). These contradictory findings highlight the need to better understand mycorrhiza biogeochemical effects as the frontier in plant-microbe interaction research (Zak et al., 2019).

ECM and ERM fungi are much more abundant than AM fungi in peatlands, especially bogs, as most of the peatland nutrients are stored in organic forms (Juan-Ovejero et al., 2020), and ECM and ERM fungi are often associated with plant species commonly found in ombrotrophic peatlands (Thormann and Rice, 2007). For example, ericaceous shrubs, which rely heavily on ERM for nutrient acquisition, thrive in nutrient-poor and acidic environments characteristic of ombrotrophic peatlands (Gavazov et al., 2016). ECM and ERM fungi in peatlands are also found to promote the SOC accumulation through suppression of saprotrophic activities (Wiedermann et al., 2017) and production of recalcitrant necromass (Fernandez et al., 2019), maintaining the peatlands' C sink function. They also play other important roles in peatland biogeochemical cycling regarding the mediation of the nutrient cycles (Vesala et al., 2021), interacting with non-mycorrhizal plant communities (Chiapusio et al., 2018) and regulating the system's response to climate change (Bragazza et al., 2015; Defrenne et al., 2020). Understanding mycorrhiza-mediated processes are thus crucial for developing a microbial process-based understanding of the peatland ecosystem (Ritson et al., 2021).

2.3. Response of peatlands to environmental changes

2.3.1. Increased nutrient deposition

Nitrogen (N) and phosphorus (P) are essential nutrients for plant growth in both terrestrial and aquatic ecosystems (Elser et al., 2007) and the primary production in ecosystems is often limited by both nutrients (Wieder et al., 2015). In recent decades, human activities like fossil-fuel combustion and excessive fertilizer application have been pouring a large amount of N and P into ecosystems worldwide (Galloway et al. 2004; Tipping et al., 2014),

leading to dramatic changes in ecosystems' biogeochemical functioning (Mack et al., 2004; Janssens et al., 2010). Given the large C storage in peatlands, it is important to understand how peatlands respond to increased nutrient availability.

Under pristine conditions, *Sphagnum* mosses typically form a continuous and dense layer that effectively absorbs airborne nutrients. Few vascular plant species can successfully compete with *Sphagnum* mosses in nutrient-poor environment, particularly in ombrotrophic peatlands that receive all their nutrients from the atmosphere (van Breemen, 1995). However, under increasing nutrient deposition, *Sphagnum* tissues become nutrient-saturated, and their absorptive capacity diminishes (Bragazza et al., 2005; Bubier et al., 2007). More exogenous nutrients could thus be available to vascular plants, increasing their competitive ability at the expense of *Sphagnum* growth and potentially leading to significant changes in peatland biogeochemical functions. Most long-term peatland fertilization experiments have reported an increase in vascular abundance and subsequent loss of *Sphagnum* mosses as expected (Bubier et al., 2007; Juutinen et al., 2010; Bragazza et al., 2012; Larmola et al., 2013; Levy et al., 2019). The changes in vegetation communities often lead to greater labile litter input and enhanced enzymatic activities, resulting in a diminished C sink for peatlands after fertilization (Bragazza et al., 2006, 2012; Bubier et al., 2007; Moore et al., 2007; Kivimäki et al., 2013; Larmola et al., 2013; Pinsonneault et al., 2016a). However, a limited response in vascular plant (Currey et al., 2011; Sheppard et al., 2014) and accelerated peat accumulation with increased nutrient input (Turunen et al., 2004; Olid et al., 2014; Berg et al., 2017) have also been found, suggesting that there could be a tipping point regarding the response of peatland function to enhanced nutrient input (Gong et al., 2019).

More importantly, recent findings have highlighted the previously ignored significance of plant-microbe interactions in regulating peatlands' response to fertilization. Ericaceous shrubs, which increase their abundance with fertilization, were reported to maintain their leaf-level photosynthetic capacity with increased leaf nutrient content (Bubier et al., 2011, Currey et al., 2011). Since increased nutrient availabilities do not result in increased photosynthesis, the observed increase in shrub growth with fertilization probably do not stem from the increased productivity. More recent evidence supports the role of mycorrhiza fungi in mediating the

response of peatland vegetation. Vesala et al. (2021) confirmed that shrubs with increased N availability have shifted their N sources away from ERM transfer to the direct root uptake. Van Geel et al., (2021) reported a negative correlation between ERM richness and nutrient availabilities across European bogs. Thus, shrubs with fertilization might be directing the C originally allocated to ERM for nutrient acquisition to their own growth, which leads to their increased biomass. However, direct evidence of changed C allocation with fertilization have yet to be found in peatlands like in other ecosystems (Eastman et al., 2021). Instead, Kiheri et al. (2020) reported increased ERM colonization with fertilization. Thus, large gaps of knowledge still exist to understand the role of mycorrhiza fungi in regulating the response of peatlands to increased nutrient input.

2.3.2. Climate change

Disproportional climate changes are projected to occur in the northern high latitudes (IPCC, 2018) where the majority of the peatlands are situated (Xu et al., 2018). Perturbations due to climate change could potentially threaten the C sequestration capacity of northern peatlands or even convert this large C sink into a C source (Wu and Roulet, 2014), which would dramatically exacerbate climate change in turn. Thus, it is of great concern how northern peatlands respond to climate change. A great many manipulative experiments including water table (WT) alteration and peatland warming have been conducted to address this question.

Lowering the WT enhances the peat decomposition by exposing the peat that is originally submerged under water to increased oxygen availability (Bragazza et al. 2016). Furthermore, the lowered WT favors the growth of woody plants like shrubs and trees (Strack et al. 2006; Potvin et al. 2015; Radu and Duval, 2018), not only because the aeration increases their rooting depth, but also because the increased nutrient mineralization with enhanced decomposition provides more nutrients for the enhanced plant growth (Munir et al., 2017; Wang et al., 2018). On the other hand, both the elevated moisture stress and increased shading of vascular plants with the WT drawdown lead to a shrinkage of *Sphagnum* mosses (Potvin et al. 2015; Radu and Duval, 2018). Thus, the C sink function of the peatland is often

threatened by both the increased decomposition and the loss of peatland engineers following WT drawdown (Munir et al., 2015; Bragazza et al. 2016). However, increased ecosystem production with the vegetation shift towards more productive drought-resistant species (Sulman et al., 2009; Ratcliffe et al., 2019) and dampened decomposition increase over time as the labile peat gets depleted (Straková et al.,2012; Ratcliffe et al., 2019) have also been reported, which could lead to recovery of C uptake capacity of peatlands after long-term WT drawdown (Munir et al., 2015; Ratcliffe et al., 2020). In comparison, peatland warming experiments have generally observed similar results as those obtained from WT drawdown experiments. Enhanced peat decomposition (Dorrepaal et al., 2009; Wilson et al., 2016), increased nutrient mineralization (Keuper et al., 2012; Song et al., 2018), vegetation shift towards increased domination of vascular plants over *Sphagnum* mosses (McPartland et al., 2019, 2020; Norby et al., 2019) have all been reported with peatland warming, which subsequently decreases the peatland's capacity to sequester C (Bragazza et al. 2016; Hanson et al., 2020). However, moderate warming has also been found to increase the C uptake of the peatlands (Ward et al., 2013; Laine et al., 2019; Salimi et al., 2021) through enhanced ecosystem production with a maintained plant community structure (Ward et al., 2013; Helbig et al., 2019).

How peatland microbial communities respond to climate change has been less studied than plant communities. WT drawdown is generally found to increase the SAP biomass (Blodau et al. 2004; Peltoniemi et al., 2012; Jassey et al., 2018) while mixed effects of warming on SAP abundance are reported (Asemaninejad et al., 2018; Liu et al., 2019; Jiang et al., 2020). Microbial thermal acclimation (Sihi et al., 2018) as well as depletion of labile C with accelerated peat decomposition (Mpamah et al., 2017) could both play a role in inhibiting the increase of SAPs with climate change. Conflicting results are also produced regarding the impact of climate change on peatland mycorrhiza fungi. A shift in microbial community from mycorrhizal to saprotrophic fungi with lower WT (Peltoniemi et al., 2012) and a loss of ERM fungi and increased ericaceous shrubs with soil warming (Defrenne et al., 2020) have been observed. However, increase in ERM accompanied by the increased ericaceous shrubs with climate change was also observed (Bragazza et al., 2015; Asemaninejad et al., 2018). These

conflicting findings highlights the complexity of the response of microbial communities and plant-microbe interactions to disturbances. As mycorrhizal fungi and saprotrophic microbes have distinct effects on peatland biogeochemical cycling, there is a clear need to better understand the response of them to climate change (Juan-Ovejero et al., 2020).

2.3.3. Elevated CO_2

Very few studies have been conducted to elucidate the effect of elevated CO_2 on the community structure and functions of peatlands. Shrubs that dominate the bogs usually show a very limited response to elevated CO_2 (Hoosbeek et al., 2001; Berendse et al., 2001; McPartland et al., 2019) whereas sedges that dominate the fens often increase (Fenner et al., 2007; Tian et al., 2020) with the CO_2 treatment. Strong nutrient limitation (Heijmans et al., 2001; Hanson et al., 2020) and acclimation of shrub photosynthetic capacity to elevated CO_2 (Ward et al., 2019) have both been proposed to explain the inertia of shrubs. Elevated CO_2 is often found to enhance the 'priming effect' of peatland plants, as suggested by the increased SAP biomass (Mitchell et al., 2003) and heterotrophic respiration (Walker et al., 2016; Leroy et al., 2017) following CO_2 treatment. Although rarely studied, mycorrhizal fungi might also benefit from the increased belowground C allocation of plants as suggested by the increased ERM colonization in a subarctic birch forest following CO_2 enhancement (Olsrud et al., 2004, 2010). All in all, due to paucity of research, a large knowledge gap still exists concerning how peatlands respond to elevated CO_2 (Anderson et al., 2013).

2.3.4. Combined effects of environmental changes

Despite these endeavors to investigate the impact of individual environmental driver, few studies exist that assess the effects of multiple drivers on peatlands simultaneously. Overall, the combination of warming and drainage (Weltzin et al., 2003; Munir et al., 2014; Jassey et al., 2019; Strack et al., 2019; Li et al., 2021), and that of warming and increased N deposition (Luan et al., 2019; Gong et al., 2021a, b) were both found to increase the dominance of vascular plants over Sphagnum mosses and reduce the peatland C sequestration capacity, as similar to the individual effect of each driver. However, interactions between these different

environmental drivers were rarely assessed. When imposed together, the effect of individual drivers might be strongly affected by other drivers, as the combined effects of multiple drivers might be synergistic or antagonistic. For example, a positive effect of CO_2 enhancement on shrub biomass was only observed when N fertilizer (Heijmans et al., 2001) or considerably high soil temperature (Norby et al., 2019) were applied together; Water level management was also found to strongly regulate the effect of warming on peatland C cycle (Samili et al., 2021); Much more efforts are needed to quantify the interactions between different environmental drivers in peatlands.

2.4. Simulation of biogeochemical processes in peatlands

Models can be useful tools for investigating the complex responses of an ecosystem to multiple external disturbance and to make long-time projections for a range of possible futures. Remarkable efforts have been made in developing peatland-specialized models (Frolking et al.,2002; St-Hilaire et al., 2010; Wu et al., 2012; Wu et al., 2013) and introducing peatlands into established ecosystem models or even global land surface models (Wania et al., 2009; Shi et al., 2015, 2021; Chaudhary et al., 2017; Wu et al., 2016; Qiu et al., 2018). Studies have used these process-based models to simulate the impact of increased nutrient deposition (Wu et al., 2015), land-use change (He et al., 2016; Young et al., 2017) and climate change (Wu and Roulet, 2014; Chaudhary et al., 2020; Qiu et al., 2020; Shi et al., 2021) on peatlands. Despite this tremendous progress, several limitations still exist in the current peatland modeling efforts.

Firstly, the decreasing substrate quality with decomposition is poorly portrayed in peatland models. Many models have adopted a simple approach of separating peat profiles into acrotelm and catotelm zones based on water table level, while assigning them with separate but constant base decomposition rates (St-Hilaire et al., 2010, Wu et al., 2016; Qiu et al., 2018). The assumption that the catotelm peat has the same decomposability as the acrotelm peat could lead to an overestimation of peatland's decomposition to dryer conditions. Other models like CoupModel and PEATBOG adopted a more realistic approach by partitioning the peat into multiple pools with different decomposability (Metzger et al.,2015;

Wu et al., 2013), but parameterization of unquantifiable pools with arbitrary decay rates may leave the models less constrained. Several long-term peat accumulation models have adopted a concise 'continuous-quality' approach (Frolking et al., 2001, 2010; Chaudhary et al., 2017) to track substrate quality change which could be parameterized with decay rates directly derived from observations. This approach is thus a combination of utility and simplicity but few fine-scale process-based peatland model that also adopted this approach for decomposition (Frolking et al., 2002; Heinemeyer et al., 2010).

Secondly, few efforts have been made to incorporate nutrient cycles into peatland models. Only a limited number of peatland models have incorporated nitrogen (N) cycle (Heijmans et al., 2008; Spahni et al., 2013; Wu et al., 2013) and only one modeling study have looked at both the N and P cycles in peatland (Shi et al., 2021). The lack of representation of nutrient cycles in peatland models have significantly hindered our ability to project peatlands' future with environmental disturbances. For example, PEATBOG was by far the only model that explicitly investigated the responses of peatlands in the long-term fertilization experiments (Wu et al., 2015), which significantly lagged behind the large number of empirical research regarding the fertilization effect on peatlands (Bubier et al., 2007; Juutinen et al., 2010; Bragazza et al., 2012; Larmola et al., 2013; Levy et al., 2019). Furthermore, current peatland projection studies have neglected the impact of nutrient limitation in future climate–carbon cycle feedbacks (Wu and Roulet, 2014; Chaudhary et al., 2017, 2020; Qiu et al., 2020), which have been found to be very important in other non-peatland modeling studies (Wieder et al., 2015). This could lead to exaggerated response of vascular plants with simulated climate change and reduce the accuracy of the model projection.

Thirdly, microbial controls on biogeochemical processes have yet to be incorporated explicitly in any peatland models. Over the past decade, explicit representation of microbial dynamics in biogeochemical models has emerged as a research focus for ecosystem modeling (Allison et al., 2010; Wang et al., 2013; Wieder et al., 2013; Kaiser et al., 2014; He et al., 2015; Abramoff et al., 2017; Wang et al., 2017; Huang et al., 2018; Fatichi et al., 2019; Chadburn et al., 2020). As reviewed earlier, the response of microbial physiological traits to changes in environmental conditions could govern the response of peatlands to climate change

(Dieleman et al., 2016; Sihi et al., 2018). Yet peatland models developed so far have all been neglecting microbial dynamics. Moreover, peatland models that incorporate nutrient cycles (Heijmans et al., 2008; Spahni et al., 2013; Wu et al., 2013; Shi et al., 2021) have failed to address the fact that the dominant plant communities in the nutrient-limited bog ecosystems primarily rely on mycorrhizal fungi for nutrient acquisition (Gavazov et al., 2016). Omitting such key microbe-mediated processes in the model hinders our ability to precisely predict the response of biogeochemical cycling in ombrotrophic peatlands, as already shown in the mycorrhizal modeling work in other nutrient limited ecosystems (Brzostek et al., 2014; Baskaran et al., 2017; Sulman et al., 2017, 2019; He et al., 2018, 2021).

Last but not least, very little effort has been devoted to parceling out the contribution of individual driver to the combined impacts of multiple drivers on peatlands. To the best of my knowledge, Müller and Joos. (2021) is the only modeling study that did so, which identified rising temperature as the main driver of future peatland loss and increasing precipitations as driver for regional peatland expansion. However, the LPX-Bern model which is adopted in Müller and Joos. (2021) does not explicitly incorporate microbial controls (Spahni et al., 2013). In addition, 'increased nutrient deposition' was not included as a driver while exploring the interaction of multiple environmental drivers in that study.

2.5. Conclusions from literature review

This review highlights the significant role of microbial dynamics and nutrient cycles in regulating the response of peatlands to environmental changes. Current peatland models are severely lacking in representations of these key processes (Ritson et al., 2021; Shi et al., 2021), which impedes our ability to accurately predict the future of the enormous C storage in peatlands. The major focus of my thesis is to address this issue by incorporating microbe-mediated Carbon-Nitrogen-Phosphorus (CNP) cycling processes into a peatland model, and to use this model to shed more lights on how microbe-mediated processes affect the function of peatland and its response to potential environmental disturbances.

Chapter 3. Integrating McGill Wetland Model (MWM) with Cohort Development and Microbial Controls

Bridging statement to Chapter 3

Models can make long projections of the fate of the massive C storage in peatlands under environmental changes. But as reviewed in Chapter 2, the decreased substrate quality with peat decomposition age is poorly portrayed in peatland models and none of those models has explicitly considered the controls of microbial dynamics on peat decomposition. To address these discrepancies, Chapter 3 presents a newly developed model McGill Wetland Model_microbe (MWMmic) that integrates cohort tracking, microbial dynamics, and solute transport with the MWM. The new model is used to simulate the C cycle in the well-characterized Mer Bleue bog. I test whether the new model could reproduce the CO_2 fluxes, DOC and microbial dynamics observed at the bog. I also examine the impact of dynamic substrate quality and altered microbial physiological traits on the response of peat decomposition to climate change. This chapter lays the foundation for the investigation of the microbe-mediated nutrient cycling and mycorrhiza fungi-saprotrophs interaction in Chapter 4.

3.1. Abstract

Peatlands store a large amount of organic carbon and are vulnerable to climate change and human disturbances. However, ecosystem-scale peatland models often do not explicitly simulate the dynamics of decomposers and substrate quality during peat decomposition, which are key controls in determining peat carbon response to a changing environment. Therefore, we incorporated cohort tracking and microbial dynamics into the McGill Wetland Model (MWMmic) to simulate the dynamics of substrate quality and microbial activities. Three major modifications were made: (1) the simple acrotelm-catotelm decomposition model in MWM was changed into a time-aggregated cohort model, to track the decrease in peat quality with decomposition age; (2) microbial growth and metabolism were introduced to control decomposition rates; and (3) vertical and horizontal transport of the dissolved organic carbon (DOC) were added and used to regulate the growth of microbial biomass.

MWMmic was evaluated against measurements from the Mer Bleue peatland, a raised ombrotrophic bog located in southern Ontario, Canada. The model was able to replicate microbial and DOC dynamics, while at the same time reproduce the ecosystem-level CO_2 and DOC fluxes. Sensitivity analysis with MWMmic showed increased peatland resilience to perturbations compared to the original MWM, because of the incorporation of substrate quality tracking. The analysis revealed the most important parameters in the model to be microbial carbon use efficiency (CUE) and turnover rate. Simulated microbial adaptation with constant CUE and turnover rates could lead to a significant carbon loss with peat warming and water table drawdown, thus the rarely explored peatland microbial physiological traits merit further research. This work paves the way for further model development to examine important microbial controls on peatland's biogeochemical cycling.

3.2. Introduction

Despite occupying only 3% of the Earth's land surface, northern peatlands store a significant amount of terrestrial carbon (Xu et al., 2018). Estimates of the carbon storage in northern peatlands have ranged from 415 to 1055 Gt (Yu, 2012; Nichols and Peteet, 2019; Hugelius et al., 2020), at least one-fourth of the global soil carbon (2000–2700 Pg C) (Ciais et al., 2013). This large amount of soil carbon (C) is a legacy of peatlands being terrestrial sinks of CO_2 for millennia. Decomposition in northern peatlands, which is dramatically constrained by the water-logged, cold environments, and biogeochemistry (Freeman et al., 2001a; Beer and Blodau, 2007), is on average less than plant production. This results in an average C accumulation rate of about 0.02–0.03 $kgCm^{-2}\ yr^{-1}$ over thousands of years (Gorham, 1995; Turunen et al., 2002; Roulet et al., 2007) which has contributed to global scale cooling over millennia (Frolking and Roulet, 2007). However, the northern high latitudes, where the majority of northern peatlands are located, are projected to experience significant changes in climate (e.g. temperature, precipitation, permafrost) in the future (Flato et al., 2013; Intergovernmental panel on climate change (IPCC), 2018). Perturbations due to climate, and, or land-use change could potentially threaten the C stores of northern peatlands (Wu and Roulet, 2014).

Models are useful tools to better understand complex system behavior and make future

projections. Remarkable efforts have been made on developing peatland-specialized models (Frolking et al.,2002; St-Hilaire et al., 2010; Wu et al., 2012; Wu et al., 2013) and introducing peatlands into established ecosystem models or even global land surface models (Zhang, 2002; Ise et al., 2008; Dimitrov et al., 2010; Wania et al., 2009a, b; Metzger et al.,2015; Shi et al., 2015; Wu et al., 2016; Qiu et al., 2018). Some of these peatland models are designed for capturing the long-term C accumulation over millennia (Frolking et al., 2010; Spahni et al., 2013; Chaudhary et al., 2017), while others are for application on finer temporal and spatial scales. The fine-scale peatland models, which have the potential to be included in global climate-C models (Frolking et al., 2011), have been evaluated for individual sites (St-Hilaire et al., 2010; Sulman et al., 2012; Wu et al., 2012; Wu et al., 2013; Abdalla et al., 2014; Wu et al., 2016), and utilized to simulate peatlands' responses to environmental changes (Wu and Roulet et al., 2014; Wu et al., 2015) or anthropogenic disturbances (He et al., 2016). However, few decomposition modules in peatland models explicitly include controls of both microbial dynamics and substrate quality changes during the decomposition, which could lead to large uncertainties in simulating peatland decomposition.

For instance, the decreasing substrate quality with decomposition, which has been identified as the critical factor in the response of peatland decomposition to lowered water table (Laiho, 2006), is poorly portrayed in peatland models. Models like McGill Wetland Model (MWM) (St-Hilaire et al., 2010), CLASS-CTEM (Wu et al., 2016) and ORCHIDEE-PEAT (Qiu et al., 2018) adopted a simple approach of separating peat profiles into acrotelm and catotelm zones based on the water table level, while assigning them with constant basic decomposition rates separately (St-Hilaire et al., 2010, Wu et al., 2016; Qiu et al., 2018). Therefore, when these models were used to simulate peatland's response to lowered water table, the deep catotelm peat exposed to oxygen would be assigned with the same high decomposition rates as the acrotelm, assuming the catotelm and acrotelm peat have the same decomposability. This could lead to an overestimation of the peatland's response to dryer conditions. Other models like CoupModel and PEATBOG partitioned the peat into multiple pools with different decomposability (Metzger et al.,2015; Wu et al., 2013). This approach realized enhanced peat refractory with decomposition, but parameterization of unquantifiable pools with arbitrary

decay rates may leave the models less constrained. In contrast, some long-term peat accumulation models have adopted a concise 'continuous-quality' approach (Ågren and Bosatta, 1996) to track substrate quality change, which could be parameterized with decay rates directly derived from observations. This approach has successfully reproduced peat profiles that match the observations (Frolking et al., 2001, 2010; Chaudhary et al., 2017) and is thus a combination of utility and simplicity. To the best of our knowledge, PCARS (Frolking et al., 2002) is the only fine-scale process-based peatland model that also adopted this approach for decomposition.

Furthermore, current peatland decomposition models are also criticized for not explicitly considering any microbial physiological processes (Sihi et al., 2018). Microbial roles in regulating soil organic matter (SOM) formation and persistence have been increasingly recognized in recent studies (Conant et al., 2011; Schmidt et al., 2011; Cotrufo et al., 2013; Glassman et al., 2018). Therefore, moving away from the traditional first-order approach where an environmental covariant is used as a proxy to implicitly represent microbial activities towards the explicit incorporation of microbial dynamics emerges as a research focus for decomposition modelling over the past decade (Allison et al., 2010; Wang et al., 2013; Wieder et al., 2013; Kaiser et al., 2014; He et al., 2015; Abramoff et al., 2017; Wang et al., 2017; Huang et al., 2018; Fatichi et al., 2019). A growing number of empirical studies have also identified the importance of microbial metabolism in peatland biogeochemistry (Andersen et al., 2013). Microbial physiological properties like carbon use efficiency (Dieleman et al., 2016), community structures (Tveit et al., 2013; Bragazza et al., 2015), necromass generation (Weedon et al., 2013; Fernandez et al., 2019), and enzymatic activities (Fenner and Freeman et al., 2011; Pinsonneault et al., 2016b) all help understand peatlands' response to environmental changes. However, microbial dynamics have not yet been incorporated into peatland models. Despite requiring greater numbers of parameters and equations, microbial decomposition models have been shown to better explain the biogeochemical phenomena than the first-order models, including the priming effect (Drake et al., 2013), alleviation of stoichiometric constraint during litter decay (Kaiser et al., 2014), opposing effects of fertilization on decomposition (Averill and Waring, 2018), and stability of soil organic carbon

(SOC) with warming (Allison et al., 2010; Li et al., 2019). Hence omitting microbial processes in peatland models could hinder our ability to project peatlands' future facing perturbations.

To address the underrepresentation of substrate quality and microbial dynamics in peatland models, we developed MWMmic to explicitly incorporate these processes in MWM and to explore the effects of substrate and microbial limitation on peatlands' response to environmental changes. We first described the general structure and governing equations that we adopt in MWMmic. Then we presented an evaluation of CO_2 fluxes and C pools simulated by the model against measurements in the well-characterized Mer Bleue Bog (MB), Ontario, Canada. Finally, we conducted a series of sensitivity analysis to diagnose model's behavior and tested different hypotheses regarding the important microbial processes that affect long-term peatland stability with climate change. Our work addresses the following questions:

(1). Could we build a microbial peatland model that matches the observation of C fluxes and microbial biomass in peatlands?,

(2). How does incorporating cohort development influence the model's behavior? and

(3). Which microbial processes are key in determining the response of decomposition to environmental changes? How different parameterizations of those key microbial processes affect model's response to environmental disturbances?

3.3. Materials and Methods

3.3.1. Model description

MWM is a process-oriented model of the carbon balance of northern peatlands (St-Hilaire et al., 2010) that was developed based on the Peatland Carbon Simulator (PCARS) (Frolking et al., 2002). MWM estimates the carbon storage in two plant pools—leaves, and roots, and two soil pools—litter and peat. Carbon enters the system through photosynthesis of vascular plants and mosses and leaves the system via either autotrophic respiration (AR) or heterotrophic respiration (HR), i.e. decomposition. Once the vascular plant tissue and moss die, they become litter and are decomposed for one year in the litter pool and then transferred to the peat carbon pool for further decomposition. To account for the changes in peat decomposability with depth and microbial controls, following modifications are made to the

decomposition module of the original St_Hilarie et al. (2010) version of MWM (Figure 3.1):

1. The simple two-compartment peat decomposition model is converted back to the annual cohort, multi-layer model, similar to the approach of Frolking et al. (2002),
2. A microbial carbon (MBC) pool as well as dissolved organic carbon (DOC) pool are added as two additional carbon pools. Microbial metabolism and its effect on peat decomposition are explicitly simulated in the new model version, and
3. A simple solute transport scheme is developed to account for DOC exports through runoff and percolation.

Conversion to annual cohort model

The basic premise of the cohort model is that litter/peat can be modeled as a collection of vertically stratified layers of increasing age down the peat profile (Frolking et al., 2002). Each year's cohort is formed by the aboveground litterfall within that particular year. Thus, a new layer is added to the top of the peat profile every year and other cohort layers are buried progressively deeper in the profile. Cohort decomposition is modeled as a first-order process, with the decomposition rate k declining linearly with mass loss as:

$$k = k_0 * \frac{m_t}{m_0} \quad (1)$$

Where k_0 is the initial decomposition rate. m_0 is the initial mass and m_t is the remaining cohort mass at time t. Litter produced by different plant functional types (PFTs) are assigned different initial decomposition rates and are tracked separately within an annual cohort layer (Frolking et al., 2002). Therefore, the decomposition rate of each litter component in each layer is modeled as:

$$\frac{dm_{i,j}}{dt} = -k_{i,j} * m_{i,j} * f(T_j) * f(W_j) \quad (2)$$

Where $k_{i,j}$ is the decomposition rate for litter component i in cohort j, $m_{i,j}$ is the remaining mass of litter component i in cohort j, $f(T_j)$ and $f(W_j)$ are the temperature and moisture multiplier in cohort j respectively and are identical to those adopted in PCARS (Frolking et al., 2002) (See Text. S1). Calculation of T_j and W_j also followed that in PCARS where T_j is calculated by linearly interpolating between depths provided by the input data and W_j in the unsaturated

zone above the water table is calculated using water retention curves parameterized for peatlands by Letts et al. (2000). In addition, cohort receives fresh root litter inputs throughout the root zone and root litter is assumed to be produced uniformly within the root zone (Frolking et al., 2002).

Microbial interaction

Decomposition in peatlands is controlled by microorganisms through exudation of extracellular enzymes to break down complex biomolecules into simple monomers that can be directly utilized by themselves (Limpen et al., 2008). Heterotrophic respiration (HR) is essentially the product of microbial metabolism processes including growth and maintenance. To describe this microbial-driven decomposition, we use a framework similar to that of Allison et al. (2010), Moorhead et al. (2012) and Xu et al. (2014). Briefly, the decomposition module consists of three pools: Soil Organic Carbon (SOC), Microbial Biomass Carbon (MBC) and DOC. SOC is first depolymerized into DOC that is assimilated by microbes for metabolism. MBC constrains SOC degradation and is returned to the DOC and SOC pool after microbial death. How the C fluxes connect to these three pools is elaborated below.

SOC degradation is catalyzed by extracellular enzymes through hydrolytic, or oxidative processes. Hence, enzymes are often treated as an individual C pool in microbial decomposition models (Allison et al., 2010). However, explicitly simulating enzyme production and turnover could lead to over-parameterization given the lack of measurements of enzymes in peatlands. Thus, we made SOC depolymerization directly dependent on MBC, assuming that extracellular enzyme levels scale with the MBC (Moorhead et al., 2012). The dependence of decomposition on microbial biomass is described in a reverse Michaelis–Menten (MM) manner instead of a forward one according to Moorehead and Weintraub (2018), as peatlands are systems saturated with C substrates, rather than enzymes. The decomposition rates from Eq.1 are adopted here as the maximum depolymerization rates as in Xu et al. (2014):

$$D_{i,j} = SOC_{i,j} * k_{i,j} * \frac{MBC_j}{MBC_j + K_{m,B} * \sum_i SOC_{i,j}} * f(T_j) * f(W_j) \quad (3)$$

where $D_{i,j}$ is the depolymerization of $SOC_{i,j}$ and $SOC_{i,j}$ is the SOC in component *i* in cohort *j*, MBC_j is the MBC in cohort *j*, $K_{m,B}$ is the half-saturation constant. Eq. 3 replaces the Eq. 2

calculation of cohort mass loss in the original MWM, and $k_{i,j}$ remains as described by Eq. 1.

Microbes take up DOC to support growth and maintenance processes. The ability of microbes to assimilate DOC will be limiting DOC uptake at high DOC concentrations, which is described using Michaelis–Menten kinetics (Allison et al. (2010) (Eq. 4)). Assimilated DOC is partitioned between biomass growth and respiration loss based on a microbial Carbon Use Efficiency (CUE) (Eq. 5, 6). Microbial biomass turnover is a first-order process with a death rate m_r modified by a moisture multiplier.

$$Uptake_j = V_{max,U} * MBC_j * \frac{DOC_j}{DOC_j + K_{m,U} * V_j} * f(T_j) * f(W_j) \quad (4)$$

$$Growth_j = Uptake_j * CUE \quad (5)$$

$$CUE = CUE_0 + CUE_{slope} * T \quad (6)$$

$$Death_j = MBC_j * m_r * f(W_j) \quad (7)$$

where $V_{max,U}$ is the maximum DOC uptake rate of microbes. $K_{m,U}$ is the half-saturation constant for DOC assimilation, V_j is the volume of cohort *j*. CUE_0 is the reference *CUE* at 0°C and CUE_{slope} describes the temperature sensitivity of CUE. Partition of microbial respiration into maintenance and growth with both being a fraction of microbial biomass could lead to overparameterization and not proven to perform better compared to the simpler CUE approach (Hararuk et al., 2019). CUE_{slope} is set to be negative since CUE is generally found to decrease with higher temperature because of increasing energy demand for microbial metabolism. This pattern has already been represented as a simple linear temperature sensitivity function in many microbial-explicit SOC models (Allison et al., 2010; Wang et al., 2013; Li et al., 2019). We therefore adopt the same approach as shown in Eq.5. How microbial turnover rate is impacted by environmental factors has not been well-studied. While no temperature sensitivity is assigned to microbial turnover rate, the same moisture sensitivity as the decomposition and microbial metabolism have is adopted here. How different descriptions of the environmental factors on CUE and microbial turnover will affect the model's behavior is discussed later. Finally, as in Allison et al. (2010), a fixed proportion (g_D) of dead microbial mass is recycled to the DOC pool, with the remainder returned to the SOC pool as the necromass. The necromass is partitioned into different cohort components with fixed coefficient $fnec_i$. f_{nec_moss} is the fraction of necromass that is allocated to moss litter while f_{nec_shrub} ($1-f_{nec\_moss}$) is the

fraction of necromass that is allocated to shrub litter. With the microbial metabolism model built here, we would be able to simulate the priming effect, in which the DOC exudated by the plant roots could increase the microbial biomass and thus the peat decomposition.

Solute transport

In order to simulate the movement of DOC without explicitly modeling the water cycle, a simple, empirical model (Fraser et al., 2001) is adopted to calculate daily runoff (R) and percolation. R in mm/d, is empirically related to water table depth (WTD) in m, as:

$$R = 63.77 - 202.27 * (10.75\text{-}WTD)^{-0.5} \quad (8)$$

Runoff is distributed along the peat profile based on calculated hydraulic conductivity profile. The same calculation method of cohort hydraulic conductivities in PEATBOG (Wu et al., 2013). Since catotelm cohorts stays saturated, thus the water content of the whole catotelm stays constant, meaning its water input (percolation from acrotelm) should equal output (catotelm runoff). Thus, percolation from acrotelm to the whole catotelm (i.e. the top cohort in catotelm) is back-calculated here, as the product of the runoff and the ratio of the integrated hydraulic conductivity in the catotelm to the integrated hydraulic conductivity for the entire profile:

$$R_j = R * \frac{Kh_j * \lambda_j}{\Sigma(Kh_j * \lambda_j)} \quad (9)$$

$$Perc_{acr} = R_{cat} = R * \frac{\Sigma_{cat}(Kh_j * \lambda_j)}{\Sigma(Kh_j * \lambda_j)} \quad (10)$$

where R_i is the runoff in cohort j, R_{cat} is the runoff from the whole catotelm, $Perc_{acr}$ indicates the percolation from the acrotelm to the catotelm. Kh_j is the hydraulic conductivity in cohort j, λ_j is the thickness of cohort j. To keep the water content constant for all the catotelm cohorts, their own water input should equal their water output. Thus, for all the cohorts in the catotelm:

$$Perc_{j\_top} = R_j - Perc_{j\_bot} \quad (11)$$

$$Perc_{j\_bot} = Perc_{j\text{-}1\_top} \quad (12)$$

where $Perc_{j\_top}$ is the percolation to cohort j from the cohort above, $Perc_{j\_bot}$ is the percolation from cohort j to the cohort below. Since we could not calculate the water loss of

each cohort due to evapotranspiration here without applying a much more complicated model, a constant percolation rate (eq. 10) throughout the acrotelm profile is assumed.

With the water fluxes calculated by the module described above, DOC transport by water is simply calculated as the product of water fluxes and DOC concentration. Fick's law is applied to calculate the DOC diffusion between cohorts with a diffusion coefficient corrected for moisture content:

$$DOC\_diff_{bot,j} = \begin{cases} \frac{DOCconc_j - DOCconc_{j+1}}{\lambda_i} * D_j & if\ DOCconc_j \geq DOCconc_{j+1} \\ \frac{DOCconc_{j+1} - DOCconc_j}{\lambda_j} * D_j & if\ DOCconc_{j+1} < DOCconc_j \end{cases} \quad (13)$$

$$DOC\_diff_{top,j} = DOC\_diff_{bot,\ j-1} \quad (14)$$

$$D_j = D_0 * Porosity_j^2 \quad (15)$$

where $DOC\_diff_{bot,j}$ is the DOC diffusion in cohort *j* to cohort below and $DOC\_diff_{top,j}$ is the DOC diffusion to cohort *j* from the cohort above, the $DOCconc_j$ is the DOC concentration in cohort *j*, D_j is the effective diffusion coefficient in cohort *j*, D_0 is the base diffusion coefficient, $Porosity_j$ is the porosity in cohort *j* which is calculated based on the degree of decomposition (Frolking et al., 2010).

Aside from the development in the decomposition module, several modifications were also made on the vegetation module to down-regulate the large autotrophic respiration in shrubs generated in the original MWM, which produced considerably smaller shrub litter production compared to measurements. This modification produced much larger shrub litter production compared to the original MWM, which was also much closer to measured litterfall values in the fields (Bubier et al., 2007; Murphy et al., 2010). This part of modification is not discussed here for it is out of the scope of this study. But its impact on the model's partitioning of ecosystem C fluxes will be briefly discussed in the section 4.1.

3.3.2.Site description, data, and model initialization

MWMmic was applied to the Mer Bleue Bog (MB) for 16 years from 1999 to 2014 to evaluate the model's performance of simulating C cycle against observations. The Mer Bleue Bog, located 10 km east of Ottawa, Ontario, Canada (45.41°N, 75.48°W, 69 m above mean sea level), was formed over 8400 years ago as a fen and switched to the bog phase around 7000

years ago. It is now a raised acidic ombrotrophic bog of 28 km^2 with dominant vegetation of shrubs and mosses and sparse coverage of sedges (Moore et al., 2002, 2003; Bubier et al., 2006). The peat depth is around 5-6m near the center to less than 0.3m at the margin (Roulet et al., 2007). The climate of the region is mid-continental, cool temperate, with a 30 year (1971–2000) mean annual air temperature of 6.0°C and annual mean precipitation of 943 mm (http://climateweatherofficeecgcca/climate_normals (2018)).

The current input variables for the stand-alone version of the MWM are net radiation, photosynthetic photon flux density, precipitation (rain or snow), water table depth (WTD), air and soil temperature, relative humidity, wind speed, atmospheric pressure, and air CO_2 concentration. These hourly meteorological input data is from the MB flux tower dataset (https://daac.ornl.gov/FLUXNET/guides/FLUXNET_Canada.html). The outputs are Gross Primary Production (GPP), Autotrophic Respiration (AR) for each PFT, oxic and anoxic decomposition, microbial biomass carbon and DOC export for the peat profile.

Most of the new parameters in the model are either calibrated or directly derived from the values adopted by previously published models (Table 1). Exceptions are $K_{M,B}$ which is obtained from observations at MB reported in the literature (Blodau et al., 2004), f_{anox} which is calibrated for the ranges described in the literature (Keiluweit et al., 2016) and f_{nec} which is calibrated without any reference. Sensitivity analysis of those parameters is described in section 2.4. The model is calibrated through matching the model outputs from 1999 to 2006, the first six years of observed daily CO_2 fluxes, measured MBC pools and DOC concentration from different depths. During the calibration processes, we gradually changed the parameter values and visually evaluated the goodness of model fit based on observations.

The spin-up of the model was conducted by repeatedly using the 16-year meteorological data for over hundreds of years until the outputs approached steady state. The initial peat depth starts at zero, which means the whole peat profile is built with the simulated 16-year C accumulation rates during the spin-up. The decomposition started to plateau after a period longer than 800 years, with the inert peat in deep catotelm producing little HR. A spin-up run over 6000 years could ‘generate’ a peat depth over 5m deep. The outputs generated from the last 8 years of model runs are deemed as simulated results.

3.3.3.Model evaluation, sensitivity analysis and experiments

Model evaluation

The simulated results from 2007 to 2014 are evaluated against the observations. The observed daily C flux data from Fluxnet Canada (https://daac.ornl.gov/FLUXNET/guides/FLUXNET_Canada.html), together with microbial biomass carbon and DOC pool data obtained from published literature are adopted here for model evaluation. The original model was also applied on MB with the same 16-year input data to compare with the new MWMmic. Evaluation was conducted using time series and goodness of fit quantified by the root mean square error (RMSE) and linear regression coefficient (R^2) (Willmott, 1982).

Sensitivity analysis

In order to assess the robustness and the behavior of the model, we conducted two sets of sensitivity analysis on endogenous and exogenous parameters respectively. The first one is done on endogenous parameters by changing one parameter at a time over a ±25% range around the baseline values (Table 1). For the scope of this study we focused on the effect of parameter changes solely on the belowground C pools and fluxes including HR, MBC and DOC; the other one is conducted by adjusting the two main environmental variables: water table depth and soil temperature. Water table depth is decreased by 5cm, 10cm and 20cm respectively to mimic the potential future of drying. Soil temperature is increased by 1°C, 2°C and 5°C respectively to simulate different levels of warming. We highlighted the impact of this simulated environmental changes on HR and compared its response with that of the original MWM.

Model experiments

We furthered our model experiments by testing different hypotheses regarding of the two most uncertain microbial physiological variables: CUE and microbial turnover. In current

MWMmic, CUE is hypothesized to stay constant with different soil moisture conditions while decrease linearly with temperature increase (Eq. 6); microbial turnover is assumed to vary proportionally with the decomposition moisture multiplier and insensitive to different temperature changes (Eq. 7). However, all these premises have been challenged in other studies and different parameterization of those two variables were shown to have a profound impact on model's behavior to perturbations (Li et al., 2019).

Parameterization of the temperature (T) sensitivity of CUE and turnover rates plays a key role in microbial model's projection of soil C feedbacks to climate warming (Allison et al., 2010; Li et al., 2019). Most empirical studies have reported decreased CUE with temperature rise (DeVêvre et al., 2000). However, contradictory evidence of Frey et al. (2013) and Ye et al. (2019) demonstrated possible acclimation of CUE with warming. Similarly, most microbial models adopt T-insensitive microbial turnover rates, but it was also found that soil warming could accelerate the turnover rate (Hagerty et al., 2014). To examine how different T sensitivities of these two parameters might affect the behavior of MWMmic, we conducted two scenarios of model experiments for CUE and m_r respectively, including a "T-insensitive" scenario and a ''T-sensitive scenario" (See Text. S2). For each scenario, we first spun up the model over 6000 years using the same 16-year input data that we adopted for Mer Bleue bog. Then we ran each scenario under control and heated conditions (soil temperature increased by 5°C, SoilT + 5) for another 96 years.

High water levels and the consequent anoxia are considered the major causes for the inhibited microbial decomposition in peatland (Laiho, 2006). The effect of soil water content (SWC) and anoxia on microbial CUE and turnover is, however, rarely reported in the literature (Schimel et al., 2007; Manzoni et al., 2018). To the best of our knowledge, only one microbial model has parameterized the effect of SWC on m_r with the assumption that microbial metabolism and death have the same SWC sensitivity (Xu et al., 2014). No model has parameterized SWC sensitivity of CUE, but empirical studies have discovered decreases of CUE with both anoxia (Šantrůčková et al., 2004) and drought (Tiemann and Billings et al., 2011), suggesting there exists an optimum SWC for CUE. To investigate how different SWC sensitivities of these two parameters could affect the behavior of MWMmic, we also

conducted two scenarios of model experiments for CUE and m_r respectively, including a "SWC-insensitive" scenario and a ''SWC-sensitive" scenario (See Text. S2). We ran the model with the same datasets and processes as described above in the T-sensitivity experiments, except that we ran each scenario under control and drier conditions (water table depth dropped by 20cm, WTD+0.2).

Due to the downregulation of both depolymerization and metabolism rates with anoxia (Eq. 3 and 4), microbial biomass would drastically decline to 0 after the cohort entered catotelm unless the microbial turnover is comparably downregulated. Thus to still 'sustain' a microbial community in the catotelm under ''SWC-sensitive CUE" and "SWC-insensitive m_r" scenario, a new density-dependent formulation of microbial turnover, modified from Georgiou et al. (2017) was applied here:

$$Death_j = MBC_j * (\frac{dMBC_j}{dMBC\_ref})^{\beta} * m_r \quad (16)$$

Where $dMBC_j$ is the density of microbial biomass C in cohort *j*; *dMBC_ref* is the reference density (in gC/m^3); β is the density-dependence exponent whose value is larger than 0, which makes the microbial death become exponentially lower with decreased MBC density, preventing the microbes from dying off in all circumstances. This function was incorporated into both ''SWC-sensitive CUE" and ''SWC-insensitive m_r" scenarios and was separately calibrated. The detailed parameterizations of all the different scenarios mentioned in this section could be found in Text. S2.

3.4. Results

3.4.1. CO_2 fluxes and budgets

The robustness of the original MWM in reproducing C dynamics in MB (St-Hilaire et al., 2010; Wu et al., 2012) was demonstrated again over the 16-year simulation period (Figure S3.1). Similarly, the overall daily C fluxes simulated with the MWMmic were shown to agree well with the measurements (Figure 3.2). For both the total GPP and total Ecosystem Respiration (ER), the R^2 coefficients between the simulated and observed fluxes have exceeded 0.88 and the index of agreement have reached 0.97 (Figure 3.2). We also calculated

the main components of the net carbon balance (NECB), with the exception of the methane flux, simulated by both the model and compared them against measurements (Figure 3.3). The annual DOC export simulated by MWMmic, which was not part of MWM outputs, was close to the measurements. The overall annual total GPP, ER and NEE simulated by MWMmic also agreed well with the observations.

3.4.2. Validation of MBC and DOC

As shown in Figure 3.4, the simulated MBC matched the measurements both temporally and spatially. Our model successfully reproduced the seasonal pattern observed by Basiliko et al. (2005): MBC concentration tended to increase in the late fall and winter while decrease in the summer. The vertical profile of simulated MBC generally mimicked the measurements while discrepancies seemed to be greater in deeper peat. The model overestimated MBC in the 10-20 cm depth segment, while underestimated it in the 20-30cm segment compared to the observation from both Basiliko et al. (2005) (Figure 3.4 (a)) and Blodau et al. (2004) (Figure 3.4 (b)). On the other hand, the model appears to overestimate MBC in deeper peat (>35cm) near the transition to the catotelm (Figure 3.4 (b)). Excessive reduction of the rate of microbial turnover with anoxia (Eq. 5) could cause this overestimation of MBC concentration in the catotelm.

Several studies have measured DOC concentration ([DOC]) in the peat porewater from different depths during different time of the year (Fraser et al., 2001; Blodau et al., 2004; Rattle, 2006). These observations are plotted individually as colour-filled circles in Figure 3.5 with the different filled color representing different concentrations, to compared with the values simulated by MWMmic. Overall, our simulation captured the decrease of [DOC] with peat depth. Our simulation agreed with the measurements in 2005 while underestimated the [DOC] compared to observations made in 2003 and 2004.

3.4.3. Sensitivity analysis of endogenous parameters

The model's sensitivity varies depending on the parameters being assessed and what outputs are examined. MBC, DOC and HR are all insensitive to g_D, f_{nec_moss} and f_{anox} (Table 2).

Generally, HR was not very sensitive to changes in all the parameters tested here. K_0, microbial turnover rate m_r and CUE were the three parameters that affected HR the most, but the sensitivity was still relatively small. The negative response of MBC with increased/decreased k_0 and $k_{M,B}$ resulted from the opposing effects of depolymerization rates on the equilibrium MBC after spin-up. Larger depolymerization rates produced more DOC for MBC to uptake but depletion of labile carbon with overly large depolymerization rates can lead to decreased MBC, thus a unimodal response of MBC to k_0 and $k_{M,B}$ is generated from the model (Figure S3.2). Changes in DOC uptake parameters: $V_{max,U}$ and $K_{M,U}$ resulted in considerable changes in DOC, but a fairly limited response in MBC and HR (Table 2). Microbial turnover rate and CUE exerted a high leverage on model outputs. Increasing (decreasing) the overall CUE by 25% changed both MBC and DOC by over 25%, and similarly high sensitivity was identified for m_r too. CUE and microbial turnover rate were the most important governing parameters in our model, as also indicated in other microbial modeling studies (Allison et al., 2010; Hagerty et al., 2014; Li et al., 2019).

3.4.4.Sensitivity analysis of exogenous parameters

The sensitivity analysis with exogenous environmental variables showed that HR increased with temperature rise and water table drawdown, but the relative changes decreased considerably in the long term (referred to as the change after 64 years of disturbance) compared to that in the short term (referred to as the change after 16 years of disturbance) (Figure 3.6). In the long run, the HR from temperature rise and water table drawdown were quite close to each other despite the large difference in the beginning. In contrast, temperature rise and water table drawdown led to similar MBC increase in the short term, but the impacts diverged in the long term (Figure S3.3). The MBC increase with water table drop is in line with the observations in field experiments (Blodau et al., 2004). The T and SWC sensitivities of microbial CUE and turnover have a significant impact on the model's response to climate change (Figure 3.8-3.9). Scenarios of no T sensitivity for both CUE and m_r led to higher T sensitivity for HR produced from the model (Figure 3.8). In comparison, the scenarios with either higher SWC sensitivity of CUE or no SWC sensitivity of m_r were clearly

more sensitive to WTD increase.

3.5. Discussion

3.5.1. Peatland carbon cycle

Overall, MWMmic and MWM both successfully reproduced the carbon fluxes measured in Mer Bleue (Figure 3.2). However, there was a distinct difference in how HR and AR were partitioned, albeit the total GPP, ER and NEE fluxes simulated by MWM and MWMmic did not vary significantly (Figure 3.3). Although the simulated GPP and ER from the original MWM do have a marginally higher R2, the slopes of the regression line from MWMmic are much closer to 1.0 (Figure 3.2). NEE simulated by MWMmic has a higher R2 but smaller slope compared to MWM. The overall RMSEs between simulated and measured daily fluxes generated by MWMmic is slightly lower than those from MWM (Figure 3.2 and Figure S3.1). In addition, MWMmic has the tendency as MWM to underestimate the highest C fluxes.

The overall annual total C fluxes produced by the two models also agreed with the observations, with MWMmic generating a little bit higher GPP and ER while fitting the values calculated from the observation slightly better. Although the two models generated overall similar total fluxes, MWMmic produced much higher HR compared to the original MWM. HR simulated from MWM was less than 7% of the total ER whereas HR generated by MWMmic contributed to nearly half of the total ER, which clearly fit better with the latest measurements on Mer Bleue showing that HR accounted for 50% of the total ER (Rankin, unpublished data). Earlier studies in other peatlands also showed that the contribution of HR to the total ER ranges from 46% to 80% (Riutta et al., 2007; Hicks Pries et al., 2015; Järveoja et al., 2018), much larger than the number produced by the original MWM. Additionally, the higher shrub NPP produced by MWMmic also agreed better with the field observation (Murphy et al., 2010; Juutinen et al., 2010), compared to MWM. These different carbon flux components mentioned here have different sensitivities to environmental changes, which essentially determined the C sink strength of peatlands (Ahlström et al., 2015; McGuire et al., 2012)). Therefore, a thorough understanding of how different C fluxes are partitioned and what are

their controls is important to discerning the ecosystem-level C dynamics (Savage et al., 2013). Limited empirical studies have been conducted on partitioning different respiration components in peatlands (Riutta et al., 2007; Hicks Pries et al., 2015; Järveoja et al., 2018) and more studies are required to validate the different partitioning schemes that are seen here from the two models. But given the measurements done so far (Rankin, unpublished data), it can be inferred that MWMmic performed more realistically in partitioning different C fluxes.

Furthermore, MWMmic is currently the only model, as far as we are aware, that has explicitly tested model-simulated microbial activities in peatlands. MWMmic was shown to perform well in simulating MBC dynamics (Figure 3.4). The MBC concentration measured at Mer Bleue bog (around 3 mg g^{-1} peat in the top 30 cm) (Blodau et al., 2004; Basiliko et al., 2005, 2006; Xing et al., 2010) is much lower compared to the observed globally average microbial concentration in the soil (12 mg g^{-1} SOC) (Xu et al., 2013). However, the value is comparable to values obtained for other peatland studies (Anderson et al., 2006; Preston et al., 2012; Parvin et al., 2018). To attain such low MBC pool, MWMmic has adopted a relatively low CUE with the maximum CUE at 0.3512, compared to those adopted in other microbial models with the maximum CUE over 0.60 (Allison et al., 2010; Wang et al., 2013). This demonstrated the overall inhibition of microbial activities in peatlands is similar to other ecosystems, probably due to the anoxic environment that is characteristic of peatlands (Freeman et al., 2001a). Both DOC concentration and export simulated by MWMmic agreed well with observations (Figure 3.3 and Figure 3.5), showing the robustness of both the decomposition model and the empirical runoff model (Fraser et al., 2001). The average [DOC] in runoff generated from the model was about 39.8 mg L^{-1} which gave an annual runoff loss of DOC around 15.3 gC yr^{-1}. This concentration is a bit lower compared to the average measured [DOC] in the outflow which was 47.5 mg L^{-1} (Fraser et al., 2001). Meanwhile the simulated DOC runoff loss of 15.3 gC yr^{-1} is right within the range reported from the literature, i.e., between 14.9 gC yr^{-1} estimated from Roulet et al. (2007) and 16.4 gC yr^{-1} obtained from Dinsmore et al. (2009). It is also noteworthy that DOC adsorption to mineral surfaces is not modeled here like some other microbial models do (Wang et al., 2013; Abramoff et al., 2018). This is in line with the fact hydrologic pathways in peatland rarely encounter mineral soils

upon which DOC adsorption occurs (Moore, 2009) before leaving the peatlands or leaching to the mineral layers below the peat. Therefore, DOC export is indispensable when accounting for peatlands' carbon budget (Roulet et al., 2007).

3.5.2.Simulated response to climate change: depletion of labile carbon

The sensitivity analysis with exogenous environmental variables showed that HR with the MWMmic was less sensitive to environmental changes compared to the original MWM (St-Hilaire et al., 2010), and relative changes in HR decreased considerably in the long run compared to the short run (Figure 3.6). This was caused by the reduction in peat decomposability. Increase in soil T or WTD led to higher values of temperature and moisture multipliers (Eq. 2), thus increased the cohort decomposition rates and caused HR to rise rapidly (Figure 3.6) along with MBC (Figure S3.3) in the short term. But as time went by, larger decomposition diminished the higher quality substrates leading to the remaining peat being relatively more recalcitrant, leading to a gradual drop in HR (Figure 3.6) or even MBC (Figure S3.3) in the long run. In comparison, the original MWM assigned fixed decomposition rates for oxic and anoxic decomposition respectively, neglecting the changes of peat quality with the degree of decomposition, which will certainly exaggerate the response of HR response to environmental changes.

The model was clearly more insensitive to WTD increase than temperature rise, particularly in the short term (Figure 3.6). The reason behind that is most likely that Mer Bleue is a relatively dry bog with WTD often deeper than 0.3m in the growing season (Moore et al., 2003). As the cohort substrate become more and more recalcitrant with decomposition, most of the labile carbon is already depleted by the time the cohort reaches the catotelm. Therefore, exposing more recalcitrant peat in the catotelm to oxygen will not increase the overall HR by a great deal even in the short term (Figure 3.7). This high resilience of HR to water table changes simulated by MWMmic agrees well with studies that identified the lack of a strong dependency of ER on water table at the Mer Bleue Bog (Lafleur et al.,2003; Goud et al., 2017). It is reported that peatlands with lower water table tend to be depleted in labile carbon at deeper depth and thus their decomposition is more resistant to water table drop (Laiho, 2006;

Sulman et al., 2010; Ratcliffe et al., 2019). In comparison to peatlands with similar climates but higher water table, the observed peat composition in MB bog showed a greater decline in carbohydrates with depth (Hodgkins et al., 2018). Therefore, MB Bog is relatively insensitive to water table lowering as shown by our modeling analysis. Our sensitivity analysis also demonstrated that the HR's response to perturbation in the long term is constrained by the low decomposability in the catotelm C. This is in line with deep peat warming study that identified the stability of catotelm C (Wilson et al., 2016) and several peatland WT manipulation studies that observed the nonlinear HR response with the largest CO_2 losses upon the initial lowering of WT (Hargreaves et al., 2003; Laiho, 2006; Straková et al.,2012)

The decomposition rate of the peat cohort is constantly downregulated as it gets older with less labile C remaining. With the cohort substrate becoming more and more recalcitrant with decomposition, microbes could not grow its biomass with overly small decomposition rates thus gradually died off as seen in the simulated deep peat profile (Figure 3.10 (a). blue line), Therefore, the increase in substrate recalcitrancy combined with the resulted gradual extinction of microbes led to gradually stopped decomposition in the deep peat. This colimitation by substrate and decomposers were also identified in all the microbial models parameterized with forward-MM depolymerization equations (Wutzler and Reichstein, 2008; Walker et al., 2018), where the decreasing SOC concentration with decomposition halted the decomposition process itself in the end of the decomposition. This inert 'leftover' from decomposition corresponds to the observations of many upland litterbag studies, which can be best modelled with an asymptotic function by inferring a limit value that is not decomposed in finite time (Bottner et al., 2000; Prescott et al., 2010; Berg et al., 2014). Fernandez et al. (2019) also found such asymptotic functions to be the best fit to the decay pattern of mycorrhizal necromass in peatlands. The idea that there exists an inert pool in soil C is already adopted in several non-microbial SOC models (Falloon and Smith, 2000; Zhao et al., 2013). Our modeling study might also provide grounds for the existence of such pool from a microbial perspective: microbes simply cannot benefit from investing energy on breaking down too recalcitrant substrate.

However, the limited value identified in MWMmic may not necessarily mean a complete

shutdown in decomposition. Wutzler and Reichstein (2008) showed that continuous addition of DOC and MBC into the system, which represented the priming effect, could lead to sustained decomposition. Field studies showed that vascular plants in peatlands could promote ancient peat loss through priming (Walker et al., 2016; Gavazov et al., 2018). This could be the mechanism through which plants acquired nutrients for growth from the otherwise 'locked-up' pools (Gavazov et al., 2016). A model that incorporated both nutrient cycling and plant-microbes interaction is required to better understand the dynamics here.

3.5.3. Response to climate change: microbial CUE and turnover

Scenarios of no T sensitivity for both CUE and m_r led to higher T sensitivity for HR produced from the model (Figure 3.8). CUE had contrasting effects on HR (Manzoni et al., 2012): Lower CUE with higher T means that microbes invest more proportion of their assimilated C to respiration. In the meantime, less assimilated C allocated to biomass growth limits the size of the microbial community (Allison et al., 2010) and thus reduce the rate of enzymatic depolymerization which is the rate-limiting step for decomposition (Bengtson and Bengtsson, 2007). In our T sensitivity experiments, all scenarios showed a sharp increase in HR with warming in the beginning and gradual decline in HR after decades of continued warming (Ågren and Bosatta 2002). The overall low CUE and small MBC determined that a constant CUE with higher T would yield higher HR, compared to a lower CUE with higher T. Likewise, higher microbial turnover rates with higher temperature limited the growth of microbial community size and ultimately HR as well. Noticeably, the simulated HR with 'T-sensitive m_r' scenario in the end became even smaller than the simulated HR without warming (Figure 3.9 (b)).

In our SWC sensitivity experiments, simulated HR from all scenarios increased in the beginning of WTD drop and gradually decreased later. The scenarios with either higher SWC sensitivity of CUE or no SWC sensitivity of m_r were clearly more sensitive to WTD increase. Microbes may decrease their CUE and microbial turnover rates to adapt to the harsh anoxic environment (Malik et al., 2020). Once the anoxia stress is relieved with WTD increase, models that allow microbes to either increase their CUE (higher SWC sensitivity for CUE) or maintain

their low turnover rate (lower SWC sensitivity for m_r) will have higher MBC and thus higher HR, as shown in our results here. However, the inclusion of the density-dependent microbial turnover function in both ''SWC-sensitive CUE" and ''SWC-insensitive m_r" scenarios may also play an important role in generating higher MBC and HR. As mentioned in section 2.3.3, this new death function could preclude microbes from dying off under all conditions and is necessary for the models to sustain catotelm microbial activity in ''SWC-sensitive CUE" and ''SWC-insensitive m_r" scenarios where anoxia unproportionally depressed microbial metabolism compared to microbial death. Figure 3.10 demonstrated that, while simulated MBC from the original MWMmic decreased radically and essentially died off in the bottom peat, the MBC from the other two scenarios gradually "stabilized" in the deeper profile. Since neither the decreased CUE with anoxia from "SWC-sensitive CUE" scenario nor the constant m_r with anoxia from ''SWC-insensitive m_r" could lead to this "preservation" of microbial activity in the catotelm, this could only be the result of the density-dependent function which dramatically decreased microbial turnover rate when the microbial density became lower in the catotelm. Therefore, microbes parameterized this way became 'tougher' and can survive much harsher conditions. The peat that was previously indecomposable now became more labile to these 'tougher' microbes, which results in model's higher sensitivity to WTD drawdown.

3.5.4. Microbial CUE

CUE has been identified as the critical synthetic representation of microbial community C metabolism in most microbial models (Allison et al., 2010; Wang et al., 2013). A great many studies have been conducted on CUE values in different ecosystems (Manzoni et al., 2018) and how it varies with variables including temperature (Frey et al., 2013), soil moisture (Šantrůčková et al., 2004; Tiemann and Billings, 2011), pH (Malik et al., 2018), substrate quality and stoichiometry (Sinsabaugh et al., 2016; Takriti et al., 2018) and microbial communities (Sinsabaugh et al., 2013; Soares and Rousk, 2019). Malik et al., (2018a) generalized the different observed patterns as microbes' strategic trade-offs among traits that are linked to growth yield, stress tolerance and nutrient acquisition: microbial communities downregulate

their growth yield (CUE) to cope with scarce resources or stressful abiotic conditions while maximize it with the absence of nutrient limitation and stress.

Studies on microbial CUE in peatlands are few (Sihi et al., 2018; Hill et al., 2014) and no measurements had been taken on the MB bog. Due to the lack of information, the CUE in MWMmic is parameterized by adopting the CUE-T function of microbes utilizing phenols from Frey et al. (2013), in line with the ubiquity of phenols in peatlands (Freeman et al., 2001a; Pinsonneault et al., 2016a). The good agreement between the simulated MBC concentration with the measured ones showed the robustness of this approach (Figure 3.4). The CUE value we calibrated for our "T-insensitive CUE" model was 0.25 (Text. S2; Figure 3.9 (a)). As mentioned earlier, this was low compared to the average measured CUE in terrestrial ecosystems of 0.45 but identical to the average value of 0.25 obtained in aquatic ecosystems (Manzoni et al., 2018). This might be attributed to the fact that wetlands are transitional ecosystems between terrestrial and aquatic environments, and Mer Bleue is an acidic and nutrient-deficient bog resulting in high microbial investments into activities related to stress tolerance and nutrient acquisition (Malik et al., 2020).

Our modeling showed the significance of CUE parameterization in determining both the magnitude and direction of the response of the peat C dynamics to environmental perturbations (Figure 3.8 and Figure 3.9), as shown in other microbial modeling studies too (Allison et al., 2010; Li et al., 2019). Contrasting evidence exist in the literature on how CUE varies with temperature. Earlier studies tended to agree with the idea that increased respiratory costs and heat stress responses with temperature rise resulted in lower microbial CUE (Apple et al., 2006), which got validated in different laboratory soil incubations (DeVêvre and Horwáth 2000; Steinweg et al. 2008; Tucker et al., 2013) and applied in many microbial models (Allison et al., 2010; Wang et al., 2013). Decrease in microbial CUEs with warming were also observed in two laboratory peat warming experiments, offering support for our T-sensitive CUE parameterization in MWMmic (Sihi et al., 2018; Wen et al., 2019). However, many other studies have reported different CUE responses with warming, including no change in CUE (Dijkstra et al., 2011) and limited increase in the long term (Frey et al., 2013) and even positive temperature-CUE relationships based on global-scale cross-biome datasets (Ye et al.,

2019; Bradford et al., 2019), challenging the classic theory that maintenance energy demands exceeded growth energy demands with warming (Bradford et al., 2013; Zheng et al., 2019). Even less certain is our understanding about the response of CUE to different moisture content. With very limited studies so far (Šantrůčková et al., 2014; Tiemann and Billings, 2011; Zheng et al., 2019), CUE was generally thought to reach maximum with an optimum soil moisture content while decrease when the soil got wetter or dryer (Manzoni et al., 2012). Unlike the CUE decrease with temperature rise which releases more CO_2, the C overflow with CUE drop in anaerobic metabolism is released as exudation (Šantrůčková et al., 2014). These observed nonlinear responses of CUE to disturbances could result from the fact that CUE is an emergent property of multiple microbial process (Bradfordet al., 2013). Therefore, studies have suggested that future microbial models should account for microbial C allocation strategies instead of adopting CUE as a single parameter (Manzoni et al., 2017; Hagerty et al., 2018).

3.5.5.Microbial turnover

Determining microbial death and necromass production, microbial turnover rate is another important parameter in microbial models. It is now widely accepted in mineral soil studies that the sorption of microbial necromass onto mineral binding sites is the determining process for long-term SOM stabilization (Conant et al., 2011; Schmidt et al., 2011; Cotrufo et al., 2013). The lack of mineral content in bog peatlands precludes this mineral-protection mechanism from occurring, but the importance of necromass production in peatland biogeochemistry is getting recognized recently. Weedon et al. (2013) found that seasonal increases in microbe-derived substrate input can have stronger effects than temperature and plant-derived substrate on peat C and N cycle processes and suggested the incorporation of realistic microbial biomass dynamics into peatland models. Fernandez et al. (2019) identified the significance of the mycorrhizal fungal necromass as an important input to the belowground C storage in boreal peatlands. Despite the importance of microbial turnover, however, little is known to date about the exact turnover time of the microbial biomass, which is partly due to the paucity of proper methods to access the microbial biomass turnover time in soil (Spohn et al., 2016a, b). Hagerty et al. (2014) is the only study that have looked at

microbial turnover rate at a peatland, which turned out to be a bit lower than that in a mineral soil, in line with what we adopted in MWMmic (Table 2).

Microbial turnover rate was reported to increase with temperature rise (Hagerty et al., 2014). Our modeling exercise showed that a T-sensitive microbial turnover rate with a Q10 function (Text. S2) could strongly inhibit the peat loss with warming in the long run, in line with the modeling results in Hagerty et al. (2014). However, Li et al. (2019) found that T sensitivity of HR is rather unrelated to the temperature sensitivity of microbial turnover rates. This is probably brought by the difference in model structures. In MWMmic, similar to the Allison-Wallenstein-Bradford (AWB) model (Allison et al., 2010; Li et al., 2014) adopted in Hagerty et al. (2014), the DOC uptake rate and microbial turnover rate are decoupled from each other; while in the MEND model (Wang et al., 2013) adopted in Li et al. (2019), the intrinsic microbial DOC uptake rate is the sum of microbial growth rate and turnover rate. Therefore, higher turnover rates with warming in MEND concurrently led to higher DOC uptake rates, offsetting the effect of warming to some extent. This demonstrated that the model's behaviors are determined by their fundamental model assumptions and structures (Y. Wang et al., 2016).

Little is known about the sensitivity of microbes' turnover rates to soil moisture content and anoxia that are critical environment factors for peatlands. Drought is thought to invoke microbial dormancy as a response to unfavorable environmental condition and thus decrease in microbial turnover rates (Manzoni et al., 2012), which has been addressed in several microbial models (He et al., 2015; Salazar et al., 2018). Anoxia was recently reported to result in reduced microbial turnover rate (Zheng et al., 2019) which is also shown in MWMmic to be necessary for microbes to survive under depressed metabolism rates. This downregulation of microbial turnover rates, similar to CUE's response to stress and resource scarcity (Malik et al., 2020), was also found to occur with microbes in deep pasture soils to deal with C starvation (Spohn et al., 2016a) but not with nutrient limitation (Spohn et al., 2016b; Spohn et al., 2017). Microbes facing P limitation were reported to decrease their phosphorus (P) turnover rates while maintained carbon turnover rates (Spohn et al., 2017), adding to the complexity in understanding microbial turnover.

To better constrain the highly uncertain microbial turnover rates in the model, a better understanding of the mechanism behind microbial death is crucial for us. Incorporation of the observed density-dependent death kinetics into microbial models is a recent effort to represent microbial turnover more mechanistically (Abramoff et al., 2017; Georgiou et al., 2017). Contrary to the classic 'exponential death' pattern, Phaiboun et al. (2015) found that bacteria facing starvation does not just die exponentially but instead will persevere for extended periods of time and exhibited density-dependent kinetics. Incorporation of such kinetics was not only shown to dampen the unrealistic oscillation in MBC pool (Georgiou et al., 2017) which is characteristic with models using forward MM function (Sihi et al., 2016), but were also expected to resolve the problem of substrate and microbial depletion at the end of decomposition simulated with microbial models (Fatichi et al., 2019). Our study is the first one to demonstrate that microbial models parameterized this way could preclude microbial and substrate depletion, thus made microbial survival possible in harsh environments like the bottom catotelm peat. This agreed well with several deep peat measurements that showed abundant microbial biomass in peat over 1m deep (Preston et al., 2012) or gene copies in peat over 2m deep (Lin et al., 2014). However, the considerably high sensitivity of HR with increased WTD that came along with this density-death function (Figure 3.9 and Figure 3.10) contradicted the empirical evidence (Laiho, 2006; Ratcliffe et al., 2019) thus making this parameterization disputable. Given the importance of microbial turnover rate in microbial models, further research is in desperate need to puzzle out how to better parameterize the microbial death in a mechanistic manner.

3.6. Conclusion

With the cohort-based microbial-driven MWMmic developed, evaluated, and tested for its behavior in this study, we could answer the questions that were raised in the beginning:

(1). Could we build a microbial peatland model that matches the observation of C fluxes and microbial biomass in peatlands?

With the new MWMmic, we can not only reproduce the observed microbial and DOC dynamics well, which were not simulated by the original MWM, but are also able to simulate

the measured C fluxes more realistically compared to MWM.

(2). How does incorporating cohort development influence the model's behavior?

Incorporating the cohort development profoundly changes the model's behavior. There always exists a proportion in the peat substrate that is left indecomposable at the end of the decomposition unless with allochthonous priming effect. The sensitivity of the model to environmental disturbances becomes much smaller compared to MWM, particularly with WTD increase, agreeing with the observation.

(3). Which microbial process is key in determining the response of decomposition to environmental changes? How different parameterizations of those key microbial processes affect model's response to environmental disturbances?

Microbial CUE and turnover rate are the two most important microbial parameters in determining the response of decomposition to environmental changes. How they responded to different environmental conditions decided the direction of the model's behavior facing environmental disturbances. CUE and microbial turnover in future microbial models need to be parameterized in a more mechanistic way and extensive empirical research is needed to provide the grounds.

Overall, the newly developed MWMmic successfully replicated more components of the peatland's carbon cycle and altered peatlands' response to perturbations in a more realistic way compared to the original model. However, we also acknowledge that there are a number of limitations in this study that need to be addressed in the future:

1. Most microbial physiological parameters are adopted from experiments in other ecosystems due to lack of corresponding studies in peatlands. Although we have calibrated the model to generate good fit to the measured MBC and DOC dynamics in Mer Bleue bog, future peatland microbial models are still needed to better calibrate the model and, more importantly, expose potentially misrepresented microbial processes in peatlands.

2. Our sensitivity experiments showed the HR in the new MWMmic model is much less sensitive to environmental disturbances than previously thought with the original MWM. Although we have demonstrated evidence that could testify our result here, such as the observed lack of sensitivity in ecosystem respiration to WTD changes in Mer Bleue bog. The

lack of comprehensive environment manipulations studies in Mer Bleue halted our ability to further test our model's applicability. Applying MWMmic on sites with manipulation experiments in the future could better inform our model's parameterization.

3. Vegetation and nutrient feedbacks are not included in our studies. Lowered water table and higher temperature were both shown to increase shrubs' abundance and reduce Sphagnum mosses' cover through canopy shading (Hanson et al., 2020). This vegetation change should have profound impact on how the peatland's decomposition responds to climate change. However, we want to focus this study on the implication of adding microbial dynamics into the decomposition model thus those feedbacks are not considered here. But the inclusion of microbial dynamics into the model have paved the way for future model development to examine important microbial controls on peatland's nutrient cycling like the priming effect (Drake et al., 2013) and necromass recycling (Cui et al., 2020). It served as the first step in a line of developments to eventually include nutrients into the model and represent the peatland biogeochemical cycling in a more realistic way.

3.7. Tables and Figures

Table 1.1 General Parameters in MWMmic

Description	Parameter	Units	Literature value	References	Calibrated Value
Initial decomposition rates of different peat components	k_0 (shrub, moss)	yr^{-1}	0.32,0.08	Frolking et al. (2010)	0.32,0.08
Half-saturation constant in decomposition	$K_{M,B}$	g MBC (g peat)$^{-1}$	0.0025	Blodau et al. (2004)	0.0025
Maximum DOC uptake rate of microbes	$V_{max,U}$	g DOC (g MBC) h^{-1}	[0.000013, 0.13]	He et al. (2014)	0.01
Half-saturation constant for DOC assimilation	$K_{M,U}$	mg L^{-1}	300	Abramoff et al. (2017)	350
Intrinsic microbial turnover rate	m_r	h^{-1}	0.0002	Allison et al. (2010)	0.00018
Reference CUE at 0°C	CUE_0	g g^{-1}	0.3512	Frey et al. (2013)	0.3512
Temperature sensitivity of CUE	CUE_{slope}	g g^{-1} $°C^{-1}$	0.0095	Frey et al. (2013)	0.0095
Fraction of dead microbes that is recycled to DOC pool	g_D	-	0.5	Allison et al (2010)	0.5
Fraction of necromass that is partitioned to different peat components	f_{nec} (shrub, moss)	-	-	N/A	0.2,0.8
Rate reduction in decomposition due to anoxia	f_{anox}	-	[0.025, 0.4]	Keiluweit et al. (2016)	0.1

Table 1.2 Sensitivity of belowground C stores and fluxes to adjustment of key parameters

Parameters adjusted	Changes (%)	Changes in C storages and fluxes (%)		
		MBC	DOC	HR
k_0	+25%	-10.31%	-18.50%	5.81%
	-25%	-7.95%	2.69%	-6.59%
$K_{M,B}$	+25%	-4.04%	2.39%	-5.01%
	-25%	-1.82%	-6.65%	4.34%
$V_{max,U}$	+25%	1.63%	-21.26%	1.49%
	-25%	-2.16%	27.62%	-1.64%
$K_{M,U}$	+25%	-1.98%	24.79%	-1.48%
	-25%	1.54%	-19.85%	1.41%
m_r	+25%	-25.88%	29.72%	-6.67%

CUE	-25%	26.00%	-26.25%	5.80%
	+25%	26.54%	-18.88%	4.91%
g_D	-25%	-38.40%	37.16%	-9.56%
	+25%	0.58%	-0.74%	0.97%
f_{nec_moss}	-25%	-0.70%	0.26%	-0.65%
	+25%	-0.11%	0.28%	-0.17%
f_{anox}	-25%	0.11%	-0.27%	0.26%
	+25%	-0.09%	0.07%	0.07%
	-25%	0.09%	-0.07%	-0.13%

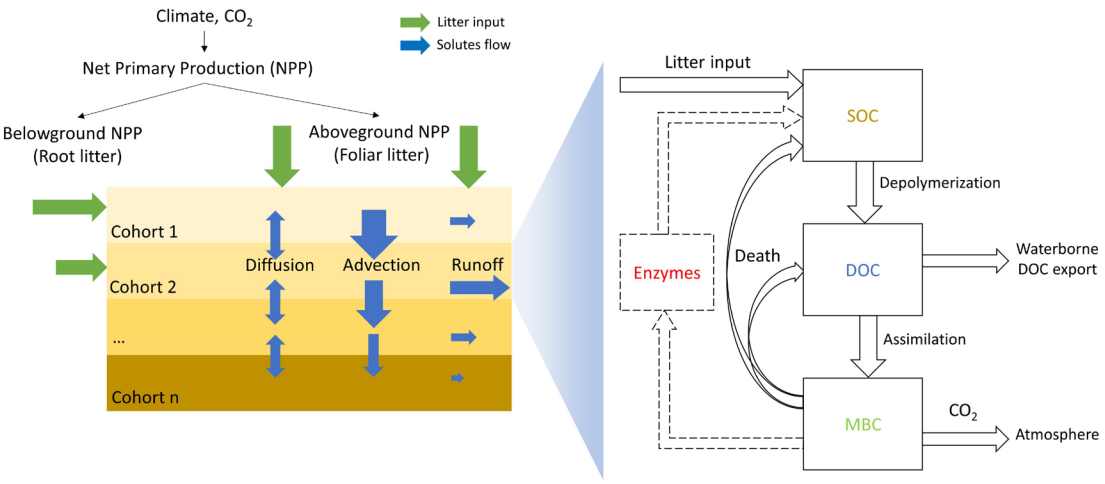

Figure 3.1 Diagrams of stores and fluxes in the decomposition module of MWMmic

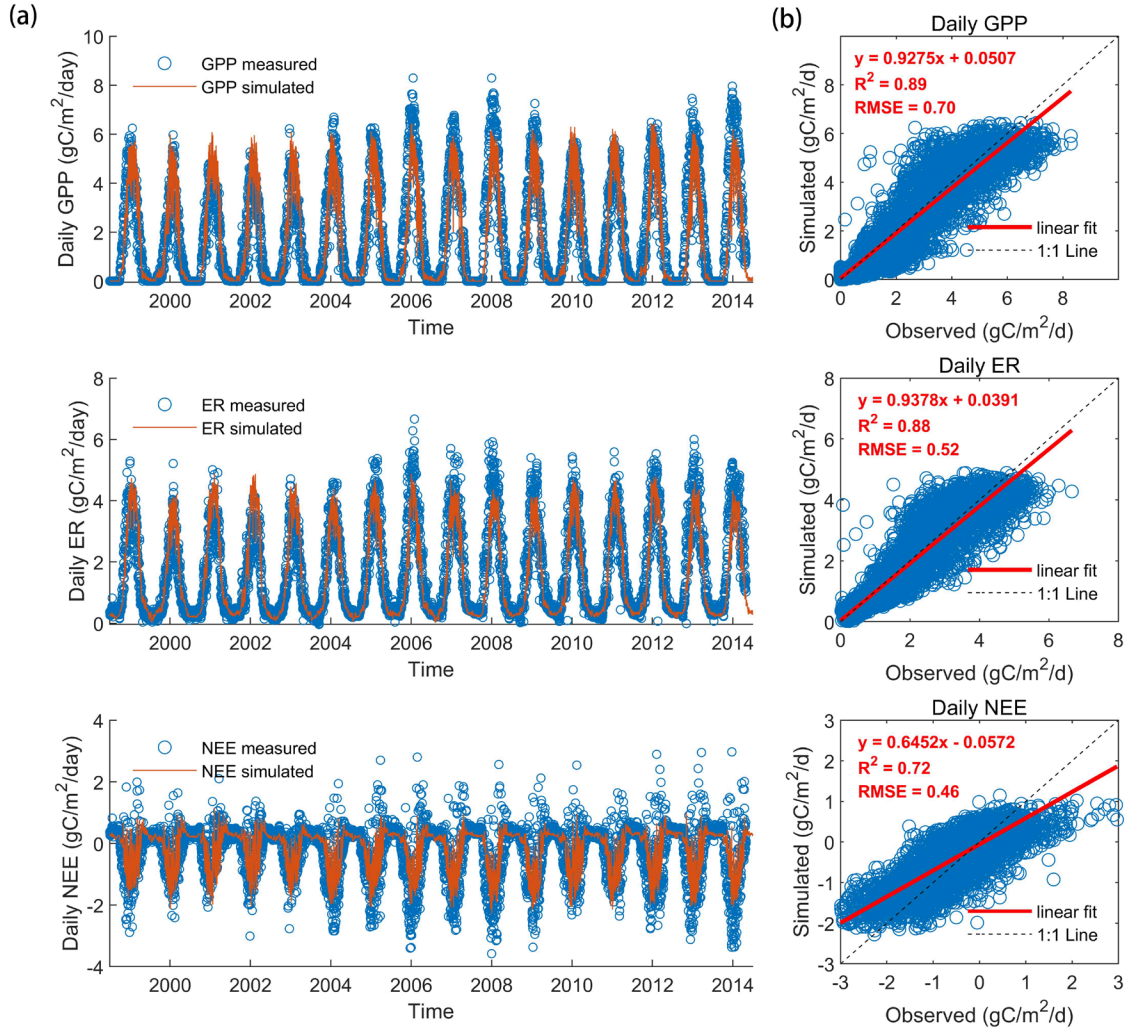

Figure 3.2 (a)Time series of observed and MWMmic-simulated daily GPP, ER and NEE. (b) Linear regression of observed and MWMmic-simulated daily GPP, ER and NEE.

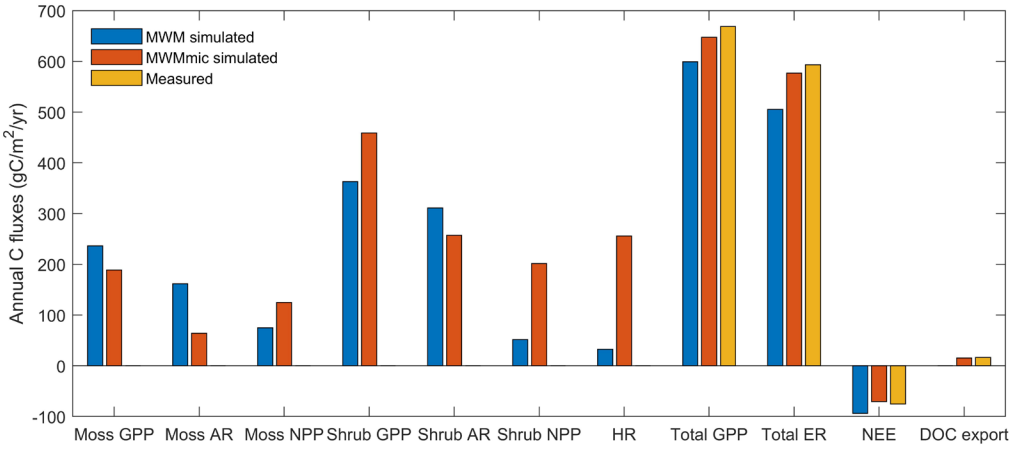

Figure 3.3 Simulated and measured mean annual C fluxes in Mer Bleue Bog from 1999 to 2014.

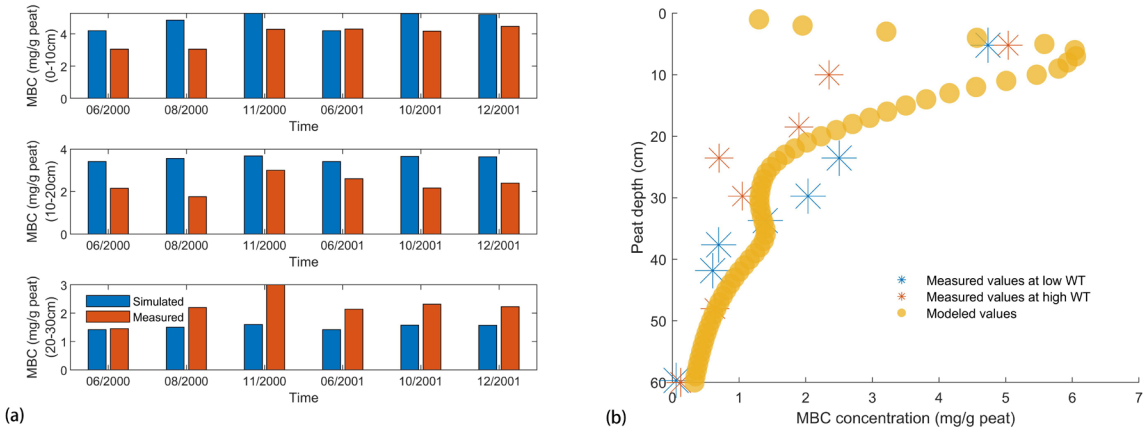

Figure 3.4 (a) Measured and simulated monthly MBC in top 30cm of the peat profile. (b) Measured and simulated MBC in the top 60cm of the peat profile.

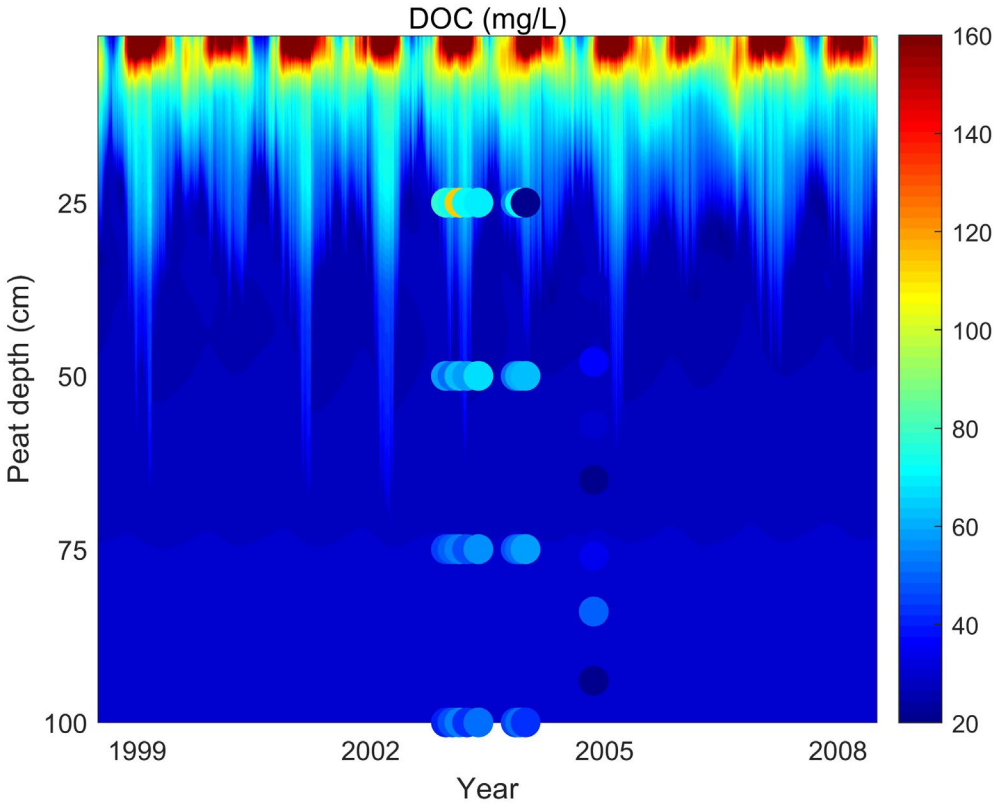

Figure 3.5 Measured and simulated DOC concentration in top 100cm of the peat profile.

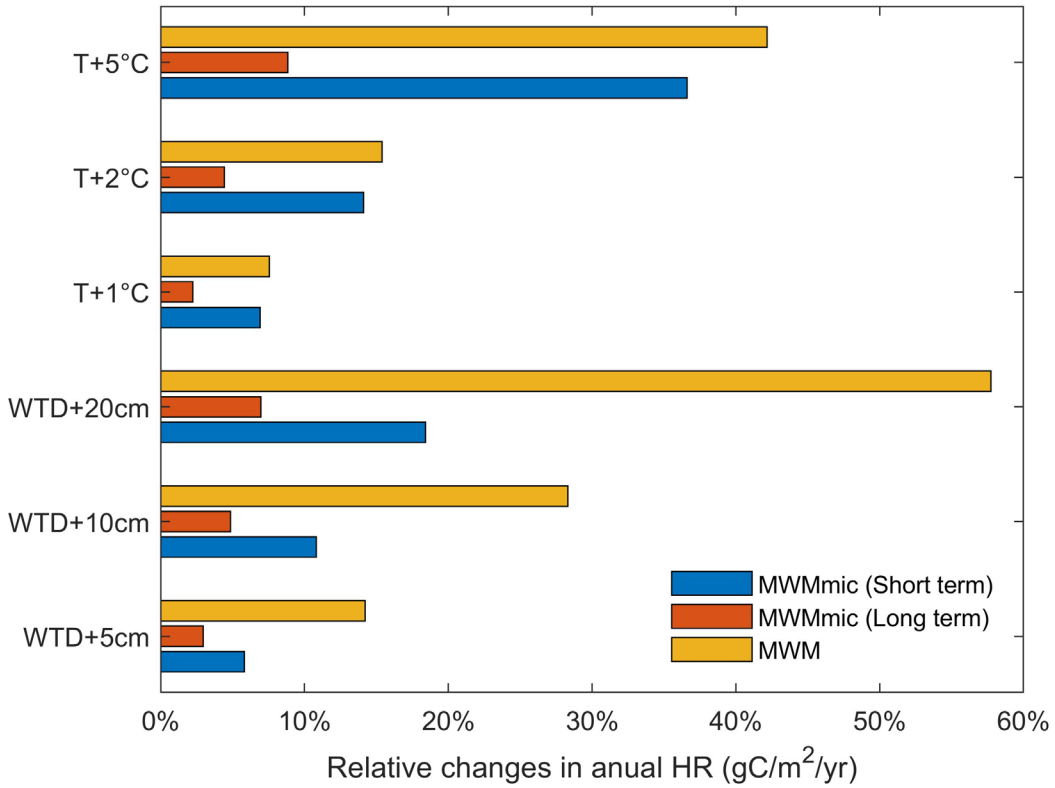

Figure 3.6 The sensitivity of simulated HR to changes in environmental parameters (water table depth and temperature) in the short term (16 years) and long term (64 years), expressed in percent change relative to the baseline simulation. The sensitivity of the original MWM to changes in environmental variables was obtained from St-Hilaire et al. (2010).

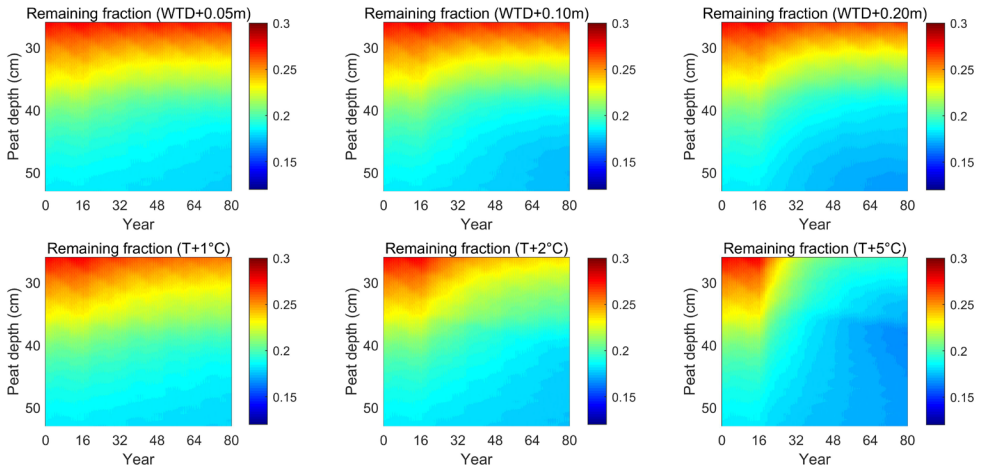

Figure 3.7 Changes in cohort remaining fraction within the 20–30 cm depth segments from simulations with different environmental parameter changes starting from 17th year.

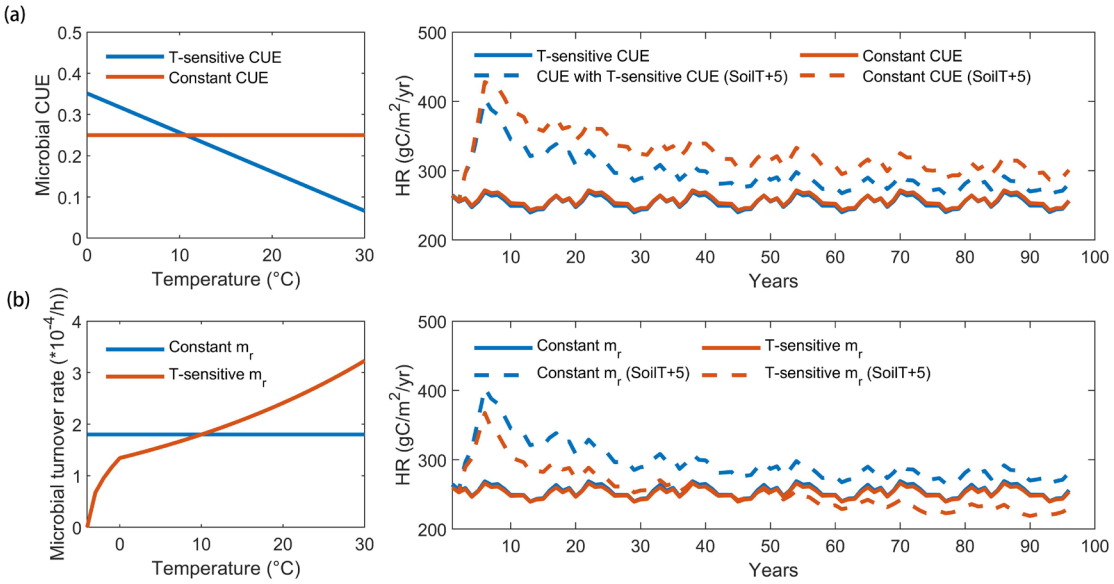

Figure 3.8 (a) The left panel: two different CUE's sensitivities to temperature and the right panel: separated trajectories (5-year moving window) of HR's sensitivity to WTD increase resulted from the different temperature sensitivities of CUE. (b) The left panel: two different microbial turnover's sensitivities to temperature and the right panel: separated trajectories (5-year moving window) of HR's sensitivity to WTD increase resulted from the different temperature sensitivities of microbial turnover.

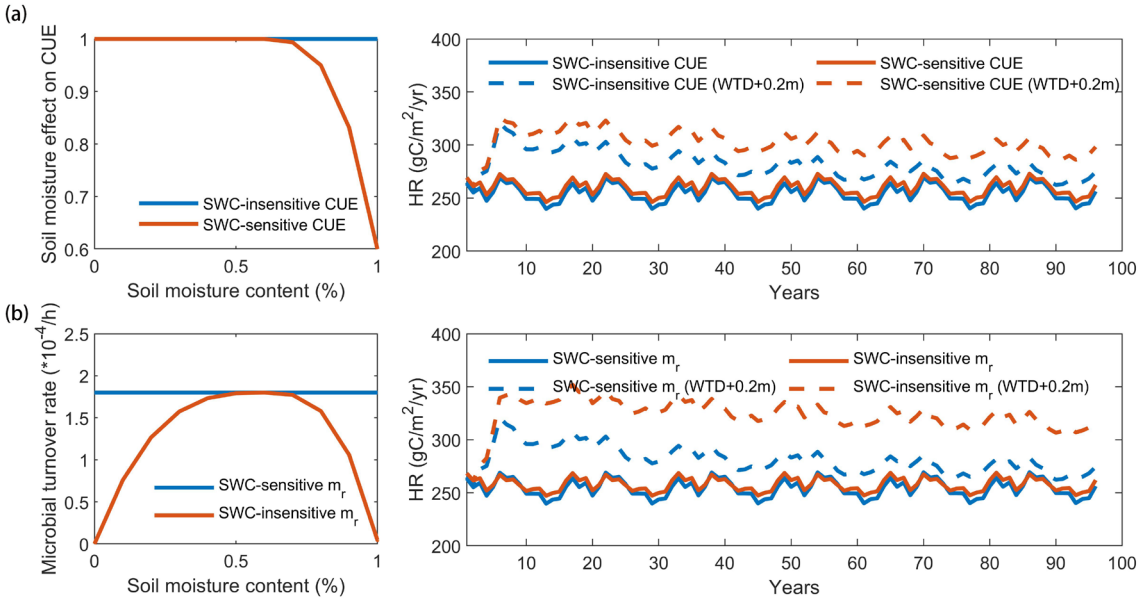

Figure 3.9 (a) The left panel: two different parameterizations of CUE's sensitivity to SWC and the right panel: separated trajectories (5-year moving window) of HR's sensitivity to WTD

increase resulted from the different SWC sensitivities of CUE. (b) The left panel: two different parameterizations of microbial turnover's sensitivity to SWC and the right panel: separated trajectories (5-year moving window) of HR's sensitivity to WTD increase resulted from the different SWC sensitivities of microbial turnover.

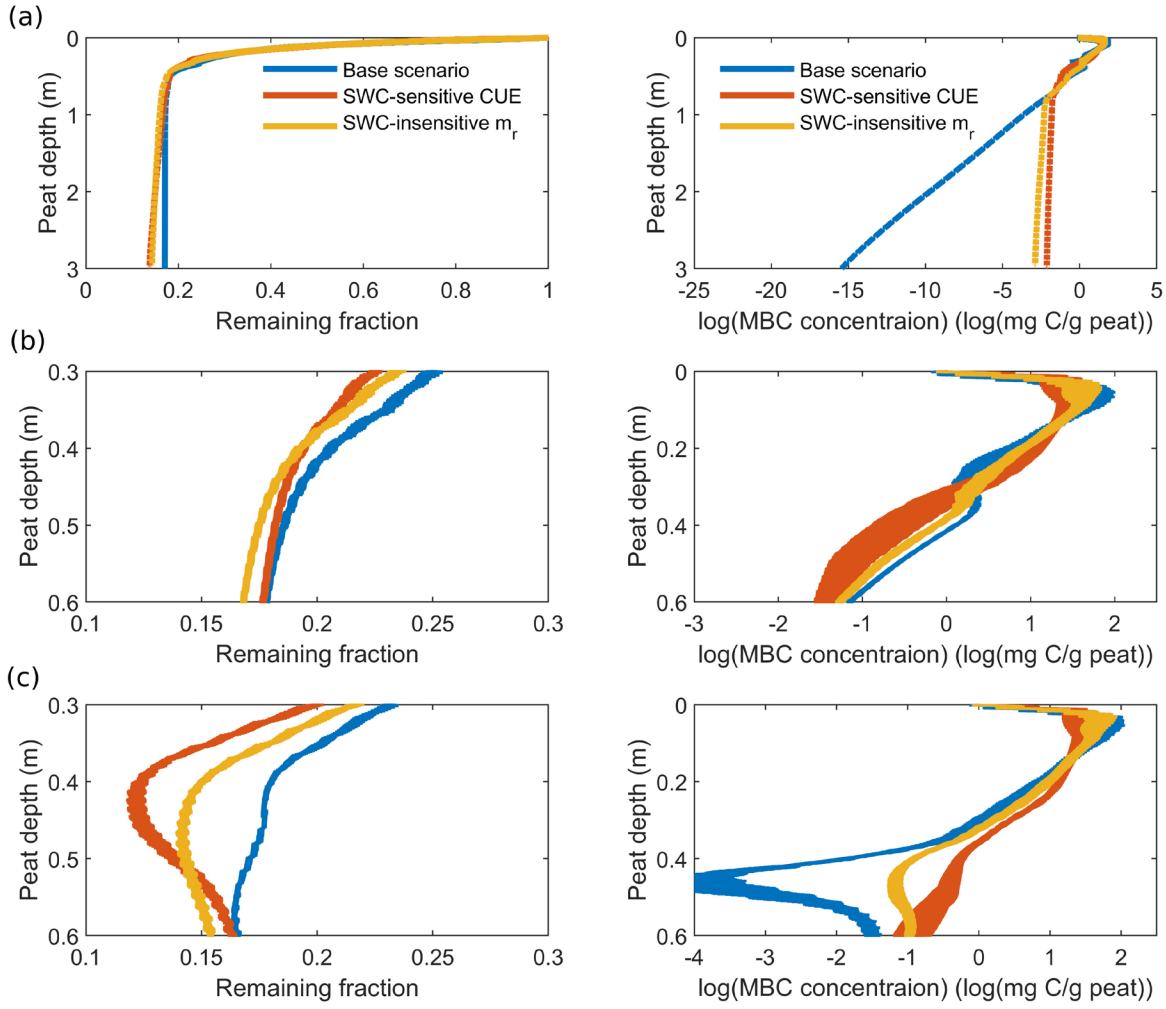

Figure 3.10 (a) 0-3m peat profiles of MBC concentration and cohort remaining fraction generated from different models. (b) 0.3-0.6m peat profiles of MBC concentration and cohort remaining fraction generated from different models. (c) 0.3-0.6m peat profiles of MBC concentration and cohort remaining fraction generated from different models subjected to WTD increase by 20cm. Blue line represents the original MWMmic; red line represents the 'SM-sensitive CUE' model with its death function multiplied by $(density/180)^{0.5}$; yellow line represents the 'SM-insensitive m_r' model with its death function multiplied by (density/180).

3.8. Supplementary materials

1. Temperature and moisture multiplier adopted in MWMmic

We adopted the same functions of temperature and moisture multiplier from PCARS (Frolking et al., 2002):

The temperature modifier was a simple exponential function (Q10 = 2) for positive temperatures and fell to zero when soil temperature dropped below Tmin as

$$f(T) = 0 \qquad T<Tmin$$

$$f(T) = \frac{T-Tmin}{|Tmin|} \qquad Tmin < T < 0\,^oC, \qquad \text{(S1)}$$

$$f(T) = Q10^{T/10} \qquad T> 0\,^oC$$

Where Tmin is set to -4 ^oC for heterotrophic metabolism

The moisture multiplier fd (Wi), was set to 1.0 at peat SWC of 0.6, declined linearly to zero as peat dessicated, and fell to a low, nonzero rate, fanox (0.025), as peat saturated. The deep peat anaerobic decomposition rate fanox, was reached either at the bottom of the root zone, if the roots penetrated below the water table, or 0.05 m below the water table and persisted to the bottom of the peat profile.

$$Z^* = max\,(zroot\,,\, zwt + 0.05) \qquad \text{(S2)}$$

$$fanox^* = fanox + \left(\frac{1-fanox}{2}\right)\left(\frac{z^*-z}{z^*-z_{wt}}\right) \qquad z_{wt}<z<z^*$$

$$fanox^* = fanox \qquad z>z^* \qquad \text{(S3)}$$

$$f(SWC) = 1 - \left(\frac{0.6-SWC}{0.6}\right)^5 \qquad SWC < 0.6$$

$$f(SWC) = 1 - (1- fanox^*)\left(\frac{SWC-0.6}{1.0-0.6}\right)^3 \quad SWC > 0.6 \qquad \text{(S4)}$$

2. Functions adopted in experiments of T and SWC sensitivity

Differences between Base Scenario and T-insensitive CUE and T-sensitive m_r scenario:

Base Scenario is the current setting adopted in MWMmic that includes “T-sensitive CUE” and “T-insensitive m_r” as described in Eq. 6 and 7. For “T insensitive CUE” scenario, CUE is calibrated to be a constant number of 0.25 to match the observed MBC value. While for “T-

sensitive m_r" scenario, we adopted similar temperature multiplier as depicted in Eq. S1 but with smaller Q10 value of 1.34 obtained from Wang et al. (2013) to describe the increase in m_r with temperature increase.

Differences between Base Scenario and SWC-sensitive CUE and SWC-insensitive m_r scenario: Base Scenario is the current setting adopted in MWMmic that includes "SWC-insensitive CUE" and "SWC-sensitive m_r" as described in Eq. 6 and 7. For "SWC-sensitive CUE" scenario, a similar soil moisture multiplier applied in Eq. 2 with fanox modified to 0.6, representing 40% decrease in the overall CUE when the environment became entirely anoxic, as found in Šantrůčková et al. (2004). Šantrůčková et al. (2004) argue that the surplus assimilated C does not contribute to microbial biomass growth due to increased anoxia but becomes DOC exudates from microbes instead of CO2 efflux. We did not include the effect of drought on CUE since we want to focus on the effect of anoxia which is characteristic of peatlands in this study. In SWC-insensitive m_r scenario, mr is set at a constant number of 0.00018 hr^{-1} (Table 1).

The density-dependent death functions calibrated for "SWC-sensitive CUE" and "SWC-insensitive m_r" scenarios are depicted in Eq. S5 and S6 respectively:

$$Death = Death * \left(\frac{Density}{180}\right)^{0.5} \qquad \text{(S5)}$$

$$Death = Death * \left(\frac{Density}{180}\right)^{1.0} \qquad \text{(S6)}$$

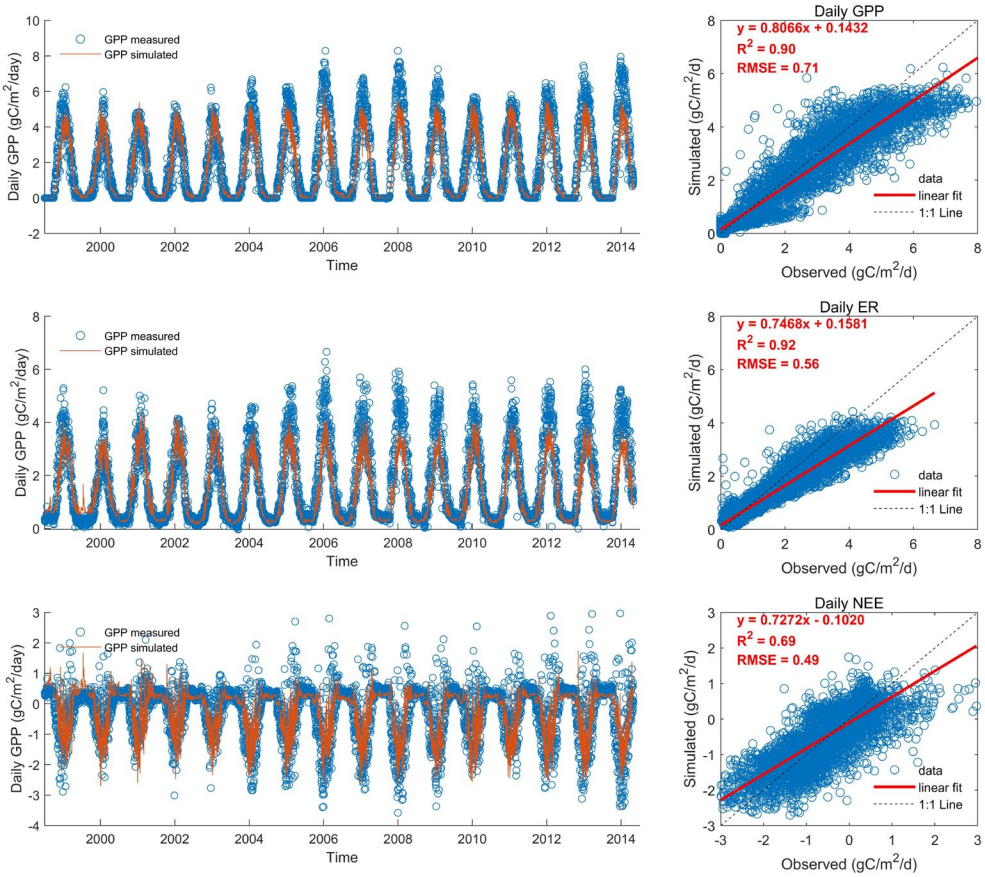

Figure S3.1 (a)Time series of observed and MWM-simulated daily GPP, ER and NEE. (b) Linear regression of observed and MWM-simulated daily GPP, ER and NEE.

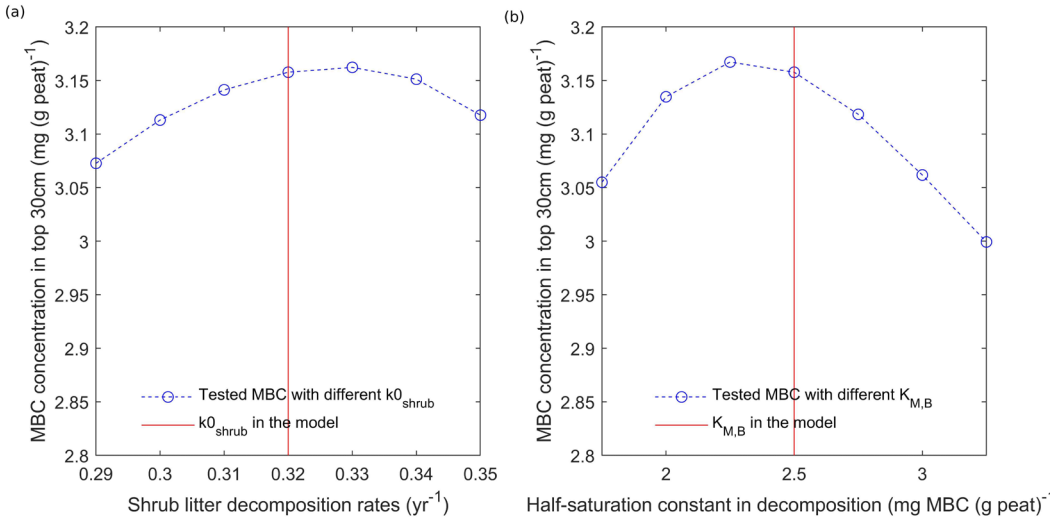

Figure S3.2 (a)MBC concentration generated with different litter decomposition rates (b) MBC concentration generated with different half-saturation constant in decomposition.

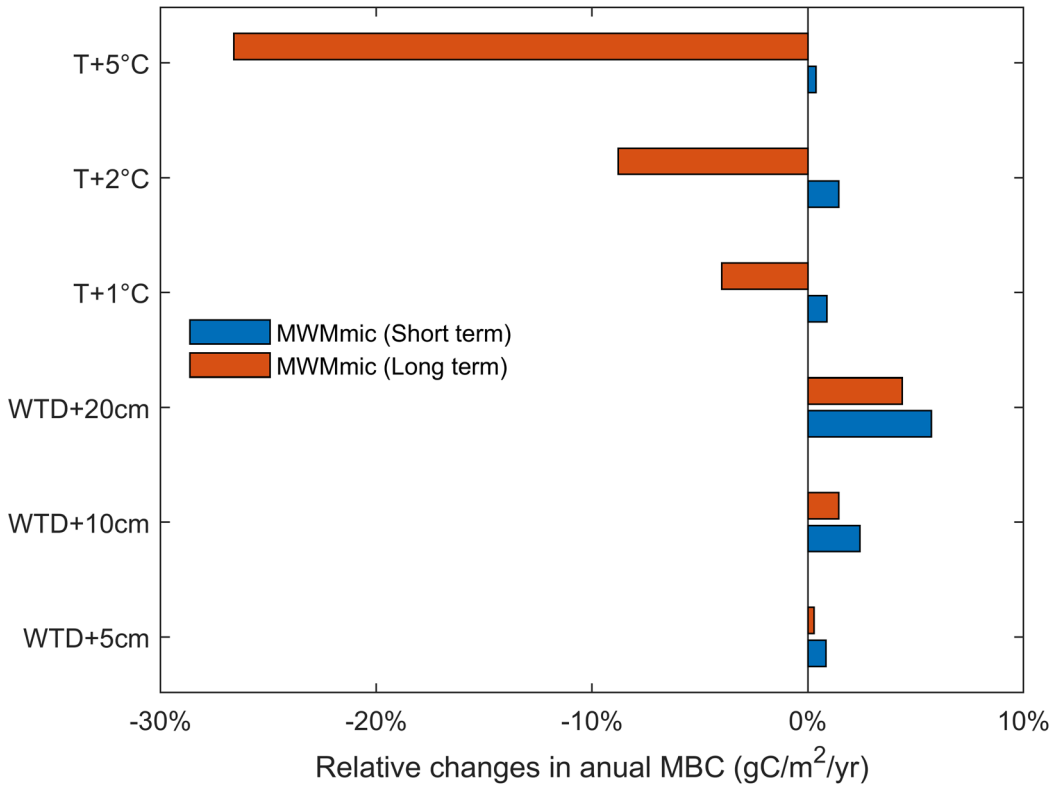

Figure S3.3 The sensitivity of simulated MBC to changes in environmental parameters (water table depth and temperature) in the short term (16 years) and long term (64 years), expressed in percent change relative to the baseline simulation.

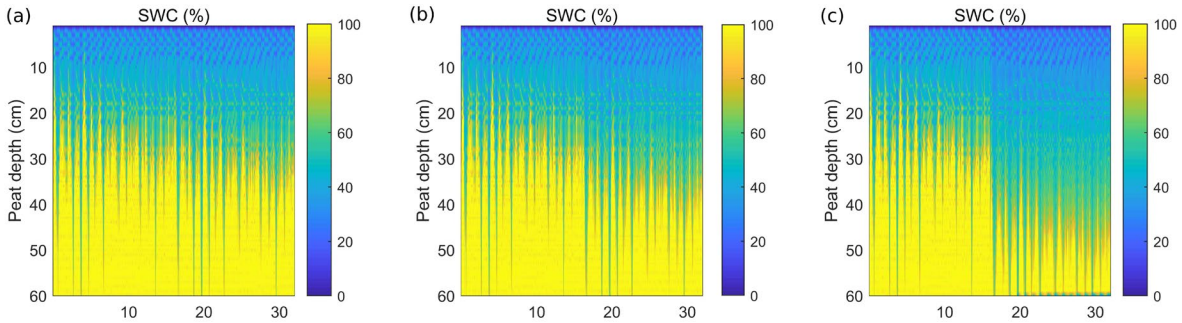

Figure S3.4 Dynamics of peat SWC profiles in the WTD manipulation experiments: (a) WTD increased by 5cm; (b) WTD increased by 10cm; (c) WTD increased by 20cm. All disturbances were introduced in the 17th year.

Chapter 4. A Mycorrhiza-mediated Carbon, Nitrogen and Phosphorus Cycling Model to Simulate Peatland's Response to Nutrient Fertilization

Bridging statement to Chapter 4

Increased nutrient deposition could induce significant changes in the bog's vegetation composition and C sink functions. The response of bog shrubs to increased nutrient input is mediated by its associated mycorrhizal fungi. However, very limited efforts have been made in incorporating either nutrient cycles or mycorrhiza fungi into peatland models, hindering our ability to understand the effect of increased nutrient deposition on peatlands. In this chapter, I further modify the MWMmic from Chapter 3 to MWMmic_NP by introducing N and P cycles, and metabolisms of ericoid mycorrhiza fungi. MWMmic_NP was evaluated against the extensive measurements from the Mer Bleue Bog, and the long-term fertilization experiments there. I test whether the new model could reproduce the C-N-P dynamics observed at the bog and examine the importance of mycorrhiza fungi in regulating the bog's response to increased nutrient deposition. The model was also used to explore the potential role of plant-mycorrhiza fungi association in maintaining the C sink function of ombrotrophic peatlands. Chapter 4, along with Chapter 3, paves the way for investigating the significance of microbe-mediate nutrient cycles in regulating the bog's C cycle in Chapter 5.

4.1. Abstract

Ombrotrophic peatlands, also known as bogs, are featured by nutrient-poor conditions. Ericaceous evergreen shrubs adapt to this harsh condition by developing organic nutrient acquisition strategies mediated by ericoid mycorrhizal fungi. However, nutrient cycles and mycorrhizal associations have been ignored in current peatland models. This has precluded accurately simulating the nutrient limitation in ombrotrophic peatlands and predict their response to disturbances such as increased nutrient deposition. To address this issue, we further developed the peatland model MWMmic into MWMmic_NP by incorporating: nitrogen and phosphorus cycles, and the metabolic activities of ericoid mycorrhizal fungi. The new model was used to simulate the carbon-nitrogen-phosphorus cycles at Mer Bleue, a

raised ombrotrophic bog located in southern Ontario Canada, and their responses to increased nutrient input. Overall, the model performed well in simulating the biogeochemical cycles in the Mer Bleue bog and reproducing its response to elevated nutrient input as observed in the fertilization experiment. In the simulated system, greater availability of inorganic nutrients with fertilization diminishes the role of mycorrhizal fungi in plant nutrient uptake. This declined mycorrhizal uptake led to more efficient carbon allocation in evergreen shrubs and ultimately remarkable changes in the bog's vegetation composition and carbon cycle. The model was also used to explore the potential role of plant-mycorrhiza fungi association in maintaining the nutrient-depleted environment of ombrotrophic peatlands. In conclusion, nutrient cycles and mycorrhizal activities, which have been overlooked in past peatland modeling studies, could play a significant role in understanding ombrotrophic peatland's biogeochemical cycles and its response to environmental disturbances.

4.2. Introduction

Peatlands stored about one third of global soil carbon (C) (Yu et al., 2012; Nichols and Peteet, 2019; Hugelius et al., 2020) due to a C imbalance between plant production and peat decomposition over millennia (Roulet et al., 2007). Ombrotrophic peatlands, also known as bogs, are peatlands that receive all their water and nutrient inputs from the atmosphere (Charman, 2002). They are often characterized by nutrient scarcity (Thormann and Bayley, 1997; Vitt, 2006; Walbridge and Navaratnam, 2006; Wang et al., 2018) and are therefore, dominated by low-productivity plant communities that are adaptive to this nutrient poor environment including ericaceous shrubs and *Sphagnum* mosses (Bubier et al., 2011; Wang and Moore 2014). This prevalence of nutrient limitation in bogs make them potentially sensitive to enhanced nutrient availability, as large amounts of active nitrogen (N) (Neff et al. 2002, Galloway et al. 2004, Dentener et al. 2006) and phosphorus (P) (Tipping et al., 2014; Brahney et al., 2015) have been added into the environment in the past decades by human activities. Given the large C storage in the ombrotrophic peatlands (Tarnocai, 2006; Loisel et al., 2014), it is important to understand how they respond to increased nutrient availability.

Several long-term peatland fertilization experiments have been established to address this question (Bubier et al., 2007; Bragazza et al., 2012; Sheppard et al., 2013; Wieder et al.,

2019). Significant increase in vascular plant biomass and decrease in the abundance of *Sphagnum* mosses are often reported in these fertilization experiments (Bubier et al., 2007; Juutinen et al., 2010; Bragazza et al., 2012; Larmola et al., 2013; Levy et al., 2019). The dramatic shift in vegetation composition led to greater labile litter input into the peat, which often resulted in a diminished C sink for peatlands after fertilization (Bubier et al., 2007; Moore et al., 2007; Bragazza et al., 2012; Larmola et al., 2013). Suppressed moss growth with increased nutrient input has been related to the direct effect of increased respiratory cost (Juutinen et al., 2016) and nutrient imbalance (Bragazza et al., 2004), or indirectly through increased shading from the taller shrubs (Chong et al., 2012). But how bog shrubs enhanced their growth with increased nutrient availabilities have yet to be clarified. In contrast to the common view that the plant photosynthetic capacity is constrained by the leaf N (Kattge et al., 2009) and P content (Walker et al., 2014), empirical measurements found that the bog shrub photosynthetic capacity does not increase with elevated N and/or P inputs (Bubier et al., 2011; Currey et al., 2011). It is proposed that these bog plants have adapted to the nutrient scarcity and do not allocate their excess nutrient content to photosynthetic processes, which is also identified in plants of other nutrient-poor environments (Shaver and Laundre, 1997 Whitehead et al., 1997). Therefore, mechanisms driving the increase of bog plants with fertilization remained to be explored.

One theory that could offer explanation is that shrubs with elevated nutrient availability may shift their C fluxes away from belowground nutrient acquisition towards aboveground productivity to acquire other limiting resources like light (Bloom et al., 1985; Eastman et al., 2021). To cope with the nutrient scarcity in the bog, ericaceous shrubs form a symbiont association with Ericoid Mycorrhiza fungi (ERM) (Smith and Read, 2010), where shrubs invest a great amount of their photosynthetic C to ERM in exchange for nutrients, as ERM fungi can access organic N and P from recalcitrant substrates via a large variety of degradative enzymes (Perotto et al., 2018, Martino et al., 2018). This C-costly mycorrhiza transfer has been identified as the major nutrient source for ericaceous shrubs in the ombrotrophic peatlands (Bragazza et al., 2012; Gavazov et al., 2016). Recent findings gave support to the 'decreased C allocation to ERM' theory: peatland shrubs were found to shift their N sources away from

mycorrhiza transfer towards direct root uptake with fertilization (Vesala et al., 2021) and increased N and P availability could lead to dramatic reduction in the richness of ERM fungi community (Van Geel et al., 2020). Despite the new evidence, empirical studies have rarely quantified the C allocation scheme of bog shrubs (Currey et al., 2011) and no study has quantified the shrub-ERM C-nutrient exchanges in peatlands due to measurement difficulty. Thus, large knowledge gap remains in understating the ERM-shrub interaction and its role in mediating the peatland's response to fertilization.

Models are useful tools to explore possible interactions and feedbacks within a system. Considerable progress has been achieved in incorporating mycorrhizal fungi into the process-based biogeochemical models for investigating the significance of plant-mycorrhiza fungi interaction. Some models adopt a simple way of using environmental indicators to quantify the C cost of mycorrhiza nutrient acquisition (Brzostek et al., 2014; Shi et al., 2016; Fatichi et al., 2019) while others simulate the metabolic processes of mycorrhiza fungi thus representing the plant-mycorrhiza interaction in a more mechanistic way (Sulman et al., 2017, 2019; He et al., 2018, 2021). Nevertheless, no such effort has yet been made in peatland modeling studies. Despite the tremendous amount of peatland models being developed in the recent decade (St-Hilaire et al., 2010; Wu et al., 2016; Qiu et al., 2018; Chaudhary et al., 2020), only a handful of those models have incorporated N cycle (Heijmans et al., 2008; Spahni et al., 2013; Wu et al., 2013; S. Wang et al., 2016) and just one of them explicitly simulated P cycles (Salmon et al., 2021) whereas none considered mycorrhizal processes. PEATBOG was the only model that is used to investigate the peatland responses to long-term fertilization (Wu et al., 2015). Although PEATBOG reproduced the overall vegetation response, it also generated results that contradicted empirical evidence like high N mineralization rates and high inorganic N uptake for shrub roots in the bog, which may result from the lack of mycorrhizal role in the model's structure. Furthermore, the lack of P cycle in the model also brings uncertainties as P drives peatland N_2 fixation (Toberman et al., 2015) and mediates the peatland's response to increased N availability (Limpens et al., 2011; Fritz et al., 2012). Thus, there is a clear need for incorporating mycorrhiza-mediated NP cycles into peatland models to make accurate projections of peatlands' response to enhanced nutrient input.

To address this need, we explicitly incorporated ERM-mediated N and P cycles into the established peatland model MWMmic to develop MWMmic_NP and applied the new model on the Mer Bleue bog where a long-term fertilization experiment is established. The major objective of the study was to investigate the potential role of ERM in mediating the response of ombrotrophic peatlands to elevated nutrient deposition. We first evaluated the model's ability to simulate the C-N-P cycles against measurements for the well-characterized Mer Bleue bog (MB). Then we tested if the model could reproduce the response of MB bog observed in the twenty-year fertilization experiments, and examined the feedbacks and interactions occurred within the system. We also explored the potential significance of ERM in regulating the bog's biogeochemical cycles using a theoretical exclusion experiment and proposed a mycorrhiza perspective in understanding the bog's biogeochemical cycling.

4.3. Materials and Methods

4.3.1. Model description

The McGill Wetland Model is a process-based model that simulated the C dynamics in northern peatlands (St-Hilaire et al., 2010). Two dominant plant functional types (PFTs) in bogs: *Sphagnum* mosses and evergreen shrubs are included in the bog version of the model. C enters the system through the plant photosynthesis and leaves the system via either autotrophic respiration (AR) or heterotrophic respiration (HR), i.e., peat decomposition. We have developed MWMmic based on the MWM by incorporating cohort tracking, microbial dynamics, and solute transport to explicitly simulate the controls of substrate quality and microbial activities on peat decomposition (Shao et al., 2021, in review). The current study extends the C-only MWMmic model with the addition of mycorrhizal-mediated nutrient cycles to produce the new MWMmic_NP model (Figure 4.1, Text S1, Table S1). A brief overview of the explicit treatment of N and P dynamics in MWMmic_NP is given in the following subsections, and a full description is given in Text S1. Following key assumptions were made during the model development.

1) Leaf-level photosynthesis is unrelated to leaf nutrient content. This contradicts the assumption applied in most nutrient cycling models that photosynthesis rates correlate

positively to plant nutrient content (Zaehle et al., 2013; Ghimire et al., 2016). However, empirical studies have found the photosynthetic capacity of ericaceous shrubs in bogs do not respond to changes in nutrient availability (Bubier et al., 2011; Currey et al., 2011). It was proposed that plants that thrive in nutrient-limited ecosystems have adapted to this environment and are unable to utilize the additional nutrients to boost photosynthesis.

2) Saprotrophic microbes regulate their P turnover rates based on P availability. P is tightly recycled within the bog ecosystem, much more so than N. Unlike N, which has two pathways to enter the bog (atmospheric deposition and N_2 fixation), P in the bog comes solely from atmospheric deposition. The discrepancy between the microbial N content and peat N content is significantly greater than that between the microbial P content and peat P content (Wang et al., 2014). Thus, soil microbes in the bog, driven by stoichiometric homeostasis, may rely more heavily on recycling to meet its P demand compared to N and C (Spohn, 2016b), which is also shown in other P-limited ecosystems (Spohn and Widdig, 2017; Chen et al., 2019). Here we assume that saprotrophs decrease their P turnover rates when their C:P ratios are high to simulate stronger P recycling when P is limiting.

3) Water table depth constrains the rooting depth of ericaceous shrubs. Shrub roots cannot penetrate deeper than the water table as they are lacking in well-developed aerenchyma (Kozlowski, 1997). Therefore, root growth below the water table is prohibited in MWMmic_NP. The distribution coefficients of root growth are parameterized using empirical relationships derived from measurements (Murphy et al., 2009, 2010) and used to determine the limitation of high water table (WT) on root growth (see Section 2.1.2 and Text. S2.2.2). Root growth in the model mostly occurs during the growing seasons, so do the changes in root distribution. Thus, we are confident with the use of empirical relationships derived from growing-season WTD and root distribution (Murphy et al., 2009, 2010). The C that cannot be allocated to root growth because of high WT limitation is directed to the C reserve pool within the shrub and could be transferred to ERM fungi when the C reserve is over-accumulated. Thus, we assume the shrubs also resort to ERM fungi for nutrient uptake when its root growth is limited by high WT.

4) Nutrients do not impact decomposition through direct amelioration of peat litter

quality. It is often found that increased N content in the litter enhances the initial rates but decreases the later rates of decomposition (Bragazza et al., 2006; Bubier et al., 2007). This effect, however, is not considered in this model, which could lead to some uncertainties in simulating changes in decomposition with fertilization. But for the purpose of this study, we believe the increased nutrient availability mainly affects the peat decomposition through directly alleviating the nutrient limitations for saprotrophs and indirectly through changes in vegetation composition and litter types (Larmola et al., 2013), which are both included in the model.

5) Several key nutrient processes are also not explicitly modeled here: nitrification and denitrification are not included in the model because of the occurrence of their low rates at the acidic Mer Bleue Bog (Rattle, 2006; Wang et al., 2018). P weathering and occlusion of P into mineral surfaces are also not considered because of the scarcity of minerals in peat soils. Sorption of dissolved inorganic and organic phosphorus into peat is not explicitly described but are accounted for by a reduced mobility in water (Eq. S16(b)).

Soil nutrient dynamics

Parameterization of soil C dynamics is described in detail in Shao et al. (2021) (in review). Soil organic nitrogen and phosphorus (SON and SOP) dynamics are assumed to follow the soil organic carbon (SOC) dynamics in accordance with the specific C:N and C:P ratio of a given pool. Dissolved organic N and P (DON and DOP) are produced from the depolymerization of the SON and SOP that is regulated by the biomass of Saprotrophic microbes (SAP) with "reverse Michaelis-Menten" kinetics (Eqs. S1-S4) (Dashed line in (Figure 4.1(a)). SAPs in our model can have a flexible stoichiometric ratio within a prescribed range. They assimilate nutrients through DOM uptake with a certain fraction of N and P (mic_{NUE} and mic_{PUE}) being incorporated into biomass and the other fraction being mineralized into DIN and DIP pools (Eq. S6). SAPs could also immobilize nutrients from the DIN and DIP pools to fulfil their stoichiometry needs (Eqs. S7(a-b)). Suppression functions for immobilization (Eqs. S7(c-d)) are introduced to gradually decrease the immobilization when the SAP nutrient content approached its maximum. Nutrient limitation for SAP occurs when its nutrient acquisition is

unable to meet the minimum nutrient demand. That leads to C overflow as a form of increased microbial respiration (Eq. S8(a)). On the other hand, N or P overflow could also happen as another form of mineralization when microbial nutrient content exceeds their stoichiometric constraints (Eq. S8(b-c)). When SAP dies, the nutrients with SAP turnover are assumed to be allocated evenly between dissolved organic nutrient and soil organic nutrient pool. To account for scarcity of P availability in ombrotrophic peatlands, microbial P is assumed to have a smaller turnover rate than C and N to simulate the recycling of P upon microbial turnover (Spohn 2016b; Spohn and Widdig, 2017). This microbial P resorption is down-regulated gradually to zero when the microbial nutrient content approached its maximum boundary (Eqs. 14(d-e)).

Plant nutrient dynamics

Plant nutrient dynamics in each structural pool follow the C dynamic and the stoichiometry of the corresponding pool. Shrub allocated its newly fixed C from photosynthesis to leaves and fine roots first following 1:1 ratio. C allocation to woody tissue (stems and coarse roots) only takes place when the maximum leaves or fine roots has been attained (Parton et al., 2010) based on a prescribed allometric relationships among biomass components (Eq. S20) (Murphy et al., 2009). Roots of ericaceous shrubs cannot penetrate deeper than the water table thus a dynamic root distribution is set here to account for this constraint on shrub root growth (Eq. S21). Distribution coefficients of shrub roots are updated with water table depth (WTD) on a monthly basis. To account for the limitation of high WT on root growth, the portion of C that is 'supposably' used for root growth underneath the WT based on the distribution coefficients is reallocated to the C reserve pool. Stoichiometric ratios of different structural pools are flexible within a prescribed range (Eqs. S22(c-d)) (Zaehle et al., 2010), allowing the stoichiometry of plants to change with nutrient availability. Nutrients leave the plant through litter production that is related to the fixed turnover rates of each plant structural pool and their stoichiometric ratios. A constant fraction of nutrient is being resorbed from the litter production back to the plants and gets stored in a reserve nutrient pool (Eqs. S28-S29).

Different nutrient acquisition pathways are prescribed for shrubs and mosses: shrubs can take up nutrients through direct root uptake from the DIN/DIP pool (Eq. S30), or through mycorrhiza mining from the SON/SOP pool (Eq. S45), while mosses get their nutrients from atmospheric deposition (Eq. S34) and direct adsorption from DIN/DIP within shallower depth (Eq. S30). Mosses could also fix N_2 as additional N source (Eqs. S35-S36). How MWMmic_NP handles the competition for nutrient uptake between different vegetation and microbial communities is given in detail in Text. S4. Once taken up, the nutrients are first stored in the plants' reserve nutrient pool and used later to construct biomass of different plant structural pools (leaves, stems, fine roots, and coarse roots). Several feedback mechanisms exist in the model to regulate the plant CNP dynamics: A maximum level for nutrient reserve pool is set up to down-regulate the nutrient uptake to prevent excessive nutrient storage within the plants (Eq. S31) (Zaehle et al., 2010; Yang et al., 2014). On the other hand, once the nutrient reserves in plants could not meet the demand for biomass building or the high WT limits the building of root biomass, the surplus C that is unable to be converted into biomass will be directed to the C reserve pool (Eq. S27, Eq. S38). The C in this reserve pool could be transferred to the ERM in exchange for nutrients, which will be described below in more detail.

Ericoid mycorrhiza fungi

Shrub transfers surplus C from its C reserve pool to ERM and root exudation when the level of C stored in the reserve pool is beyond the threshold level (Eq. S39). The rate of the transfer is determined by the maximum value of nutrient stress (Eq. S31) that is calculated by comparing the reserve nutrient pool to a target value equivalent to double the leaf and fine root nutrient content (Sulman et al., 2019). The C transfer is partitioned between ERM pathway and root exudation with a fixed coefficient (Eq. S40).

ERM converted the C transferred from shrubs into its own biomass with a constant C use efficiency (Eq. S42), and the remaining C is emitted as CO_2 (Eq. S52). ERM is parameterized with a fixed turnover rate at 0.0001 hr^{-1} (Eq. S54), which is assumed to be much slower than the free-living saprotrophs (Sulman et al., 2019). ERM could acquire nutrients through two pathways: organic nutrient mining and inorganic nutrient uptake. ERM could directly mine

organic nutrient from the soil organic nutrient pool, which is described using a function similar to that used in the SAP biomass-regulated depolymerization (Eq. S45). The rates prescribed for ERM organic nutrient mining are larger than the SOM depolymerization rates prescribed for SAP, manifesting the superior capacity of ERM in accessing nutrients from recalcitrant organic compounds in strongly acidic peat environment. ERM is also prescribed with a capacity to take up nutrients from inorganic pool (Eq. S47), similar to that of shrubs' roots. The nutrients acquired by ERM are first stored in an intermediate pool, which also takes the nutrients resorbed from ERM turnover (Sulman et al., 2019). Priority is given to ERM to extract nutrients from this intermediate pool to fulfill its own nutrient needs (Eqs. S50-S52). After ERM's own usage, the remaining nutrients stored in this pool are transferred to shrubs at a rate regulated by the size of the intermediate pool (Eq. S59). The smaller the inter mediate pool is, which suggests a high nutrient stress for ERM, the smaller the nutrient transfer rate is to preserve more nutrients within the ERM.

4.3.2.Site description and datasets

The Mer Bleue bog (MB), located 10 km east of Ottawa, Ontario, Canada (45.41°N, 75.48°W, 69m above mean sea level), is a raised acidic ombrotrophic bog of 28 km with dominant vegetation of ericaceous shrubs and *Sphagnum* mosses and sparse coverage of sedges (Bubier et al., 2006). The peat depth is around 5-6m near the center to less than 0.3m at the margins (Roulet et al., 2007). The 30-year (1971–2000) mean annual air temperature is 6.0°C and annual mean precipitation is 943 mm (http://climateweatherofficeecgcca/climate_normals (2018)). The N deposition for the Mer Bleue area is estimated to be 0.4–1.6 gN m^{-2} yr^{-1} (Moore et al., 2004) and P deposition is estimated to fall in the range of 7 to 34 mgP m^{-2} yr^{-1} (Newman, 1995; Tipping et al., 2014; Wang et al., 2015).

A fertilization experiment was established in 2000 and was continued to the present (Bubier et al., 2007), where the N loads were applied as equivalent to 5, 10, and 20 times the ambient wet summer N deposition at 1.6gN m^{-2} yr^{-1}, 3.2 gN m^{-2} yr^{-1} and 6.4gN m^{-2} yr^{-1} respectively, with or without ample phosphorus (5.0 gP m^{-2} yr^{-1}) and potassium (6.3 gK m^{-2} yr^{-}

^{1}). Based on the fertilization level, the treatments with only N are referred to as 5N, 10N and 20N, while ones with NPK additions are referred to 5NPK, 10NPK, 20NPK, and ones with only PK addition are referred to as PK. Treatments with deionized water to serve as baseline are referred to as Control.

The current input variables for the stand-alone version of the MWMmic_NP are annual N deposition, annual P deposition, net radiation, photosynthetic photon flux density, precipitation (rain or snow), water table depth (WTD), air and soil temperature, relative humidity, wind speed, atmospheric pressure, and air CO_2 concentration. The input annual N and P deposition level are derived from literature at 0.8 gN m^{-2} yr^{-1} and 30 mgP m^{-2} yr^{-1} respectively. The remaining hourly meteorological input data is from the MB flux tower dataset (https://daac.ornl.gov/FLUXNET/guides/FLUXNET_Canada.html). The observed daily C flux data also from the tower dataset is adopted here for model evaluation. We also collected the C fluxes and vegetation data measured in the fertilization plots using the method described in Bubier et al. (2007) and Larmola et al., (2013). Other data sets for model calibration and evaluation were obtained from a range of the published literature, including the peatland vegetation distribution (Bubier et al., 2006, 2007; Murphy et al., 2009, 2010; Juutinen et al., 2010; Larmola et al., 2013), peatland stoichiometry from plant to peat (Wang and Moore 2014; Wang et al., 2014; M. Wang et al., 2016), microbial communities (Basiliko et al., 2005, 2006; Xing et al., 2011), porewater chemistry (Fraser et al., 2001; Rattle, 2006; Moore et al., 2019) and specific biogeochemical processes (Wang et al., 2018; Živković, 2019).

4.3.3.Model evaluation and sensitivity analysis and experiments

For every model experiment. we first spin up the model to construct our initial peat profile and vegetation biomass. The spin-up was conducted by repeatedly using a 16-year meteorological data (from 1998 to 2014) for over thousands of years until the model's state variables reached quasi-equilibrium. The initial peat depth starts at zero, which means the whole peat profile is built with the simulated 16-year C accumulation rates during the spin-up. The decomposition started to plateau after a period longer than 800 years, with the inert peat in deep catotelm producing little HR. A spin-up run over 8000 years could 'generate' a

peat depth over 4.6m deep. The outputs generated from the last 16 years of model runs are deemed as simulated results.

Model calibration and evaluation

New parameters in the model are either calibrated or directly derived from literature (Table 1S). The model was first constructed and calibrated for N and then we repeated the process for P. Calibration for both nutrient modules was conducted in three steps, we first calibrated the model to match the peat stoichiometry profile by calibrating the saprotrophic microbial process and solute export; then we calibrated the model to agree with the vegetation biomass and litter production data; finally, we calibrated the ERM model to match the measured plant stoichiometry, nutrient fluxes and C fluxes data. These three processes were done iteratively, and parameter values were changed gradually until we could get a good fit to the overall observation data. Evaluation of simulated vegetation biomass, nutrient fluxes and stoichiometry were conducted by direct comparison against observations. Evaluation of simulated C fluxes were conducted using time series and goodness of fit quantified by the root mean square error (RMSE) and linear regression coefficient (R^2) (Willmott, 1982). We also compared the results from MWMmic_NP with the results from PEATBOG, the only carbon-nutrient model that had been applied in the MB bog before our work (Wu et al., 2013, 2015).

Sensitivity analysis

A one-at-a-time (OAT) sensitivity analysis is performed by modifying the selected key parameters that control important processes: SAP nutrient mineralization and immobilization (NUE_{SAP}, SAP nitrogen use efficiency; PUE_{SAP}, SAP phosphorus use efficiency; $V_{max,DIP}^{SAP}$, base rate for SAP's DIP immobilization); microbial P turnover (β_{SAP}^{Death}, reduction factor that describes the regulation of SAP P content on SAP P turnover); P biochemical mineralization ($V_{max,bcm}^{SAP}$, base rate of SAP's P biochemical mineralization; α_{SAP}^{P}, power of the N:P status regulation function on P biochemical mineralization); ERM growth and decay (CUE_{ERM}^{growth}, carbon use efficiency for ERM growth; $Deathrate_{ERM}$, ERM's turnover rate; $frac_{ERMnecro}^{moss}$, fraction of ERM necromass allocated to moss litter pool); ERM nutrient mining ($k_{Nmining}^{ERM}$, N

mining rates of ERM; $V_{max,bcm}^{ERM}$, base rate of ERM's P biochemical mineralization; $k_{Cmining}^{ERM}$, C mining rates of ERM); shrub-ERM C-nutrient exchange ($frac_{max}$, maximum ratio of shrub's reserve C pool to the size of shrub's storage organs for reserve C; $rate_{outerm}$, the rate for ERM's nutrient transport to shrubs; $rate_{out}^{shrub}$ is the base rate of the C translocation from the reserve C pool; $frac_{efflux}^{ERM}$ is the fraction of shrub's C translocation from reserve C pool that is allocated to ERM); Moss nutrient uptake (β_{moss}, the distribution parameter of mosses' virtual roots; $V_{max,DIP}^{moss}$, base rate of mosses' DIP uptake) (See Text S1 and Table S1 for more detailed parameter descriptions). Parameters were modified individually by ±15% while all the other parameters were kept at default values. The relative changes in the biomass of shrubs, mosses, SAP and ERM are examined to assess the sensitivity of model of these selected parameters.

Fertilization experiments

We simulated three nutrient addition scenarios that match the fertilization experiments of 20N, PK and 20PK to simulate the effect of N fertilization, P fertilization and NP fertilization. After an initial spin-up we increased the annual deposition of N and P by 6.4 gN m^{-2} yr^{-1} (in N and NP fertilization simulation) and 5.0 gP m^{-2} yr^{-1} (in P and NP fertilization simulation) respectively, starting from the 2nd year of our final 16-year model run (which means year 2000) to match the doses and time applied at the fertilization plots. In order to produce a continuous time series for model evaluation of the CO_2 fluxes in the fertilization, we have reconstructed the sparse Chamber measurements of half-hourly CO_2 exchange (Bubier et al., 2007; Juutinen et al., 2010) the same method applied in Wu et al. (2015) (Figure S4.4). A continuous daily C fluxes measurement data was thus constructed for model performance evaluation in the growing seasons (May-August) of 2001, 2003, 2009 and 2011 due to the abundance of the measurement taken in those years. We also converted our simulated moss biomass to moss cover using the relationship between the known moss cover and biomass data (Juutinen et al., 2010), to compare with the measured moss cover in the fertilization plot.

ERM-exclusion experiments

To further examine the potential significance of ERM symbiont, several species-exclusion

experiments were also conducted in this study. We ran the model with the same inputs described above but the growth parameters of the species we intended to remove were set to zero. The model was also spun-up for over thousands of years until the model's state variables reached quasi-equilibrium. Following this protocol, we conducted ERM exclusion, moss exclusion and moss-ERM exclusion experiment. Shrub exclusion was not described here since we have already eliminated both ERM and shrubs in the ERM exclusion experiment.

4.4. Results

4.4.1.Model performance

The model produced a large CNP storage in the peat over 4.6m deep, with C storage at 262.5 kg/m^2, N storage at 6.88 kg/m^2 and P storage at 285 g/m^2 (Figure 4.2). These numbers are consistent with long-term peat core records from Mer Bleue (Frolking et al., 2010; Moore et al., 2019). C and nutrients stored in the peat took over 98% of total storage in the whole bog ecosystem, while the catotelm storage took over 95% of the total peat storage. The simulated C and nutrient pools in the plants and microbes are also in line with the available measurements (Figure 4.3). The ericaceous shrubs are the second largest C pool in the system at 995.7 gC/m^2. In contrast, saprotrophs are the second largest pools for N and P, with the majority of the storage distributed at catotelm, especially for N. MWMmic_NP performed much better than MWMmic in simulating the size of vegetation pools (Figure 4.3(c-d)) as the new model used allometric relationships (Eq. S20) derived from measurements (Murphy et al., 2009). After accounting for nutrient limitation, SAP biomass produced by the new MWMmic_NP was also much closer to measured values compared to MWMmic (Figure 4.3(c)).

Overall, the profiles of nutrient distribution agreed well with the measurements (Figure 4.4). MWM_micNP captured the changes in peat stoichiometry with depth particularly well. The simulated peat C:N ratios decreased with depth while the peat C:P ratios and peat N:P ratios increased with peat depth, in line with the observation ((Figure 4.4(a, e, l))). MWM_micNP performed better in simulating C and N profiles than it did with P. The simulated microbial C and DOC profiles agreed well with the measurements (Figure 4.4(i-j)). A decreased microbial C:N ratio, increased microbial N:P ratio and increased DIN concentration with peat depth was

also produced by the model, in agreement with the observed patterns (Figure 4.4(b, d, k)). An initial decreased microbial C:P ratio with depth, which is in line with the measurement, was produced by the model, but the observed increasing microbial C:P ratio with deeper depth was not achieved (Figure 4.4(f)). The simulated DOP and DIP concentrations are larger and smaller than the measured values, respectively (Figure 4.4(g-h)).

The overall daily C fluxes simulated by MWMmic_NP agree well with the tower flux measurement. The R^2 values for both the total gross primary production (GPP) and total ecosystem respiration (ER) are over 0.88 (Figure S4.1(a-b)), very close to the number that MWMmic produced (Shao et al., 2021, in review). The R^2 value for the net ecosystem exchange (NEE) is 0.65, which is smaller than the number of 0.72 that MWMmic produced. But MWMmic_NP produced a much better regression coefficient (0.996) for NEE, compared to that from MWMmic (0.645). The annual C fluxes generated by MWMmic_NP agreed with the observation (Figure 4.3(a)). MWMmic_NP underestimated the NEE a bit but performed well in simulating annual GPP and ER. The simulated daily fluxes captured the seasonal and annual dynamics of carbon fluxes reconstructed from the chamber measurement (Figure S4.4). But there is a larger discrepancy between the chamber-measured and MWMmic_NP-simulated daily C fluxes (Figure S4.1(d-f)), which likely stemmed from the lack of adequate chamber measurements to construct the daily fluxes. There is still a lack of comprehensive measurement regarding to the P budget at Mer Bleue, which hampered us from doing such an evaluation on model's performance in P cycling. But MWMmic_NP produced a similar N:P ratio for the plant's foliar biomass which agreed well with measurements (Figure S4.2).

4.4.2.Sensitivity analyses

The model's sensitivity varies with the parameters being assessed and the outputs being examined (Figure S4.3). Different model outputs are sensitive to different parameters respectively, with ERM biomass being overall the most sensitive output from the model, followed by shrub biomass, mosses and SAP biomass. ERM biomass and shrub biomass have similar levels of sensitivities to several parameters. They are both very sensitive to SAP's nutrient use efficiencies (NUE_{SAP} and PUE_{SAP}), ERM's N mining rates ($k_{Nmining}^{ERM}$) and turnover

rates ($Deathrate_{ERM}$). ERM is also very sensitive to parameters that control the C transfer from shrubs to ERM ($frac_{max}$ and $rate_{out}^{shrub}$) while shrub biomass is sensitive to the parameter that determines mosses' nutrient uptake capacity (β_{moss}). Mosses and SAP biomass also share similar levels of sensitivities to several parameters. They are both quite sensitive to NUE_{SAP}, β_{moss}, and SAP's P biochemical mineralization rates ($V_{max,bcm}^{SAP}$), and much less sensitive to ERM-related parameters that shrub and ERM biomass are sensitive to.

4.4.3. Fertilization experiments

MWMmic_NP successfully reproduced the overall response patterns of plant dynamics to nutrient fertilization measured in the field (Figure 4.5). In line with the observations, simulated elevated nutrient availabilities increased shrub biomass while decreased moss cover. Maintaining the shading effect at control produced increased moss biomass with NP fertilization by over 30% (not shown here), suggesting that intensified shading (Figure S4.5) is the major contributor to the shrinking of mosses. The plant response is the greatest when the plot is fertilized with both N and P. MWM_NPmic overestimated the response of shrubs to N-only or P- only fertilization (referred to as single-nutrient fertilization below) while performed well in simulating shrubs' response to NP fertilization. The moss cover simulated by MWMmic_NP agreed better with the overall moss cover (*Sphagnum* + *Polytrichum strictum*) than *Sphagnum* cover, as field measurements showed that *Sphagnum* mosses got replaced by *Polytrichum* mosses in the N- only or P- only fertilization experiments while both mosses are decimated in the NP fertilization. Simulated shrubs switched their nutrient sources with fertilization (Figure 4.6 and Figure S4.6). Before fertilization, shrubs relied almost entirely on ERM transfer to provide nutrients for them. This dependency decreased with single-nutrient fertilization and completely disappeared with NP fertilization.

The simulated C budget of the peatland also changed considerably with fertilization (Figure S4.7). Mosses C fluxes were massively reduced with fertilization, especially with both NP fertilization where moss litter production is reduced by 86.2%. ERM respiration also declined sharply, so did its biomass (Figure S4.8). Its proportion in the total belowground respiration (peat decomposition + root respiration + ERM respiration) decreased from 29.7%

to 15.5% and 19.4% in N-only and P-only fertilization respectively, and to effectively 0 in the NP fertilization. Shrub GPP was only slightly increased with fertilization while its respiration and litter production were significantly enhanced. Shrub's total litter production (foliar + root) has increased by 52% in NP fertilization. The overall GPP and ER simulated by MWMmic decreased with fertilization, which did not quite match the observed increased GPP and ER in the fertilization plots (Figure S4.4). The model produced notable reduction in net ecosystem carbon balance following fertilization, as also indicated by the chamber measurements (Figure S4.4).

Simulated NP budget of the peatland was also significantly altered by fertilization. MWM_micNP has produced markedly increased nutrient availability with simulated fertilization, in line with what was reported in the fertilization plots (Figure S4.9). Fertilization considerably increased the nutrient export and decreased net mineralization (Figure S4.10). ERM nutrient extraction and N_2 fixation were significantly decreased with fertilization while shrub's root uptake and litter nutrient input significantly increased (Figure S4.11). The nutrient budget, which was initially dominated by organic nutrient fluxes, was now dominated with inorganic nutrient fluxes after fertilization.

4.4.4. ERM-exclusion experiments

Excluding ERM in the model results in a notable reduction in moss biomass and a complete elimination of shrubs (Figure 4.7(a-b)). The reduction in moss biomass was caused by strong P limitation as indicated by the larger N:P ratios in moss biomass with "ERM excluded" treatment (Figure S4.12(a)). The complete elimination of shrubs results from the severe nutrient limitation due to the paucity of inorganic nutrients and strong competition from the mosses. But even when mosses are concomitantly removed with the ERM, shrubs could not grow as well as in the control scenario. Only excluding mosses in the model led to a dramatic increase in shrub biomass (Figure 4.7(b)). HR was the lowest in the "ERM excluded" run and the highest in the "ERM and moss exclusion" run (Figure 4.7(c)). The net ecosystem production (NEP) was the lowest in the "ERM and moss exclusion" run and the highest in the control run, while the "ERM excluded" and the "Moss excluded" runs produced very similar

NEP (Figure 4.7(d) and Figure S4.13).

4.5. Discussion

4.5.1. Model's performance on peatland CNP cycles

Ombrotrophic peatlands are nutrient-poor ecosystems with all their nutrient inputs coming from the atmosphere. Growth of vegetation and microbes in such an impoverished environment need to rely heavily on recycling or energy costly pathways to actively acquire nutrients from the surroundings. The newly developed MWMmic_NP captured this feature and successfully reproduced major fluxes and pools reported for the CNP cycles in the MB bog.

Peatland N cycle

To the best of our knowledge, MWMmic_NP is one of the only two peatland models that were applied to both explicitly simulate the peatland nutrient cycles and validate against the measurements (Wu et al., 2013). The newly developed MWMmic_NP has successfully reproduced the overall N budget observed at MB bog. Important N fluxes, including N mineralization rates (Wang et al., 2018), N export rates (Rattle, 2006), and N_2 fixation rates (Živković et al., 2019) simulated by MWMmic_NP were much closer to their observed values at MB bog, compared to the values simulated by PEATBOG (Figure 4.3). MWMmic_NP also captured the pattern of decreased peat C:N ratio and increased peat DIN concentration with peat depth observed in empirical studies (Rattle, 2006; Wang et al., 2014). N in the peat is mostly locked up at deeper depth beneath the water table and thus inaccessible to shrub roots which adapt poorly to anoxia. This gave rise to the high dependance of shrubs on ERM for acquiring nutrients. The simulation result showed that most of the shrub N came from the ERM N transfer. N mining rates of ERM was the dominant N flux in the whole N cycle at 2.52 gN m^{-2} yr^{-1} (Figure S4.11(a)), which was over twice the amount of total N input into the peatland (N deposition plus N_2 fixation: 1.23 gN m^{-2} yr^{-1}). 68% of those mined N is transferred to shrubs from ERM in exchange for C. Such reliance of ericaceous shrubs on ERM for N was supported by the much lower $\delta^{15}N$ values of evergreen shrubs (-5 to -9‰) than

nonmycorrhizal sedges and herbs (-1 to -1‰) (Moore et al., 2020; Vesala et al., 2021), as ericoid mycorrhizal symbiosis was widely reported to decrease the $\delta^{15}N$ value of its host plants (Hobbie and Högberg, 2012; Gavazov et al., 2016). In contrast to shrubs, mosses mainly rely on atmospheric deposition as their major N sources, which accounted for 60% of their total N supply. N_2 fixation accounted for about 32.7 % of simulated mosses' N supply, which was higher than the number 22% reported in Živković et al., (2019). Summing up all the simulated N fluxes gave a total N accumulation rate in the MB bog of 0.85 gN m^{-2} yr^{-1}. This number fell within the ranges of the long-term N accumulation rates derived from various measurements (0.6-0.9 gN m^{-2} yr^{-1}) (Moore et al., 2005; Wang et al., 2014, M. Wang et al., 2016). Simulated MB bog gained about 1.23 gN m^{-2} yr^{-1} from the atmosphere through N deposition and N_2 fixation while lost 0.38 gN m^{-2} yr^{-1} through fluvial export. These two numbers approximated the values summarized in Moore et al. (2020), which estimated a total N input of 1.0 gN m^{-2} yr^{-1} and export of 0.4 gN m^{-2} yr^{-1}. Note that nitrification and denitrification processes were not simulated by the model, in line with their low values reported at MB bog (Moore et al., 2020).

Peatland P cycle

MWMmic_NP is currently the only model, as far as we are aware, that explicitly simulated the peatland P dynamics. P cycle in MB bog is much less studied than C and N (Wang et al., 2014), which precluded us from doing a more comprehensive evaluation of model's performance on simulating P cycle. Nevertheless, MWMmic_NP successfully reproduced the increase of C:P ratio with peat depth at the acrotelm as observed in MB bog and many other peatlands (Wang et al., 2015; Worrall et al., 2016), which suggested a rapid P recycling at shallow depth. Our simulation results showed that this rapid recycling of P could be engineered by the ERM, whose P mining rate in the model was 192 mgP m^{-2} yr^{-1} (Figure S4.11(e)), over six times the amount of P deposition we adopted in our model runs (30 mgP m^{-2} yr^{-1}). The tight recycling feature of P extended beyond ERM throughout the whole ecosystem. To produce the high microbial P content obtained from measurements (Basiliko et al., 2005, 2006) (Figure 4.4(f)), SAPs in MWMmic_NP are assumed to resorb P upon their death. P resorption increased with decrease in microbial P content, resulting in a smaller

microbial P turnover rate with stronger P limitation. This reduced P turnover rate with low P availability was reported by Spohn and Widdig (2017) and identified as a potentially important process by which microbes adapt to low-P environment. DIP was also strongly recycled within the system, which was characterized by the large DIP immobilization by SAPs (Figure S4.10(e)) and large DIP absorption by mosses (Figure S4.11(e)). DIP absorption by mosses accounted for ~56% of the mosses' P supply. This large P uptake of moss from peat P pool was in line with the evidence of *Sphagnum* mosses processing a high capacity to absorb phosphates (Rydin and Clymo, 1989; Bates and Bakken, 2018). Simulated P export was very small at around 6 mgP m^{-2} yr^{-1} because of the strong internal recycling and the reduced leaching rates we have prescribed. Summing up all the simulated P fluxes gave a total P accumulation rate in the MB bog of 24 mgP m^{-2} yr^{-1} which was close to but larger than the 17 mgP m^{-2} yr^{-1} derived from peat core analysis (Wang et al., 2014). This might be attributed to the mismatch between measured and simulated P content in the catotelm. MWMmic_NP produced increased peat P concentrations with depth for peat below the water table where shrub roots cannot reach, while measurement showed that the peat in the catotelm is still losing relatively more P than C (Wang et al., 2015, Worrall et al., 2016). One possible explanation for this is the increased release of soluble P via reduction of Fe under anoxic conditions (Moore and Reddy, 1994; Herndon et al., 2019). Exclusion of adsorption and desorption in MWMmic_NP hampered us from simulating this process, which may ultimately lead to an overestimation of P accumulation rates.

Peatland C cycle

MWMmic_NP successfully reproduced the C fluxes measured at MB (Figure S4.1). The ecosystem-level C fluxes generated from MWMmic_NP were also close to the measurements and the simulated results from MWMmic (Figure 4.3). However, MWMmic_NP has a completely different C allocation scheme compares to MWMmic. Shrubs in MWMmic_NP allocated 26% of its GPP to ERM. Shrub-mediated ERM respiration accounted for 23% of the total belowground respiration and ERM necromass production accounted for 17.3% of the overall shrub NPP (Figure S4.14). In contrast, shrubs in MWMmic had higher autotrophic

respiration and higher shrub litter production. These higher shrub C fluxes from MWMmic made up for the non-existent ERM respiration and necromass production in the model thus resulted in ecosystem-level C fluxes similar to those from MWMmic_NP. A lack of ERM measurement at MB bog precluded us from concluding which allocation scheme here is more accurate. But the simulated amount of C allocated to ERM is comparable to empirical studies that quantified the C allocation to mycorrhiza in other ecosystems. The simulated fraction of NPP allocated to ERM (17.3%) fell within the range (1% to 21%) reported from Hobbie (2006). Furthermore, our simulated contribution of ERM respiration to total soil respiration (23%) is comparable to numbers recently reported for ECM respiration from studies of boreal forest (14%-26%) (Hagenbo et al., 2019) and temperate forest (18%–44%) (Heinemeyer et al., 2012; Andrew et al. (2014); Neumann and Matzner, 2014). In additon, the shrub litter production produced from MWMmic_NP was closer to the measurements than MWMmic (Figure S4.14), providing grounds for the large contribution of ERM respiration in the whole C cycle of MB bog, as simulated by our new model.

4.5.2.Simulated peatland response to fertilization

Response of vegetation dynamics to fertilization

Fertilization experiment at MB bog was reported to greatly impact the vegetation composition by increasing shrub biomass and decreasing *Sphagnum* mosses (Juutinen et al., 2010; Larmola et al., 2013). In contrast to the common assumption applied in N-cycle model that increased N availability enhances plant photosynthetic capacity (Wu et al., 2015), Bubier et al., (2011) reported unchanged shrub's photosynthetic capacity with increased N content. They proposed that bog shrubs adapted to the nutrient poor environment and did not shift their resource allocation to photosynthetic processes even with more nutrient availability. MWMmic_NP adopted the findings from Bubier et al., (2011) and attributed the bog shrub growth with fertilization to the altered C allocation. With increased nutrient availability brought by fertilization (Figure S4.9), shrub could rely more on root direct uptake rather than the energy costly ERM transfer to acquire nutrients (Figure 4.6). Thus, shrub decreased its C

transfer to ERM and used this portion of C for its own growth (Figure 4.6). This increased shrub growth resulted in strong reduction of PAR that reached the moss layer (Figure S4.5) (Chong et al., 2012) and thus led to large reduction in moss biomass. Compared to PEATBOG, results generated with MWMmic_NP agreed better with the observations (Figure 4.3)

A number of studies can provide support to the fertilization effects on shrubs proposed by our model results here. From a plant perspective, our simulation results were in line with the findings that nutrient limitation induces surplus C accumulation within plants (Prescott et al., 2020) and leads to large C investment of plants to roots or symbiosis facilitating nutrient acquisition (Litton et al., 2007; Vicca et al., 2012; Gill and Finzi, 2016). Contrastingly, plants with high-nutrient availability use more of their photosynthates for more efficient biomass production (Vicca et al., 2012). Increased C allocation to biomass production with nutrient fertilization was recently reported in temperate forests (Eastman et al., 2021). From a mycorrhizal perspective, it has been widely reported that both ECM (van der Linde et al., 2018; Lilleskov et al., 2019) and AM (Jiang et al., 2018; Ceulemans et al., 2019) respond negatively to nutrient fertilization, presumably caused by diminished resource allocation from hots plants (Treseder, 2004). The effects of fertilization on ERM are much less studied and opposite results have been reported (Johansson, 2000; Calvo-Fernández et al., 2018; Wu et al., 2021). Kiheri et al. (2020) reported that fertilization decreased the activities of ERM root enzymes for nutrient acquisition but increased the ERM colonization of shrub roots at Whim Bog. This may be caused by the increased sedge and decreased shrub abundance observed at Whim bog fertilization plots (Levy et al. 2019), or the potential for ERM to switch from mutualistic to more saprotrophic lifestyle (Martino et al., 2018). A recent large-scale study showed that nutrient pollution resulted in a potentially 40% loss of ERM species in European bogs across a gradient of N deposition and ERM richness was negatively correlated to both N and P availability (Van Geel et al., 2021), supporting our simulated decrease in ERM biomass with fertilization (Figure S4.8). Whether ERM at MB responded to fertilization in accordance with the simulation presented in this study remained to be unfolded. But from a nutrient-uptake perspective, the simulated diminished role of ERM in ericoid shrub nutrient uptake was directly supported by the increased foliar $\delta^{15}N$ values of shrubs after N fertilization at both

MB bog and Whim bog (Vesala et al., 2021), suggesting ERM fungi were less important for N supply with N fertilization. This shift of plant nutrient uptake strategies was also observed on AM-associated plants with fertilization (Jach-Smith and Jackson, 2020) and mycorrhiza modeling studies examining the effects of increased nutrient input (Meyer et al., 2012; Franklin et al., 2014).

Response of CNP cycles to fertilization

Fertilization considerably impacted the C cycle of MB bog. Overall, the alteration in plant community structure led to a weaker carbon sink in MB (Figure S4.7) which was in line with the observation (Larmola et al., 2013). The simulated 20NPK fertilization led to the greatest increase in shrub litter production (82 gC m^{-2} yr^{-1}) among all treatments. However, this large increase in shrub litter cannot compensate for the drastic decline in moss litter production (77.51 gC m^{-2} yr^{-1}) combined with the loss of ERM necromass production (32.82 gC m^{-2} yr^{-1}). Besides, *Sphagnum* moss litter possess cell-wall pectin-like polysaccharides (Hájek et al., 2011) and ERM is reported to produce heavily melanized necromass (Clemmensen et al., 2013, 2015). Both those litters are much more resistant to degradation compared to shrub litter. Therefore, the fertilization-induced increase in labile litter input and concomitant decrease in refractory litter input resulted in a reduced C sequestration capacity. The NEP after 16 years of 20NPK fertilization was simulated to decrease over 73% compared to control plots (Figure S4.7). In contrast, the C cycle is much less affected by single nutrient fertilization manifested by the less increased shrub biomass and more moss biomass being preserved (Figure 4.5). This showed that shrubs in MB bog were co-limited by both N and P (Wang and Moore et al., 2014). This NP co-limitation was also indicated by the simulated dynamics of shrub foliar N:P ratios (Figure S4.2) which could serve as a reliable indicator of nutrient limitation status (Sterner and Elser, 2017). The simulated dynamics of shrub N:P ratio agreed with the measurements (M. Wang et al., 2016) (Figure S4.2) and suggested that shrubs become more N/P limited when applied with P-only/N-only fertilizers. Therefore, only applying N and P fertilization together could alleviate the shrubs at MBC bog from nutrient limitation.

Fertilization also dramatically altered the nutrient dynamics in MB bog. Before

fertilization, the nutrient cycles in MB big is featured by its strong internal recycling. ERM nutrient mining was the most dominant flux in the nutrient cycle, followed by shrub litter input and ERM nutrient transfer to shrubs (Figure S4.11). Thus, the shrub-mycorrhiza association had formed a closed internal recycling within itself. This resulted in a strong nutrient retention rate for N (78%) and P (80%) in MB bog and made the system a strong N and P sink. Fertilization, however, had changed the bog from being an organic flux-dominant closed system to an inorganic flux dominant open system through diminishing the role of ERM in shrub's nutrient uptake. The initially dominant ERM nutrient mining became effectively zero after 16 years of 20NPK fertilization. Moss's N_2 fixation was also suppressed by N fertilization, in line with the measurement (Živkovic et al., 2019). Nutrient retention rates of the MB bog after 16 years of fertilization dropped to 50% for N and 21% for P (Figure S4.10), which suggested that the system was approaching nutrient saturation along with its decreased C sequestration capacity (Lovett and Goodale, 2011). The ability of bogs to act as a significant nutrient sink was severely weakened.

4.5.3. ERM and its role in peatland CNP cycles

Our 'ERM-exclusion' model experiments provided a unique perspective to how vascular plants, mosses and microbial communities might interact in terms of nutrient cycling. As expected, the modeling results showed that losing ERM could severely suppress shrub growth (Figure 4.7). More surprisingly, *Sphagnum* mosses suffered from the exclusion of ERM and shrubs as well. Although *Sphagnum* mosses possess strong capacity to assimilate nutrients from surrounding environment (Bates and Bakken, 2018), the lack of roots precludes them from getting P, which cannot be fixed from the atmosphere, from the deep peat. In contrast, ERM-shrub root association in the control experiment could extract P from deeper peat and deliver it to shrubs' aboveground biomass, thus *Sphagnum* moss could take up those phosphates released from the decomposition of shrub litter. This difference ultimately led to a stronger P limitation for *Sphagnum* mosses in the "ERM-excluded" experiment compared to that in the control experiment (Figure S4.12).

Nutrient competition is often thought to prevail between *Sphagnum* moss and vascular

plants interactions in peatlands (Malmer et al., 2003), but here we showed that Sphagnum mosses might rely on ERM-Shrub association to extract P from deep peat thus could also benefit from a moderate amount of shrub presence, supporting the previous findings that vascular plants can facilitate *Sphagnum* growth under certain conditions (Malmer et al., 1994; Pouliot et al., 2011) from a nutrient-cycling perspective. This also demonstrated how the nutrient dynamics of different PFTs in ombrotrophic peatlands could be interconnected through ERM: Not only shrubs could directly utilize the ERM to pilfer the N that mosses fixed from the atmosphere (Zackrisson et al., 1997; Lindo et al., 2013), but mosses could also assimilate P that shrubs take up from deep peat with the help of ERM. These interconnections thus formed a shrub-ERM-*Sphagnum* association at the center of the biogeochemical cycling within the MB bog (Figure 4.2). The mutual benefit of shrub-ERM association is supported by ample evidence in the literature. Ericaceous shrubs in peatlands were reported to gain a competitive advantage over other PFTs by tightening the nutrient cycle through ERM (Bragazza et al., 2012; Gavazov et al., 2016). In turn, ericaceous shrub litter created acidic (Cornelissen et al., 2006; Adamczyk et al., 2016) and phenolic-rich (Wang et al., 2015; Pinsonneault et al., 2016a) environment that the ERM could have a competitive advantage over other microbes (Kohout et al., 2017). In contrast, little research has been done regarding the interaction between *Sphagnum* moss and ERM. But recent studies reported that *Sphagnum* phenolics could drive ericoid mycorrhization (Chiapusio et al., 2018) and our modeling study here further showed that that *Sphagnum* mosses might benefit from the ERM's presence. Therefore, this shrub-ERM-*Sphagnum* association could potentially exist to the benefit of each 'stakeholder' and together they dominated the nutrient cycling within the ombrotrophic peatlands (Figure 4.2).

As this shrub-ERM-*Sphagnum* association effectively recycled nutrients within itself, it limited the nutrient supply to other competitors both below- and above-ground thus could exert a considerable impact on the system's C cycling. Belowground saprotrophic microbes could suffer from this intense nutrient competition from ERM, which could limit their activities and thus inhibit peat decomposition. The existence of such competition was supported with our modeling result that the "ERM and moss exclusion" run produced the highest HR despite

the “Moss exclusion” run had the largest shrub biomass and the most labile litter input (Figure 4.7). This echoed with the classic phenomenon known as the ‘Gadgil effect’ that the competition between mycorrhiza and few-living decomposers slows decomposition (Gadgil and Gadgil, 1971; Fernandez and Kennedy, 2016; Wiedermann et al., 2017), which could promote soil C storage (Averil et al., 2014). As to the aboveground part, besides the established notion that ericaceous shrubs compete with fast-growing plant species through the short-circuited nutrient cycle mediated by ERM (Bragazza et al., 2012; Gavazov et al., 2016; Vowles and Björk, 2019), our model results showed that the presence of ERM could also benefit the growth of Sphagnum mosses (Figure 4.7(a)). Thus, the ERM appeared to favor slow-growing plant species that shed highly phenolic litters and created acidic environments (Rydin and Jeglum, 2013) that further inhibited activities of other soil microbes (Freeman et al., 2001a) to the benefit of ERM itself. Therefore, this shrub-ERM-*Sphagnum* association could potentially self-reinforce itself as it developed and ultimately resulted in a system featured with closed nutrient cycle and large SOC accumulation which resembled ombrotrophic peatlands. Our modeling result offered support to this development as the experiment with the intact shrub-ERM-*Sphagnum* association produced the largest NEP among all exclusion experiments (Figure 4.7(d)). This is in congruence with the recent findings that ERM association led to progressive nutrient limitation and facilitated the long-term humus build-up in late successional-stage boreal forest (Näsholm et al., 2013; Franklin et al., 2014; Clemmensen et al., 2015; Högberg et al., 2017; Ward et al., 2021). Our study thus provided a new insight into the role of ERM in mediating the biogeochemical cycling of the ombrotrophic peatlands like the MB bog (Frey, 2019; Juan-Ovejero et al., 2020).

4.6. Conclusion and future directions

A new model MWMmic_NP that integrates peatland carbon, nitrogen and phosphorus cycles with mycorrhiza controls was developed in this study. To the best of our knowledge, MWMmic_NP is the first model that explicitly simulates the C-N-P cycles in peatlands. We have parameterized and ran our model in the well-characterized MB bog. The model was demonstrated to perform well in simulating the overall C-N-P cycles observed in the MB bog. Compared to the previous nutrient modeling work, the MWMmic_NP performed much better

in capturing the tight recycling features of the nutrient cycle observed in the bog. The Bog plants were shown to adapt to bogs' nutrient-poor environment by investing a large amount of C into nutrient acquisition. This plant-invested C feeds the ERM symbiont and renders the nutrient mining of ERM fungi the most dominant nutrient flow. MWMmic_NP was also demonstrated to successfully reproduce the response of the bog to nutrient fertilization experiment. Shrubs benefited from the increased nutrient availability and diminished their C investment to ERM, which led to a series of changes observed in plant community composition and C cycling. MWMmic_NP was also used to explore the possible shrub-ERM-moss association in maintaining the nutrient-depleted environment that benefit the association itself. We conclude that ERM may play a central role in regulating the overall biogeochemical cycles of ombrotrophic peatlands like the MB bog. This study served as a pioneering step into compressively simulating the C-N-P cycles in ombrotrophic peatlands and addressing the potential significance of symbiont microbes in these nutrient limited ecosystems.

Based on this study, we suggest future peatland research should focus on following areas to further our understanding. Firstly, the overall P profiles in the peat were not well reproduced by the model, particularly compared to C and N. This may stem from the several simplified assumptions that were applied when simulating the P cycle in peatlands. A lack of study in P cycles in peatland compared to C and N also precluded us from well-constructing the overall P budget in the MB bog. As bogs like MB are often co-limited by N and P, we called for more P measurements conducted in the ombrotrophic peatlands to better constrain the model. Secondly, the mycorrhiza model was constructed using data from studies done in other ecosystems or simply based on calibrated numbers. A comprehensive evaluation of our mycorrhiza model was not conducted here due to the lack of measurement. Future peatland studies on mycorrhiza fungi are needed to better calibrate the mycorrhiza model and more importantly, expose the potentially misrepresented processes in the model. Thirdly, MWMmic_NP did not produce a higher GPP or ER for MB bog after fertilization as shown from measurements (Figure S4.4). This might result from the fact that MWMmic_NP only included the two most dominant bog PFTs. Several other PFTs were also reported to increase in

abundance after fertilization, including the tall moss *Polytrichum strictum*, deciduous shrubs such as *B. populifolia* and *V. myrtilloides* and new colonizing ferns (Larmola et al., 2013). The lack of non-mycorrhiza vascular plants like sedges also inhibited our ability to apply the model into mineratrophic peatlands where these PFTs are likely to dominate. Therefore, future inclusion of more PFTs into the model will expand its applicability on different types of peatland ecosystems.

4.7. Tables and Figures

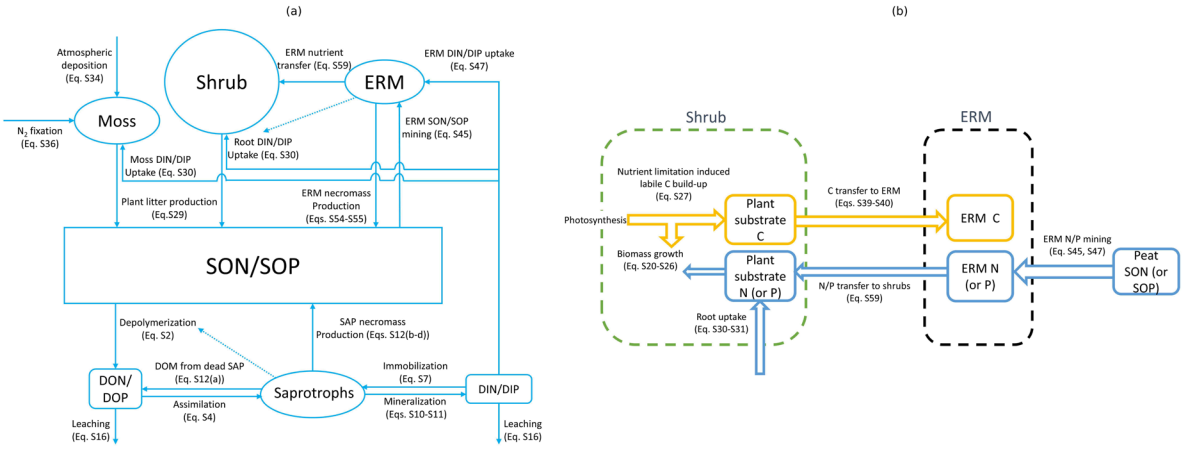

Figure 4.1 (a) Schematic representation of the model structure. Ellipse: plant or microbial nutrient pools; rectangles: soil organic nutrient pools; rounded rectangles: dissolved nutrient pools; solid lines: nutrient flows; dotted lines: effects; (b) Schematic representation of the shrub-ERM carbon-nutrient exchange model. Orange boxes: C pools; orange arrows: C fluxes; blue boxes: nutrient pools; orange arrows: nutrient fluxes; green dotted boxes: shrub; black dotted boxes: ERM.

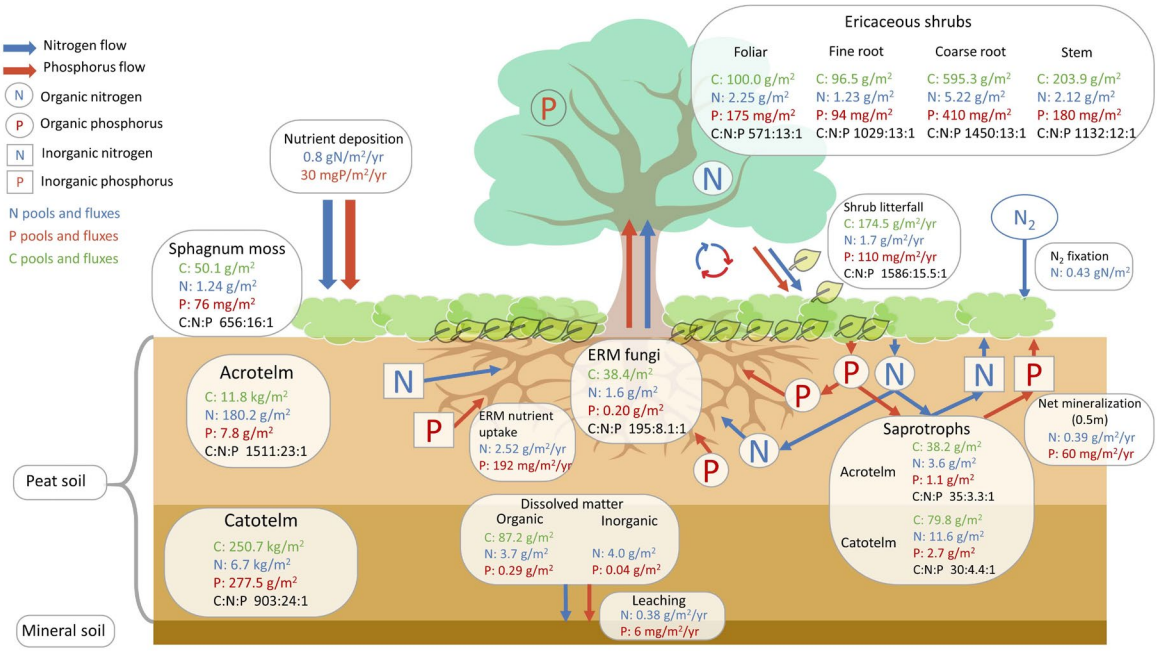

Figure 4.2 The nutrient flow diagram in ombrotrophic peatlands. Ellipse: organic nutrient pools; rectangles: inorganic nutrient pools; Simulated values for the major C, N and P pools and fluxes are shown here, represented with green, blue, and red colors, respectively. The system relied heavily on internal nutrient recycling where ERM organic nutrient mining plays a central role.

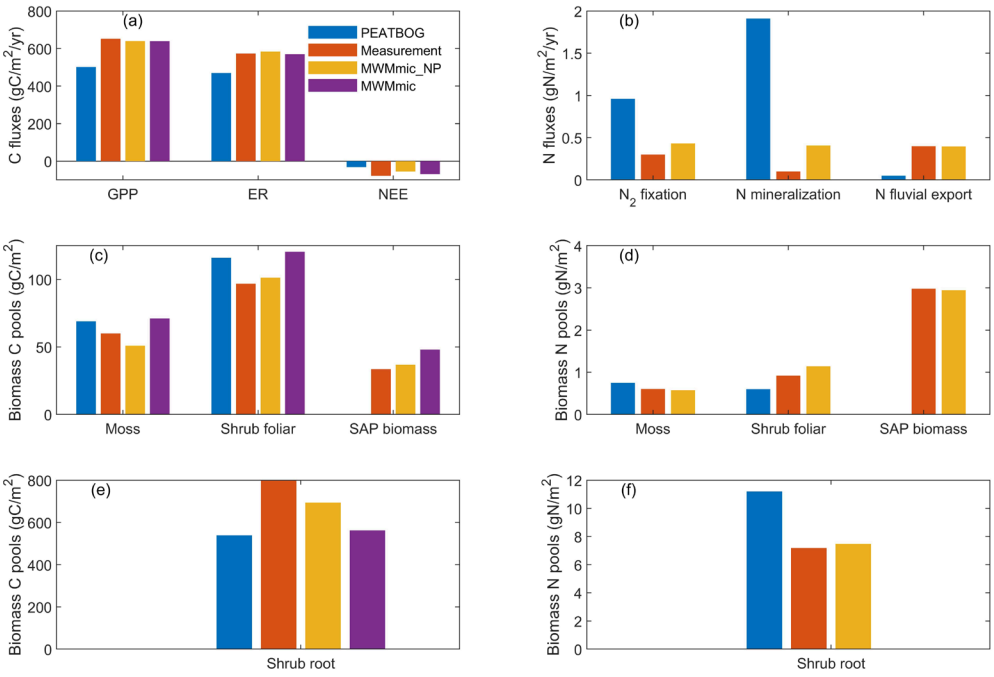

Figure 4.3 The measured (blue bars), PEATBOG simulated (red bars), MWMmic_NP simulated (yellow bars) and MWMmic simulated (purple bars) (a) plant C pools, (b) plant N pools, (c) ecosystem C fluxes (aggregated from tower measurements), (d) ecosystem N fluxes.

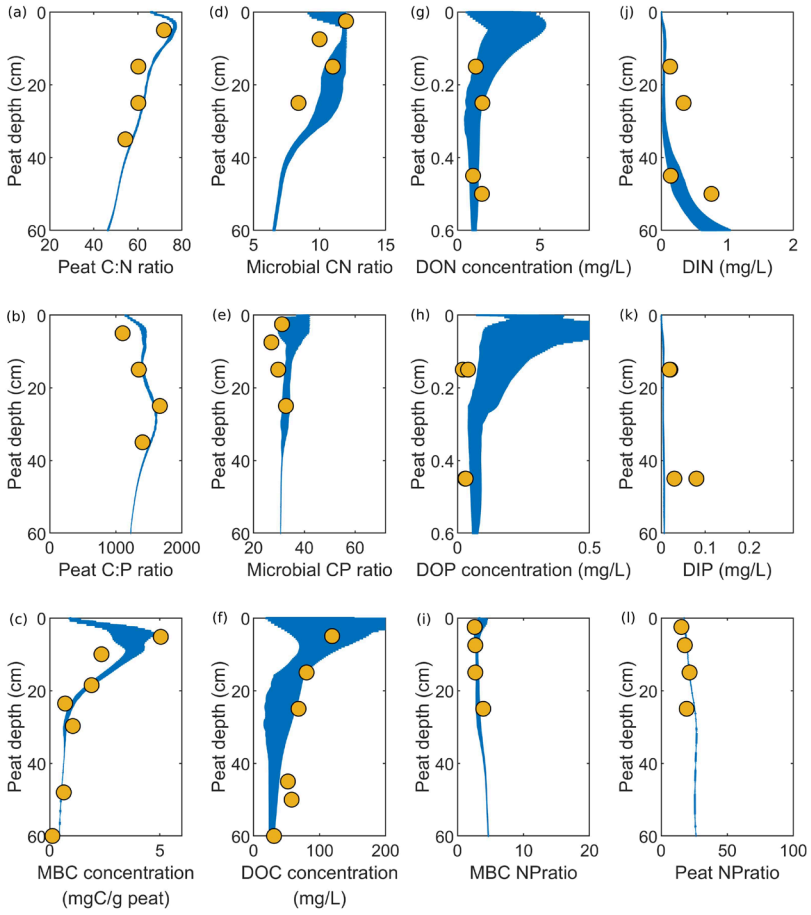

Figure 4.4 Simulated (blue lines) and observed (yellow dots) (a) C:N ratio in peat, (b) C:N ratio in saprotrophic microbes, (c) DON concentration, (d) DIN concentration, (e) C:P ratio in peat, (f) C:P ratio in saprotrophic microbes, (g) DOP concentration, (h) DIP concentration, (i) C content in saprotrophic microbes, (j) DOC concentration, (k) N:P ratio in saprotrophic microbes, (l) N:P ratio in peat at Mer Bleue bog up to 60cm peat depth.

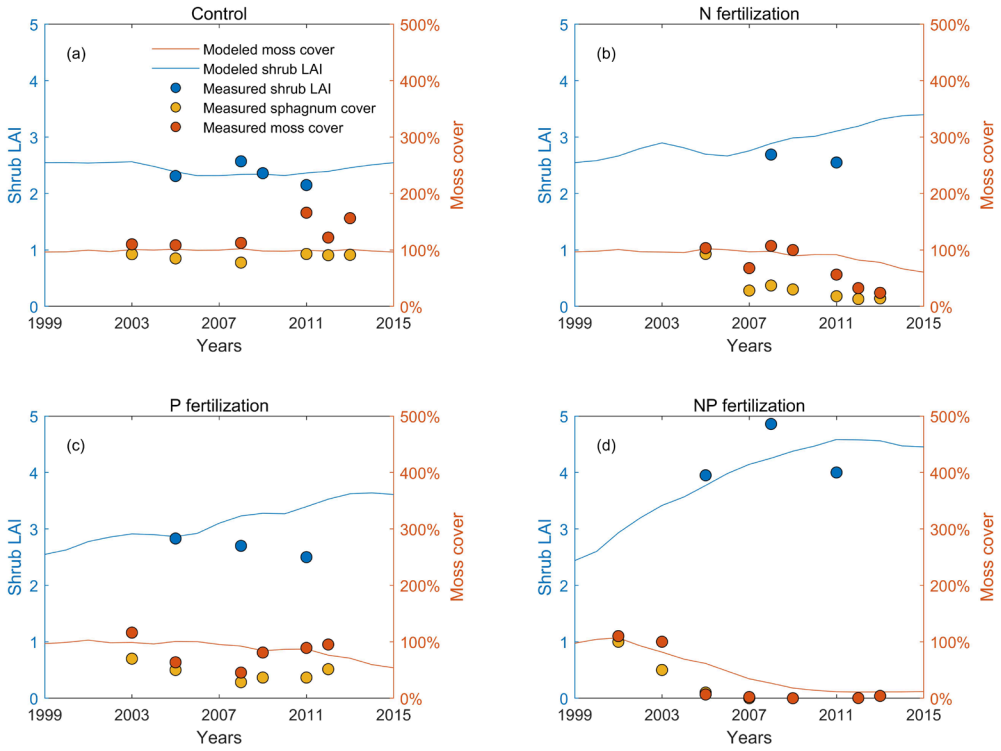

Figure 4.5 Simulated (lines) and observed (dots) plant dynamics in experiments of (a) no fertilization, (b) 20N fertilization, (c) PK fertilization, (d) 20NPK fertilization.

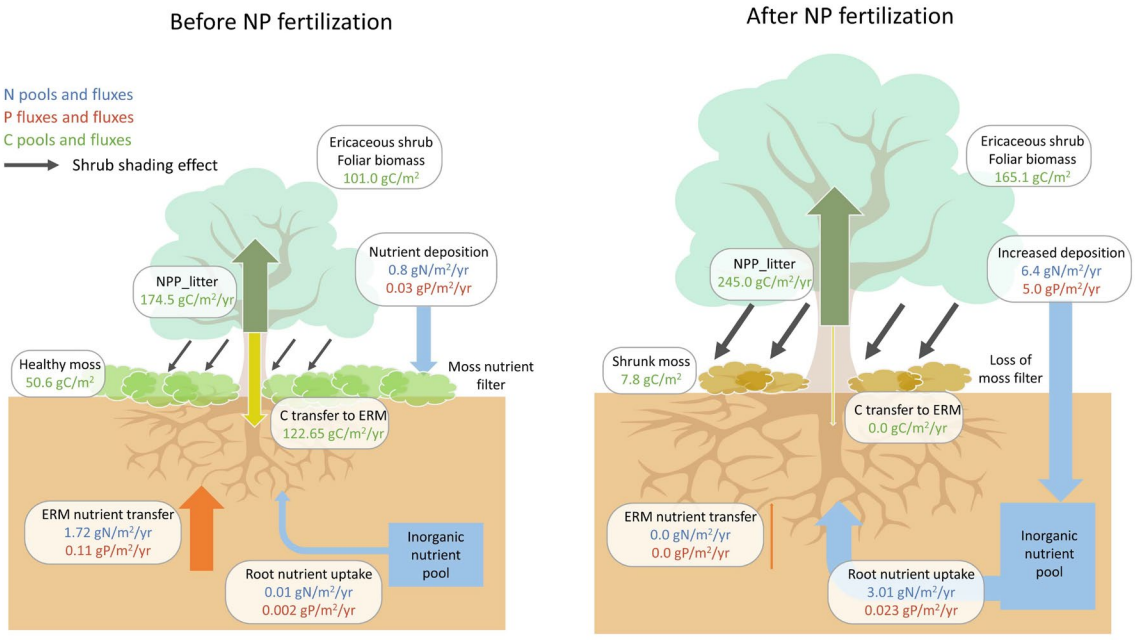

Figure 4.6 Simulated changes in shrub nutrient uptake pathways and C allocation schemes, and subsequent changes in vegetation communities before and after NP fertilization.

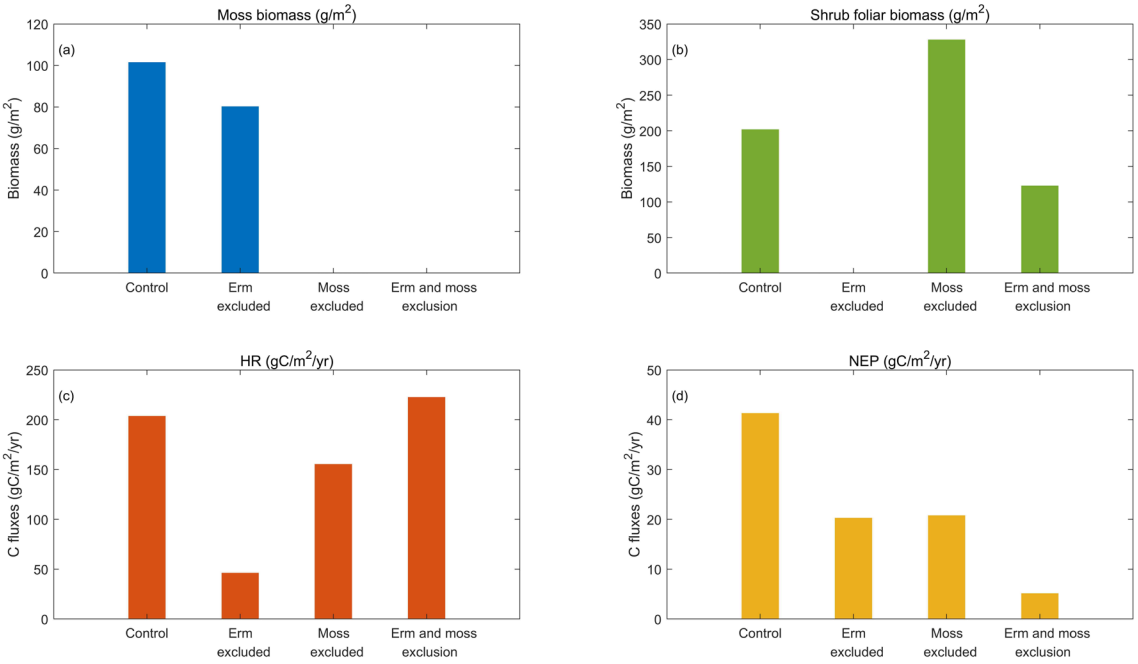

Figure 4.7 Simulated plant biomass and NEP from different 'Exclusion' experiments: (a) mosses biomass; (b) shrub biomass; (3) NEP.

4.8. Supplementary materials

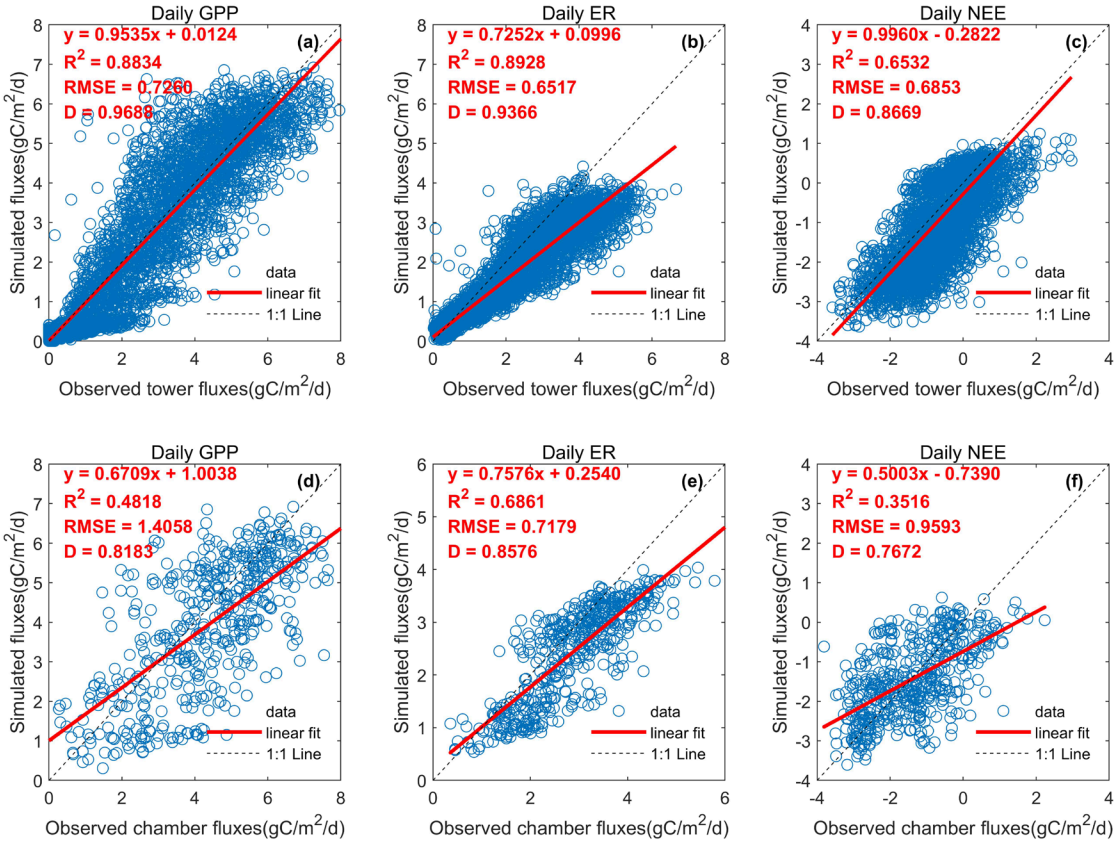

Figure S4.1 (a-c) Linear regression of flux tower-observed and MWMmic_NP-simulated daily GPP, ER and NEE; (d-f) Linear regression of chamber-measured and MWMmic_NP-simulated daily GPP, ER and NEE.

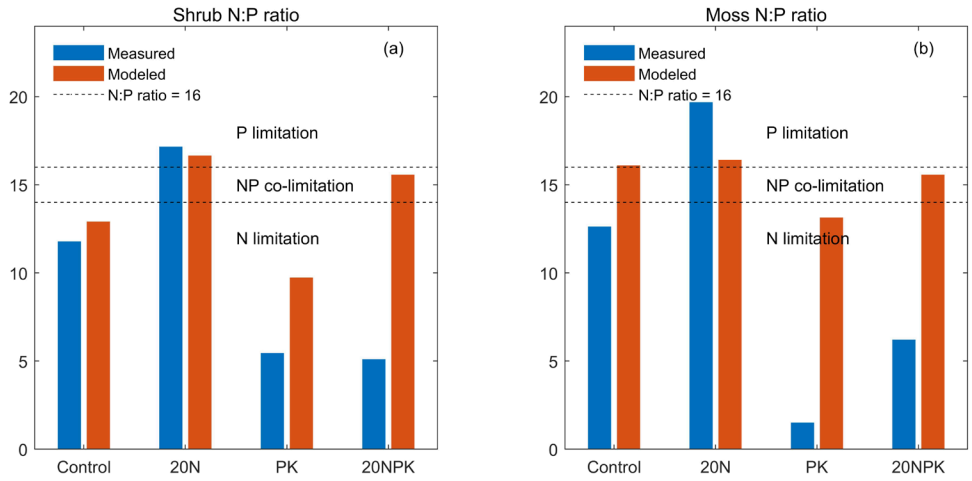

Figure S4.2 Simulated and observed N:P ratios in the foliar biomass of (a) shrubs and (b) mosses. N:P ratio greater than 16 or smaller than 14 suggested P or N limitation, respectively and N:P ratio between 14 and 16 indicated NP co-limitation.

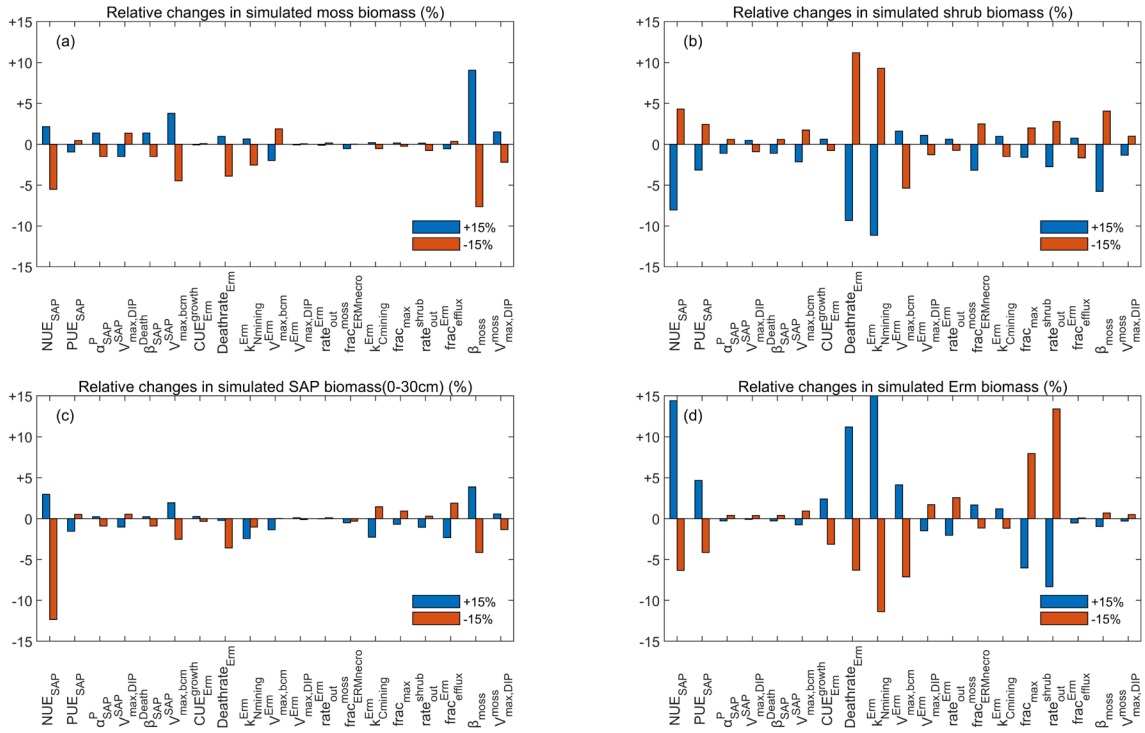

Figure S4.3 Relative changes in simulated (a) moss biomass, (b) shrub biomass, (c) SAP biomass, (4) ERM biomass from varying one model parameter by ±15% at a time.

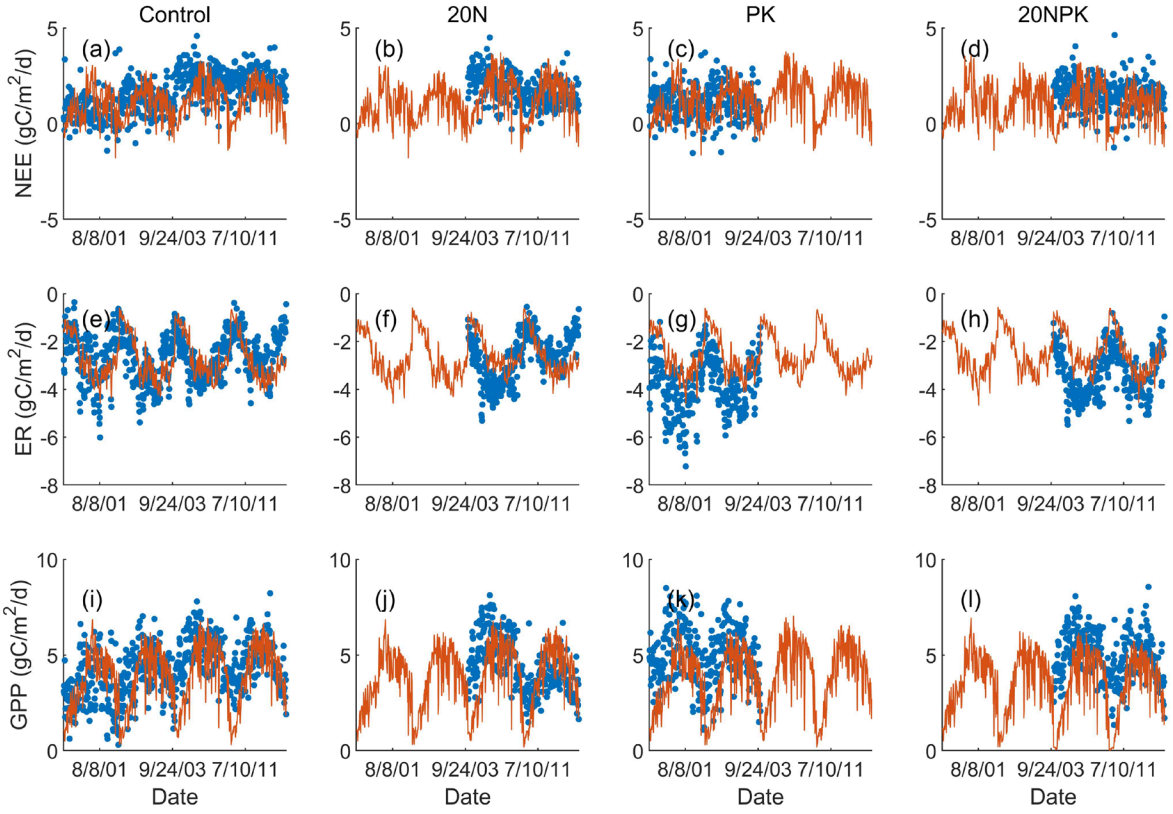

Figure S4.4 (a-d) Simulated and observed daily net ecosystem exchange (NEE), (e-h) ecosystem respiration (ER) and (i-l) gross primary production (GPP) from May to September in year 2001, 2003, 2009, 2011.

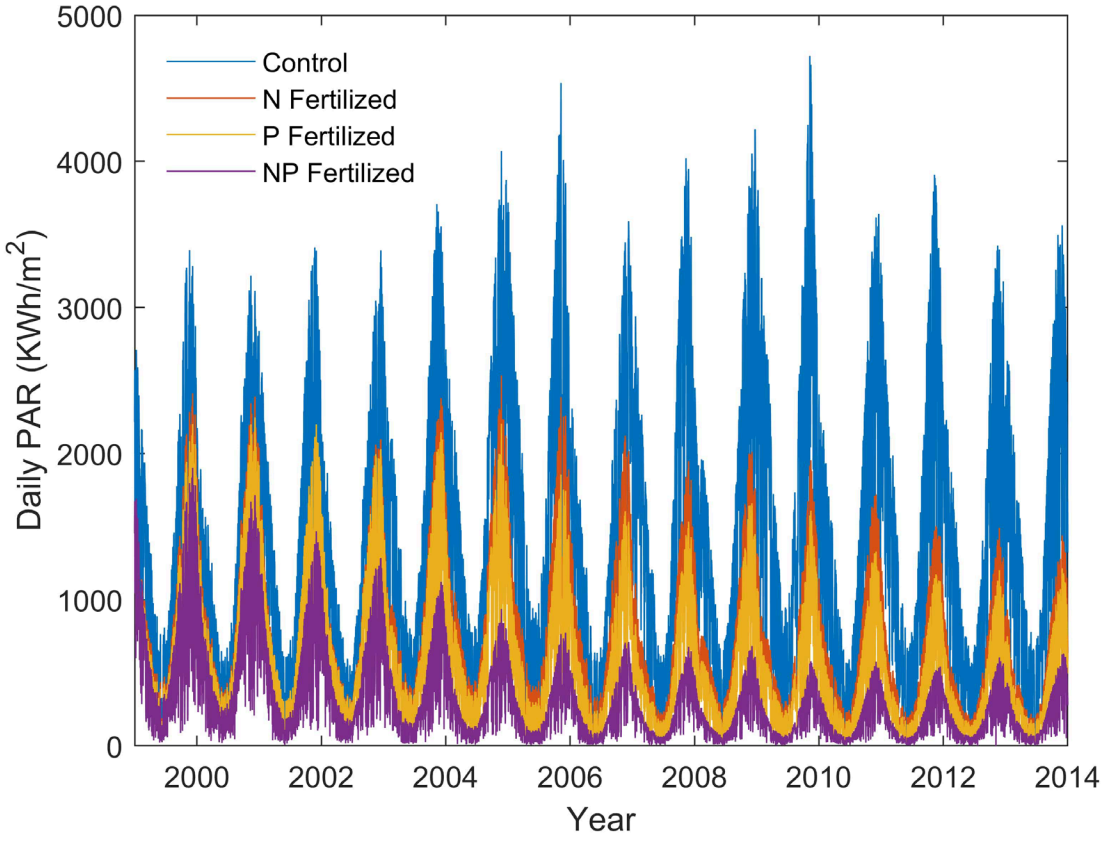

Figure S4.5 Simulated photosynthetically active radition (PAR) that reaches the moss layer in different fertilization experiments.

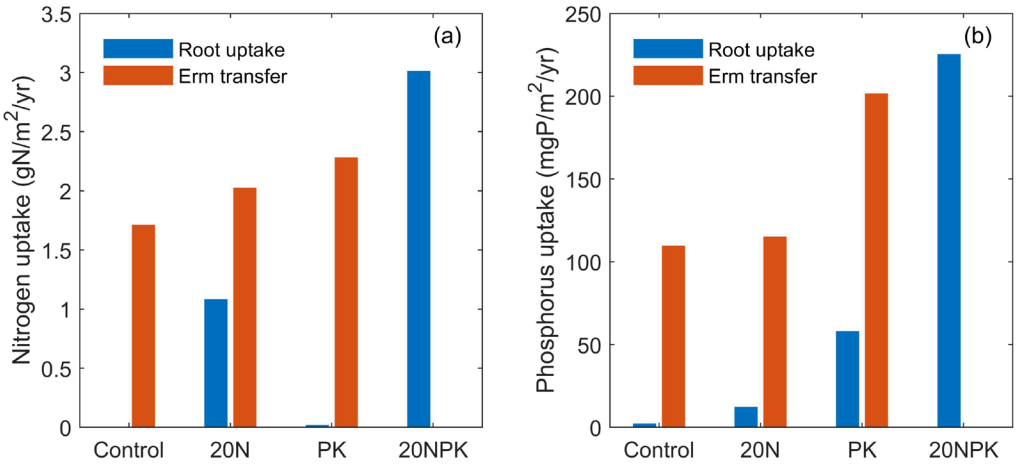

Figure S4.6 Simulated shrub nutrient uptake by roots and nutrient transfer from ERM in different fertilization experiments. (a) for N and (b) for P.

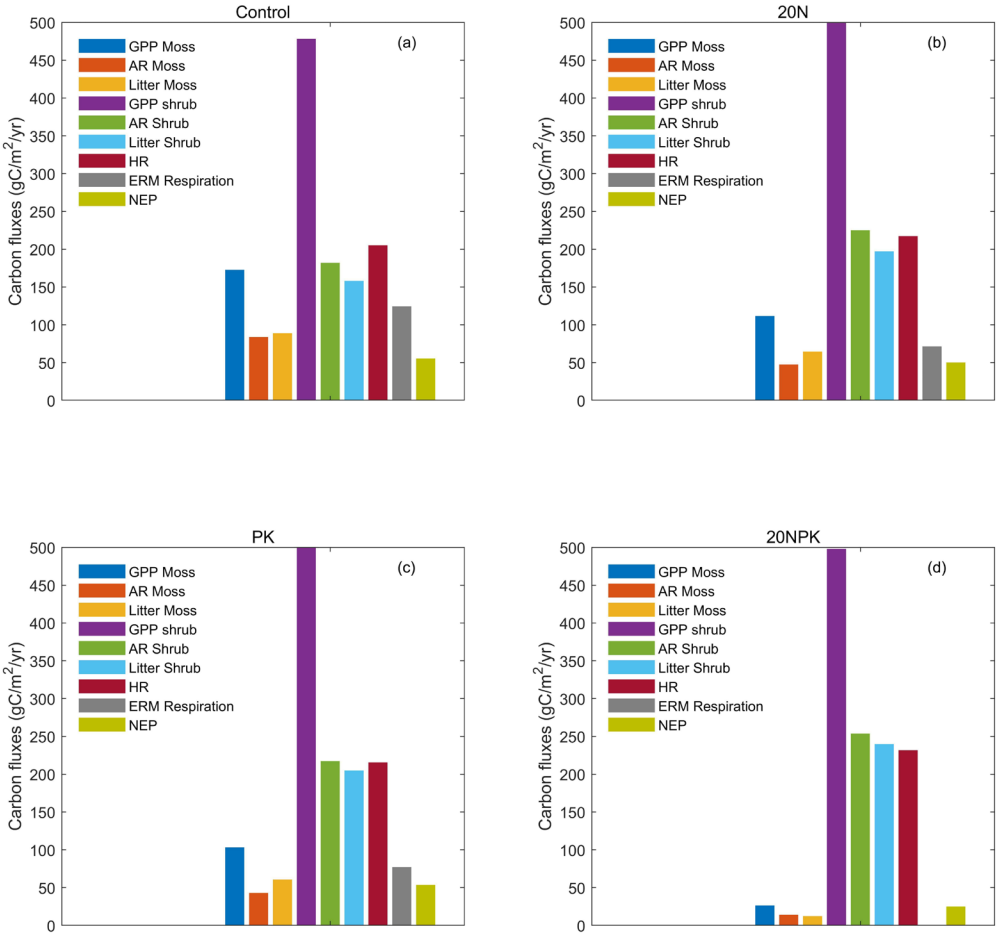

Figure S4.7 Simulated Mer Bleue C fluxes (a) without fertilization, (b) after 16 years of 20N fertilization, (c) after 16 years of PK fertilization, (d) after 16 years of 20NPK fertilization.

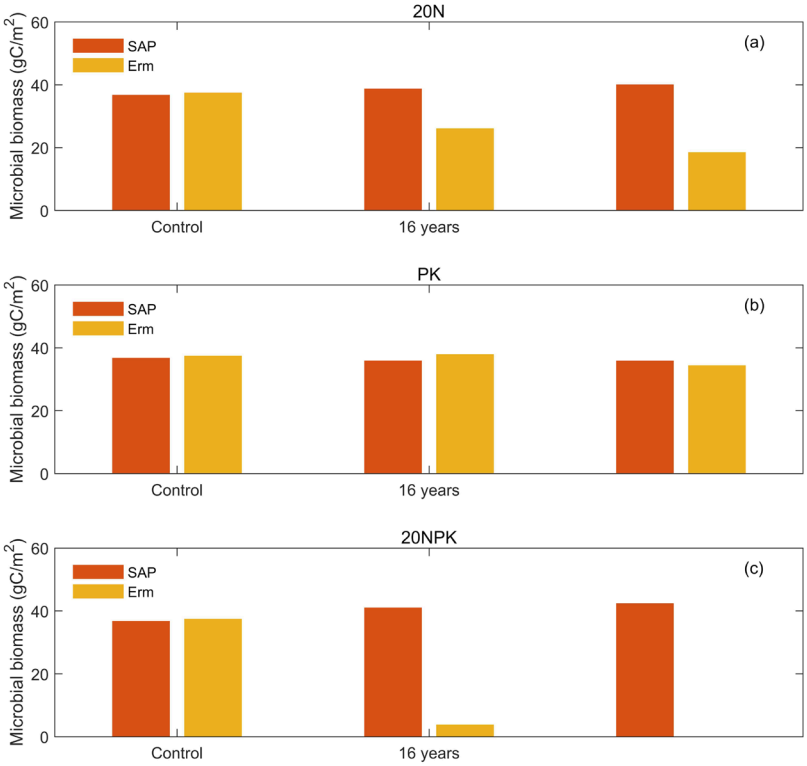

Figure S4.8 Simulated microbial dynamics in experiments of (a) no fertilization, (b) 20N fertilization, (c) PK fertilization, (d) 20NPK fertilization.

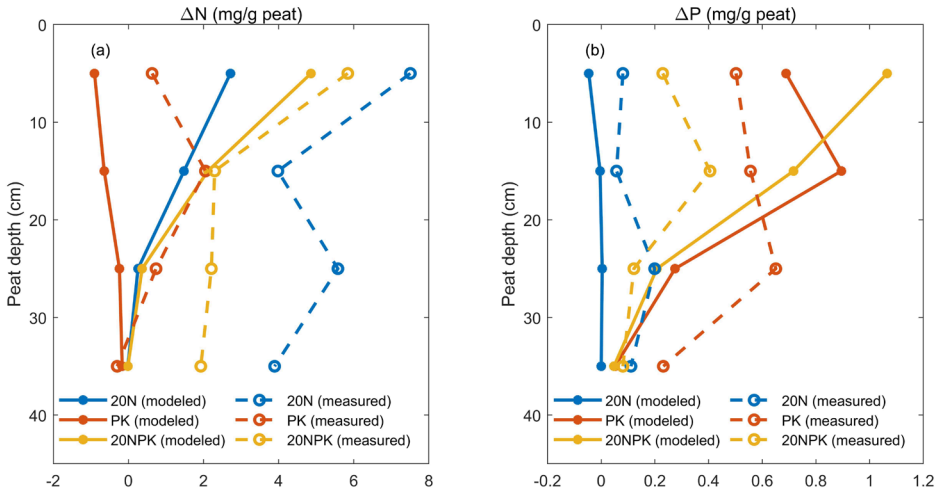

Figure S4.9 Observed (dashed lines and circle marker) and simulated (solid lines and filled circle markers) differences in (a) N concentrations and (b) P concentrations between treated and control peat cores at equivalent depths.

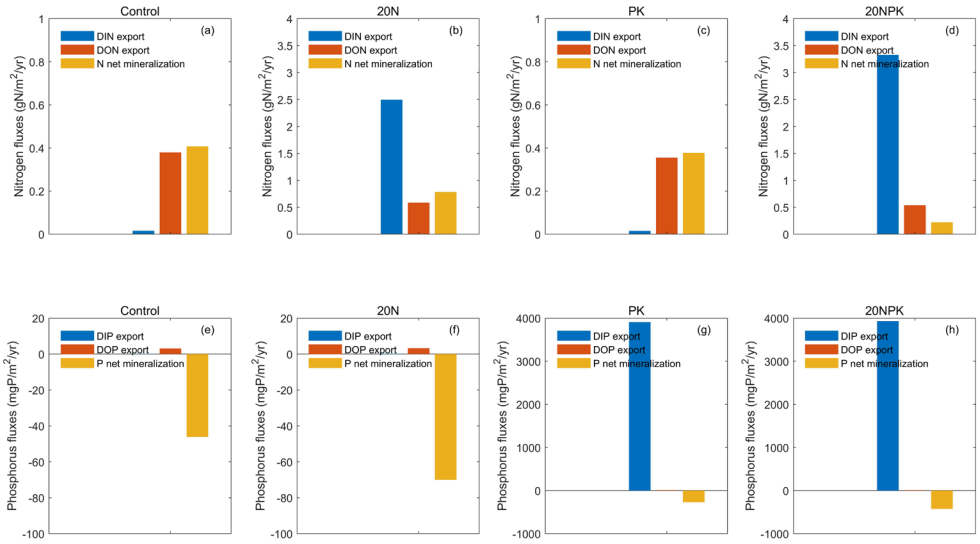

Figure S4.10 Simulated NP fluxes within the peat at Mer Bleue (a) without fertilization, (b) after 16 years of 20N fertilization, (c) after 16 years of PK fertilization, (d) after 16 years of 20NPK fertilization.

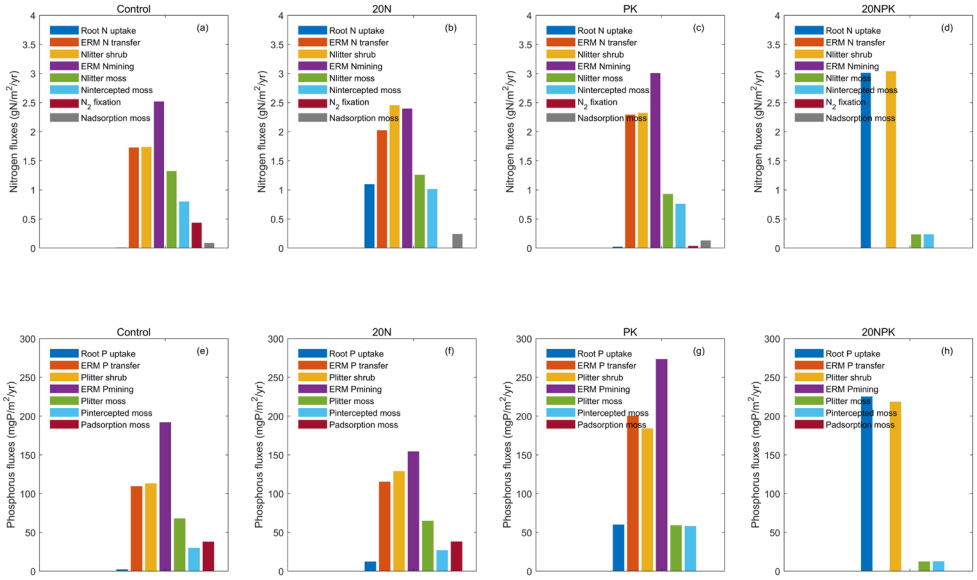

Figure S4.11 Simulated NP fluxes of plants and ERM at Mer Bleue (a) without fertilization, (b) after 16 years of 20N fertilization, (c) after 16 years of PK fertilization, (d) after 16 years of

20NPK fertilization.

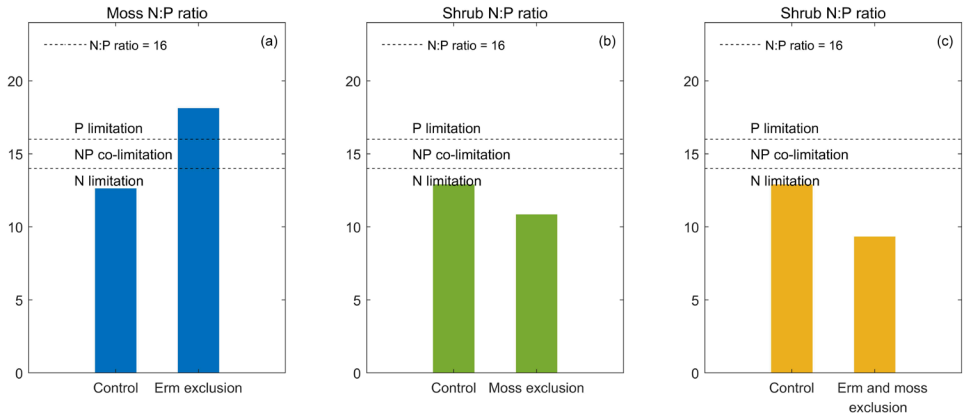

Figure S4.12 Simulated N:P ratios for (a) mosses biomass and (b) shrub foliar biomass from different ‘Exclusion’ experiments

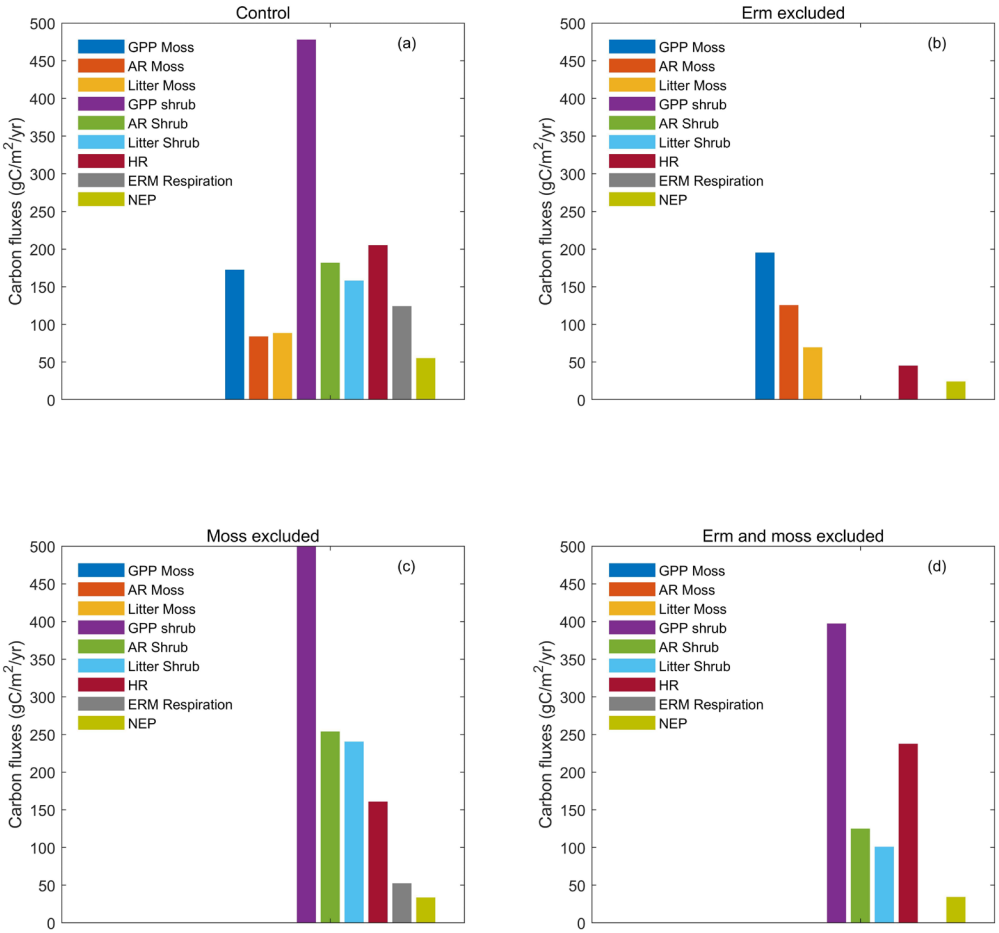

Figure S4.13 Simulated C fluxes from different model runs: (a) control; (b) ERM-exclusion experiment; (c) moss-exclusion experiment.

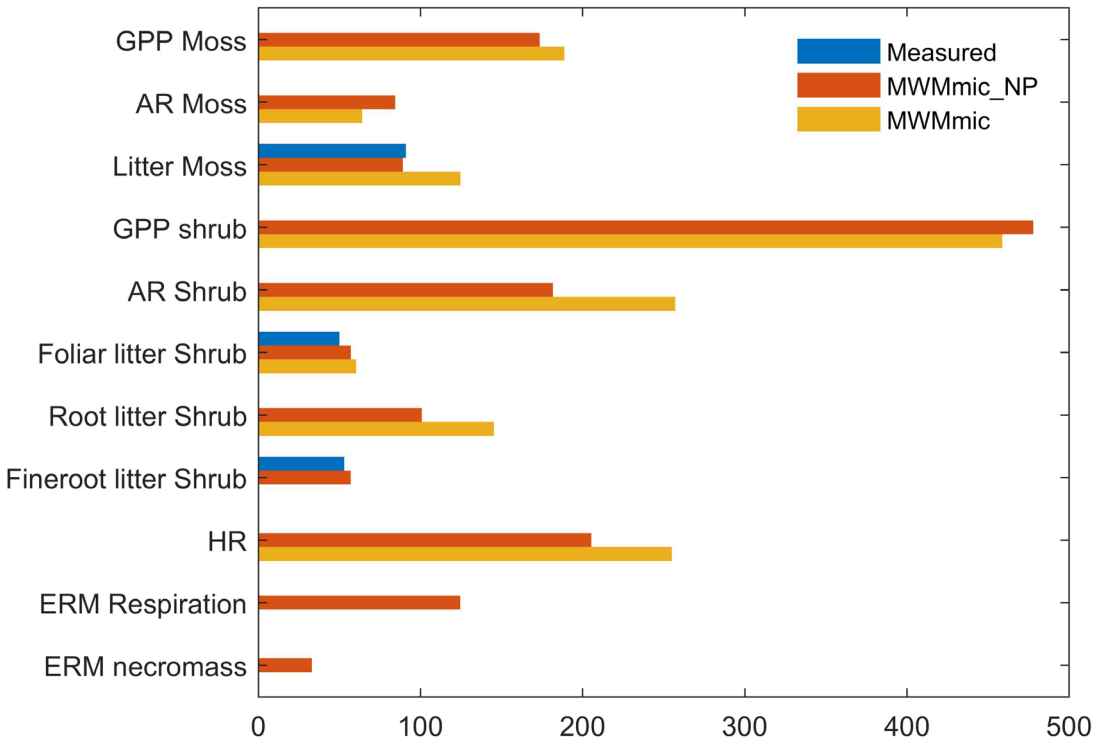

Figure S4.14 A breakdown of C budget simulated by MWMmic_NP and MWMmic, compared to available measurements.

Supplementary Text: Detailed description and equations of C-N-P model.

S1 Soil nutrient dynamics

S1.1 SOM depolymerization and DOM assimilation

Depolymerization of SOC into DOC is regulated by the biomass of Saprotrophs (SAP), substrate quantity and quality, and environmental conditions. Depolymerization of SON and SOP follows that of SOC in accordance with the stoichiometric ratios of SOM. Similarly, SAP takes up DON and DOP follows the stoichiometric ratios of the DOM.

$$DC_i^{deploy} = SOC_i * k_i^{SAP} * f(Q) * \frac{SAP\_C}{SAP\_C + KM_D^{SAP} * \sum_i SOC_i} * f(T) * f(W) \quad \text{(S1)}$$

$$DN_i^{deploy} = \frac{DC_i^{deploy}}{CN_{SOM,i}} \quad \text{(S2a)}$$

$$DP_i^{deploy} = \frac{DC_i^{deploy}}{CP_{SOM,i}} \quad \text{(S2b)}$$

$$DOC_{uptake} = V_{max,U} * SAP\_C * \frac{DOC}{DOC + KM_U^{SAP}} * f(T) * f(W) \quad \text{(S3)}$$

$$DON_{uptake} = \frac{DOC_{uptake}}{CN_{DOM}} \quad \text{(S4a)}$$

$$DOP_{uptake} = \frac{DOC_{uptake}}{CP_{DOM}} \quad \text{(S4b)}$$

where i represents the litter component (mosses or shrubs) in the cohort and k_i^{SAP} is the depolymerization base rate for the different component, $f(Q)$ is the substrate-quality multiplier which is determined by the remaining fraction of the peat with decomposition (see Section 2.1 in Chapter 1), $f(T)$ and $f(W)$ are the soil temperature and moisture multiplier, respectively (see Text. S1 in Chapter 1). KM_D^{SAP} and KM_U^{SAP} are the half-concentration constants for depolymerization and microbial DOC uptake, respectively.

1.2 SAP growth

The potential C assimilation by the SAP is the product of the SAP DOC uptake and the temperature-sensitive carbon use efficiency of SAPs (see Section 2.1 in Chapter 1).

$$SAP\_C^* = SAP\_C + CUE_{SAP} * DOC_{uptake} \quad \text{(S5)}$$

1.2.1 SAP nutrient assimilation

SAP could get its nutrients through DOM uptake and inorganic nutrient immobilization. We first calculated the potential nutrient uptake of SAPs from these two pathways (SAP_N^* and SAP_P^*). From the DOM uptake, there is a maximum fraction of nutrients that SAP could assimilate (NUE_{SAP} and PUE_{SAP}). Inorganic nutrient immobilization is regulated by the instant stoichiometric ratios of the SAP, which is volatile within the prescribed range.

$$SAP\_N^* = SAP\_N + DON_{uptake} * NUE_{SAP} + DIN_{immob}^{SAP} \quad \text{(S6a)}$$

$$SAP\_P^* = SAP\_P + DOP_{uptake} * PUE_{SAP} + DIP_{immob}^{SAP} \quad \text{(S6b)}$$

$$DIN_{immob}^{SAP} = V_{max,DIN}^{SAP} * SAP\_C * \frac{DIN}{DIN + KM_{DIN}^{SAP}} * N_{stress}^{SAP} * f(T) * f(W) \quad \text{(S7a)}$$

$$DIP_{immob}^{SAP} = V_{max,DIP}^{SAP} * SAP\_C * \frac{DIP}{DIP + KM_{DIP}^{SAP}} * P_{stress}^{SAP} * f(T) * f(W) \quad \text{(S7b)}$$

$$N_{stress}^{SAP} = min\left(max\left(\frac{CN\_SAP - CN\_SAP_{min}}{CN\_SAP_{max} - CN\_SAP_{min}}, 0.0\right), 1.0\right) \quad \text{(S7c)}$$

$$P_{stress}^{SAP} = \min\left(\max\left(\frac{CP\_SAP - CP\_SAP_{min}}{CP\_SAP_{max} - CP\_SAP_{min}}, 0.0\right), 1.0\right) \quad \text{(S7d)}$$

Where $V_{max,DIN}^{SAP}$ and $V_{max,DIP}^{SAP}$ are the base rates for SAP's DIN and DIP immobilization, respectively, KM_{DIN}^{SAP} and KM_{DIN}^{SAP} are the corresponding half saturation constants, CN_SAP and CP_SAP are SAP's instant C:N ratio and C:P ratio, CN_SAP_{min}, CN_SAP_{max}, CP_SAP_{min} and CP_SAP_{max} are the prescribed stoichiometric ranges for SAPs. N_{stress}^{SAP} and P_{stress}^{SAP} are the scaling factors relating the SAP's instant nutrient content (CN_SAP and CP_SAP) to the rates of inorganic nutrient immobilization. Immobilization is the largest when the nutrient content in the SAP is at its minimum and approached zero when the nutrient content in SAP reaches its maximum (Blagodatsky et al., 2011).

1.2.2 SAP C-N-P overflow

Overflow occurs when the potential C, N and P assimilation of SAP calculated from (Eq. S5-S6) result in a saturated element content of SAP outside its prescribed stoichiometric range. C saturation leads to C overflow in the form of increased microbial respiration. N or P saturation results in N or P overflow in the form of increased DIN or DIP mineralization.

$$IF\ SAP\_C^* > min\left(\frac{SAP\_N^*}{CN\_SAP_{max}}, \frac{SAP\_P^*}{CP\_SAP_{max}}\right)$$
$$THEN\ C_{overflow}^{SAP} = SAP\_C^* - min\left(\frac{SAP\_N^*}{CN\_SAP_{max}}, \frac{SAP\_P^*}{CP\_SAP_{max}}\right), ELSE\ C_{overflow}^{SAP} = 0.0 \quad \text{(S8a)}$$

$$IF\ SAP\_N^* > min\frac{\left(SAP\_C^*, \frac{SAP\_P^*}{CP\_SAP_{max}}\right)}{CN\_SAP_{min}}$$
$$THEN\ N_{overflow}^{SAP} = SAP\_N^* - min\frac{\left(SAP\_C^*, \frac{SAP\_P^*}{CP\_SAP_{max}}\right)}{CN\_SAP_{min}}, ELSE\ N_{overflow}^{SAP} = 0.0 \quad \text{(S8b)}$$

$$IF\ SAP\_P^* > min\frac{\left(SAP\_C^*, \frac{SAP\_N^*}{CN\_SAP_{max}}\right)}{CP\_SAP_{min}}$$
$$THEN\ P_{overflow}^{SAP} = SAP\_P^* - min\frac{\left(SAP\_C^*, \frac{SAP\_N^*}{CN\_SAP_{max}}\right)}{CP\_SAP_{min}}, ELSE\ P_{overflow}^{SAP} = 0.0 \quad \text{(S8c)}$$

$$SAP\_C_{growth} = DOC_{uptake} * CUE_{SAP} - C_{overflow} \quad \text{(S9a)}$$

$$SAP\_N_{growth} = DON_{uptake} * NUE_{SAP} + DIN_{immob} - N_{overflow} \quad \text{(S9b)}$$

$$SAP\_P_{growth} = DOP_{uptake} * PUE_{SAP} + DIP_{immob} - P_{overflow} \quad \text{(S9c)}$$

where SAP_C_{growth}, SAP_N_{growth} and SAP_P_{growth} are the actual SAP growth in C, N and P content after accounting for the C, N and P overflow, which are $C_{overflow}$, $N_{overflow}$ and $P_{overflow}$ respectively. These overflows add to the gross mineralization of the corresponding element.

$$R_{SAP} = DOC_{uptake} * (1 - CUE_{SAP}) + C_{overflow} \quad \text{(S10a)}$$

$$DIN_{mineral}^{SAP} = DON_{uptake} * (1 - NUE_{SAP}) + N_{overflow} \quad \text{(S10b)}$$

$$DIP_{mineral}^{SAP} = DOP_{uptake} * (1 - PUE_{SAP}) + P_{overflow} \quad \text{(S10c)}$$

Strongly controlled by the demand for P rather than the need for energy, inorganic P could be biochemically mineralized (phosphatase enzymes-mediated) from organic matter without releasing CO_2 (McGill and Cole 1981). Phosphatase enzymes are rich in N. Studies have shown that terrestrial plants and microbes can allocate excess N to produce the phosphatase enzymes to alleviate P limitation (Marklein and Houlton 2012; Chen et al., 2020). To account for this observed link, P biochemical mineralization of SAP are regulated by its N:P status (Goll et al., 2017).

$$P_{bcm,i}^{SAP} = SOP_i * V_{max,bcm}^{SAP} * \frac{SAP_C}{SAP_C + KM_D^{SAP} * \sum_i SOC_i} * f(T) * f(W) * f(CP_{SOM,i}) * f(NP_{SAP}) \quad \text{(S11a)}$$

$$f(CP_{SOM}) = \frac{1}{1 + CP_{SOM,i} * K_{bcm}^{CP}} \quad \text{(S11b)}$$

$$f(NP_{SAP}) = \min\left(\max\left(\left(\frac{NP\_SAP - NP\_SAP_{min}}{NP\_SAP_{max} - NP\_SAP_{min}}\right)^{\alpha_{SAP}^{P}}, 0.0\right), 1.0\right) \quad \text{(S11c)}$$

where $V_{max,bcm}^{SAP}$ is the substrate-independent base rate of SAP's P biochemical mineralization, $f(CP_{SOM})$ is the scaler constraining the P biochemical mineralization rates under high peat C:P ratio, K_{bcm}^{CP} is the half-saturation constant of peat P:C ratio. $f(NP_{SAP})$ is the scaler relating the instant NP status of SAP to its P biochemical mineralization, NP_SAP is SAP's instant N:P ratio. Maximum P biochemical rate is reached when NP_SAP equals NP_SAP_{max}, and P biochemical rate is zero when NP_SAP reaches NP_SAP_{min}. α_{SAP}^{P} represented the power of the N:P status regulation, and the larger it is the stronger the regulation is.

1.3 SAP turnover

When SAPs die, 50% of the dead SAP is recycled back to the SOM pool as necromass, while the other 50% is back to the DOM pool. 20% of the necromass is recycled to the moss pool while the other 80% to the shrub pool.

$$Death_{SAP}^{DOM} = frac_{Death_{SAP}}^{DOM} * SAP\_M_{death} \quad \text{(S12a)}$$

$$Death_{SAP}^{SOM} = frac_{Death_{SAP}}^{SOM} * SAP\_M_{death} \quad \text{(S12b)}$$

$$Death_{SAP}^{SOM_{moss}} = frac_{SAP_{necro}}^{moss} * Death_{SAP}^{SOM} \quad \text{(S12c)}$$

$$Death_{SAP}^{SOM_{shrub}} = frac_{SAP_{necro}}^{shrub} * Death_{SAP}^{SOM} \quad \text{(S12d)}$$

where M here represents C, N or P, $Death_{SAP}^{SOM}$ and $Death_{SAP}^{DOM}$ are the part of dead SAP that is recycled to SOM and DOM pool, respectively, $frac_{Death_{SAP}}^{DOM}$ and $frac_{Death_{SAP}}^{SOM}$ are the proportions of SAP death allocated to DOM and SOM pools, and both of them equal 50%, $Death_{SAP}^{SOM_{moss}}$ and $Death_{SAP}^{SOM_{shrub}}$ represent the part of SAP necromass that is recycled to moss and shrub pool. $frac_{SAP_{necro}}^{moss}$ and $frac_{SAP_{necro}}^{shrub}$ are the proportions of SAP necromass allocated to the moss and shrub litter pools, which equal 20% and 80%, respectively.

Turnover rate of SAP is a density-dependent function (See Section 3.3, Chapter 1). Turnover of SAP_N follows that of SAP_C. However, SAP_P turnover rate is down-regulated here by P_{stress}^{SAP} to attain the relatively high microbial P content measured at the Mer Bleue (Basiliko et al., 2006) with very low P availability in the peat. Microbes facing P limitation were reported to decrease their phosphorus (P) turnover rates while maintained carbon turnover rates (Spohn et al., 2016b). Thus, a scaling factor is added here to decrease the turnover rate of SAP_P when it is low.

$$Deathrate_{SAP} = Deathrate0_{SAP} * \left(\frac{Density_{SAP\_C}}{Ref\_Density_{SAP\_C}}\right)^{\beta_{SAP}^{Death}} * f(W) \quad \text{(S13)}$$

$$SAP\_C_{death} = SAP\_C * Deathrate_{SAP} \quad \text{(S14a)}$$

$$SAP\_N_{death} = SAP\_N * Deathrate_{SAP} \quad \text{(S14b)}$$

$$SAP\_P_{death} = SAP\_P * Deathrate_{SAP} * scal_{SAP}^{P} \quad \text{(S14c)}$$

$$scal_{SAP}^{P} = exp(\beta_{SAP}^{Pdeath} * P_{stress}^{SAP}) \quad \text{(S14d)}$$

where $Ref\_Density_{SAP\_C}$ and β_{SAP}^{Death} are parameters that control the magnitude of turnover rate down-regulation when microbial density is low, $scal_{SAP}^{P}$ is the scaling factor relating the P_{stress}^{SAP} to turnover rate of SAP_P. β_{SAP}^{Pdeath} is the reduction factor describing the magnitude of SAP_P_{death} downregulation with high P_{stress}^{SAP}.

1.4 Solute transport

Fick's law is applied to calculate the diffusion of different dissolved solutes between

cohorts with a diffusion coefficient corrected for moisture content:

$$DM_{diff_{bot,j}} = \begin{cases} \frac{DMconc_j - DMconc_{j+1}}{\lambda_i} * D_{DM,j}, & DMconc_j \geq DMconc_{j+1} \\ \frac{DMconc_{j+1} - DMconc_j}{\lambda_j} * D_{DM,j}, & DMconc_{j+1} < DMconc_j \end{cases} \quad \text{(S15a)}$$

$$DM_{diff_{top,j}} = DM_{diff_{bot,j}} - 1 \quad \text{(S15b)}$$

$$D_{DM,j} = D_{DM,0} * Porosity_j^2 \quad \text{(S15c)}$$

where j represent the serial number of a certain cohort layer counting from the peat surface, DM stands for all the dissolved matter (DOC, DON, DIN, DOP, DIP). $DM_{diff_{bot,j}}$ is the DM diffusion in cohort j to cohort below and $DM_{diff_{top,j}}$ is the DM diffusion to cohort j from the cohort above, the $DMconc_j$ is the DM concentration in cohort j, $D_{DM,j}$ is the effective diffusion coefficient in cohort j, $D_{DM,0}$ is the base diffusion coefficient, $Porosity_j$ is the porosity in cohort j which is calculated based on the degree of decomposition (Frolking et al., 2010).

Calculation of water fluxes including runoff and advection could be found in Section 2.1, Chapter 1. Dissolved N transport N_{leach} is simply calculated as the product of water fluxes and DOC concentration, while Dissolved P transport is downregulated by a scaler $f_{leach,P}$ to implicitly account for the reduced mobility of P in water resulted from its sorption onto SOM.

$$N_{leach} = \frac{N_{sol}}{W*\lambda}(runoff + advection) \quad \text{(S16a)}$$

$$P_{leach} = \frac{P_{sol}}{W*\lambda} * (runoff + advection) * f_{leach,P} \quad \text{(S16b)}$$

where N_{sol} represents all the dissolved N pools, P_{sol} represents all the dissolved pools. Here we assumed that DIP and DOP have the same mobility, because research into the movement of DOP is still unclear (McDowell et al., 2021), and contrasting results about the mobility of DOP compared to DIP have been reported (Berg and Joern, 2006).

S2 Plant nutrient dynamics

2.1 C allocation to respiration

The potential C available for plant growth is derived from subtracting plant maintenance

respiration from the newly fixed C from photosynthesis. Plant's total maintenance respiration CF_{mr} is the sum of each compartment's own maintenance respiration, which is determined by temperature and the N content of each compartment, respectively.

$$G_{C,pot} = GPP - CF_{mr} - CF_{GPP,reserv\_repl} \quad \text{(S17a)}$$

$$CF_{mr} = \sum_{X} X\_N * MR_{base} * f_{veg}(T)) \quad \text{(S17b)}$$

$$f_{veg}(T) = \left(3.22 - (0.046 * Tair)\right)^{\left(\frac{Tair-20.0}{10.0}\right)} \quad \text{(S18)}$$

where GPP is the gross primary production representing the newly fixed C from photosynthesis, $G_{C,pot}$ is the potential C available for plant growth, CF_{mr} is the plant's total maintenance respiration needed to support live tissues, X represents different plant tissues (foliar, fine roots, stems, and coarse roots), X_N is the nitrogen content of each plant tissue, MR_{base} is the base maintenance respiration rate, $f_{veg}(T)$ represents the temperature multiplier.

C is extracted from the reserve C pool when GPP is smaller than the total maintenance respiration. To account for scenarios when the reserve C pool is depleted, we adopted the method from the Community Land Model (CLM) (Lawrence et al., 2011): The C storage in the reserve pool can run a deficit at any time and get replenished later by the newly fixed C when GPP is larger than the maintenance respiration again. The C reserve pool will continuously get replenished from GPP until it reaches the minimum level required for the plants to survive (defined as a fraction of the size of the storage organ, which are the woody tissues) (Dietze et al., 2014). A great advantage of this approach is the elimination of the need to know in advance the total C requirement for maintenance respiration in any period (Lawrence et al., 2011).

$$CF_{reserv,mr} = \begin{cases} 0, & CF_{mr} \le GPP \\ CF_{mr} - GPP, & CF_{mr} > GPP \end{cases} \quad \text{(S19a)}$$

$$CF_{GPP,reserv}^{repl,pot} = \begin{cases} 0, & CF_{mr} > GPP \\ C_{res,min} - C_{res}/\tau_{repl}, & CF_{mr} \le GPP \end{cases} \quad \text{(S19b)}$$

$$C_{res,min} = frac_{min} * (croot\_C + stem\_C) \quad \text{(S19c)}$$

$$CF_{GPP,reserv}^{repl} = \begin{cases} 0, & CF_{GPP,reserv}^{repl,pot} \le GPP - CF_{mr} \\ \max(GPP - CF_{mr}, 0), & CF_{GPP,reserv}^{repl,pot} > GPP - CF_{mr} \end{cases} \quad \text{(S19d)}$$

Where $CF_{reserv,mr}$ is the extraction of C from the reserve C pool to meet the needs of maintenance respiration, $C_{res,min}$ is the prescribed minimum level of the reserve C pool inside the storage organs that is required to sustain the plant, $frac_{min}$ is the prescribed ratio of $C_{res,min}$ to the size of the woody tissues as storage organs (note that due to the lack of woody tissues, the $C_{res,min}$ and $frac_{min}$ are both set to be zero for mosses), $CF_{GPP,reserv}^{repl,pot}$ and $CF_{GPP,reserv\_repl}$ are the potential and actual C allocated from GPP to replenish the C reserve pool, respectively, τ_{repl} is the time constant controlling the rate of replenishment of C_{res}.

2.2 C allocation to growth

2.2.1 Growth allometry

The newly fixed C, after accounting for plant maintenance respiration is allocated to grow foliar biomass (B_{foliar}) and fine root biomass (B_{froot}) based on a 1:1 ratio (Thornton et al., 2007). For the growth of woody tissue, stems (B_{stem}) and coarse roots (B_{croot}), we adopted the approach of ForCent model (Parton et al., 2010) that C allocation to woody tissues only takes place when the maximum leaves or fine roots that can be supported by the biomass of current woody tissues has been attained. Measurements of shrub compartments at Mer Bleue Bog (Murphy et al., 2009, 2010; Xing et al., 2010) are used to derive the relationship between B_{foliar} and $B_{stem,min}$ (the minimum stem biomass needed to support it), and the relationship between $(B_{foliar} + B_{stem})$ (shoot biomass) and $B_{croot,min}$ (the minimum coarse root biomass needed to support it) both in the form of power function.

$$B_{stem,min} = a_1 * \left(B_{foliar}\right)^{a_2} \quad \text{(S20a)}$$

$$B_{croot,min} = a_3 * \left(B_{foliar} + B_{stem}\right)^{a_4} \quad \text{(S20b)}$$

Where a_1, a_2, a_3, and a_1 are all parameters derived from curve-fitting. The exponential a_2 is larger than 1.0, suggesting that more stem biomass is proportionally required to support more foliar biomass. This is in line with that upward tree growth requires an increase in supporting stem diameter (Sitch et al., 2003) and a constant ratio of leaf area to sapwood cross-sectional area from the classic pipe model (Shinozaki et al., 1964). On the

contrary, the exponential a_4 is smaller than 1.0, consistent with the finding from Mokany et al. (2006) that the root: shoot ratios were found to be negatively related to shoot biomass.

2.2.2 Root

Vertical root distribution is modeled using the asymptotic equation described by Gale and Grigal (1987) and Jackson et al. (1996). The root systems of the ericaceous shrubs at Mer Bleue adapt poorly to anoxia thus have a high distribution parameter β (Murphy et al., 2009, 2010). To account for the negative effects of high WT on shrub root growth, a scaling factor is deployed here relating the WTD to root growth status. β could also increase with larger WTD, indicating greater root production at depth with lower water table (Murphy et al.,2010). We adopted the empirical functions derived from Murphy et al. (2010) to account for this dynamic root distribution.

$$frac\_root_{cumulative} = 1 - \beta^d \quad \text{(S21a)}$$

$$scal_{root,X} = 1 - (\beta_X)^{WTD} \quad \text{(S21b)}$$

$$\beta_{froot} = a_5 * \left(WTD_{growing\_season}\right)^{a_6} \quad \text{(S21c)}$$

$$\beta_{croot} = a_7 * WTD_{growing\_season} + a_8 \quad \text{(S21d)}$$

Where Eq. S18(a) is the classic root distribution equation adopted from Jackson et al. (1996), β is the distribution parameter and high β indicates greater root distribution at depth, d is the depth, $scal_{root,X}$ is the scaling factor accounting for the inhibition effects of WT on shrub root growth with its calculation based on Eq. S18(a) and the assumption that WTD is the maximum rooting depth, a_5, a_6, a_7, and a_8 are all parameters derived from Murphy et al. (2010) to describe the dynamic root distribution with changing growing-season water table. The root growth coefficient is updated on a monthly basis.

2.3 CNP allocation to growth

2.3.1 Potential CNP allocation to growth

The minimum nutrients needed to grow plant biomass using the $G_{C,pot}$ (see Section S2.1), is calculated based on fractions of C allocated to each plant tissue (see Section S2.2), and the

minimum stoichiometric needs of each plant tissue.

$$G_{N,pot\_min} = (CN_{fol,max}f_{fol} + CN_{froot,max}f_{froot} + CN_{stem,max}f_{stem} + CN_{croot,max}f_{croot}) * (1 - r_g) * G_{C,pot} \quad \text{(S22a)}$$

$$G_{P,pot\_min} = (CP_{fol,max}f_{fol} + CP_{froot,max}f_{froot} + CP_{stem,max}f_{stem} + CP_{croot,max}f_{croot}) * (1 - r_g) * G_{C,pot} \quad \text{(S22b)}$$

where G_{N,pot_min} and G_{P,pot_min} are the minimum N and P needed to build plant tissues with the $G_{C,pot}$, $CM_{X,max}$ (M represents N or P, X represents different plant tissues) is the minimum stoichiometric needs to build different compartment, r_g is the fraction of allocated C lost as growth respiration.

Flexible stoichiometry for plant compartment is applied here, allowing the plant to build biomass with nutrient concentrations greater than the minimum stoichiometric needs when nutrient supply is high.

$$G_{N,pot\_max} = G_{N,pot\_min} * (1 + D^N_{leaf}) \quad \text{(S22c)}$$

$$G_{P,pot\_max} = G_{P,pot\_min} * (1 + D^P_{leaf}) \quad \text{(S22d)}$$

$$D^N_{leaf} = 1 + D_{max} * \left(\frac{CN_{fol} - CN_{fol,min}}{CN_{fol,max} - CN_{fol,min}}\right) \quad \text{(S23a)}$$

$$D^P_{leaf} = 1 + D_{max} * \left(\frac{CP_{fol} - CP_{fol,min}}{CP_{fol,max} - CP_{fol,min}}\right) \quad \text{(S23b)}$$

where G_{N,pot_max} and G_{P,pot_max} are maximum amount of N and P that the plant's new growth could incorporate, G_{N,pot_min} and G_{P,pot_min} are minimum amount of N and P that the plant's new potential growth requires, D^N_{leaf} and D^P_{leaf} are elasticity parameters used to dampen the temporal variations in tissue nutrient content (Zaehle et al., 2010; Goll et al., 2017), $CN_{fol,min}$, $CN_{fol,max}$, $CP_{fol,min}$, and $CP_{fol,max}$ are stoichiometric boundaries for foliar biomass which are used to calculate the D^N_{leaf} and D^P_{leaf}. D_{max} is the parameter that determined the stoichiometry elasticity.

2.3.1 Actual CNP allocation to growth

Plant uses nutrients stored in the nutrient reserve pool to build its biomass. When nutrient supply is more than enough to support the minimum nutrients need (G_{N,pot_min} and G_{P,pot_min}), plant uses more N and P to build its biomass. The surplus N and P used for plant growth is determined by the minimum of the nutrient reserve pool, and G_{M,pot_min} (M

represents N or P) after accounting for the maximum elasticity in nutrient concentration.

$$G_N = \min(N_{reserve}^{veg}, G_{N,pot\_max}) \quad \text{(S24a)}$$

$$G_P = \min(P_{reserve}^{veg}, G_{P,pot\_max}) \quad \text{(S24b)}$$

Where G_N and G_P are the actual N and P used for plant growth, $N_{reserve}^{veg}$ and $P_{reserve}^{veg}$ represent the N and P reserve pool, respectively.

Nutrient limitation occurs when the nutrients stored in the nutrient reserve pool are not enough to support the minimum nutrients needed to grow plant biomass using the $G_{C,pot}$. The actual C that is used for plant growth is proportionally downregulated from $G_{C,pot}$. This will lead to a C overflow from GPP into the C reserve pool to account for the C that is not able to be converted into plant biomass. Similarly, when high WT inhibits the root growth (see Section S2.2), a C overflow into the C reserve pool will also occur to account for the C that is not able to be converted into root tissue.

$$G_C = \begin{cases} min\left(\frac{N_{reserve}^{veg}}{G_{N,pot\_min}}, \frac{P_{reserve}^{veg}}{G_{P,pot\_min}}\right) * G_{C,pot}, & N_{reserve}^{veg} < G_{N,pot\_min} \; or \; P_{reserve}^{veg} < G_{P,pot\_min} \\ G_{C,pot}, & N_{reserve}^{veg} \geq G_{N,pot\_min} \; and \; P_{reserve}^{veg} \geq G_{P,pot\_min} \end{cases} \quad \text{(S25)}$$

$$IF\ min\left(\frac{N_{reserve}^{veg}}{G_{N,pot\_min}}, \frac{P_{reserve}^{veg}}{G_{P,pot\_min}}\right) > 1.0, \quad THEN\ No\ NP\ limitation, N_{limit} = 1.0, P_{limit} = 1.0 \quad \text{(S26a)}$$

$$IF\ \frac{N_{reserve}^{veg}}{G_{N,pot\_min}} < 1.0, \quad THEN\ N\ limitation, N_{limit} = max\ (0.0, \frac{N_{reserve}^{veg}}{G_{N,pot\_min}}) \quad \text{(S26b)}$$

$$IF\ \frac{P_{reserve}^{veg}}{G_{P,pot\_min}} < 1.0, \quad THEN\ P\ limitation, P_{limit} = max\ (0.0, \frac{P_{reserve}^{veg}}{G_{P,pot\_min}}) \quad \text{(S26c)}$$

$$CF_{GPP,reserv}^{overflow} = max(0.0, G_{C,pot} - G_C) + \sum_{X}^{X=froot_{shrub}, croot_{shrub}} CF_{GPP,X} * (1 - scal_{root,X}) \quad \text{(S27)}$$

where G_C is the actual C from GPP that is used for plant growth, N_{limit} and P_{limit} described the degree of N and P limitation, respectively, $CF_{GPP,reserv}^{overflow}$ is the C overflow resulted from either nutrient limitation on plant growth and/or high-WT inhibition on shrub root growth, $scal_{root,X}$ is the scaling factor accounting for the inhibition effects of WT on shrub root growth (Eq. S21(b)).

2.4 Nutrient resorption and acquisition

We parameterized different pathways for mosses and shrubs to acquire nutrients. Shrub

can acquire nutrients from direct root uptake, ERM organic nutrient transfer and nutrient resorption from litter production. Mosses in our model do not have access to ERM nutrients, but they can get nutrients directly from atmospheric deposition and fix N2 from the atmosphere (Živković 2019). We have also parameterized a "virtual root" for mosses to take up nutrients directly from the inorganic nutrient pools like the shrub roots, in line with the evidence of Sphagnum mosses taking up nutrients through capillary water transport (Damman et al., 1978; Jauhiainen et al., 1999). All the acquired nutrients are placed in the nutrient reserve pool first and are later used to grow plant biomass (see Section S2.3.2).

$$\frac{\partial}{\partial t}N_{reserve}^{veg} = N_{uptake}^{root,veg} + N_{resorp}^{veg} + N_{transfer}^{Erm,shrub} + N_{deposition}^{moss} + N_{N_2\,fixation}^{moss} - G_N \quad \text{(S28a)}$$

$$\frac{\partial}{\partial t}P_{reserve}^{veg} = P_{uptake}^{root,veg} + P_{resorp}^{veg} + P_{deposition}^{moss} + P_{transfer}^{Erm,shrub} - G_P \quad \text{(S28b)}$$

Where $N_{uptake}^{root,veg}$ and $P_{uptake}^{root,veg}$ is the nutrients uptake by the shrub roots or the "virtual root" of mosses, N_{resorp}^{veg} and P_{resorp}^{veg} are the nutrients resorbed from litter production $N_{transfer}^{Erm,shrub}$ and $P_{transfer}^{Erm,shrub}$ are the nutrients transferred from ERM to shrubs, $N_{deposition}^{moss}$ and $N_{N_2\,fixation}^{moss}$ are nutrients moss absorbed from atmospheric deposition and N_2 fixation, respectively, which is described in more detail in Section 2.4.3.

2.4.1 Nutrient resorption

Plants in the model resorb a fix fraction of nutrients and carbon from litter production.

$$N_{resorp}^{veg} = \sum_X (N_X * \frac{frac_{resorp,X}^{N}}{\tau_{X,veg}}) \quad \text{(S29a)}$$

$$P_{resorp}^{veg} = \sum_X (P_X * \frac{frac_{resorp,X}^{P}}{\tau_{X,veg}}) \quad \text{(S29b)}$$

$$C_{resorp}^{veg} = \sum_X (C_X * \frac{frac_{resorp,X}^{C}}{\tau_{X,veg}}) \quad \text{(S29c)}$$

Where N_{resorp}^{veg}, P_{resorp}^{veg}, and C_{resorp}^{veg} are the amount of resorption for N, P, and C respectively for different plant tissues, $frac_{resorp,X}^{P}$, $frac_{resorp,X}^{P}$ and $frac_{resorp,X}^{P}$ are the fixed resorption efficiencies for each elements, $\tau_{X,veg}$ are their corresponding turnover time of each tissue of each PFT.

2.4.2 Nutrient root uptake

Plant nutrient uptake is assumed to be proportional to the fine root biomass and regulated by the availability of the soil inorganic nutrient, the nutrient status of the plants and environmental conditions (Zaehle et al., 2010). The effect of soil nutrient availability is described in the form of a Michaelis-Menten function (Ghimire et al., 2016). A nutrient demand scaler is adopted here to account for the observed increase in nutrient uptake in nutrient starved plants (Cardenas-Navarro et al., 1999), which is calculated as follows: Firstly, we adopted the method utilized in Sulman et al. (2019) to calculate the nutrient stress scaler, which is calculated by comparing the reserve nutrient pool to a target value equivalent to double the leaf and fine root nutrient content (only leaves in the case of mosses); then the nutrient demand scaler is the minimum of 1.0 and nutrient stress to avoid the nutrient uptake rate exceeds its prescribed capacity.

$$N_{uptake,veg}^{root}$$

$$= \begin{cases} V_{max,DIN}^{shrub} * B_{froot} * \dfrac{DIN}{DIN + KM_{DIN,shrub}} * f_{veg}(T) * f(W) * scal_{veg}^{N} * scal_{ERM}, & veg = shrub \\ V_{max,DIN}^{moss} * B_{moss} * \dfrac{DIN}{DIN + KM_{DIN,moss}} * f_{veg}(T) * f(W) * scal_{veg}^{N} * scal_{moss}^{N}, & veg = moss \end{cases} \quad \text{(S30a)}$$

$$P_{uptake,veg}^{root}$$

$$= \begin{cases} V_{max,DIP}^{shrub} * B_{froot} * \dfrac{DIP}{DIP + KM_{DIP,shrub}} * f_{veg}(T) * f(W) * scal_{veg}^{P} * scal_{ERM}, & veg = shrub \\ V_{max,DIP}^{moss} * B_{moss} * \dfrac{DIP}{DIP + KM_{DIP,moss}} * f_{veg}(T) * f(W) * scal_{veg}^{P} * scal_{moss}^{P}, & veg = moss \end{cases} \quad \text{(S30b)}$$

$$scal_{veg}^{N} = min\,(1{,}0, N_{stress}^{veg}) \quad \text{(S31a)}$$

$$scal_{veg}^{P} = min\,(1{,}0, P_{stress}^{veg}) \quad \text{(S31b)}$$

$$N_{stress}^{veg} = \frac{2*(foliar\_N + froot\_N) - N_{reserve}^{veg}}{2*(foliar\_N + froot\_N)} \quad \text{(S31c)}$$

$$P_{stress}^{veg} = \frac{2*(foliar\_P + froot\_P) - P_{reserve}^{veg}}{2*(foliar\_P + froot\_P)} \quad \text{(S31d)}$$

where $V_{max,DIN}^{veg}$ and $V_{max,DIP}^{veg}$ (veg is shrub or moss) are the base uptake rates of DIN and DIP, respectively, B_{froot} is the shrub root biomass and B_{froot} is the moss biomass, the distribution of those biomass in the peat profile for nutrient uptake is calculated based on their root distribution parameter β (see Section 2.2.2), $KM_{DIN,veg}$ and $KM_{DIP,veg}$ are the half saturation constant for the calculation of DIN and DIP availability, $f_{veg}(T)$ is the temperature multiplier, $f(W)$ are the soil moisture multiplier, N_{stress}^{veg} and P_{stress}^{veg} are the N and P stress

scaler, respectively, $scal_{ERM}$, $scal_{moss}^{N}$ and $scal_{moss}^{P}$ are the additional scalers that modify the shrub and moss uptake, respectively. Shrub root uptake is inhibited by mycorrhiza colonization (Taylor and Alexander 2005; Hobbie et al., 2008), whereas moss nutrient uptake is regulated by its NP status. sphagnum N:P imbalance could impose physiological stress (Limpens et al., 2011) (Eq. S36), so we assume in the model that mosses could upregulate its P uptake to alleviate the negative effects of excessive N concentration.

$$scal_{ERM} = exp\left(m_1 * min\ (1.0, \frac{Erm\_C}{m_2 * froot\_C})\right) \quad \text{(S32a)}$$

$$scal_{moss}^{N} = max\left(min\left(\frac{NP_{moss} - NP_{moss,min}}{NP_{moss,max} - NP_{moss,min}}\right), 0.0\right) \quad \text{(S33a)}$$

$$scal_{moss}^{P} = 1 - scal_{moss}^{N} \quad \text{(S33b)}$$

Where Erm_C is the C content in ERM biomass, $froot\_C$ is the C content in fine root biomass, m_1 and m_2 are the parameters determining the magnitude of ERM inhibition effect on root, $NP_{moss,max}$ and $NP_{moss,min}$ are the stoichiometric boundaries used to calculate $scal_{moss}^{N}$ and $scal_{moss}^{P}$.

2.4.3 Specific processes for mosses

Mosses can directly assimilate nutrients from atmospheric deposition. Here we parameterize this process to be relatively passive: the assimilation of the airborne nutrients only ceases when the nutrient saturation is reached (nutrient stress scaler equals zero). The part of nutrient deposition that cannot be assimilated by moss due to saturation becomes nutrient throughfall and is added into the soil inorganic nutrient pool of the peat surface cohort.

$$M_{deposition}^{moss} = \begin{cases} M_{dep}, & scal_{moss}^{M} > 0 \\ 0.0, & scal_{moss}^{M} = 0 \end{cases} \quad \text{(S34a)}$$

$$M_{throughfall} = M_{dep} - M_{deposition}^{moss} \quad \text{(S34b)}$$

where M represents N or P, $M_{deposition}^{moss}$ is the amount of nutrient deposition that is directly assimilated by mosses, $M_{throughfall}$ is the amount of nutrient deposition that reaches the peat surface.

When the growth of mosses is nutrient limited, the resulted surplus C in mosses is directly respired out as an C overflow due to the lack of woody tissues as storage organs for C

reserve. However, the C overflow caused by N limitation (see Section S2.3.2) is assumed to be spent on N_2 fixation in the model. The rate of N_2 fixation is calculated by dividing the total C expenditure on N_2 fixation by its C cost (Fisher et al., 2010). The C cost of N_2 fixation is dependent on temperature, with the dependence function adapted from Houlton et al. (2008) and Meyerholt et al., (2016).

$$CF_{GPP,moss}^{overflow} = max\left(0.0, G_{C,pot} - G_C\right) \quad \text{(S35a)}$$

$$C_{fixation}^{moss} = \begin{cases} max\left(0.0, G_{C,pot} - G_C\right), & N_{limit} < P_{limit} \\ 0.0, & N_{limit} \geq P_{limit} \end{cases} \quad \text{(S35b)}$$

$$N_{fixation}^{moss} = \frac{C_{fixation}^{moss}}{N_{fixation\_cost}} \ (when\ N_{limit} < P_{limit}) \quad \text{(S36a)}$$

$$N_{fixation\_cost} = \frac{Cost0_{fix}}{exp\left(a_{fix} + b_{fix} * Tair * \left(1 - \frac{Tair}{c_{fix}}\right)\right)} \quad \text{(S36b)}$$

where $C_{fixation}^{moss}$ is the total C expenditure on N_2 fixation, $N_{fixation\_cost}$ is the C cost of N_2 fixation, $Cost0_{fix}$ is the base cost, a_{fix}, b_{fix} and c_{fix} are all parameters used to describe the dependance of C cost of N_2 fixation on temperature. $N_{fixation\_cost}$ decreases with increased temperature, indicating that the rate of N_2 fixation increases with higher temperature.

A scaler relating the excessive N concentration in moss to its C fixation is parameterized here, in a manner similar to that proposed by PEATBOG (Wu et al., 2013). This is in line with the finding that sphagnum N:P imbalance could impose physiological stress.

$$f_{N,toxic} = 1 - max\left(0.0, a_{N,tocix} * \left(NP_{moss} - 16.0\right)\right) \quad \text{(S37)}$$

where $f_{N,toxic}$ is the scaler applied to moss photosynthesis and respiration, $a_{N,tocix}$ determines the magnitude of the N toxic effect on mosses.

S3 Ericoid mycorrhiza fungi

3.1 C transfer from shrub to ERM

Non-structural carbohydrates (NSC) accumulate in the C reserve pool because of nutrient limitation of plant growth and/or high-WT inhibition on shrub root growth (Eq. S27). The size of this reserve pool is limited by the size of the storage organ (woody tissues) and a threshold

value for the ratio of C_{reserv}^{shrub} to $(stem\_C + croot\_C)$ is prescribed here (Zaehle et al., 2010) to avoid unrealistically high accumulation of NSC in plants (Edwards et al., 2002). If the storage level of C_{reserv}^{shrub} exceeds this threshold, shrubs start to translocate the excessive C out to ERM and root exudates (Schiestl-Aalto et al., 2019). This parameterization is in line with the finding that plant allocates C to mycorrhiza as an overflow (Corrêa et al., 2012) and the evidence that mycorrhiza fungi had access to stored C in the plant that is later used to support its maintenance respiration (Heinemeyer et al., 2012). The rate of this translocation is regulated by the level of nutrient stress (Sulman et al., 2019). The partitioning between root exudates and C transfer to ERM is fixed in the model.

$$\frac{\partial}{\partial t} C_{reserv}^{shrub} = CF_{GPP,reserv}^{overflow} + CF_{resorp} - CF_{reserv,mr} - C_{efflux} \quad \text{(S38)}$$

$$C_{efflux} = \begin{cases} 0, & C_{reserv}^{shrub} \le frac_{max} * (stem\_C + croot\_C) \\ C_{reserv}^{shrub} * rate_{out}^{shrub} * max(N_{stress}^{shrub}, P_{stress}^{shrub}), & C_{reserv}^{shrub} > frac_{max} * (stem\_C + croot\_C) \end{cases} \quad \text{(S39)}$$

$$C_{transfer}^{ERM} = C_{efflux} * frac_{efflux}^{ERM} \quad \text{(S40a)}$$

$$C_{exudates} = C_{efflux} * (1 - frac_{efflux}^{ERM}) \quad \text{(S40b)}$$

where $CF_{GPP,reserv}^{overflow}$ is the C overflow directed from GPP to C reserve pool (Eq. S27), CF_{resorp} is the C resorption from litter production, $CF_{reserv,mr}$ is the C extracted from the reserve pool to meet the demands for maintenance respiration, C_{efflux} is the translocation of C from C reserve pool when the storage level exceeds the prescribed threshold, $frac_{max}$is the prescribed maximum ratio of C_{reserv}^{shrub} to the size of storage organs $(stem\_C + croot\_C)$, $rate_{out}^{shrub}$ is the base rate of the C translocation from the reserve pool, $frac_{efflux}^{ERM}$ is the fixed parameter that partitions C_{efflux} to ERM $C_{transfer}^{ERM}$ and root exudates $C_{exudates}$.

3.2 CNP acquisition of ERM

To make easier the parameterization of carbon-nutrient exchange between shrub and ERM, we set up two pools for all the elements in ERM: a structural biomass pool and a separated reserve pool, in conformity with shrubs. The C transferred from shrub to ERM is first stored in the C reserve pool of ERM, which also takes in the C that ERM directly mines from the peat. ERM assimilates C from its C reserve pool in a manner similar to SAP's DOC uptake (Eq. S3).

$$\frac{\partial}{\partial t} C_{reserv}^{Erm} = C_{transfer}^{Erm} + C_{mining,assim}^{Erm} - C_{uptake}^{Erm} \quad \text{(S41)}$$

$$C_{uptake}^{Erm} = V_{max,U}^{Erm} * Erm\_C * \frac{C_{reserv}^{Erm}}{C_{reserv}^{Erm} + KM_U^{Erm}} * f(T) * f(W) \quad \text{(S42)}$$

where $C_{transfer}^{Erm}$ is the C transferred from shrub to ERM, $C_{mining,assim}^{Erm}$ is the C that ERM directly mines from the SOC pool, C_{uptake}^{Erm} is the C assimilation of ERM from the C reserve pool, C_{reserv}^{Erm} is ERM's reserve C pool, $V_{max,U}^{Erm}$ is the maximum C uptake rate, KM_U^{Erm} is the half saturation constant of ERM C assimilation, $f(T)$ and $f(W)$ are the soil temperature and moisture multiplier, the same ones applied for SAP's DOC uptake (Eq. S3).

Similar to plants, the nutrients acquired by ERM are first stored in the reserve nutrient pools. The maximum size of the reserve pool is limited, based on the prescribed minimum stoichiometric ratios which account for both the C and nutrient reserve pools. A nutrient stress scaler is calculated based on the size of the reserve nutrient pool and used to regulate the nutrient acquisition.

$$CNratio_{ERM} = \frac{(C_{reserve}^{ERM} + ERM\_C)}{(N_{reserve}^{ERM} + ERM\_N)} \quad \text{(S43a)}$$

$$CPratio_{ERM} = \frac{(C_{reserve}^{Erm} + ERM\_C)}{(P_{reserve}^{ERM} + ERM\_P)} \quad \text{(S43b)}$$

$$N_{stress}^{ERM} = min\left(max\left(\frac{CNratio_{ERM} - CNratio_{ERM}^{min}}{CNratio_{ERM}^{max} - CNratio_{ERM}^{min}}, 0.0\right), 1.0\right) \quad \text{(S44a)}$$

$$P_{stress}^{ERM} = max\left(min\left(\frac{CPratio_{ERM} - CPratio_{ERM}^{min}}{CPratio_{Erm}^{max} - CPratio_{ERM}^{min}}, 0.0\right), 1.0\right) \quad \text{(S44b)}$$

Where ERM_C, ERM_N, and ERM_P are the structural C, N and P content in ERM biomass, M_{reserv}^{ERM} is ERM's reserve nutrient pool (M stands for N or P), M_{stress}^{ERM} is the nutrient stress scaler calculated based on the nutrient status of ERM ($CMratio_{ERM}$), $CMratio_{ERM}^{max}$ and $CMratio_{ERM}^{min}$ are the prescribed boundaries. ERM builds its structural biomass based on a fixed stoichiometric ratio, which equals the $CMratio_{ERM}^{max}$, since $CMratio_{ERM}$ reaches $CMratio_{ERM}^{max}$ when M_{reserv}^{ERM} equals zero, indicating the depletion of nutrients in the nutrient reserve pool.

ERM is known to produce enzymes to break down a wide range of recalcitrant substrates for nutrient extraction (Smith and Read, 2010). This organic nutrient 'mining' is described using a Michaelis-Menten function similar to that used in the SAP biomass-regulated depolymerization. We have prescribed higher rates for ERM organic nutrient mining than

SAP's SOM depolymerization. This is in line with the superior capacity of ERM in accessing nutrients from recalcitrant substrates so that it can dominate the infertile soils characterized by acidic conditions and high content of polyphenolic compounds (Perotto et al., 2018).

A scaler relating N:P status of ERM to its P mining is applied here to account for the effect of N availability on P biochemical mineralization, similar to Eq. S11(b) adopted for SAP P biochemical mineralization. Although the effects of P availability on N cycling are much less understood and results varied across different fertilization studies (Chen et al., 2017; Xiao et al., 2018), activities of N acquisition enzymes were reported to significantly increased with the P fertilization treatment at Mer Bleue Bog (Pinsonneault et al., 2016a). Considering the fact that ERM could have larger investments on phosphatase enzyme production to satisfy the P need of shrubs, a weak-dependence function of N mining on P:N status is parameterized only for ERM N mining here.

$$N_{mining}^{ERM} = SON_i * k_{i,Nmining}^{ERM} * \frac{ERM\_C}{ERM\_C + KM_{mining}^{ERM} * \sum_i SOC_i} * N_{stress}^{ERM} * f(Q) * f(T) * f(W) * f(PN_{ERM}) \quad \text{(S45a)}$$

$$P_{mining}^{ERM} = SOP_i * V_{max,bcm}^{ERM} * \frac{ERM\_C}{ERM\_C + KM_{mining}^{ERM} * \sum_i SOC_i} * P_{stress}^{ERM} * f(T) * f(W) * f(NP_{ERM}) \quad \text{(S45b)}$$

$$f(PN_{ERM}) = \left(\frac{PNratio_{ERM} - PNratio_{ERM}^{min}}{PNratio_{ERM}^{max} - PNratio_{ERM}^{min}}\right)^{\alpha_{ERM}^{N}} \quad \text{(S45c)}$$

$$f(NP_{ERM}) = \left(\frac{NPratio_{ERM} - NPratio_{ERM}^{min}}{NPratio_{ERM}^{max} - NPratio_{ERM}^{min}}\right)^{\alpha_{Erm}^{P}} \quad \text{(S45d)}$$

$$NPratio_{ERM} = \frac{CNratio_{ERM}}{CPratio_{ERM}} \quad \text{(S46a)}$$

$$PNratio_{ERM} = \frac{1}{NPratio_{ERM}} \quad \text{(S46b)}$$

where $k_{i,Nmining}^{ERM}$ (i represents the litter component (mosses or shrubs) in the peat cohort) is the N mining rates of ERM, $V_{max,bcm}^{ERM}$ is the substrate-independent base rate of ERM's P biochemical mineralization, KM_{mining}^{ERM} is the half saturation constant accounting for the regulation of ERM biomass on nutrient mining, $f(Q)$, $f(T)$ and $f(W)$ are the same substrate-quality, soil temperature and soil moisture multipliers parameterized for SAP (see Section S1.1), $f(PN_{ERM})$ and $f(NP_{ERM})$ are the NP status scaler used to regulate ERM's N and P mining rate, respectively: maximum P (or N) mining rate is reached when $NPratio_{ERM}$ (or $PNratio_{ERM}$) equals $NPratio_{ERM}^{max}$ (or $PNratio_{ERM}^{max}$), α_{ERM}^{P} (or α_{ERM}^{N}) represents the

power of ERM's N:P status (or P:N status) regulation, and the larger it is the stronger the regulation is.

ERM in the model could also immobilize inorganic nutrients (Rains and Bledsoe, 2007), which is parameterized in a manner similar to that used for SAP nutrient immobilization (Eq. S7(a-b))

$$DIN_{immob}^{ERM} = V_{max,DIN}^{ERM} * \frac{DIN}{DIN+KM_{DIN}^{ERM}} * N_{stress}^{ERM} * f(T) * f(W) \quad \text{(S47a)}$$

$$DIP_{immob}^{ERM} = V_{max,DIP}^{ERM} * \frac{DIP}{DIP+KM_{DIP}^{ERM}} * P_{stress}^{ERM} * f(T) * f(W) \quad \text{(S47b)}$$

where $V_{max,DIN}^{ERM}$ and $V_{max,DIP}^{ERM}$ are the base rates for ERM's DIN and DIP immobilization, respectively, KM_{DIN}^{ERM} and KM_{DIN}^{ERM} are the corresponding half saturation constants.

We have also parameterized a C mining pathway for ERM to account for the observed saprotrophic capabilities of ERM fungi and a possible dual lifestyle (Martino et al., 2018). The Cmining rates prescribed for ERM are much smaller than SAP to let ERM in our model depend mostly on shrub C transfer. After accounting for the carbon use efficiency of the C mining (Sulman et al., 2019), the C mined from the peat is assimilated into the reserve C pool of ERM first (Eq. S41).

$$C_{mining}^{ERM} = SOC_i * k_{i,Cmining}^{ERM} * \frac{ERM\_C}{ERM\_C + KM_{mining}^{ERM} * \sum_i SOC_i} * f(Q) * f(T) * f(W) \quad \text{(S48a)}$$

$$C_{mining,assim}^{ERM} = C_{mining}^{ERM} * CUE_{Erm}^{Cmining} \quad \text{(S48b)}$$

where $k_{i,Cmining}^{ERM}$ (i represents the litter component (mosses or shrubs) in the peat cohort) is the C mining rates of ERM, $CUE_{ERM}^{Cmining}$ is the carbon use efficiency of ERM's C mining: ratio of the mined C that is assimilated into the C reserve pool to the ERM's total C mining.

The potential C, N and P assimilation of ERM into its structural biomass pools is thus calculated by summing up all the C-N-P acquisition flows described above:

$$ERM\_C^* = ERM\_C + CUE_{ERM}^{growth} * C_{uptake}^{ERM} \quad \text{(S49a)}$$

$$ERM\_N^* = ERM\_N + DIN_{immob}^{ERM} + N_{mining}^{ERM} \quad \text{(S49b)}$$

$$ERM\_P^* = ERM\_P + DIP_{immob}^{ERM} + P_{mining}^{ERM} \quad \text{(S49c)}$$

where ERM_C^*, ERM_N^* and ERM_P^* is the potential C, N and P assimilation of ERM into its structural biomass pools, respectively, CUE_{ERM}^{growth} is the fixed carbon use efficiency for ERM growth.

3.3 ERM C-N-P overflow

Like shrubs, ERM in the model can extract N and P from its corresponding nutrient reserve pool to fulfill its stoichiometric needs. ERM overflow occurs when the potential C, N and P assimilation of ERM (Eq. S49) combined with the demand-based extraction of nutrients from the reserve pools results in a saturated element content inside the ERM structural biomass (according to the prescribed fixed stoichiometric ratio of ERM structural biomass). While the C overflow leads to increased ERM respiration (Eq. S52), N and P overflows are directed into the corresponding reserve nutrient pool and awaits transport into the shrubs (Eq. S58). The actual growth of ERM structural biomass is thus calculated by subtracting the overflows from the potential growth.

$$IF\ ERM\_C^* > min\left(\frac{ERM\_N^*+N_{reserve}^{ERM}}{CN\_ERM}, \frac{ERM\_P^*+P_{reserve}^{ERM}}{CP\_ERM}\right)$$

$$THEN\ C_{overflow}^{ERM} = ERM\_C^* - min\left(\frac{ERM\_N^*+N_{reserve}^{ERM}}{CN\_ERM}, \frac{ERM\_P^*+P_{reserve}^{ERM}}{CP\_ERM}\right), ELSE\ C_{overflow}^{ERM} = 0.0 \quad \text{(S50a)}$$

$$IF\ (ERM\_N^* + N_{reserve}^{ERM}) > min\frac{\left(ERM\_C^*, \frac{ERM\_P^*+P_{reserve}^{ERM}}{CP\_ERM}\right)}{CN\_ERM}$$

$$THEN\ N_{overflow}^{ERM} = max\left(ERM\_N^* - \frac{min\left(ERM\_C^*, \frac{ERM\_P^* + P_{reserve}^{ERM}}{CP_{ERM}}\right)}{CN\_ERM}, 0.0\right), N_{extract}^{ERM} = \max\left(min\left(ERM\_C^*, \frac{ERM\_P^* + P_{reserve}^{ERM}}{CP\_ERM}\right) - ERM\_N^*, 0.0\right) \quad \text{(S50b)}$$

$$ELSE\ N_{overflow}^{ERM} = 0.0, N_{extract}^{ERM} = N_{reserve}^{ERM}$$

$$IF\ (ERM\_P^* + P_{reserve}^{ERM}) > min\frac{\left(ERM\_C^*, \frac{ERM\_N^*+N_{reserve}^{ERM}}{CN\_ERM}\right)}{CP\_ERM}$$

$$THEN\ P_{overflow}^{ERM} = max\left(ERM\_P^* - \frac{min\left(ERM\_C^*, \frac{ERM\_N^* + N_{reserve}^{ERM}}{CN_{ERM}}\right)}{CP\_ERM}, 0.0\right), P_{extract}^{ERM} = \max\left(min\left(ERM\_C^*, \frac{ERM\_N^* + N_{reserve}^{ERM}}{CN\_ERM}\right) - ERM\_P^*, 0.0\right) \quad \text{(S50c)}$$

$$ELSE\ P_{overflow}^{ERM} = 0.0, P_{extract}^{ERM} = P_{reserve}^{ERM}$$

$$ERM\_C_{growth} = ERM\_C^* - C_{overflow}^{ERM} \quad \text{(S51a)}$$

$$ERM\_N_{growth} = ERM\_N^* + N_{extract}^{ERM} - N_{overflow}^{ERM} \quad \text{(S51b)}$$

$$ERM\_P_{growth} = ERM\_P^* + P_{extract}^{ERM} - P_{overflow}^{ERM} \quad \text{(S51c)}$$

$$R_{ERM} = C_{overflow}^{ERM} + C_{mining}^{ERM} * \left(1 - CUE_{ERM}^{Cmining}\right) + C_{uptake}^{ERM} * \left(1 - CUE_{ERM}^{growth}\right) \quad \text{(S52)}$$

where CN_ERM and CP_ERM are the fixed stoichiometric ratios for ERM's structural biomass, $N_{reserve}^{ERM}$ and $P_{reserve}^{ERM}$ are the N and P stored in the ERM's reserve nutrient pools,

$N_{extract}^{ERM}$ and $P_{extract}^{ERM}$ are the nutrient extraction from the reserve pools to build ERM's structural biomass, $C_{overflow}^{ERM}$ is the C overflow of ERM as a result of nutrient limitation, $N_{overflow}^{ERM}$ and $P_{overflow}^{ERM}$ are ERM's nutrient overflows as a result of C limitation (Eq. S55), ERM_C_{growth}, ERM_N_{growth} and ERM_P_{growth} are the actual growth in ERM's structural biomass, R_{ERM} is the total respiration of ERM summing up all the C overflow processes described above.

3.4 ERM death and nutrient transfer

ERM in the model turns over at a fixed rate. When ERM dies, 100% of the SAP is recycled back to the SOM pool as necromass. Half of the necromass is recycled to the moss peat pool while the other half is recycled to the shrub peat pool. We have parameterized the necromass of ERM to be much more recalcitrant than that of SAP. This is in line with the finding that necromass of ERM fungi may contribute to the large storage of SOM in boreal ecosystems (Clemmensen et al.2015, Fernandez et al., 2019).

$$Erm\_M_{death} = Erm\_M * Deathrate_{Erm} \quad (S54)$$

$$Death_{Erm}^{SOM} = frac_{Death_{Erm}}^{SOM} * Erm\_M_{death} \quad (S55a)$$

$$Death_{Erm}^{DOM} = frac_{Death_{Erm}}^{DOM} * Erm\_M_{death} \quad (S55b)$$

$$Death_{Erm}^{SOM_{moss}} = frac_{Erm_{necro}}^{moss} * Death_{Erm}^{SOM} \quad (S56a)$$

$$Death_{Erm}^{SOM_{shrub}} = frac_{Erm_{necro}}^{shrub} * Death_{Erm}^{SOM} \quad (S56b)$$

where Erm_M_{death} (M stands for C, N and P) is the ERM death fluxes, $Deathrate_{Erm}$ is the fixed ERM's turnover rate, $Death_{Erm}^{SOM}$ and $Death_{Erm}^{DOM}$ are the part of dead ERM that is recycled to the SOM and DOM pool, respectively, $frac_{Death_{Erm}}^{DOM}$ and $frac_{Death_{Erm}}^{SOM}$ are the proportions of SAP death allocated to DOM and SOM pools, which equal 0% and 100%, respectively, $frac_{Erm_{necro}}^{moss}$ and $frac_{Erm_{necro}}^{shrub}$ are the proportions of ERM necromass that is allocated to the moss and shrub litter pools, and both of them equal 50%, $Death_{Erm}^{SOM_{moss}}$ and $Death_{Erm}^{SOM_{shrub}}$ represent the amount of SAP necromass that is recycled to corresponding litter

pool.

ERM in the model resorb a fix fraction of nutrients from its death fluxes.

$$N_{resorp}^{Erm} = \sum_{X}(Erm\_N_{death} * frac_{resorp,Erm}^{N}) \quad \text{(S57a)}$$

$$P_{resorp}^{Erm} = \sum_{X}(Erm\_P_{death} * frac_{resorp,Erm}^{P}) \quad \text{(S57b)}$$

Where N_{resorp}^{Erm} and P_{resorp}^{Erm} are the nutrient resorption fluxes, $frac_{resorp,Erm}^{N}$ and $frac_{resorp,Erm}^{P}$ are the fixed resorption efficiencies for N, P respectively for ERM. The resorbed nutrients are directed into the nutrient reserve pools and awaits transport into the shrubs. Thus, mycorrhiza death in the model serves as a major source for the nutrients transferred to the shrubs (Rosinger et al., 2020).

Nutrient reserve pools of ERM takes in the nutrient overflows resulted from C limitation for ERM growth ($N_{overflow}^{Erm}$ and $P_{overflow}^{Erm}$, Eq. S50(b-c)) and the nutrient resorptions from ERM turnover (N_{resorp}^{Erm} and P_{resorp}^{Erm}, Eq. S57). Outflows from the reserve nutrient pool include the extraction of nutrients to ERM growth ($N_{extract}^{Erm}$ and $P_{extract}^{Erm}$, Eq. S50(b-c)) and the transport into the shrubs ($N_{transfer}^{Erm}$ and $P_{transfer}^{Erm}$, Eq. S59). The nutrient transport is determined by the size of the reserve nutrient pools and a fixed nutrient transport rate, regulated by ERM's nutrient stress status. ERM decreases (or increases) its nutrient transfer to shrubs when its nutrient stress is high (or low).

$$\frac{\partial}{\partial t}N_{reserv}^{Erm} = N_{overflow}^{Erm} + N_{resorp}^{Erm} - N_{extract}^{Erm} - N_{transfer}^{Erm} \quad \text{(S58a)}$$

$$\frac{\partial}{\partial t}P_{reserv}^{Erm} = P_{overflow}^{Erm} + P_{resorp}^{Erm} - P_{extract}^{Erm} - P_{transfer}^{Erm} \quad \text{(S58b)}$$

$$N_{transfer}^{Erm} = N_{reserv}^{Erm} * rate_{out}^{Erm} * (1 - N_{stress}^{Erm}) \quad \text{(S59a)}$$

$$P_{transfer}^{Erm} = P_{reserv}^{Erm} * rate_{out}^{Erm} * (1 - P_{stress}^{Erm}) \quad \text{(S59b)}$$

where $rate_{out}^{Erm}$ is the fixed rate prescribed for ERM's nutrient transport to shrubs. N_{stress}^{Erm} and P_{stress}^{Erm} are ERM's N and P stress scalers (Eq. S44).

S4 Competition for nutrients between plant and microbial communities

Different plant and microbial communities have different nutrient sources in the model. As described in the earlier sections, *Sphagnum* mosses and shrub plant roots only take up dissolved inorganic nutrients from the soil solution (Eq. S30); Saprotrophs take up both

dissolved inorganic nutrients (Eq. S7) and dissolved organic nutrients (Eq. S4) from the soil solution; ERM fungi take up dissolved inorganic nutrients (Eq. S47) from the soil solution, but their major nutrient source comes from the direct mining from the SOM (Eq. S45) as they are majorly responsible for short-circuiting the nutrient cycles in peatlands (Gavazov et al., 2016). Dissolved organic nutrients are not directly taken up by plants and mycorrhiza fungi. This is not the case in reality, but it is a valid approach in the model as to separate saprotrophic activities and root-mycorrhiza activities, otherwise the interaction between them could be too complicated to be investigated. According to the nutrient sources summarized here, two sets of nutrient competition exist in the model:

Firstly, SAP, Sphagnum mosses, shrub root and ERM fungi compete for inorganic nutrient pools in the peat soil. Access to the inorganic nutrient pool is given in the following order of priority: SAP immobilization, moss adsorption, shrub root uptake and ERM fungi. Gross nutrient immobilization for SAP is given the first priority here, in line with the 'microbe-first' approach adopted in O-CN model (Zaehle & Friend, 2010). Sphagnum moss is assumed to have a superior capacity for nutrient absorption over shrub thus it is placed the second. For competition between shrub root and ERM fungi, priority is given to the shrub root. This approach is more arbitrary and is based on the assumption that shrub roots rely on inorganic nutrients while ERM fungi mainly attack organic nutrients. Secondly, SAP and ERM fungi directly compete for soil organic nutrient pools in the peat. As ERM fungi are perceived to have superior capability to extract nutrient from complex SOM than saprotrophs, priority is given to ERM fungi on soil organic nutrients; Furthermore, ERM is also set up with larger mining rates compared to the depolymerization rates parameterized for SAP, in line with ERM's superior capability in depolymerizing SOM (Sulman et al. 2019).

Table S2.1 MWMmic_NP parameters

Description	Parameter	Units	Literature value	Calibrated value	Equation	Reference/Comment
Soil nutrient dynamics: SOM depolymerization and DOM assimilation						
Initial decomposition rates of different peat components	k_i^{SAP} (i = shrub, moss)	yr^{-1}	0.32,0.08	0.32,0.08	S1	Frolking et al. (2010)
Half-saturation constant of SAP biomass in depolymerization	KM_D^{SAP}	gMBC (g peat)$^{-1}$	2.5e-3	2.5e-3	S1	Blodau et al. (2004)
Maximum DOC uptake rate of microbes	$V_{max,U}$	gDOC (g MBC)$^{-1}$ h^{-1}	[1.3e-5, 0.13]	0.02	S3	He et al. (2015)
Half-saturation constant of DOC concentration for DOC assimilation	KM_U^{SAP}	mg L^{-1}	300	350	S3	Abramoff et al. (2018)
Soil nutrient dynamics: SAP growth						
Base rates for SAP's DIN immobilization	$V_{max,DIN}^{SAP}$	gN (g MBC)$^{-1}$ h^{-1}	1.344e-4	1.5e-4	S7	Kuzyakov et al. (2013) Calibrated to make DIN immobilization rate 3 times the DIP immobilization rate in accordance with the observed microbial N:P ratio around 3.0 at Mer Bleue bog (Basiliko et al., 2006)
Half saturation constant of DIN concentration for immobilization	KM_{DIN}^{SAP}	mgN L^{-1}	0.28	0.75	S7	Kuzyakov et al. (2013)
Base rates for SAP's DIP immobilization	$V_{max,DIP}^{SAP}$	gP (g MBC)$^{-1}$ h^{-1}	4.87e-4	5e-4	S7	Yu et al. (2020)
Half saturation constant of DIP concentration for immobilization	KM_{DIP}^{SAP}	mgP L^{-1}	0.02	0.075	S7	Yu et al. (2020) Calibrated in line with the much smaller DIP concentration in the peat water
Minimum C:N ratio for SAP	CN_SAP_{min}	gC gN^{-1}	6.7	6	S7	Basiliko et al. (2006)
Maximum C:N ratio for SAP	CN_SAP_{max}	gC gN^{-1}	12.0	12	S7	Basiliko et al. (2006)
Minimum C:P ratio for SAP	CP_SAP_{min}	gC gP^{-1}	9.38	12	S7	Basiliko et al. (2006)
Minimum C:P ratio for SAP	CP_SAP_{max}	gC gP^{-1}	32.8	42	S7	Basiliko et al. (2006) Calibrated to generate SAP biomass in line with measurements
Soil nutrient dynamics: SAP C-N-P overflow						
SAP nitrogen use efficiency	NUE_{SAP}	-	0.804	0.85	S10	Sinsabaugh et al. (2016)
SAP phosphorus use efficiency	PUE_{SAP}	-	0.814	0.85	S10	Sinsabaugh et al. (2016)
Base rate of SAP's P biochemical mineralization	$V_{max,bcm}^{SAP}$	yr^{-1} gP^{-1}	-	0.12	S11	Goll et al. (2017) set the P biochemical mineralization rates to be half the turnover times used for SOM decomposition. Here we calibrated to be between the k_{moss}^{SAP} and k_{shrub}^{SAP} and make it substrate independent as did Yang et al (2014) and Yu et al. (2020).
Half-saturation constant of peat P:C ratio	K_{bcm}^{CP}	gN gP^{-1}	5.8e-3	2.0e-3	S11	Yu et al., (2020) Calibrated to generated peat C:P ratio profile in

						line with measurements
Minimum N:P ratio for SAP	NP_SAP_{min}	gN gP^{-1}	1.4	2.0	S11	Basiliko et al. (2006)
Maximum N:P ratio for SAP	NP_SAP_{max}	gN gP^{-1}	3.9	7.0	S11	Basiliko et al. (2006)
Power of the N:P status regulation	α_{SAP}^{P}	-	0.2	1.0	S11	Yang et al. (2014) Calibrated to make P biochemical mineralization less dependent on N to match the more prevalent N limitation observed in the Mer Bleue bog
Soil nutrient dynamics: SAP turnover						
Proportion of SAP death allocated to DOM	$frac_{Death_{SAP}}^{DOM}$	-	0.5	0.5	S12	Allison et al. (2010)
Proportion of SAP death allocated to SOM	$frac_{Death_{SAP}}^{SOM}$	-	0.5	0.5	S12	Allison et al. (2010)
Proportion of SAP necromass that is recycled to moss litter pool.	$frac_{SAP_{necro}}^{moss}$	-	-	0.2	S12	Calibrated
Proportion of SAP necromass that is recycled to shrub litter pool.	$frac_{SAP_{necro}}^{shrub}$	-	-	0.8	S12	Calibrated
Base turnover rate for SAP	$Deathrate0_{SAP}$	h^{-1}	1.5e-4	1.5e-4	S13	Abramoff et al. (2018)
Reference microbial density that is used to regulate microbial turnover	$Ref\_Density_{SAP\_C}$	g MBC m^{-3}	-	70	S13	Calibrated to match the MBC concentration measured throughout the peat profile (Blodau et al., 2004; Basiliko et al., 2006)
Power of the regulation function for microbial turnover	ρ_{SAP}^{Death}	-	-	0.2	S13	Calibrated to match the MBC concentration measured throughout the peat profile (Blodau et al., 2004; Basiliko et al., 2006)
Reduction factor that describes the magnitude of SAP P-turnover downregulation with high P stress.	ρ_{SAP}^{Pdeath}	-	-	-2.3	S14	Calibrated to the degree that microbes decrease their P turnover rates to 10% of the reference value when its C:P ratio is at the highest
Soil nutrient dynamics: Solute transport						
base diffusion coefficient	$D_{DM,0}$ (DM = DOC, DON, DIN, DOP, DIP)	$m^2\ d^{-1}$	1.19e-5 (DOC, DON) 6e-5 (DIN) 2e-4 (DOP, DIP)	1.19e-5 (DOC, DON) 6e-5 (DIN) 2e-4 (DOP, DIP)	S15	Wu and Blodau (2013)
Scaler to implicitly account for the reduced mobility of P in water	$f_{leach,P}$	-	-	0.2	S16	Calibrated to match the DIP and DOP concentration in the peat profile
Plant nutrient dynamics: Carbon allocation to respiration						
Base maintenance respiration rate	MR_{base}	gC $gN^{-1}\ s^{-1}$	2.525e-6	2.525e-6	S17	Lawrence et al. (2011)
Time constant controlling the rate of replenishment of plant's reserve C pool	τ_{repl}	d	30	30	S19	Lawrence et al. (2011)
Minimum ratio of NSC pool to the size of the woody tissues	$frac_{min}$	-	0.012	0.02	S19	Furze et al. (2018) Calibrated
Plant nutrient dynamics: C allocation to growth						

Coefficient for foliar and stem biomass relationship	a_1	-	0.2843	0.2843	S20	Murphy et al. (2009); Xing et al. (2011)
Same as above	a_2	-	1.324	1.324	S20	Murphy et al. (2009); Xing et al. (2011)
Coefficient for shoot and coarse root biomass relationship	a_3	-	154.22	154.22	S20	Murphy et al. (2009); Xing et al. (2011)
Same as above	a_4	-	0.3195	0.3195	S20	Murphy et al. (2009); Xing et al. (2011)
Root distribution parameter for mosses' virtual root	β_{moss}	-	-	0.55	S21	Calibrated Assuming 95% of mosses' 'roots' are distributed within 5cm depth.
Coefficient for dynamic fine root distribution with water table depth	a_5	-	0.61	0.61	S21	Murphy et al. (2010)
Same as above	a_6	-	0.11	0.11	S21	Murphy et al. (2010)
Coefficient for dynamic coarse root distribution with water table depth	a_7	-	0.9158	0.9158	S21	Murphy et al. (2010)
Same as above	a_8	-	1.1e-3	1.1e-3	S21	Murphy et al. (2010)
Fraction of C allocated to growth that is respired out as CO_2	r_g	-	0.11	0.1	S22	Atkin et al. (2017)
Elasticity parameter used to dampen the temporal variations in tissue N content	D_{leaf}^{N}	-	0.25	0.025	S22	Zaehle et al. (2010)
Elasticity parameter used to dampen the temporal variations in tissue P content	D_{leaf}^{P}	-	0.25	0.025	S22	Zaehle et al. (2010) Calibrated to be much smaller to match the little seasonal variation observed (Wang and Moore 2014)
Minimum C:N ratio for foliar biomass	$CN_{fol,min}^{veg}$ (veg = shrub, moss)	gC gN^{-1}	30, 38.4	30, 38.4	S23	M. Wang et al. (2016)
Maximum C:N ratio for foliar biomass	$CN_{fol,max}^{veg}$ (veg = shrub, moss)	gC gN^{-1}	45, 48	45, 48	S23	M. Wang et al. (2016)
Minimum C:N ratio for foliar biomass	$CP_{fol,min}^{veg}$ (veg = shrub, moss)	gC gP^{-1}	467, 250	467, 250	S23	M. Wang et al. (2016)
Maximum C:N ratio for foliar biomass	$CP_{fol,max}^{veg}$ (veg = shrub, moss)	gC gP^{-1}	700, 720	700, 720	S23	M. Wang et al. (2016)
Plant nutrient dynamics: Nutrient resorption and acquisition						
N resorption efficiencies	$frac_{resorp,veg}^{N}$ (veg = shrub moss)	-	0.4	0.4	S29	Wang et al. (2014)
P resorption efficiencies	$frac_{resorp,veg}^{P}$ (veg = shrub moss)	-	0.5	0.5	S29	Wang et al. (2014)
C resorption efficiencies	$frac_{resorp,veg}^{C}$ (veg = shrub moss)	-	0.15	0.15	S29	Wang et al. (2014)
Turnover time for each tissue of each PFT	$\tau_{X,veg}$ (X=foliar, froot, croot, stem) (veg = shrub moss)	yr	1.5, 1.5, 12, 65 (shrub) 0.7 (moss)	1.5, 1.5, 12, 65 (shrub) 0.57 (moss)	S29	Wu et al. (2016)
Base rates for shrub root DIN uptake	$V_{max,DIN}^{shrub}$	gN (gC root)$^{-1}$ h^{-1}	[2.14e-7 1.5e-3]	1.0e-4	S30	Zaehle et al. (2010) Yu et al., (2020)
Half saturation constant of DIN	$KM_{DIN,shrub}$	mg L^{-1}	5.0	5.0	S30	Sulman et al. (2019)

concentration for shrub root uptake						
Base rates for moss DIN uptake	$V_{max,DIN}^{moss}$	gN (gC moss)$^{-1}$ h^{-1}	-	5.0e-4	S30	Calibrated to be large than shrub roots and match the measured moss N content
Half saturation constant of DIN concentration for moss uptake	$KM_{DIN,moss}$	mg L^{-1}	-	0.7	S30	Calibrated as above
Base rates for shrub root DIP uptake	$V_{max,DIP}^{shrub}$	gP (gC root)$^{-1}$ h^{-1}	[1.73e-4 4.1e-4]	4.0e-5	S30	Kavka and Polle et al. (2017) Thum et al. (2019)
Half saturation constant of DIP concentration for shrub root uptake	$KM_{DIP,shrub}$	mg L^{-1}	0.61	0.7	S30	Kavka and Polle et al. (2017)
Base rates for moss DIP uptake	$V_{max,DIP}^{moss}$	gN (gC moss)$^{-1}$ h^{-1}	-	3.75e-4	S30	Calibrated to be large than shrub roots and match the measured moss P content
Half saturation constant of DIP concentration for moss uptake	$KM_{DIP,moss}$	mg L^{-1}	-	0.7	S30	Calibrated as above
Coeffiicents for ERM inhibition effect on shrub root	m_1	-	-0.5	-2.0	S32	He et al. (2018) Calibrated to be stronger. As Meyer et al. (2012) set up a 100% inhibition when ERM colonization is 100%, we calibrated our value to be in the middle of these two.
Coeffiicents for ERM inhibition effect on shrub root	m_2	-	0.3	0.3	S32	He et al. (2018)
Base cost for moss N_2 fixation	$Cost0_{fix}$	gC gN^{-1}yr^{-1}	6	15	S36	Meyerholt et al., (2016) Calibrated
Parameters used to describe the dependance of C cost of N2 fixation on temperature	a_{fix}	-	-3.62	-3.62	S36	Meyerholt et al., (2016)
Same as above	b_{fix}	$^{\circ}$C^{-1}	0.27	0.27	S36	Meyerholt et al., (2016)
Same as above	c_{fix}	$^{\circ}$C	25.15	25.15	S36	Meyerholt et al., (2016)
Parameter for the N toxic effect on mosses	$a_{N,tocix}$	-	0.1	0.1	S37	Calibrated
Ericoid mycorrhiza fungi: C transfer from shrub to ERM						
Base rate of the C translocation from the shrub's C reserve pool	$rate_{out}^{shrub}$	h^{-1}	-	2.5e-4	S39	Calibrated to generate reasonable amount of amount of ERM biomass and C reserve pool for shrubs
Maximum ratio of shrub C reserve pool to the size of storage organs	$frac_{max}$	-	0.05	0.05	S39	Zaehle et al. (2010)
Proportion of shrub overflow that is directed to ERM	$frac_{efflux}^{Erm}$	-	-	0.9	S40	Calibrated, assuming a small fraction of shrub C overflow is constantly allocated to exudates (Sulman et al., 2019)
Ericoid mycorrhiza fungi: CNP acquisition of ERM						
Maximum C uptake rate of ERM from its reserve C pool	$V_{max,U}^{Erm}$	gC (gC ERM)$^{-1}$ h^{-1}	-	4.0e-3	S42	Calibrated to generate reasonable amount of ERM biomass
Half saturation constant of ERM C assimilation from its reserve C pool	KM_U^{Erm}	gC (gC ERM)$^{-1}$	-	0.01	S42	Calibrated to generate reasonable amount of ERM biomass

Minimum C:N ratio for ERM to constrain the size of labile N pool	$CNratio_{Erm}^{min}$	gC gN^{-1}	18	15	S44	He et al. (2018) Calibrated
Maximum C:N ratio for ERM, equivalent to C:N ratio of ERM structural biomass	$CNratio_{ERM}^{max}$	gC gN^{-1}	30	25	S44	He et al. (2018) Calibrated
Minimum C:N ratio for ERM to constrain the size of labile P pool	$CPratio_{ERM}^{min}$	gC gP^{-1}	100	100	S44	He et al. (2021)
Maximum C:P ratio for ERM, equivalent to C:P ratio of ERM structural biomass	$CPratio_{Erm}^{max}$	gC gP^{-1}	200	200	S44	He et al. (2021)
Base N mining rates of ERM	$k_{i,Nmining}^{ERM}$ (i = shrub, moss)	yr^{-1}	-	0.1, 0.4	S45	Calibrated to be larger than SAP depolymerization rates
Half saturation constant accounting for the regulation of ERM biomass on nutrient mining	KM_{mining}^{ERM}	gC ERM (g peat)$^{-1}$	-	2.5e-3	S45	Assumed to be the same as SAP (Sulman et al., 2019)
Base rate of ERM's P biochemical mineralization	$V_{max,bcm}^{ERM}$	yr^{-1} gP^{-1}	-	0.16	S45	Calibrated to be larger than SAP P biochemical mineralization rates
The power of ERM's P:N status regulation on N mining	α_{Erm}^{P}	-	-	0.5	S45	Calibrated to be smaller than that of SAP in line with the larger nutrient mining rates of ERM demanding larger N to build enzymes.
The power of ERM's N:P status regulation on P mining	α_{ERM}^{N}	-	-	0.2	S45	Calibrated to be smaller than the N:P status control on P mining.
Minimum N:P ratio for ERM to constrain the size of labile N and P pool	$NPratio_{ERM}^{max}$	-	-	10.0	S45	Calibrated based on the boundaries of C:N ratios and C:P ratios set up for ERM
Maximum N:P ratio for ERM to constrain the size of labile N and P pool	$NPratio_{ERM}^{min}$	-	-	5.0	S45	Same as above
Base rates for ERM DIN uptake	$V_{max,DIN}^{ERM}$	gN (g ERM)$^{-1}$ h^{-1}	-	1.0e-4	S47	Calibrated with KM_{DIN}^{ERM} to let the DIN uptake capacity of ERM be stronger than shrub root but smaller than SAP (Rains and Bledsoe 2007)
Half saturation constant of DIN concentration for ERM uptake	KM_{DIN}^{ERM}	mgN L^{-1}	-	1.0	S47	Same as above
Base rates for ERM DIP uptake	$V_{max,DIP}^{ERM}$	gP (g ERM)$^{-1}$ h^{-1}	-	5.0e-5	S47	Calibrated with KM_{DIP}^{ERM} to let the DIP uptake capacity of ERM be stronger than shrub root but smaller than SAP
Half saturation constant of DIP concentration for ERM uptake	KM_{DIP}^{ERM}	mgP L^{-1}	-	0.7	S47	Same as above
Base C mining rates of ERM	$k_{i,Cmining}^{ERM}$ (i = shrub, moss)	yr^{-1}	-	0.16,0.04	S48	Assumed to be much smaller than SAP C depolymerization rates
C use efficiency of ERM's C mining	$CUE_{Erm}^{Cmining}$	-	0.1	0.1	S48	(Sulman et al., 2019)
C use efficiency for ERM growth	CUE_{ERM}^{growth}	-	0.5	0.5	S49	Sulman et al. (2019)
Ericoid mycorrhiza fungi: ERM death and nutrient transfer						
ERM's turnover rate	$Deathrate_{Erm}$	yr^{-1}	1.14e-4	1.0e-4	S54	Sulman et al. (2019)

Proportion of dead ERM that is recycled to the SOM	$frac_{Death_{Erm}}^{SOM}$	-	-	1.0	S55	Calibrated to let ERM death be much more recalcitrant than SAP death, in line with Clemmensen et al. (2015)
Proportion of ERM necromass that is recycled to the moss litter pool	$frac_{Erm_{necro}}^{moss}$	-	-	0.5	S56	Same as above
Resorption efficiencies of N for ERM	$frac_{resorp,Erm}^{N}$	-	0.5	0.4	S57	Calibrated to be equivalent to the value for shrub and mosses
Resorption efficiencies of P for ERM	$frac_{resorp,Erm}^{P}$	-	0.5	0.5	S57	Calibrated to be equivalent to the value for shrub and mosses
Rate for transport from ERM's nutrient reserve pool to shrubs	$rate_{out}^{Erm}$	-	0.0285	0.025	S59	Sulman et al. (2019) Calibrated

Chapter 5. Simulating the impacts of climatic change, increased nutrient deposition and elevated CO_2 on ombrotrophic peatlands

Bridging statement to Chapter 5

It is of great concern whether or not peatlands could still maintain their C sink function under future environmental changes. Models have been used for predictions of peatlands' future, but as reviewed in Chapter 2, most peatland models do not include nutrient cycles and microbial processes. To address this, Chapter 5 presents a scenario simulation using the newly developed MWMmic_NP that fully integrates microbe-mediated nutrient cycles with C cycle. The simulation was conducted on the Mer Bleue bog. Different combinations of six selected environmental drivers including elevated N deposition, elevated P deposition, rising atmospheric CO_2, rising air temperature, rising soil temperature and lowered water table are used to construct the potential scenarios of environment change. I aim to assess the response of the ombrotrophic peatlands to multiple simultaneous disturbances. I also examine the interactions between different drivers and disentangle the contribution of each driver to the combined impacts of multiple disturbances. The role of microbe-mediated nutrient cycling in mediating the response of bog's C cycle to disturbances is thoroughly investigated here.

5.1. Abstract

Northern peatlands have acted as a net carbon sink for millennia and thus store about 30% of global soil organic carbon. Potential environmental disturbances including climate warming, increased nutrient deposition, and altered hydrological conditions could reduce the carbon sequestration capacity and put this large carbon reservoir in jeopardy. However, peatland models used for projections of environmental change impacts have omitted important processes including nutrient cycling and plant-microbe interaction, which could reduce the accuracy of the model predictions. To address this issue, we applied the newly developed MWMmic_NP which explicitly integrated carbon-nutrient cycles with mycorrhiza controls to simulate the impact of environmental changes on an ombrotrophic peatland. We assessed the combined and interactive effects of elevated nitrogen deposition, elevated

phosphorus deposition, rising atmospheric CO_2, rising air temperature, rising soil temperature and lowered water table on the composition of both vegetation and microbial communities as well as the biogeochemical cycles in the peatland. Most scenarios of environmental changes were projected to shift the vegetation communities towards shrub-domination and the microbial communities towards saprotroph-domination and reduced carbon sequestration capacity for the bog. Rising soil temperature and lowered water table were the primary drivers for the weakening of carbon sink while rising air temperature, elevated CO_2 and increased phosphorus deposition could potentially lead to enhanced carbon uptake. The diminished nutrient transfer from ericoid mycorrhizal fungi to shrubs were found to be the key process responsible for the decrease in the bog's carbon sequestration. We therefore identified the significance of shrub-ERM association in maintaining the C sink function of ombrotrophic peatlands and called for more research into this area.

5.2. Introduction

Despite only occupying 3% of the Earth's land surface (Xu et al., 2018), northern peatlands have stored approximately one-third of the global terrestrial soil carbon (C) (Yu et al., 2012), a result of persistent C imbalance between plant production and organic matter decomposition throughout the Holocene (Roulet et al., 2007). The prevalent waterlogged conditions and low peat temperature are key determinants for the reduced decomposition and consequent C accumulation in northern peatlands (Limpens et al., 2008). The low availability of nutrients also contributes to the C sink strength, especially in ombrotrophic peatlands (bogs) exclusively fed by atmospheric deposition, as it favors the dominance of the peat-forming *Sphagnum* mosses (van Breemen, 1995; Bragazza et al., 2006). However, these key environmental conditions for C accumulation are subject to significant changes in the future, as disproportional climate changes are projected to occur in the northern high latitudes (IPCC, 2018) and human activities could dramatically alter the nutrient and hydrological conditions in peatlands (Strack et al., 2006; Hedwall et al., 2017). Thus, it is of great concern whether these northern peatlands will continue functioning as C sinks in the future of environmental change.

To address this question, a great many field manipulative experiments have been

conducted, which have reported an enormous effect of environmental changes on the structure and functioning of peatland ecosystems. For example, climate change could pose severe threats to peatlands' large C storage either directly through increased decomposition (Dorrepaal et al., 2009; Bragazza et al., 2016), or indirectly through the consequent increased dominance of vascular plants over *Sphagnum* mosses (Gavazov et al., 2018; McPartland et al., 2019; Norby et al., 2019). Increased nutrient availability could also result in enhanced growth of vascular plants at expense of *Sphagnum* mosses (Bubier et al., 2007; Juutinen et al., 2010), thus leading to reduction in C sequestration capacity (Bragazza et al., 2012; Larmola et al., 2013). Changes in microbial communities with environmental changes (Basiliko et al., 2006; Anderson et al., 2013; Asemaninejad et al., 2018) also contributed to the diminished C sink function of peatlands (Juan-Ovejero et al., 2020). Nevertheless, the increase in plant production and peatland C accumulation with both warmer climate (Ward et al., 2013; Helbig et al. 2019) and increased nutrient deposition (Turunen et al., 2004) have also been reported, showing the non-linearity of peatland's response to environmental disturbances. Despite these endeavors, most of these field studies only focused on the impact of individual environmental driver and few studies exist that assessed the effects of multiple drivers on peatlands simultaneously (Weltzin et al., 2003; Dielemen et al., 2015; Luan et al., 2019; Gong et al., 2021a, b). As environmental drivers interact in complex ways, prediction of their collective effect cannot rely on simply combining their individual impacts and thus remains challenging (Dise, 2009).

Process-based models allow the trajectory of a system to emerge from the interaction of important internal processes, which could help elucidate the complex responses of an ecosystem to multiple external disturbances (Evans, 2012). Tremendous efforts have been made into developing peatland-specialized models (Frolking et al.,2002; St-Hilaire et al., 2010; Wu et al., 2012; Wu et al., 2013) and introducing peatlands into established ecosystem models or even global land surface models (Wania et al., 2009; Shi et al., 2015, 2021; Chaudhary et al., 2017; Wu et al., 2016; Qiu et al., 2018). Studies have used these process-based models to simulate the impact of increased nutrient deposition (Wu et al., 2015), land-use change (He et al., 2016; Young et al., 2017) and climate change (Wu and Roulet, 2014; Chaudhary et al.,

2020; Qiu et al., 2020) on peatlands. Despite the progress made so far, limited effort has been devoted to disentangling the contribution of individual driver to the combined impacts of multiple disturbances. To the best of our knowledge, Müller and Joos. (2021) is the only modeling study that isolated the contribution of each driver and identified rising temperature as the main driver of future peatland loss and increasing precipitations as driver for regional peatland expansion.

Furthermore, most peatland models lack important processes that could greatly impact the projection of the peatland's response to environmental changes. Firstly, only a limited number of peatland models have incorporated nitrogen (N) cycle (Heijmans et al., 2008; Spahni et al., 2013; Wu et al., 2013) and none has explicitly simulated phosphorus (P) cycle. Modeling studies in non-peatland ecosystems have found the impact of nutrient limitation in projecting future climate–carbon cycle feedbacks to be significant (Wieder et al., 2015), but no such studies have been done for peatlands, let alone assessing the combined effect of altered nutrient deposition and climate change (Utstøl-Klein et al., 2015). Secondly, given the increasing awareness of the importance of microbial communities in ecosystem function (Crowther et al., 2019), a new generation of ecosystem models have started incorporating microbial metabolism (Allison et al., 2010). Such efforts, however, have been significantly lacking in peatland modeling studies (Chadburn et al., 2020) despite the well-acknowledged significance of microbial process in peatland functions (Anderson et al., 2013; Juan-Ovejero et al., 2020). Plant-microbe interactions were particularly important for the nutrient-limited bog ecosystems, as the nutrient acquisition of the dominant ericaceous shrubs primarily depend on the C-demanding symbiotic exchange with ericoid mycorrhiza fungi (ERM) (Read et al., 2004; Thormann, 2006; Defrenne et al., 2020). Direct evidence for the significance of ERM in regulating peatland's response to climate change has been reported (Bragazza et al., 2015; Fernandez et al., 2019). Therefore, omitting key microbe-mediated processes in the model hinders our ability to understand the response of biogeochemical cycling in ombrotrophic peatlands, as already shown in the modeling work of other nutrient-limited ecosystems (Sulman et al., 2019).

To address some of these knowledge gaps, we applied the newly developed

MWMmic_NP (Shao et al., 2021, in prep) which explicitly integrates CNP cycles with mycorrhiza controls to simulate the impact of environmental changes on ombrotrophic peatlands. Simulations were conducted for the well-characterized Mer Bleue bog, where the model has been previously validated. Different combinations of six selected environmental drivers including elevated N deposition, elevated P deposition, rising atmospheric CO_2, rising air temperature, rising soil temperature and lowered water table were used to construct the potential scenarios of environment change. We assessed the combined effects of multiple environmental drivers on different model outputs meanwhile separated the contribution of each driver to identify the most influencing one. With the incorporation of both nutrient cycles and microbial controls, the role of microbe-mediated nutrient cycling in the response of peatlands to environmental disturbances was also explored for the first time.

5.3. Materials and Methods

5.3.1. Model description

The McGill Wetland Model is a process-based model that simulates the CO_2 dynamics in northern peatlands on an hourly basis (St-Hilaire et al., 2010). We have extensively developed MWM into MWMmic_NP by integrating cohort tracking, solute transport, microbial dynamics, and nutrient cycles into the model's bog version. The details of model development can be found in Chapter 3 and 4. In summary, C enters the bog through photosynthesis of the two dominant plant functional types (PFTs) in bogs: *Sphagnum* mosses and ericaceous evergreen shrubs, and leaves the system via plants' autotrophic respiration, microbial respiration, and the export of dissolved organic carbon (DOC) with runoff. The aboveground litter production forms a new cohort of peat every year. The cohort moves downward as the peat depth develops and gets replenished with the root litter and microbial necromass. Two types of microbes: saprotrophs (SAP) and ericoid mycorrhizal fungi (ERM) are currently included in the model, mediating the system's biogeochemical cycles. While SAP feeds on the C from peat substrate, ERM mainly relies on the C transferred from shrubs when low nutrient availability or high water table limits shrubs' growth and leads to accumulation of surplus photosynthates. Nutrient saturation/scarcity in SAP biomass leads to net mineralization/immobilization of

inorganic nutrients. In contrast, ERM could directly 'mine' organic nutrients from the peat and deliver them to shrubs without producing any inorganic nutrients. Nutrients enter the system through atmospheric deposition and N_2 fixation while leave the system through leaching with runoff.

The current input variables for the stand-alone version of the MWMmic_NP are annual N deposition, annual P deposition and hourly variables including net radiation, photosynthetic photon flux density, precipitation (rain or snow), water table depth (WTD), air and soil temperature, relative humidity, wind speed, atmospheric pressure, and air CO_2 concentration. The model outputs all the major fluxes that constitutes the CNP budget of the ombrotrophic peatland (see Chapter 3 and 4).

5.3.2.Study site and dataset

We based our study at the Mer Bleue (MB) bog, an acidic ombrotrophic peatland located 10km east of Ottawa, Ontario, Canada (45.41°N, 75.48°W, 69m above mean sea level). It is a slightly domed bog with a peat depth of 5–6 m in the center. The vegetation coverage is dominated by mosses (e.g. *Sphagnum capillifolium*, *S. angustifolium*, *S. magellanicum* and *Polytrichum strictum*) and evergreen shrubs (e.g. *Chamaedaphne calyculata* and *Ledum groenlandicum*). Some deciduous shrubs (*Vaccinium myrtilloides*), sedges (*Eriphorum Vaginatum*), black spruce (*Picea marinana*) and larch also constitute a sparse cover. The climate of the region is mid-continental, cool temperate, with a 30 year (1971–2000) mean annual air temperature of 6.0°C and annual mean precipitation of 943 mm (http://climateweatherofficeecgcca/climate_normals (2018)).

MWMmic_NP has been successfully applied at the MB bog and evaluated against the extensive measurements (see Chapter 3 and 4). To run the model under the non-disturbance condition, we used the hourly meteorological input data from the MB flux tower dataset (https://daac.ornl.gov/FLUXNET/guides/FLUXNET_Canada.html). The input annual N and P deposition under the non-disturbance scenario are derived from literature at 0.8 gN m^{-2} yr^{-1} and 30 mgP m^{-2} yr^{-1} respectively (Moore and Bubier, 2020; Wang et al., 2015).

5.3.3.Simulation set-up and result analysis

Six environmental drivers were considered for their impacts on the biogeochemical cycles of the MB bog: (i) increased N deposition, (ii) increased P deposition, (iii) rising CO_2 concentration, (iv) water table drawdown, (v) rising air temperature, and (vi) rising soil temperature. For each driver, we set two levels of alteration: a median level and a high level. Combined with the values under the non-disturbance condition, we thus had 3 values for each environmental variable that were investigated here (Table 1). Capital letters “B”, “M” and “H” were used here to indicate the condition of non-disturbance, median-level disturbance, and high-level disturbance for each environmental variable in the rest of the paper. A ‘scenario’ is any combination of the 6 environmental variables with one of their 3 different values. We thus constructed a total of 729 scenarios (36) to run the model. Simulations for all scenarios were implemented following the same protocol: the model was first spun up for over 6000 years by repeatedly using the 16-year meteorological data (from 1998 to 2014) from the MB bog until the outputs approached steady state, then the model was run for 80 years using the altered environmental conditions assigned for each scenario. The results for the last 96 years were extracted as the simulation results (16-year non-disturbance period plus 80-year disturbance period) and used for analysis described below.

Two sets of analysis were conducted to examine the impact of the drivers (Figure 5.1). Firstly, the scenario where all variables are set at the non-disturbance level are referred to as the reference scenario, representing the trajectory of the MB bog under current environmental conditions. Therefore, the combined impact of the drivers could be represented by the difference between the simulation outputs from each scenario and the reference scenario. Heat maps were constructed to demonstrate the combined impact on different model outputs and the axes of each heat map were adjusted accordingly to show a notable pattern. Secondly, to isolate the contribution of each driver from the calculated combined impact, we subtracted results from any two scenarios that differ only in the investigated driver being on or off, resulting in a total of 243 (35) subtractions. Time-series and violin plots (Hintze and Nelson, 1998) were used to depict the distribution of each driver’s contribution under the 243 relevant scenarios.

For all the analysis, we examined the impact of drivers on the following 16 model outputs: moss biomass, shrub biomass, SAP biomass in the top 35cm, ERM fungi biomass in the top 35cm, gross primary production (GPP), ecosystem respiration (ER), heterotrophic respiration (HR), net ecosystem production (NEP), direct N uptake of shrub roots, direct P uptake of shrub roots, N transfer from ERM to shrub, P transfer from ERM to shrub, dissolved inorganic N (DIN) in the top 50cm, dissolved inorganic P (DIP) in the top 50cm, net N mineralization in the top 50cm, net P mineralization in the top 50cm.

5.3.4.Mycorrhizal adaptation experiment

To further examine the implication of mycorrhiza-mediated nutrient cycling to the changing environments, we repeated the simulation process described above but with modifications for ERM in the model to account for their adaptation. Adaptive ERM was set to actively control its nutrient transfer to shrubs based on the C to nutrient exchange ratios. Therefore, ERM could reduce its nutrient transfer to shrubs in response to decreased C transfer from shrubs to potentially maintain the shrubs' reliance on them (See text in supplementary information for details). We then compared the simulation results from the new "mycorrhizal adaptation" models with the results from the original model to investigate the potential effect of ERM-mediated nutrient cycling.

5.4. Results

For simplicity, we use abbreviations to represent different environmental variables here. N refers to N deposition (N_dep), P refers to P deposition (P_dep), C refers to CO_2 concentration, Ta refers to air temperature (Tair), Ts refers to soil temperature (Tsoil) and WTD refers to water table depth (WTD). Coupled with the different levels of the changes described in Section 5.3.3, scenarios of environmental change are all represented in abbreviations. For example, "BWTD MN HC" represents scenarios with 'base-level non-disturbed' WTD, 'median-level disturbed' nitrogen deposition and 'high-level disturbed' CO_2 concentration.

5.4.1.Impacts on vegetation and microbial community

Under most scenarios, the environmental change altered the vegetation composition by increasing shrub biomass and decreasing moss biomass (Figure 5.2(a-b)) and the effects on both vegetation biomass appeared cumulative over time (Figure S5.1). However, the moss biomass could also increase with environmental changes when Tsoil, WTD and N_dep were all maintained at their base levels or the combination of "BT BWTD MN HC HP" was imposed (Figure 5.2(b)). The dominant factor for the overall vegetation shift was the increase in CO_2 concentration (Figure 5.4(a-b)). Its effect was even boosted when coinciding with other drivers. On the other hand, increased N_dep, Tsoil, Tair and WTD, could also contribute to the shrub domination over mosses. But their effects, except for the increased Tair, were diminished when co-occurring with other drivers. Increased P_dep had a relatively neutral effect but could considerably increase the moss domination over shrubs when imposed alone. The effects of most drivers on moss biomass were the opposite of those on shrub biomass. But the higher Tsoil had a slightly negative effect for both vegetation types in general.

Simulated environmental changes generally led to increased SAP biomass and decreased ERM biomass (Figure 5.2(c-d)). The effects of environmental change on ERM biomass appeared cumulative over time, whereas the initial positive effects on SAP could dampen with time or even switch to negative effects in the long run (Figure S5.2). SAP changes generally followed those of shrubs except for the co-occurrence of shrub increase and SAP decrease with high Tair. Similarly, changes of ERM biomass followed those of mosses, except for the co-occurrence of moss decrease and ERM increase under scenarios with "BN BTs HC". As shown in Figure 5.4(c-d), N_dep and Tsoil were the most consistent driving forces for microbial community shift. Increased N_dep and Tsoil both led to decrease in ERM biomass while SAP biomass was increased by increased N_dep and decreased by rising Tsoil. Increased CO_2 and Tair had a distinctly positive and negative impact on SAP biomass, respectively. But their overall impacts on ERM biomass were relatively neutral even though they can considerably boost ERM biomass when imposed alone. On the contrary, increased WTD decreased the ERM biomass but its overall impact on SAP was neutral. The overall impact of increased P_dep was the smallest among all drivers. But it could boost ERM biomass when imposed alone, as did

the increased CO_2 and Tair.

5.4.2.Impacts on carbon cycle

Environmental changes also considerably impacted the carbon budget of the system. The impact on GPP were generally cumulative over time while the short-term positive effect on ER appeared to dampen over long time (Figure S5.3). Overall, the GPP and ER change was mostly driven by the level of increase in CO_2 concentration and Tair (Figure 5.3(a-b)). The interaction with other drivers considerably reduced the positive effects of CO_2 increase on both GPP and ER but did not really affect those of rising Tair (Figure 5.4(e-f)). GPP was negatively impacted by increased N_dep and WTD and the largest GPP increase occurred under scenarios with B-level WTD and N_dep. In contrast, ER was negatively affected by increased N_dep while positively impacted by greater WTD.

Environmental changes led to increase in HR and overall decrease in NEP (Figure 5.3(c-d)). While the short-term effect of WTD and Tsoil increase on both HR and NEP appeared to dampen over long time, the effects of the other 4 drivers were time-cumulative (Figure S5.4). The increaseed Tsoil and increased WTD had a positive and negative effect on HR and NEP, respectively. Tsoil had the largest impact among all drivers on HR and NEP, followed by WTD (Figure 5.4(g-h)). However, when interacting with other drivers, the effects of increased Tsoil and WTD on HR was reduced but their negative effects on NEP was enhanced. It is worth pointing out that every scenario of environmental changes had led to increased HR. Besides Tsoil and WTD increase, the overall effects on HR of the other 4 investigated drivers were all positive. But the overall effects of P_dep and Tair increase on HR were diminished to almost neutral when co-occurring with other drivers. Similarly, NEP was boosted by increased CO_2 and P_dep when these two drivers were imposed alone but their overall impacts were also relatively neutral (Figure 5.4(h)). In contrast to the unidirectional effects on HR, NEP could increase with environmental changes when Tsoil and WTD were both maintained at their base levels and N_dep was below its highest level (Figure 5.4(h)).

5.4.3.Impacts on nutrient mineralization and inorganic nutrient pools

For both N and P, environmental changes had a profound impact on the size of their inorganic nutrient pools and net mineralization rates, but the patterns among different combinations of drivers differed considerably between the two nutrients (Figure 5.5). Increased N_dep, greater WTD and higher Tsoil all led to an increased DIN pool (Figure 5.5(a)). DIN increase with environmental change could even be over 200 times under scenarios with both H-level N_dep and H-level WTD. Those three drivers also led to an increase in DIP pool but on a much smaller scale (Figure 5.5(b)). Increased P_dep had the largest positive impact on the size of DIP as did N_dep on the size of DIN pool (Figure 5.7(a)). In contrast to the notable impact of N_dep on DIP (Figure 5.7(d)), P deposition did not seem to affect DIN that much (Figure 5.7(a)). Rising CO_2 had an overall neutral effect on the sizes of both inorganic nutrient pools (Figure 5.7(a, d)).

The overall changes of net N mineralization rates generally followed that of DIN pool, whereas the change of net P mineralization appeared much more complicated (Figure 5.5(c-d)). Generally, all drivers but increased P_dep and rising CO_2 led to increased net N mineralization (Figure 5.7(b)). Increased P_dep had an overall neutral effect while rising CO_2 had an overall negative effect on net N mineralization. This resulted in increased net N mineralization with environmental changes in general. In contrast, the overall effects of environmental changes on net P mineralization seemed much more neutral (Figure 5.7(e)). Only increased N_dep and Tsoil led to an increased net P mineralization. Increased CO_2, Tair and WTD had an overall neutral impact on net P mineralization although they all had a positive impact when imposed alone, suggesting strong interactive effects among different drivers. Different from all other drivers, increased P_dep had a strong negative effect on net P mineralization in general, despite having a positive effect when imposed alone (Figure 5.7(e)).

5.4.4.Impacts on nutrient uptake

In response to environmental changes, shrubs generally shifted their nutrient sources from being ERM transfer-dominated towards root uptake-dominated (Figure 5.6). This

nutrient source shift for both N and P were mainly driven by the increased N_dep as it substantially increased the root uptake and decreased ERM transfer for both N and P (Figure S5.5(c, f)). In contrast, the positive effect of increased P_dep on shrub's nutrient source shift was much weaker, as it had an overall neutral effect on ERM P transfer and root N uptake (Figure S5.5(a, d)). The other 4 drivers: Higher Tair, Tsoil, WTD and CO_2 level also played a role in driving the shift of the shrubs' nutrient source towards root uptake, with higher Tsoil exerting the second largest effect which was only smaller than that of higher N_dep. Higher Tair, Tsoil and WTD had an overall positive and a negative effect on root nutrient uptake and ERM nutrient transfer, respectively, whereas elevated CO_2 had a positive effect on both nutrient uptake pathways (Figure S5.5). However, except for increased N_dep and Tsoil, the other 4 drivers almost have no effect on reshaping the nutrient sources for shrubs when they are applied alone, suggesting the strong interactive effect between drivers. Furthermore, elevated CO_2 and P_dep alone considerably increased shrub's reliance on ERM for N and P, respectively (Figure S5.5(c-d)).

5.4.5. Effects of microbial adaptation

Simulated mycorrhizal adaptation substantially increased the resilience of the corresponding microbes in response to environmental changes and subsequently altered the system's responsive behavior. The negative feedback of ERM to decreased C transfer from shrubs led to much more neutral effect of environmental changes on ERM biomass (Figure 5.6(d)). As a result, this led to the attenuated shift from moss dominated to shrub dominated systems in response to environmental changes (Figure 5.8(a-b)). In many cases, moss biomass even increased while shrub biomass slightly decreased with the environmental disturbances under scenarios with B-level N_dep. This led to much higher GPP, ER and ultimately less C loss from the system in response to environmental changes (Figure 5.9). Accounting for mycorrhizal adaptation also changed the contribution of different drivers to the combined impact of environmental changes. ERM adaptation significantly increased the overall negative effect of elevated N_dep on moss biomass, ERM biomass, GPP and NEP (Figure S5.6). Meanwhile, it also dramatically decreased the negative effect of N_dep on those same model

outputs when elevated N_dep was applied alone (Figure S5.6). The overall positive effect of increased N_dep on SAP biomass and HR was switched to being negative with ERM adaptation. The overall slightly positive effect of rising CO_2 on NEP was also changed to being slightly negative.

5.5. Discussion

5.5.1. Response of peatland vegetation

Our simulations showed that, most scenarios of environmental changes shifted the Mer Bleue bog from being *Sphagnum* moss-dominated to evergreen shrub dominated. The increase in CO_2 level was the most important driver of this shift, followed by increased N deposition, water table depth and air temperature. Increased N deposition and lowered water table depth could both alleviate the nutrient limitation for shrubs while elevated CO_2 level and higher air temperature could directly boost the growth of shrubs. In contrast, the increase in soil temperature and P deposition could drive the system towards the opposite direction at times and thus played a more complicated role in shaping the vegetation composition. Increased soil temperature alone favored shrub dominance as it increased the nutrient availability for shrubs. But meanwhile higher soil temperature led to increased root respiration thus it often had a negative net impact on shrubs provided other drivers had already alleviated the nutrient limitation of shrubs. *Sphagnum* mosses are more P limited while shrubs are more N limited, thus increased P deposition alone could boost moss growth and further strengthened the dominance of mosses over shrubs.

Our simulation results are in accordance with most experiments of N fertilization (Bubier et al., 2007; Juutinen et al., 2010; Bragazza et al., 2012; Larmola et al., 2013; Levy et al., 2019), warming (Bragazza et al., 2013; Buttler et al., 2015; McPartland et al., 2019, 2020; Norby et al., 2019) and water table drawdown (Strack et al. 2006; Breeuwer et al. 2009; Strakova et al. 2012; Potvin et al. 2015; Radu and Duval, 2018; McPartland et al. 2019, 2020), where a shrinkage of moss cover and increase in woody shrub abundance were observed. Such shift in vegetation composition was also found in studies where two or more drivers were assessed simultaneously including warming plus drying (Weltzin et al., 2000, 2003; Munir et al., 2014;

Jassey et al., 2019; Strack et al., 2019), warming plus increased N deposition (Hedwall et al., 2017; Luan et al., 2019) and the combination of warming, drying and increased N deposition (Pinceloup et al., 2020). In contrast, the experiments with P fertilization and CO_2 enhancement often yielded mixed results. P fertilization alone was found to be either beneficial to (Limpens et al., 2004; Fritz et al., 2012) or detrimental (Li et al., 2018) to *Sphagnum* growth, depending on the amount of P applied. When P fertilizer was applied together with N fertilizer, P could either accelerate the shift in vegetation composition observed with only N fertilizer (Bubier et al., 2007; Juutinen et al., 2010; Larmola et al., 2013; Levy et al., 2019) or ameliorate the negative effect of N enrichment on mosses (Limpens et al., 2011). These findings are in line with the mixed effect of increased P deposition exhibited in our simulation. Treatments with only CO_2 enhancement generated a very limited response of the shrub (Hoosbeek et al., 2001; Berendse et al., 2001; McPartland et al., 2019, 2020) presumably because of strong nutrient limitation (Hanson et al., 2020). Our modeling result partially agreed with the observations as the simulated positive effect of CO_2 rise on shrubs was much less when CO_2 rise was the only driver. But the strong boost in shrub growth by the simulated elevated CO_2 when multiple drivers were applied has not been reported in manipulation experiments so far. Only minor increase in shrubs by elevated CO_2 was observed when N fertilizer (Heijmans et al., 2001) or considerably high soil temperature (Norby et al., 2019) was applied together with CO_2. Besides strong nutrient limitation, this inertia of shrubs could also result from the acclimation of shrub's photosynthetic capacity to elevated CO_2 (Ward et al., 2019).

5.5.2. Response of peatland microbial community

Simulated environmental changes have led to overall losses of ERM and increased SAP biomass. The dominant driver for this shift is the increased N_dep, as it reduced the dependency of shrubs on ERM to acquire N. In contrast, increased P_dep, CO_2 or Tair alone could all exerted the opposite effect on microbial community (Figure 5.4(c-d)). Elevated P_dep mostly benefited the highly P-limited moss growth, which exacerbated the N limitation for shrubs (Čapek et al., 2018) and elevated CO_2 and Tair aggregated the limitation of both nutrients for shrubs. Therefore, all these three scenarios led to increased dependency of

shrubs on ERM thus increased the dominance of ERM over SAP. Increased Tsoil and WTD alone could increase the nutrient availability for shrubs thus also contributed to the increase in SAP and the loss of ERM. But their overall effects on SAP biomass is only positive in the short term and became neutral or even negative in the long term. This resulted from the large increase in HR with these two drivers which depleted the labile carbon in the peat and made the "food source" of SAP more recalcitrant in the long run. The decrease of microbial carbon use efficiency (CUE) with higher temperature further limited microbial growth thus led to largest decrease in SAP biomass caused by Tsoil rise (Figure 5.4(c)).

Matching our simulation result here, field studies have reported increased SAP biomass in peatlands with water table drawdown (Blodau et al. 2004, Peltoniemi et al., 2012; Jassey et al., 2018). In contrast, warming experiments often reported mixed results on SAP biomass, with some studies showing increase in SAP biomass (Asemaninejad et al., 2018; Liu et al., 2019; Jiang et al., 2020) while others showing decrease (Sihi et al., 2018; Basińska et al., 2020) or only changed seasonal patterns (Weedon et al., 2012). These inconsistent findings could be attributed to the different optimal temperature for different microbial communities (Thormann et al., 2004) or different extent of microbial thermal acclimation (Davidson and Janssens, 2006; Sihi et al., 2018). It is also thought that longer term of climate change could lead to depletion of labile SOC and smaller microbial community as shown by previous modeling studies (Knorr et al., 2005; Allison et al., 2010) and ours here. Mpamah et al. (2017) reported decrease in microbial biomass at bogs with long-term drainage presumably caused by depletion in labile carbon as proposed here. But more long-term experimental studies, especially on the effect of warming, are still needed to confirm this mechanism (Anderson et al., 2013; Juan-Ovejero et al., 2020). Studies on how peatland ERM responded to climate change were limited and produced conflicting outcomes. Matching our simulation result here, Defrenne et al. (2020) reported loss of ERM fungi along with the increased shrub abundance by deep soil warming and Peltoniemi et al. (2012) reported fungal community shift from mycorrhizal to saprotrophic fungi with higher WTD. But increase in ERM with hotter and drier climate accompanied by the increased dominance of ericaceous shrubs was also reported in other studies (Bragazza et al., 2015; Asemaninejad et al., 2018). These mixed results could

stem from the nonlinear change of ericaceous shrubs' dependencies on ERM with different environmental conditions. As our modeling result showed here: higher Tair and Tsoil with warmer climate exerted the opposite effects on the ERM dominance (Figure 5.4(d)) and higher WTD could increase the dominance of both ERM and ericaceous shrubs when the initial WT is very high (Figure S5.7). Therefore, how peatland microbial communities respond to climate change depends on the different ecological niches present in peatlands (Kennedy et al., 2018; Juan-Ovejero et al., 2020).

There is a large gap in understanding how microbial communities in peatlands respond to elevated CO_2 due to the scarcity of relevant research (Anderson et al., 2013). Nonetheless, our simulation result agreed with observed increase in SAP biomass at a *Sphagnum* peatland (Mitchell et al., 2003) and ERM colonization in a subarctic birch forest (Olsrud et al., 2004, 2010) following CO_2 enhancement. Increases in both microbial communities were proposed to result from the increased belowground C allocation of plants (Mitchell et al., 2003; Olsrud et al., 2004, 2010), as shown in our simulation too. Furthermore, increased nutrient availability was generally found to increase the SAP biomass (Basiliko et al., 2006; Juutinen et al., 2010; Peltoniemi et al., 2020) and decrease the diversity of ERM fungi (Van Geel et al., 2020), which also agreed with our modeling result. Yet contrarily, studies in peatlands reported increased ERM biomass and colonization with nutrient fertilization (Kiheri et al., 2020), which was also found in other boreal ecosystems (Johansson et al., 2000; Wu et al., 2021). This resiliency of ERM still needs further research but could be due to its important ecological roles as both mutualists and saprotrophs (Martino et al., 2018).

5.5.3. Response of peatland carbon cycle

Our simulation results showed differentiated responses to environmental changes for different components of the C cycle. GPP showed the most inconsistent response and could either increase or decrease with environmental changes. This is caused by the overall opposing directions of changes between shrubs and mosses, with the increase of shrubs often accompanied by a decrease in mosses. The elevated CO_2 and increased Tair contributed the most to the increase of total GPP since those two drivers could boost the photosynthetic rates

at the leaf level. The combination of AR and ERM respiration (Figure S5.8) followed the changing pattern of GPP in general (Figure 5.3(a)), showing the tight correlation of photosynthesis and plant-mediated respiration. HR, on the hand, consistently increased to all the simulated environmental changes, which was mostly driven by the larger depolymerization rates with higher Tsoil and increased O_2 availability with higher WTD. Meanwhile the indirect impact of the improved litter decomposability with the vegetation shifts also contributed to the consistently increased HR. The ER, which was the sum of HR, AR and ERM respiration, generally increased with environmental changes as the HR did. But ER also decreased when the increased respiration from shrubs and SAP could not compensate for decreased respiration with the loss of moss and ERM. In the end, NEP was decreased by most scenarios of environmental changes. Higher Tair, CO_2, or P deposition combined with base-level Tsoil and WTD could lead to increase in NEP, as the large increase in GPP exceeded the relatively small increase in HR, which is in line with the predictions from Gallego-Sala et al. (2018).

Manipulation studies have also reported mixed effects of environmental changes on GPP. In line with our simulation result, increased Tair was often found to have a positive effect on the primary production (Johnson et al., 2013; Ward et al., 2013; Munir et al., 2015; Helbig et al., 2019; Laine et al., 2019). In contrast, no conclusion about the effect of WTD alteration on GPP has been reached yet in empirical studies (Gong et al., 2020). Both decrease (Bubier et al. 2003; Blodau et al., 2004; Churchill et al., 2015; Lund et al., 2015; Munir et al., 2015; Minkkinen et al., 2018; Laine et al., 2019) and increase in GPP (Sulman et al., 2009; Ratcliffe et al., 2019; Fortuniak et al., 2021) has been reported. This challenged the consistently negative effect of water table drawdown on GPP simulated by MWMmic_NP which may stem from a lack of more drought-adaptive woody species in the model. The effect of N fertilization on GPP often depended on the experimental duration and switched from being positive to negative in the long run (Bubier et al., 2007; Juutinen et al., 2010; Gong et al., 2020), which partially supported our simulation result. The effect of P deposition was rarely explored alone but significant increase in GPP was observed when both N and P fertilizers were applied (Bubier et al., 2007; Larmola et al., 2013; Kivimäki et al., 2013; Gong et al., 2020). In contrast,

GPP increase with NP fertilization in our simulation was only generated when M-level N_dep was applied, which may result from the lack of more N-demanding species in the model. No empirical studies have looked at the impact of elevated CO_2 on GPP directly. Based on the observed inertia of shrub biomass (McPartland et al., 2019, 2020), elevated CO_2 should lead to only limited impact on the primary production, which challenged the leading role of CO_2 simulated in this study.

On the other hand, the increase in HR and overall decrease in NEP with environmental changes have been well documented in peatland manipulation experiments, which is in line with our simulation results. Higher temperature (Dorrepaal et al., 2009; Wilson et al., 2016; Gill et al., 2017; Hopple et al., 2020), lowered water table (Laiho, 2006; Ise et al., 2008; Fenner and Freeman 2011; Bragazza et al. 2016), increased nutrient availability (Bragazza et al., 2012; Larmola et al., 2013; Pinsonneault et al., 2016a) and subsequent vegetation shift (Walker et al., 2016; Gavazov et al., 2018) could all contribute to higher peat decomposition and ultimately a decrease in the C uptake capacity of peatlands (Larmola et al., 2013; Munir et al., 2015; Bragazza et al. 2016; Ratcliffe et al., 2019; Hanson et al., 2020; Zhang et al., 2020; Fortuniak et al., 2021). Our result was in line with the finding from Müller and Joos. (2021) that temperature and precipitation are the most important determinants for the future fate of peatland, but we further highlighted the different effects of Tair and Tsoil on peatland C cycling. It is worth noticing that our simulation also successfully reproduced the observed dampened decomposition increase over time as the labile peat got depleted (Laiho, 2006; Straková et al.,2012; Ratcliffe et al., 2019), which could lead to recovery of C uptake capacity of peatlands in the long run (Munir et al., 2015; Minkkinen et al., 2018; Ratcliffe et al., 2020). Furthermore, several studies reported increased C uptake for peatlands with moderate air warming (Ward et al., 2013; Helbig et al., 2019; Laine et al., 2019), cooccurrence of warming and higher precipitation (Vitt et al., 2000; Bäckstrand et al., 2010) and increased nutrient deposition (Turunen et al., 2004; Olid et al., 2014), which also agreed with our simulation result.

5.5.4.Response of peatland nutrient cycles

In general, environmental changes have led to increased availability of inorganic nutrients in the peat. Besides the elevated nutrient deposition, the increase in inorganic nutrients could also be caused by the increased net nutrient mineralization with climate change. The simulated increase in both N and P net mineralization are mostly driven by higher Tsoil, which accelerated both the depolymerization and microbial growth rates while decreased the microbial CUE. All those changes could contribute to more nutrient 'leakage' from microbial metabolism processes (Melillo et al., 2011). Greater WTD could also stimulate N mineralization as it exposed the peat with smaller C:N ratio. But its effect on P mineralization was more neutral as it exposed deeper peat with lower C:P ratio meanwhile boosted P biochemical mineralization with higher N availability. Increased N_dep led to increased net mineralization for N while increased P_dep resulted in decreased net P mineralization for P. This resulted from the relatively wider range of C:P ratios compared to C:N ratios prescribed for both SAP (Camenzind et al., 2021) and shrub litter, which made N immobilization more demand-driven while P immobilization more supply-driven. Therefore, higher availability of DIN relieved the N limitation for SAP and led to much higher production of N 'waste' whereas increased DIP resulted in much higher P immobilization for SAP and led to smaller net mineralization for P. On the other hand, increased N_dep boosted P biochemical mineralization thus could also drive the increase in P net mineralization.

Previous studies often found increased nutrient mineralization and availability in peatlands with soil warming (Keuper et al., 2012; Weedon et al., 2012; Song et al., 2018) and water table drawdown (Macrae et al., 2013; Munir et al., 2017; Marttila et al., 2018; Wang et al., 2018;), which generally agreed with our simulation results here. Several studies have also reported different responsive dynamics for N and P mineralization to environmental changes (Bridgham and Richardson, 2003; Aerts et al., 2012; Mettrop et al., 2015; Morison et al., 2018). What caused the relative inertia of P mineralization in our simulation is in line with the framework proposed by Bridgham and Richardson (2003) that the immobilization-mineralization dynamics of N and P were largely driven by a source-sink relationship. The wide C:P ratio ranges prescribed for both SAP and shrub litter led to a strong capacity for P sinks, which

resulted in larger increase in P immobilization than mineralization with increased P availability. However, it is worth pointing out that our simulation predicted extremely high DIN accumulation under scenarios with high level Tsoil, WTD and N_dep. The lack of N_2O production in our model reduced the credibility of this projection here as previous studies have reported increase in peatland N_2O productions with climate change (Minkkinen et al., 2020) and N fertilization (Gong et al., 2019).

5.5.5. Microbe-plant interaction on biogeochemical cycling

As most environmental changes simulated here increased the availability of inorganic nutrients in the peat (Figure 5.5), the ericaceous shrubs shifted their major nutrient sources from the "C-costly" ERM transfer to "C-free" direct root uptake (Figure 5.6). This shift in nutrient sources thus increased the available C allocated to shrub growth and contributed to the overall increase in shrub's dominance over mosses with environmental changes. In contrast, when CO_2, Tair or only P_dep was increased while Tsoil, WTD and N_dep were maintained at their base levels, shrubs increased their C allocation to ERM to acquire more nutrients, especially N, to meet their growth demands (Figure S5.9). But not only did the increased ERM not alleviate the nutrient limitation for the shrubs, it decreased inorganic nutrients in the peat and increased shrubs' reliance on ERM to acquire nutrients, which led to limited increase in shrubs and even increase in peatland's NEP (Figure 5.3(d)).

To further investigate the significance of mycorrhiza-mediated nutrient cycling, ERM adaptation was introduced into the simulation which enabled ERM to actively decrease their nutrient transfer to maintain shrubs' high reliance on them. With the adaptive ERM, the high dependency of shrubs on ERM for nutrient acquisition was much better maintained and only cut down by elevated nutrient inputs or high-level climate change (Figure S5.10). As a result, the resilience of ERM and moss biomass was substantially enhanced while the increase in shrub and SAP biomass was dramatically reduced (Figure 5.8), leading to much less C loss in response to environmental disturbances (Figure 5.9(d)). Since all the climate conditions were the same between the experiments with and without ERM adaptation (see section 2.4), the attenuated shrub increases with adaptive ERM could only result from the sustained shrubs'

large C allocation to ERM nutrient transfer. Therefore, a large portion of the original shrub increase with environmental changes could be attributed to the changes in nutrient sources for shrubs besides the improved climate conditions. The mycorrhiza-mediated nutrient cycling thus played a paramount role in determining the bog's response to environmental changes.

Studies in non-peatland ecosystems have shown that increased nutrient availability could lead to changes in plant nutrient sources (Högberg et al., 2014; Jach-Smith and Jackson, 2020; Pellitier et al., 2021), decline in plants' belowground C allocation (Bae et al., 2015; Gill and Finzi, 2016; Eastman et al., 2021) and shifts in plant-microbe interactions (Carrara et al., 2018; Dunleavy and Mack, 2021), which ultimately drove the changes in the ecosystem as our modeling results demonstrated here. More studies are still needed to validate these mechanisms in peatlands, but peatland fertilization experiments have already reported some supporting evidence including shifts in shrub's nutrient sources (Vesala et al., 2021), decrease in ERM diversity (Van Geel et al., 2020) and enzyme production (Kiheri et al., 2020) with increased nutrient availability. Furthermore, our simulation results are in line with the findings from previous ectomycorrhiza (ECM) studies that mycorrhizal fungi could trap the ecosystem in N limitation by forming a positive feedback loop among the increased C allocation to mycorrhiza, higher mycorrhiza N immobilization, decreased soil N availability and aggregated N limitation (Näsholm et al. 2013; Franklin et al. 2014; Henriksson et al., 2021). Interestingly, recent evidence seemed to find this mechanism applied even better on ERM fungi: mycorrhiza shift from ECM to ERM during long-term succession in boreal forest was found to aggregate N limitation, decrease aboveground plant productivity, and increase SOC accumulation (Clemmensen et al., 2013, 2015, 2021), and ECM plants exhibited a greater increase in above-ground biomass in CO_2-enrichment studies than plants associated with ERM (Terrer et al., 2021; Bastos and Fleischer, 2021). Therefore, ERM-mediated nutrient cycling could be significantly responsible for the high nutrient limitation environment, the low plant production and high C accumulation in ombrotrophic peatlands, as already shown in Chapter 4.

Furthermore, our ERM adaptation experiments showed that the negative effect of ERM on shrubs could worsen into complete parasitism with environmental changes if the

mycorrhiza can actively control its nutrient transfer based on the C benefit from the host. This experimental ERM control we applied here agrees with the 'biological market' theory (Kiers et al., 2011; Werner et al., 2014) which has been proposed to explain the complex mycorrhiza-host interactions along a continuum of mutualism to parasitism (Johnson et al., 1997, 2010). Evidence on this theory is found that arbuscular mycorrhizal fungi could store nutrients in a form inaccessible to hosts to gain a better "carbon price" (Hammer et al., 2011; van't Padje et al., 2021b) and actively select the host that could provide a larger benefit (Fellbaum et al., 2012, 2014; van't Padje et al., 2021a). An ECM modeling study applying the market theory also discovered that the market mechanisms lead to stabilization of ECM-plant symbiont in expense of reduced growth for host, thus could be used to explain strong N limitation ubiquitous in boreal forests (Franklin et al., 2014), which is in line with our modeling result. Therefore, by simulating the potential ERM adaptation, our model has further highlighted the significant role of ERM in regulating the biogeochemical cycling in ombrotrophic peatlands, challenging the more prevalent plant-centric views (Dieleman et al., 2015; Goud et al., 2017).

5.6. Conclusion and way forward

In this study, we applied the newly developed model MWMmic_NP that integrates peatland C, N and P cycles with mycorrhiza controls to simulate the responses of an ombrotrophic peatland to changes in climate conditions, nutrient depositions, and CO_2 level. We found a general change from mosses to shrubs in vegetation community composition, and from ERM to SAP in microbial community composition in response to most scenarios of environmental changes. These community shifts were accompanied by a more open nutrient cycle and a reduced C sink strength for the bog. We also examined the interaction between different drivers and disentangled the contribution of each driver in causing the simulated changes. Soil warming and water table drawdown were identified as the two most important drivers leading to losses in peatland C sequestration capacity. Considering the insulation effect of peat (Wisser et al., 2011), moderate air warming and CO_2 level rise in the future could lead to increased C sequestration for the bog if the water table is maintained. ERM-mediated nutrient cycling was found to play an instrumental role in determining the response of the bog. The diminished role of ERM transfer in the ericaceous shrubs' nutrient sources was

primarily responsible for the bogs' simulated changes with the environmental disturbances. Persistence of ERM with potential adaptive strategies could increase the resilience of the ombrotrophic peatlands and needs further research. Meanwhile we also acknowledge there are several limitations in this study:

1. MWMmic_NP lacked a complete hydrological model and adopted water table depth as a meteorological input, which hindered the model's ability to examine important hydrological feedbacks that exist in peatlands. For instance, the higher decomposition following water table drawdown could lead to peat subsidence and compaction, which helped maintain the water table and limited the impact brought by drainage or drought (Strack and Waddington 2007). Therefore, our simulated result with WTD increase should be interpreted with caution.

2. Only two PFTs and one mycorrhiza type were currently represented in the model. Responses of other vegetation types like trees and deciduous shrubs were reported to play an important role in the long-term response of the bog to disturbances (Talbot et al., 2014). Since the non-ericaceous woody plant species in bogs were mostly associated with ECM (Thormann, 2006), ECM and its interaction with ERM could determine the dominant plant species with environmental changes (Vowles and Björk, 2019). Therefore, exclusion of these plant and microbial species could lead to uncertainties in our model's long-term prediction.

3. The production of other important GHGs (greenhouse gases) including CH_4 and N_2O is not simulated in the model. MWM adopted a simple methane module from PCARS (Frolking et al., 2002), but for the scope of this research, that module was not adapted into the newly developed MWM. Previous studies have shown dramatic changes in the emissions of these GHGs with environmental changes (Gong et al., 2019; Minkkinen et al., 2020). Since CH_4 and N_2O have different radiative efficacies and lifetimes from CO_2 (Etminan et al., 2016), the changes in global warming potential in peatlands with environmental changes cannot be assessed here.

Despite the limitations, our study is, to the best of our knowledge, the first modeling study that looked at the importance of microbe-mediated nutrient cycling in the response of ombrotrophic peatland to environmental changes. Our research served as one of the first

steps to answer the calling towards a microbial process-based understanding of the resilience of peatland ecosystem service provisioning (Ritson et al., 2021).

5.7. Tables and Figures

Table 3.1 Values assigned for each environmental variable in different alteration scenarios.

Disturbance	N deposition (N_dep)	P deposition (P_dep)	CO_2 level (CO_2)	Water table depth (WTD)	Air temperature (Tair)	Soil temperature (Tsoil)
Base	BN	BP	BC	BWTD	BTa	BTs
	0.8 gN/m^2/yr	30 mgP/m^2/yr	MB input	MB input	MB input	MB input
Median	MN	MP	MC	MWTD	MTa	MTs
	1.6 gN/m^2/yr	60 mgP/m^2/yr	+150ppm	+10cm	+2.5 °C	+2.5 °C
High	HN	HP	HC	HWTD	HTa	HTs
	2.4 gN/m^2/yr	90 mgP/m^2/yr	+300ppm	+20cm	+5.0 °C	+5.0 °C

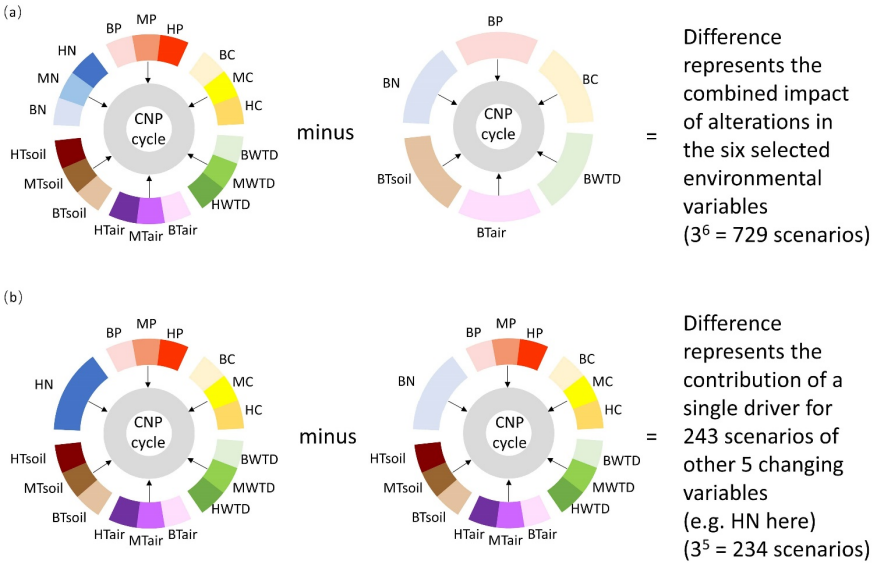

Figure 5.1 Analysis protocol of the simulation results. (a) The difference between each scenario and the base scenario represents the combined effect of concomitant change in different drivers; (b) The difference between two scenarios that differ only in the investigated driver being on and off represents the contribution of a single driver to the combined impact with other 5 drivers.

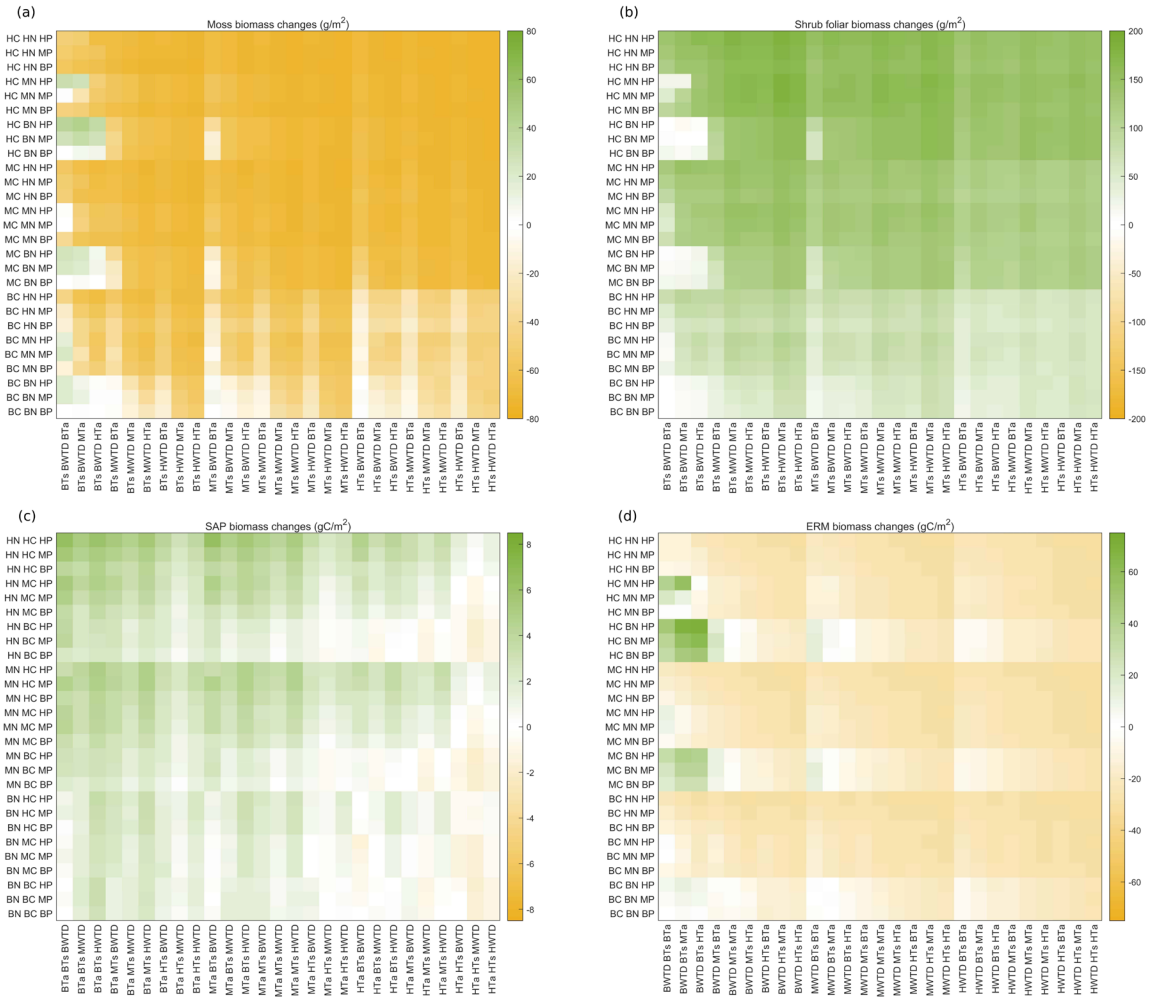

Figure 5.2 Average changes during the 80-year period of simulated disturbance under different environmental change scenarios (heat maps) in (a) shrub biomass, (b) moss biomass, (c) SAP biomass and (d) ERM biomass. The X-axis depicts the disturbance scenarios of increased Ta, Tsoil and WTD and the Y-axis depicts the disturbance scenarios of increased CO_2 level, N deposition and P deposition. This setup applies to all the heatmaps in this study.

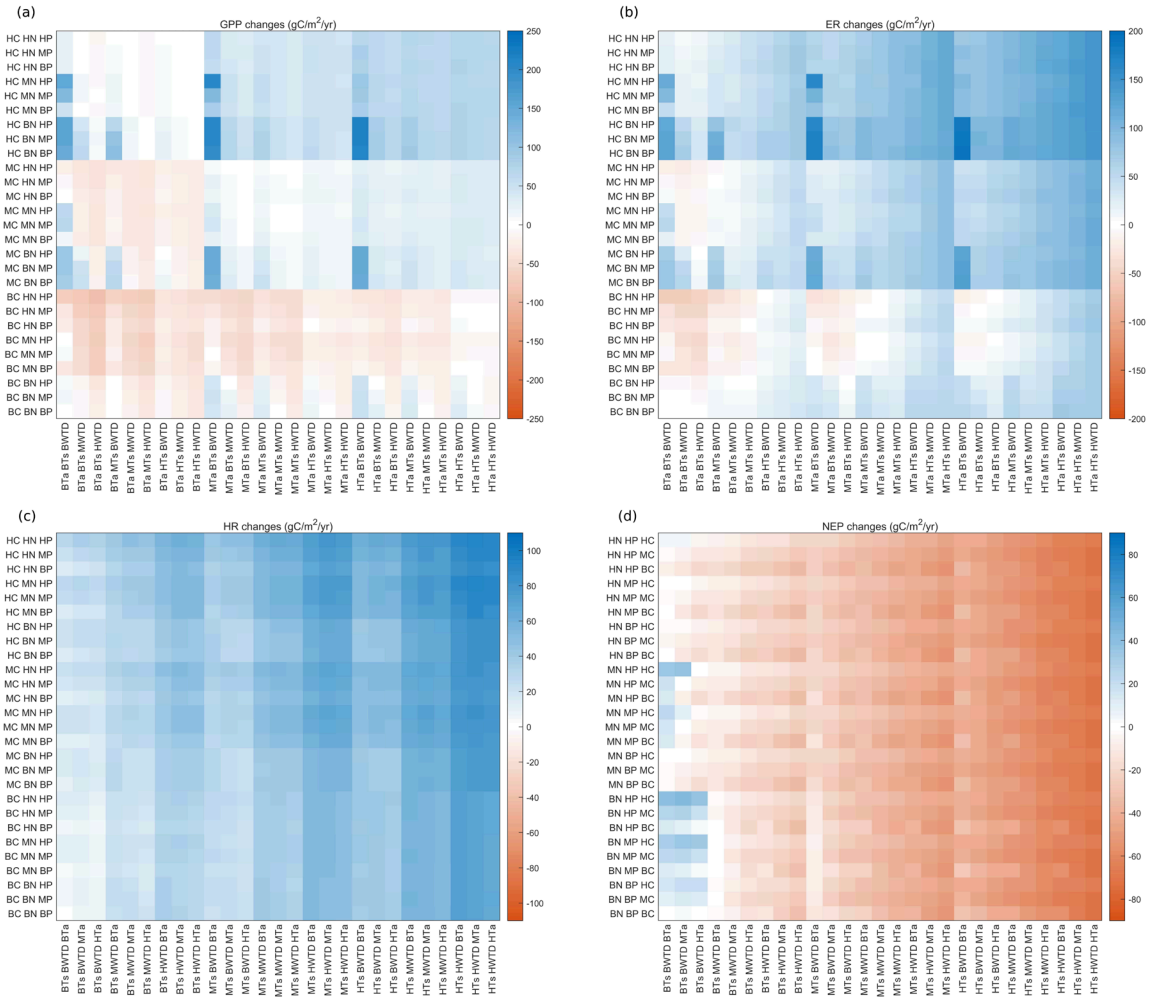

Figure 5.3 Average changes during the 80-year period of simulated disturbance under different environmental change scenarios (heat maps) in (a) GPP, (b) ER, (c) HR and (d) NEP.

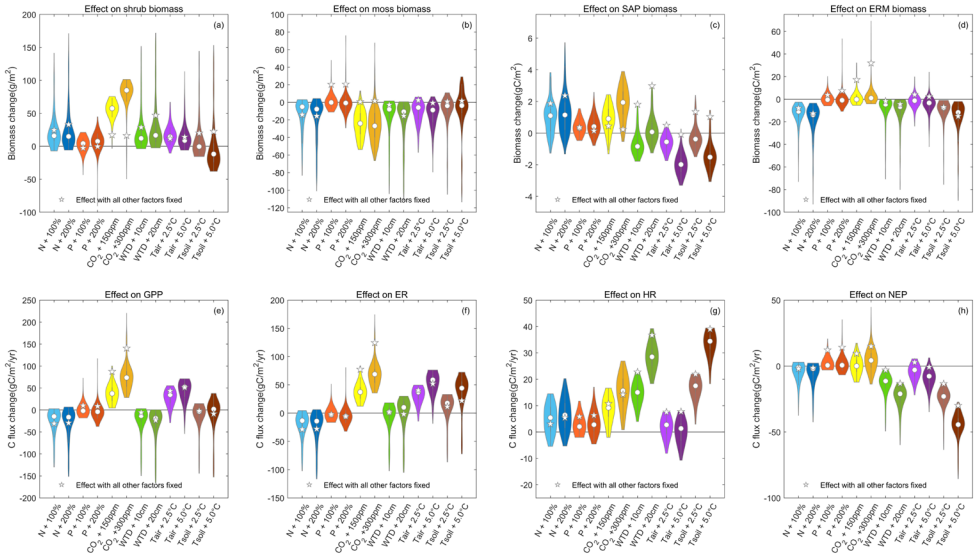

Figure 5.4 The contribution of each driver on the changes (violin plots) in (a) shrub biomass, (b) moss biomass, (c) SAP biomass, (d) ERM biomass, (e) GPP, (f) ER, (g) HR and (h) NEP.

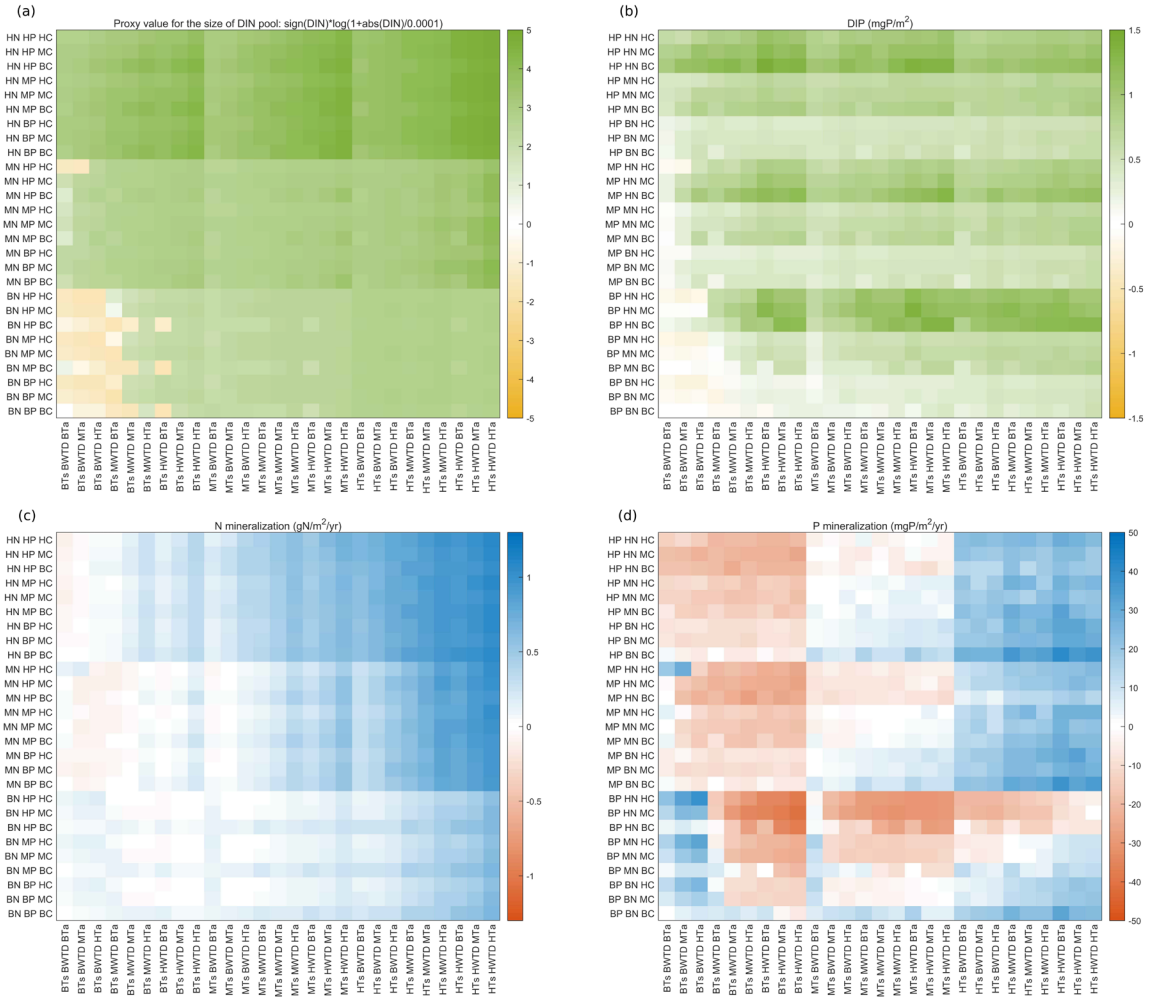

Figure 5.5 Average changes during the 80-year period of simulated disturbance under different environmental change scenarios (heat maps) in (a) the size of DIN pool, (b) the size of DIP pool, (c) net N mineralization fluxes and (d) net P mineralization fluxes within top 50cm peat. The size of DIN pool is presented using a proxy value to show the wide range of DIN change on an exponential scale.

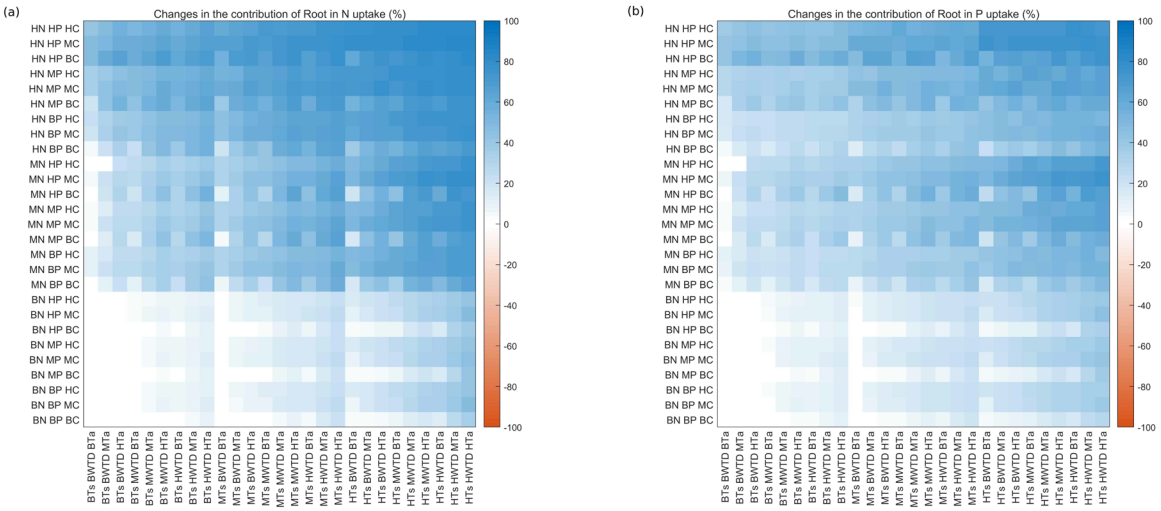

Figure 5.6 Average changes during the 80-year period of simulated disturbance under different environmental change scenarios (heat maps) in (a) N sources for shrubs and (b) P sources for shrubs.

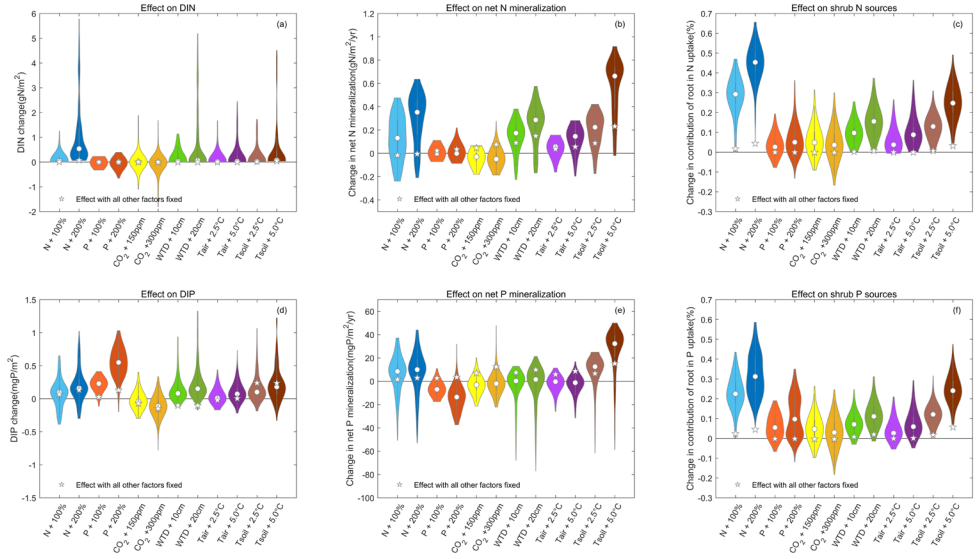

Figure 5.7 The contribution of each driver on the changes (violin plots) in (a) the size of DIN pool (top 50cm), (b) net N mineralization fluxes (top 50cm), (c) N sources for shrubs, (d) the size of DIP pool (top 50cm), (e) net P mineralization fluxes (top 50cm) and (f) P sources for shrubs.

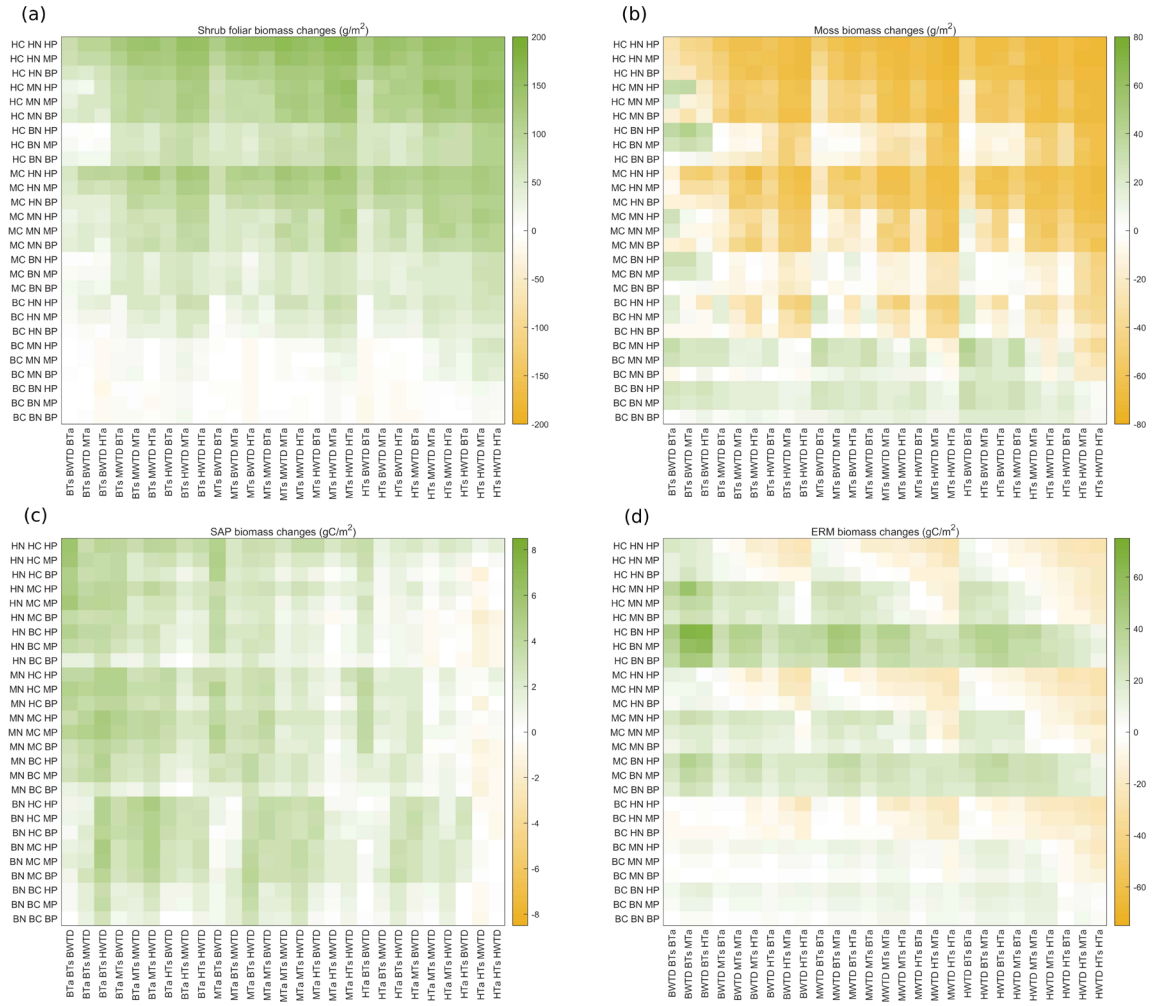

Figure 5.8 Average long-term changes in (a) shrub biomass, (b) moss biomass, (c) SAP biomass and (d) ERM biomass predicted by MWMmic_NP with adaptive ERM under different simulation scenarios.

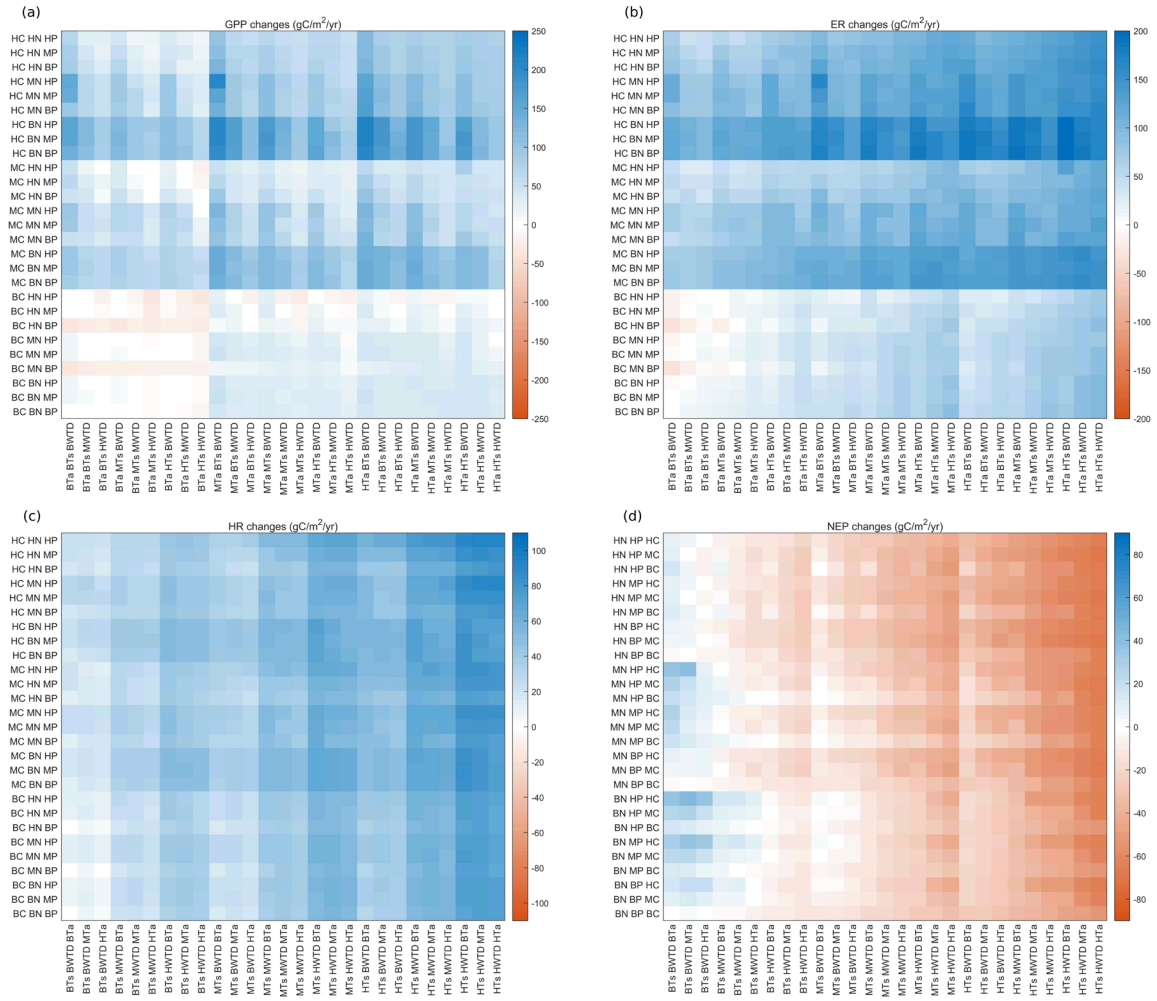

Figure 5.9 Average long-term changes in (a) GPP, (b) ER, (c) HR and (d) NEP predicted by MWMmic_NP with adaptive ERM under different simulation scenarios.

5.8. Supplementary materials

Simulating ERM's control on nutrient transfer

To simulate the active control of nutrient transfer, we applied the concept of "carbon price" from Hammer et al. (2011) and Franklin et al. (2014) to create the nutrient prices (the ratio of carbon benefit per nutrient transferred) while adopted an equation like that used for calculating the nutrient transfer from mycorrhiza to host plants in Meyer et al. (2012).

$$Cbenefit_N = \frac{Ctransfer_{annual}}{Ntransfer_{annual}} \quad \text{(S1a)}$$

$$Ntransfer_{coeff} = min\left(\left(\frac{Cbenefit_N}{Cbenefit_{N,ref}}\right)^{\alpha}, 1.0\right) \quad \text{(S1b)}$$

$$Cbenefit_P = \frac{Ctransfer_{annual}}{Ptransfer_{annual}} \quad \text{(S2a)}$$

$$Ptransfer_{coeff} = min\left(\left(\frac{Cbenefit_P}{Cbenefit_{P,ref}}\right)^{\alpha}, 1.0\right) \quad \text{(S2b)}$$

Where $Cbenefit_N$ and $Cbenefit_P$ represent the N and P price paid by ERM for C transfer from shrubs, respectively, $Ctransfer_{annual}$ is the annual accumulation of C transferred from shrubs to ERM, $Ntransfer_{annual}$ and $Ptransfer_{annual}$ are annual accumulation of N and P transferred from ERM to shrubs, respectively, α represents the power of ERM active regulation, $Ntransfer_{coeff}$ and $Ptransfer_{coeff}$ are the coefficient multipliers used to constrain the rate of N and P transfer from ERM to shrubs.

$Cbenefit_{N,ref}$ and $Cbenefit_{P,ref}$ were assigned with the value of 60gC/gN and 1000gC/gN respectively, which are derived from assigning a slightly larger number than the average N and P prices calculated for the control plots at Mer Bleue bog. The logic behind this calculation is to ensure that ERM can transfer nutrients with a coefficient multiplier around 1.0 in the control scenarios, so that the simulated peatland in controls scenarios with the "ERM adaptation" is close to that without considering "ERM adaptation". α was assigned with a value of 10.0 to ensure strong regulation from the ERM. The updating of NP transfer coefficients was conducted on the end of the year and calculated based on the 2-year average of the $Cbenefit_N$ and $Cbenefit_P$ to prevent abrupt change in ERM-shrub exchange and ensure a smooth transition from year to year.

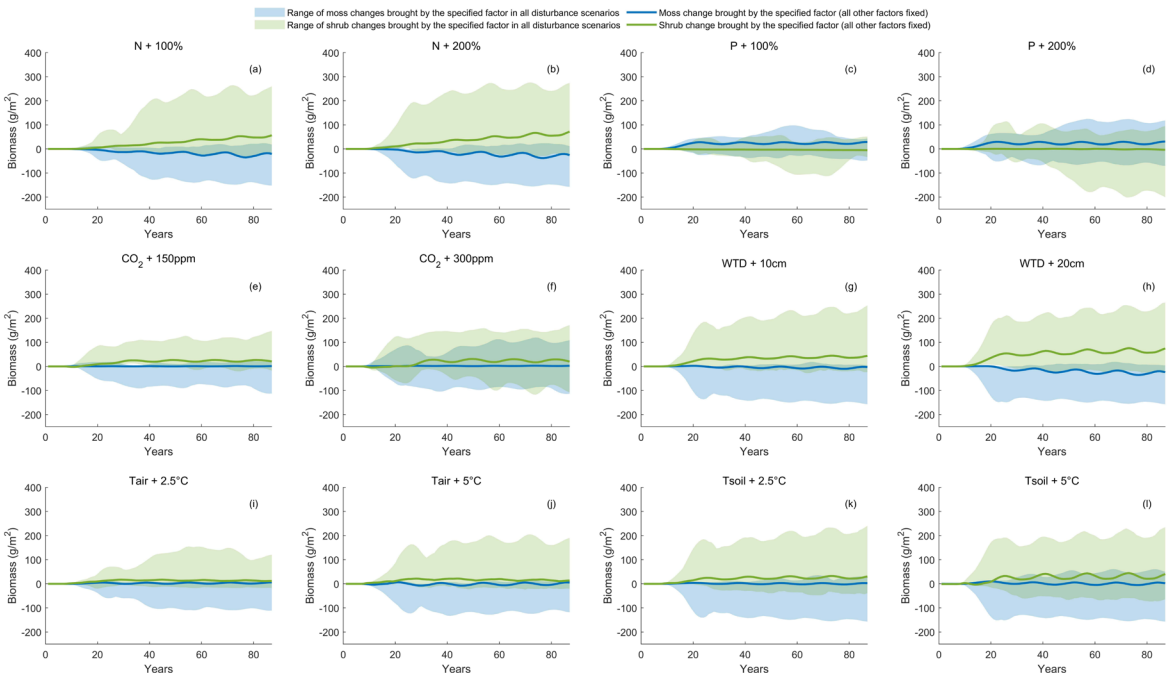

Figure S5.1 Time series of the contribution of each driver on the changes in vegetation biomass, derived from subtracting two scenario results that differ only in the specific driver being on or off.

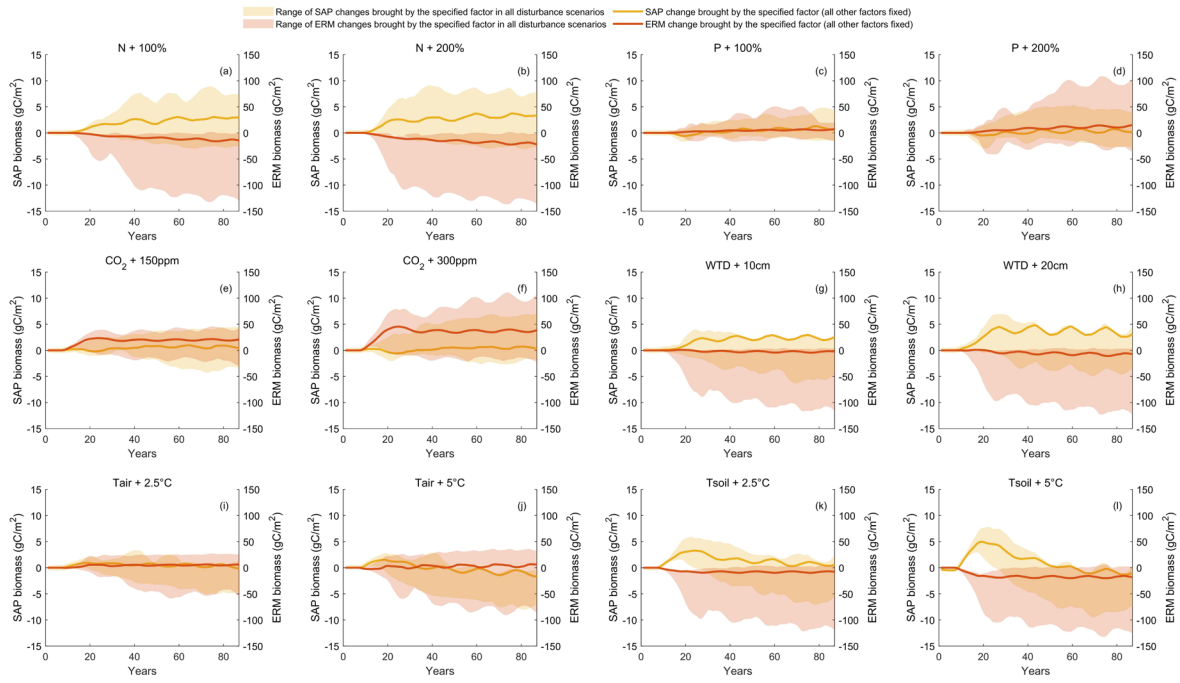

Figure S5.2 Time series of the contribution of each driver on the changes in microbial biomass, derived from subtracting two scenario results that differ only in the specific driver being on or off.

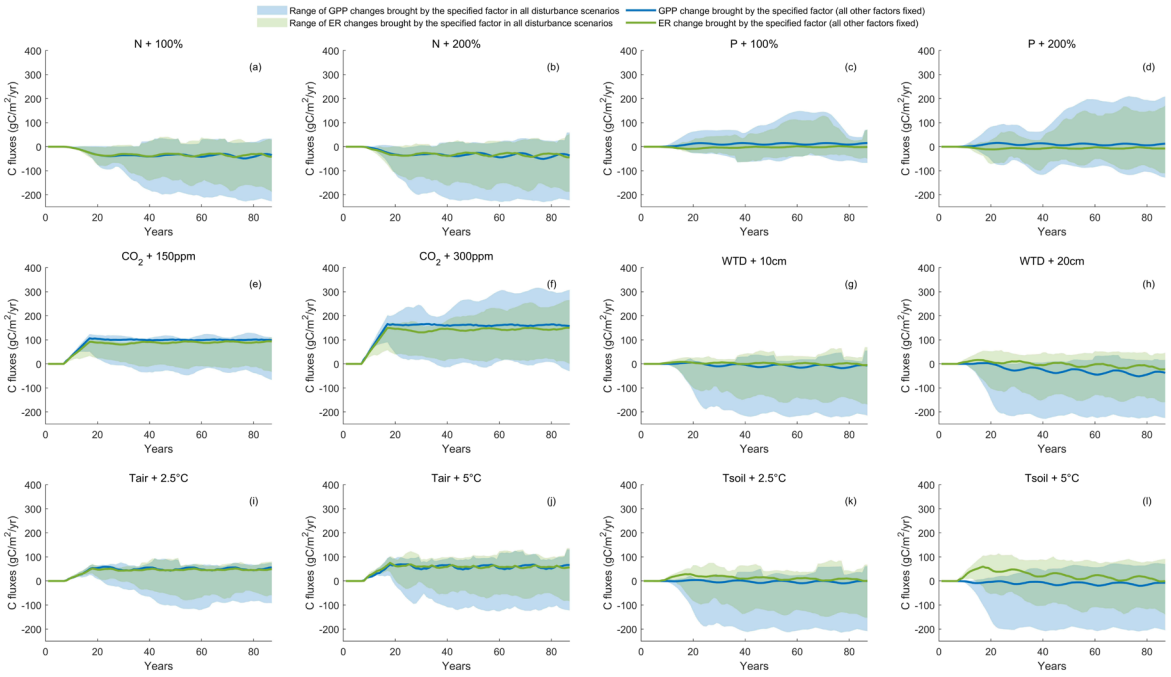

Figure S5.3 Time series of the contribution of each driver on the changes in GPP and ER, derived from subtracting two scenario results that differ only in the specific driver being on or off.

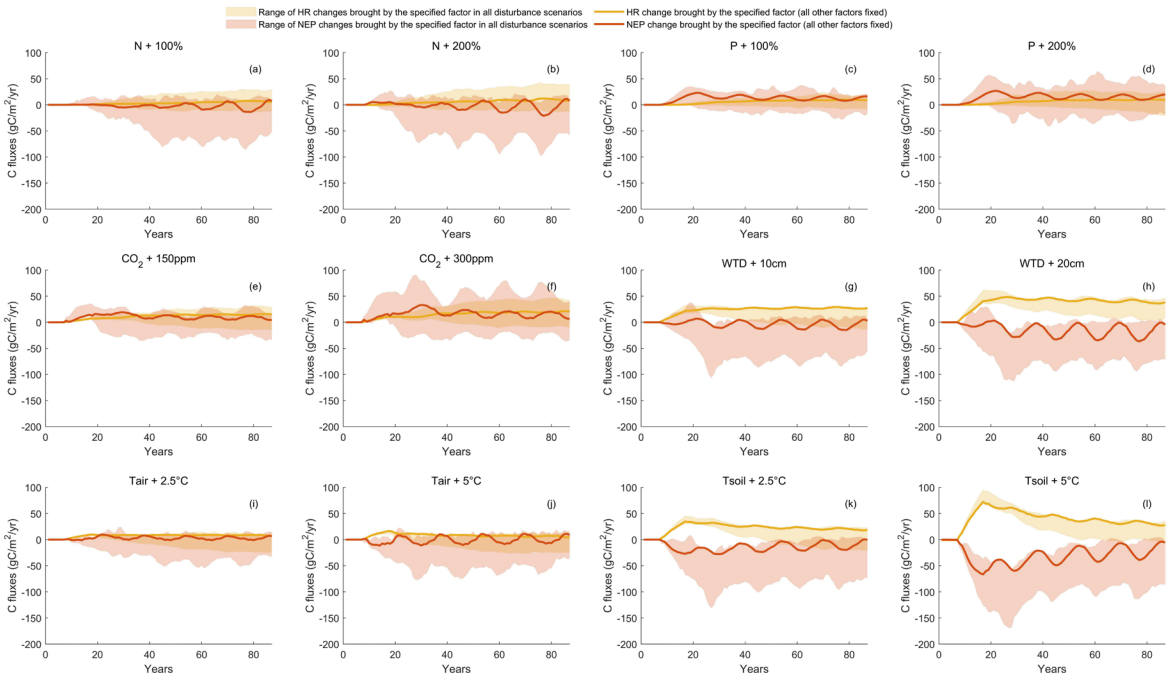

Figure S5.4 Time series of the contribution of each driver on the changes in HR and NEP, derived from subtracting two scenario results that differ only in the specific driver being on or

off.

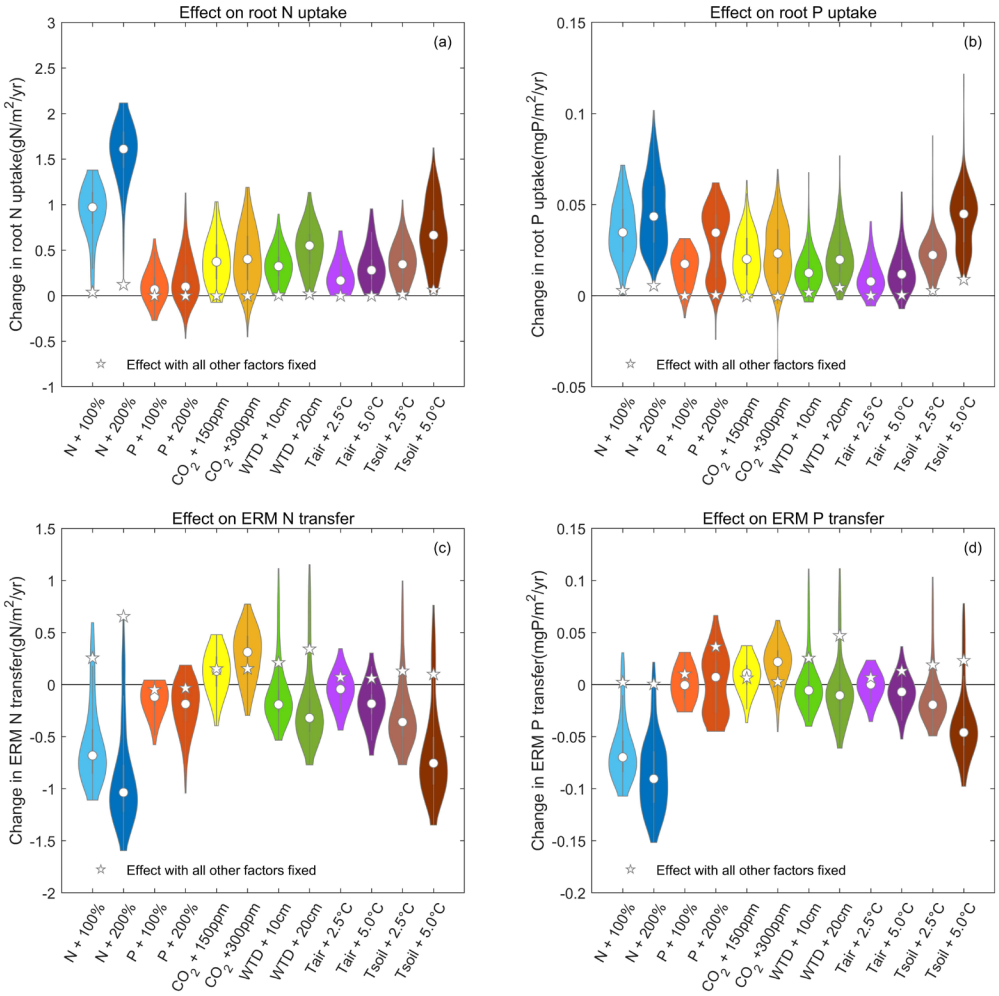

Figure S5.5 The contribution of each driver on the changes (violin plots) in (a) shrub root N uptake, (b) shrub root P uptake, (c) ERM N transfer and (d) ERM P transfer.

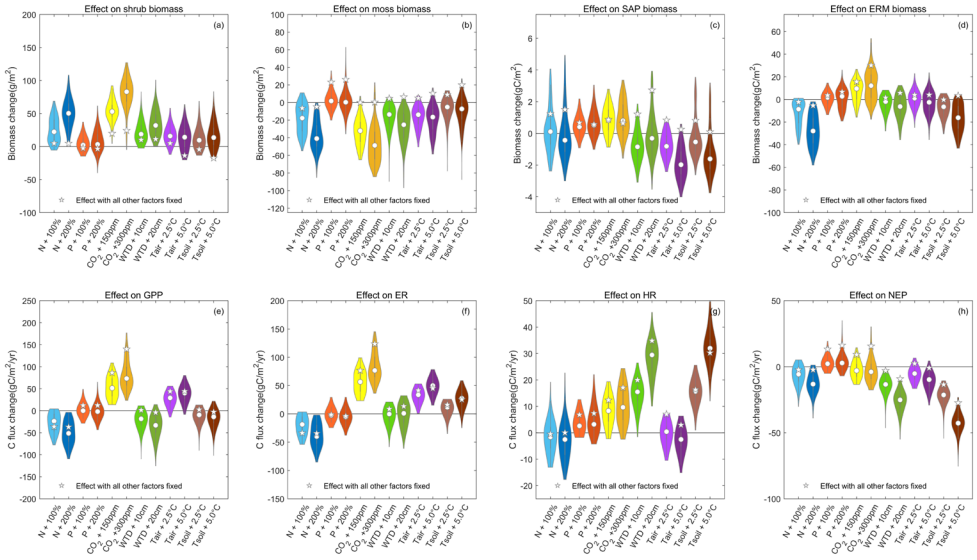

Figure S5.6 The contribution of each driver on the changes (violin plots) in vegetation and microbial biomass, and ecosystem C fluxes, predicted by MWMmic_NP with adaptive ERM.

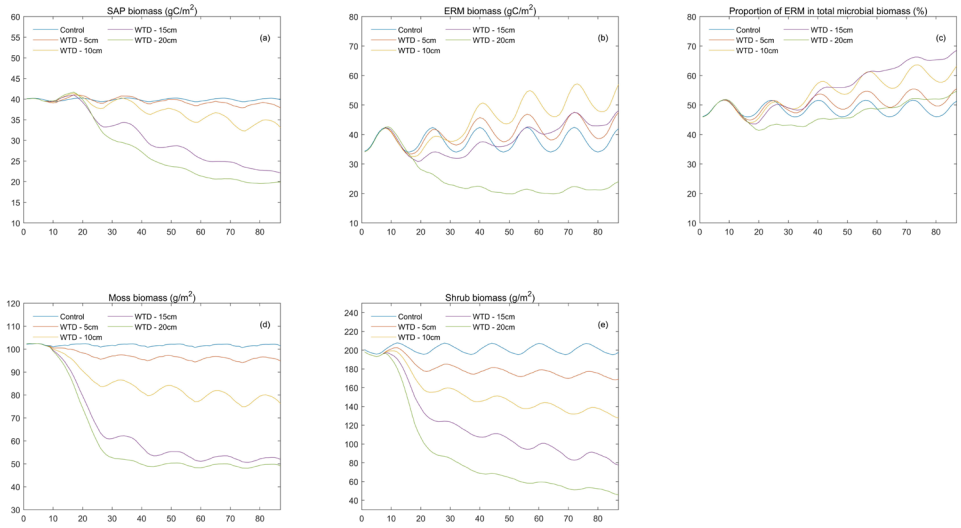

Figure S5.7 Simulated response of the vegetation and microbial communities Mer Bleue bog to elevated water table.

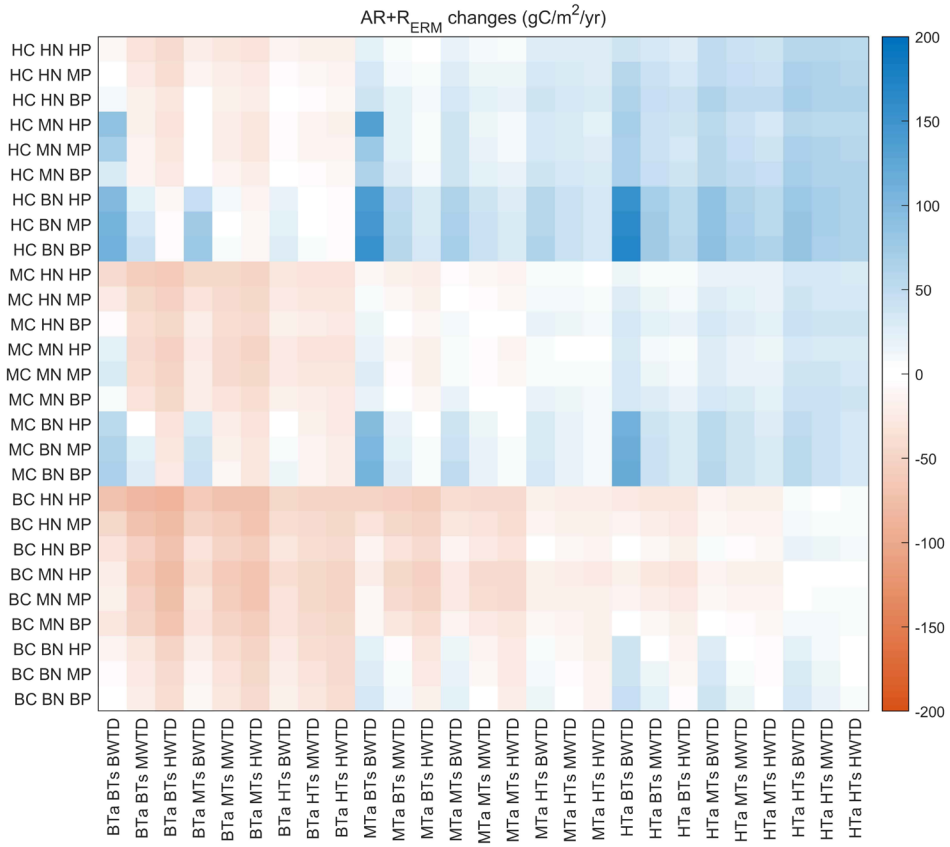

Figure S5.8 Heat map of simulated average changes in AR+ERM respiration during the 80-year period of simulated disturbance under different environmental change scenarios

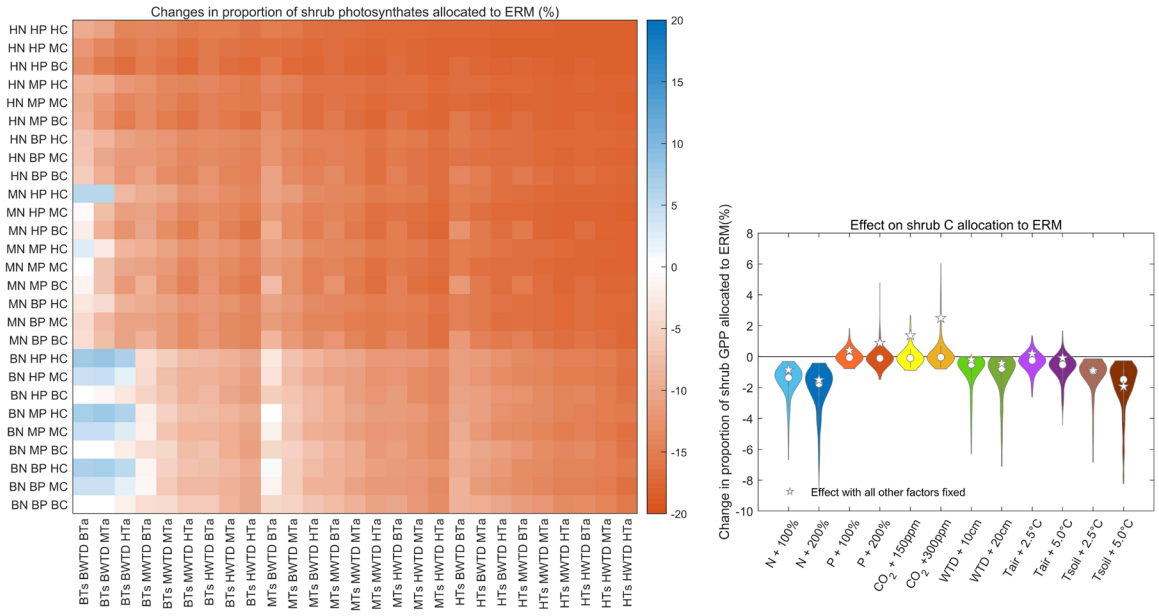

Figure S5.9 (a) Heat map of simulated average changes in the proportion of shrub photosynthates allocated to ERM during the 80-year period of simulated disturbance under

different environmental change scenarios and (b) the contribution of each driver on the changes.

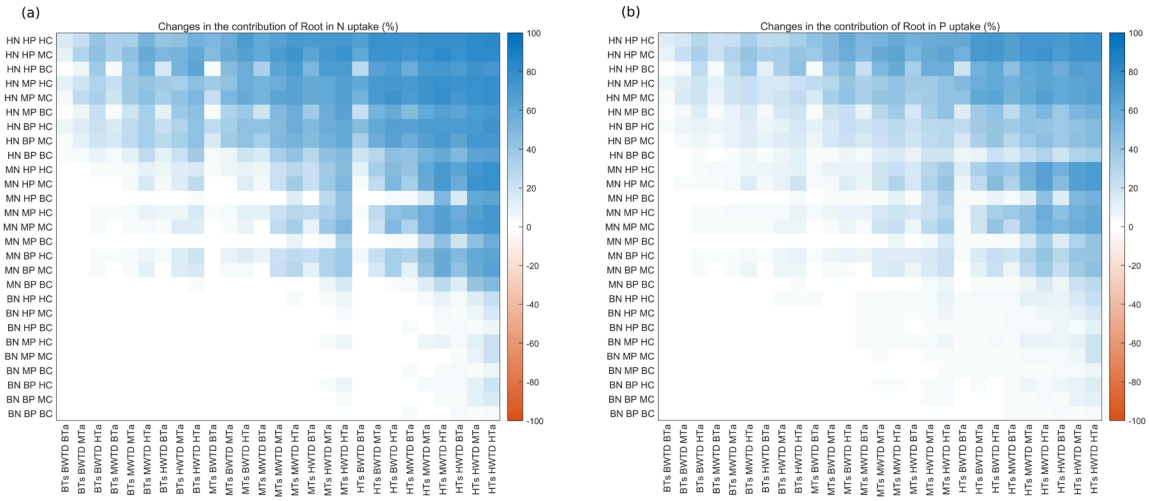

Figure S5.10 Average changes during the 80-year period of simulated disturbance under different environmental change scenarios with adaptive ERM in (a) N sources for shrubs and (b) P sources for shrubs.

Chapter 6. Synthesis, conclusions, and future directions

Despite covering less than 3% of the world land area, peatlands currently store up to a third of the global soil organic carbon. These peatlands have acted as C sinks for millennia and may be potentially sensitive to future environmental disturbances like increased nutrient deposition and climate change. Biogeochemical models can be used to examine complex interactions within an ecosystem and project its response to environmental disturbances. However, current peatland models have neglected important regulating processes like nutrient cycling and microbial metabolism. This hinders our ability to predict the future of peatland carbon balances. In this thesis, I have incorporated microbial processes and nutrient cycles into the established peatland model McGill Wetland Model (MWM), used the new model MWMmic_NP to examine the importance of microbe-mediated biogeochemical feedbacks and assessed the fate of the peatland under future environmental changes.

6.1. Chapter syntheses

In Chapter 3, I incorporated cohort development and saprotrophic microbial metabolisms into the decomposition model of MWM and applied the new model MWMmic on the Mer Bleue bog. MWMmic not only successfully reproduced the measured CO_2 fluxes at the bog, but also performed well in replicating the observed microbial and DOC dynamics. Compared to the original MWM (St-Hilaire et al., 2010), consideration of peat substrate quality with the cohort control made the modelled peatland less sensitive to environmental disturbances, especially water table drawdown, as the deep peat which has gone through large degree of decomposition is much more recalcitrant than the fresh peat substrate at shallow depth. Our modelling result demonstrates the negative feedback within the peatland that the increased peat recalcitrancy with accelerated decomposition could limit the loss of peat C with climate change. I also identified the microbial carbon use efficiency (CUE) and turnover rate as the most important microbial physiological parameters in determining the response of peat decomposition to environmental changes. Potentially more adaptive saprotrophs which maintained constant turnover rates and/or increased their CUE with favourable environmental conditions could lead to much larger increase in the peat

decomposition with warming and water table drawdown.

In Chapter 4, I incorporated ericoid mycorrhiza (ERM)-mediated nutrient cycling into MWMmic and applied the new model to the Mer Bleue bog setting. MWMmic_NP performed well in capturing the tight recycling features of the nutrient cycle observed in the bog, including the measured small N mineralization rates and increased peat C:P ratios with depth. MWMmic_NP also replicated the response of peatland to increased nutrient deposition observed in the long-term fertilization experiments at Mer Bleue. My modelling results showed that ericaceous shrubs rely mostly on ERM transfer as their nutrient sources for the scarcity of inorganic nutrients. But with increased nutrient deposition, the shrubs switched their nutrient sources to less C-costly root uptake, decreased their C expenditure on ERM and invested more C to their own growth. This result could help explain how shrubs managed to increase their biomass with unchanged photosynthetic capacity as observed in the fertilization experiment (Bubier et al., 2011). A species-exclusion experiment demonstrated that *Sphagnum* mosses in the model might also be indirectly relying on shrub-ERM to acquire P and the whole system had the largest C sequestration capacity when shrubs, mosses and ERM fungi were all present in the model. Therefore, I found that shrub-ERM-*Sphagnum* association could potentially be a mutualistic system that reinforces itself and might be ultimately responsible for closed nutrient cycle and large C accumulation in ombrotrophic peatlands.

In Chapter 5, MWMmic_NP was used to simulate the response of Mer Bleue bog to different scenarios of changes in climate conditions, nutrient depositions, and CO_2 level. In response to environmental changes, the bog generally shifted its vegetation communities towards shrub domination and its microbial communities towards saprotroph domination. These community shifts were often accompanied with a reduced C sequestration capacity for the bog. Through disentangling the contribution of each driver in causing the simulated changes, I identified the increased peat temperature and lowered water table as the two most important drivers leading to the bog's community shift and decreased C sequestration capacity. Those two drivers enhanced nutrient mineralization and led to a diminished role of ERM transfer in the ericaceous shrubs' nutrient sources, which are primarily responsible for

the simulated increased shrub biomass. In contrast, moderately warmer air temperature and elevated CO_2 levels alone could increase the reliance of shrub on ERM for nutrients, which further tightened the bog's nutrient cycling and increased the C sequestration. Therefore, ERM-mediated nutrient cycling is found to play an instrumental role in determining the response of the bog. Potentially more adaptive ERM fungi which can decrease their nutrient transfer outwards in response to the reduced C transfer from the host could significantly increase the resiliency of the ombrotrophic peatlands.

6.2. Conclusions and the broader context

My overall objective was to fill some scientific gaps in the controls of the ombrotrophic peatland biogeochemical cycles from a modeling perspective. My unique and original modeling results showed that inclusion of key processes like cohort development, microbial dynamics and nutrient cycles into the peatland model could help us better understand the understudied feedbacks and interactions that exists within the ombrotrophic peatland. First of all, increased peat recalcitrancy with progressive decomposition could present an important negative feedback within the peatland, limiting the increase of peat decomposition with favorable environmental conditions. Secondly, nutrient cycles are tightly coupled with C cycles in ombrotrophic peatlands. Increased nutrient deposition or enhanced nutrient mineralization with climate change increased the dominance of more nutrient-demanding vascular plants over *Sphagnum* mosses, which could negatively impact the bog's C sink function. On the other hand, elevated CO_2 concentration and increased air temperature could aggravate the nutrient limitation of the bogs and subsequently increased the bogs' C sequestration. Thus, the dynamics of nutrient cycles must be considered when projecting the response of the ombrotrophic peatlands' C cycles to environmental changes. Finally, the dynamics of microbes, both saprotrophs and ERM fungi, play an important role in regulating the biogeochemical cycling of ombrotrophic peatlands. Our modeling result showed that ERM fungi potentially linked ericaceous shrubs and *Sphagnum* mosses together through tightened nutrient cycling, and suppressed the saprotrophic activity through nutrient competition, thus could significantly contribute to the high nutrient limitation and C accumulation in the bog. The diminished dominance of ERM fungi with increased nutrient availability accounted for the

substantial vegetation changes and reduced C sink capacity shown in the bog's response to environmental changes. Therefore, the biogeochemical function of an ombrotrophic peatland could be potentially determined by its microbial composition. Which microbial community (ERM fungi or saprotroph) is more adaptable with disturbances may decide the trajectory of bog's response to environmental changes.

6.3. Directions for future research

There are several knowledge gaps that remained to be addressed to improve the representation of microbial dynamics and nutrient cycling in the model. Here I propose several research directions that could be pursued in future peatland empirical research and modeling effort to improve our understanding of peatland biogeochemical cycles.

First, the microbial model in MWMmic_NP was constructed using data from studies in other ecosystems or based on calibrated parameters. Data for both saprotrophs and mycorrhiza fungi in peatlands that could be used for model calibration is rare. Therefore we need more empirical measurements on peatland microbial communities, especially their important physiological traits including CUE and turnover rates, to better constrain the peatland microbial decomposition model. Furthermore, studies that elucidate the amount of C that is allocated from ericaceous shrubs to ERM fungi, and the amount of nutrients transferred the other way around would significantly improve our knowledge of the role of mycorrhiza fungi in mediating peatland biogeochemical cycles.

Second, the P cycles in peatlands merits further research. A lack of study in P cycles in peatland compared to C and N precluded us from well-constructing the overall P budget in the MB bog. In particular, the model failed to reproduce the continuously decreased P concentration with depth in the catotelm peat, suggesting mycorrhiza mining might not be sufficient to explain the observed P distribution pattern. Iron reduction-phosphate desorption in the anoxic conditions might also play a role in P distribution but have not been well categorized in any peatland model. More research into the P-related processes is needed in peatlands to construct more comprehensive P cycle models for peatlands.

Third, more plant functional types (PFTs) and microbial community types need to be included in the peatland model. In this thesis, MWMmic_NP only considered two PFTs:

ericaceous shrubs and Sphagnum mosses and two microbial community types: saprotrophs and ERM fungi. This approach might be sufficient for oligotrophic peatlands like Mer Bleue bog. But more nutritious peatland ecosystems like fens or treed bogs, other PFTs like sedges, deciduous shrubs and trees, and other microbial communities like ectomycorrhizal (ECM) fungi might play a more important role. Moreover, these more nutrient-demanding PFTs and ECM fungi could potentially become more important in the long-term response of the oligotrophic bog to climate change with increased nutrient mineralization.

Forth, MWMmic_NP only used water table depth as model input thus did not include any hydrological feedback. Increased peat decomposition with environmental changes could lead to peat subsidence and compaction, which helped maintain higher relative water table, thus presenting a negative feedback. In contrast, increased shrub or even tree dominance with environmental changes could increase the evapotranspiration and may further lower the water table, thus presenting a positive feedback. A peatland model that includes a complete hydrological cycle could help us examine these potential feedbacks and assess the response of peatlands to disturbances more accurately.

Last, but not the least, the production of other important greenhouse gases (GHGs) including CH_4 and N_2O was not simulated in the model. These two gases have different radiative efficacies and lifetimes from CO_2, and their production are also heavily regulated by microbial processes. Future modeling effort should also include CH_4 and N_2O to improve our understanding of the impact of environmental changes on the global warming potential in peatlands.

Reference

Abdalla, M., Hastings, A., Bell, M. J., Smith, J. U., Richards, M., Nilsson, M. B., ... & Smith, P. (2014). Simulation of CO_2 and attribution analysis at six European peatland sites using the ECOSSE Model. Water, Air, & Soil Pollution, 225(11), 1-14.

Abramoff, R. Z., Davidson, E. A., & Finzi, A. C. (2017). A parsimonious modular approach to building a mechanistic belowground carbon and nitrogen model. Journal of Geophysical Research: Biogeosciences, 122(9), 2418-2434.

Abramoff, R., Xu, X., Hartman, M., O'Brien, S., Feng, W., Davidson, E., ... & Mayes, M. A. (2018). The Millennial model: in search of measurable pools and transformations for modeling soil carbon in the new century. Biogeochemistry, 137(1), 51-71.

Adamczyk, B., Ahvenainen, A., Sietiö, O. M., Kanerva, S., Kieloaho, A. J., Smolander, A., ... & Heinonsalo, J. (2016). The contribution of ericoid plants to soil nitrogen chemistry and organic matter decomposition in boreal forest soil. Soil Biology and Biochemistry, 103, 394-404.

Aerts, R., Callaghan, T. V., Dorrepaal, E., Van Logtestijn, R. S. P., & Cornelissen, J. H. C. (2012). Seasonal climate manipulations have only minor effects on litter decomposition rates and N dynamics but strong effects on litter P dynamics of sub-arctic bog species. Oecologia, 170(3), 809-819.

Ågren, G. I., & Bosatta, E. (1996). Quality: a bridge between theory and experiment in soil organic matter studies. Oikos, 522-528.

Ågren, G. I., & Bosatta, E. (2002). Reconciling differences in predictions of temperature response of soil organic matter. Soil Biology and Biochemistry, 34(1), 129-132.

Ahlström, A., Xia, J., Arneth, A., Luo, Y., & Smith, B. (2015). Importance of vegetation dynamics for future terrestrial carbon cycling. Environmental Research Letters, 10(5), 054019.

Allison, S. D., Wallenstein, M. D., & Bradford, M. A. (2010). Soil-carbon response to warming dependent on microbial physiology. Nature Geoscience, 3(5), 336-340.

Andersen, R., Chapman, S. J., & Artz, R. R. E. (2013). Microbial communities in natural and disturbed peatlands: a review. Soil Biology and Biochemistry, 57, 979-994.

Andersen, R., Francez, A. J., & Rochefort, L. (2006). The physicochemical and microbiological status of a restored bog in Québec: Identification of relevant criteria to monitor success. Soil Biology and Biochemistry, 38(6), 1375-1387.

Andrew, C. J., Van Diepen, L. T., Miller, R. M., & Lilleskov, E. A. (2014). Aspen-associated mycorrhizal fungal production and respiration as a function of changing CO_2, O_3 and climatic variables. Fungal Ecology, 10, 70-80.

Apple JK, del Giorgi PA, Kemp WM (2006) Temperature regulation of bacterial production, respiration, and growth efficiency in a temperate salt-marsh estuary. Aquat Microb Ecol 43:243–254

Asemaninejad, A., Thorn, R. G., Branfireun, B. A., & Lindo, Z. (2018). Climate change favours specific fungal communities in boreal peatlands. Soil Biology and Biochemistry, 120, 28-36.

Atkin, O. K., Bahar, N. H., Bloomfield, K. J., Griffin, K. L., Heskel, M. A., Huntingford, C., ... & Turnbull, M. H. (2017). Leaf respiration in terrestrial biosphere models. In Plant respiration: metabolic fluxes and carbon balance (pp. 107-142). Springer, Cham.

Averill, C., & Hawkes, C. V. (2016). Ectomycorrhizal fungi slow soil carbon cycling. Ecology letters, 19(8), 937-947.

Averill, C., & Waring, B. (2018). Nitrogen limitation of decomposition and decay: How can it occur?. Global change biology, 24(4), 1417-1427.

Averill, C., Turner, B. L., & Finzi, A. C. (2014). Mycorrhiza-mediated competition between plants and decomposers drives soil carbon storage. Nature, 505(7484), 543-545.

Bäckstrand, K., Crill, P. M., Jackowicz-Korczynski, M., Mastepanov, M., Christensen, T. R., & Bastviken, D. (2010). Annual carbon gas budget for a subarctic peatland, Northern Sweden. Biogeosciences, 7(1), 95-108.

Bae, K., Fahey, T. J., Yanai, R. D., & Fisk, M. (2015). Soil nitrogen availability affects belowground carbon allocation and soil respiration in northern hardwood forests of New Hampshire. Ecosystems, 18(7), 1179-1191.

Basiliko, N., Moore, T. R., Jeannotte, R., & Bubier, J. L. (2006). Nutrient input and carbon and microbial dynamics in an ombrotrophic bog. Geomicrobiology Journal, 23(7), 531-543.

Basiliko, N., Moore, T. R., Lafleur, P. M., & Roulet, N. T. (2005). Seasonal and inter-annual decomposition, microbial biomass, and nitrogen dynamics in a Canadian bog. Soil Science, 170(11), 902-912.

Basińska, A. M., Reczuga, M. K., Gąbka, M., Stróżecki, M., Łuców, D., Samson, M., ... & Lamentowicz, M. (2020). Experimental warming and precipitation reduction affect the biomass of microbial communities in a Sphagnum peatland. Ecological Indicators, 112, 106059.

Baskaran, P., Hyvönen, R., Berglund, S. L., Clemmensen, K. E., Ågren, G. I., Lindahl, B. D., & Manzoni, S. (2017). Modelling the influence of ectomycorrhizal decomposition on plant nutrition and soil carbon sequestration in boreal forest ecosystems. New Phytologist, 213(3), 1452-1465.

Bastos, A., & Fleischer, K. (2021). Effects of rising CO_2 levels on carbon sequestration are coordinated above and below ground.

Bates, J. W., & Bakken, S. (2018). Nutrient retention, desiccation and redistribution in mosses. Bryology for the Twenty-first Century, 293-304.

Beer, J., & Blodau, C. (2007). Transport and thermodynamics constrain belowground carbon turnover in a northern peatland. Geochimica et Cosmochimica Acta, 71(12), 2989-3002.

Bengtson, P., & Bengtsson, G. (2007). Rapid turnover of DOC in temperate forests accounts for increased CO_2 production at elevated temperatures. Ecology letters, 10(9), 783-790.

Berendse, F., Van Breemen, N., Rydin, H., Buttler, A., Heijmans, M., Hoosbeek, M. R., ... & Wallén, B. (2001). Raised atmospheric CO_2 levels and increased N deposition cause shifts in plant species composition and production in Sphagnum bogs. Global Change Biology, 7(5), 591-598.

Berg, A. S., & Joern, B. C. (2006). Sorption dynamics of organic and inorganic phosphorus compounds in soil. Journal of environmental quality, 35(5), 1855-1862.

Berg, B. (2014). Decomposition patterns for foliar litter–a theory for influencing factors. Soil Biology and Biochemistry, 78, 222-232.

Blagodatsky, S., Grote, R., Kiese, R., Werner, C., & Butterbach-Bahl, K. (2011). Modelling of microbial carbon and nitrogen turnover in soil with special emphasis on N-trace gases

emission. Plant and soil, 346(1), 297-330.

Blodau, C., Basiliko, N., & Moore, T. R. (2004). Carbon turnover in peatland mesocosms exposed to different water table levels. Biogeochemistry, 67(3), 331-351.

Bloom, A. J., Chapin III, F. S., & Mooney, H. A. (1985). Resource limitation in plants-an economic analogy. Annual review of Ecology and Systematics, 16(1), 363-392.

Bottner, P., Coûteaux, M. M., Anderson, J. M., Berg, B., Billès, G., Bolger, T., ... & Rovira, P. (2000). Decomposition of ^{13}C-labelled plant material in a European 65–40 latitudinal transect of coniferous forest soils: simulation of climate change by translocation of soils. Soil Biology and Biochemistry, 32(4), 527-543.

Bradford, M. A., Keiser, A. D., Davies, C. A., Mersmann, C. A., & Strickland, M. S. (2013). Empirical evidence that soil carbon formation from plant inputs is positively related to microbial growth. Biogeochemistry, 113(1), 271-281.

Bradford, M. A., McCulley, R. L., Crowther, T. W., Oldfield, E. E., Wood, S. A., & Fierer, N. (2019). Cross-biome patterns in soil microbial respiration predictable from evolutionary theory on thermal adaptation. Nature Ecology & Evolution, 3(2), 223-231.

Bragazza, L., Bardgett, R. D., Mitchell, E. A., & Buttler, A. (2015). Linking soil microbial communities to vascular plant abundance along a climate gradient. New Phytologist, 205(3), 1175-1182.

Bragazza, L., Buttler, A., Habermacher, J., Brancaleoni, L., Gerdol, R., Fritze, H., ... & Johnson, D. (2012). High nitrogen deposition alters the decomposition of bog plant litter and reduces carbon accumulation. Global Change Biology, 18(3), 1163-1172.

Bragazza, L., Buttler, A., Robroek, B. J., Albrecht, R., Zaccone, C., Jassey, V. E., & Signarbieux, C. (2016). Persistent high temperature and low precipitation reduce peat carbon accumulation. Global Change Biology, 22(12), 4114-4123.

Bragazza, L., Freeman, C., Jones, T., Rydin, H., Limpens, J., Fenner, N., ... & Toberman, H. (2006). Atmospheric nitrogen deposition promotes carbon loss from peat bogs. Proceedings of the National Academy of Sciences, 103(51), 19386-19389.

Bragazza, L., Limpens, J., Gerdol, R., Grosvernier, P., Hájek, M., Hájek, T., ... & Tahvanainen, T. (2005). Nitrogen concentration and δ^{15}N signature of ombrotrophic Sphagnum mosses

at different N deposition levels in Europe. Global Change Biology, 11(1), 106-114.

Bragazza, L., Parisod, J., Buttler, A., & Bardgett, R. D. (2013). Biogeochemical plant–soil microbe feedback in response to climate warming in peatlands. Nature Climate Change, 3(3), 273-277.

Bragazza, L., Tahvanainen, T., Kutnar, L., Rydin, H., Limpens, J., Hájek, M., ... & Gerdol, R. (2004). Nutritional constraints in ombrotrophic Sphagnum plants under increasing atmospheric nitrogen deposition in Europe. New Phytologist, 163(3), 609-616.

Brahney, J., Mahowald, N., Ward, D. S., Ballantyne, A. P., & Neff, J. C. (2015). Is atmospheric phosphorus pollution altering global alpine Lake stoichiometry?. Global Biogeochemical Cycles, 29(9), 1369-1383.

Breeuwer, A., Robroek, B. J., Limpens, J., Heijmans, M. M., Schouten, M. G., & Berendse, F. (2009). Decreased summer water table depth affects peatland vegetation. Basic and Applied Ecology, 10(4), 330-339.

Bridgham, S. D., & Richardson, C. J. (2003). Endogenous versus exogenous nutrient control over decomposition and mineralization in North Carolina peatlands. Biogeochemistry, 65(2), 151-178.

Brzostek, E. R., Fisher, J. B., & Phillips, R. P. (2014). Modeling the carbon cost of plant nitrogen acquisition: Mycorrhizal trade-offs and multipath resistance uptake improve predictions of retranslocation. Journal of Geophysical Research: Biogeosciences, 119(8), 1684-1697.

Bubier, J. L., Moore, T. R., & Bledzki, L. A. (2007). Effects of nutrient addition on vegetation and carbon cycling in an ombrotrophic bog. Global Change Biology, 13(6), 1168-1186.

Bubier, J. L., Moore, T. R., & Crosby, G. (2006). Fine-scale vegetation distribution in a cool temperate peatland. Botany, 84(6), 910-923.

Bubier, J. L., Smith, R., Juutinen, S., Moore, T. R., Minocha, R., Long, S., & Minocha, S. (2011). Effects of nutrient addition on leaf chemistry, morphology, and photosynthetic capacity of three bog shrubs. Oecologia, 167(2), 355-368.

Bubier, J., Crill, P., Mosedale, A., Frolking, S., & Linder, E. (2003). Peatland responses to varying interannual moisture conditions as measured by automatic CO_2 chambers. Global Biogeochemical Cycles, 17(2).

Buttler, A., Robroek, B. J., Laggoun-Défarge, F., Jassey, V. E., Pochelon, C., Bernard, G., ... & Bragazza, L. (2015). Experimental warming interacts with soil moisture to discriminate plant responses in an ombrotrophic peatland. Journal of vegetation Science, 26(5), 964-974.

Calvo-Fernández, J., Taboada, Á., Fichtner, A., Härdtle, W., Calvo, L., & Marcos, E. (2018). Time- and age-related effects of experimentally simulated nitrogen deposition on the functioning of montane heathland ecosystems. Science of the Total Environment, 613, 149-159.

Camenzind, T., Philipp Grenz, K., Lehmann, J., & Rillig, M. C. (2021). Soil fungal mycelia have unexpectedly flexible stoichiometric C: N and C: P ratios. Ecology Letters, 24(2), 208-218.

Čapek, P., Manzoni, S., Kaštovská, E., Wild, B., Diáková, K., Bárta, J., ... & Šantrůčková, H. (2018). A plant–microbe interaction framework explaining nutrient effects on primary production. Nature ecology & evolution, 2(10), 1588-1596.

Cárdenas-Navarro, R., Adamowicz, S., & Robin, P. (1999). Nitrate accumulation in plants: a role for water. Journal of Experimental Botany, 50(334), 613-624.

Carrara, J. E., Walter, C. A., Hawkins, J. S., Peterjohn, W. T., Averill, C., & Brzostek, E. R. (2018). Interactions among plants, bacteria, and fungi reduce extracellular enzyme activities under long-term N fertilization. Global change biology, 24(6), 2721-2734.

Ceulemans, T., Van Geel, M., Jacquemyn, H., Boeraeve, M., Plue, J., Saar, L., ... & Honnay, O. (2019). Arbuscular mycorrhizal fungi in European grasslands under nutrient pollution. Global Ecology and Biogeography, 28(12), 1796-1805.

Chadburn, S. E., Aalto, T., Aurela, M., Baldocchi, D., Biasi, C., Boike, J., ... & Westermann, S. (2020). Modeled microbial dynamics explain the apparent temperature sensitivity of wetland methane emissions. Global Biogeochemical Cycles, 34(11), e2020GB006678.

Charman, D. (2002). Peatlands and environmental change. John Wiley & Sons Ltd.

Chaudhary, N., Miller, P. A., & Smith, B. (2017). Modelling Holocene peatland dynamics with an individual-based dynamic vegetation model. Biogeosciences, 14(10), 2571-2596.

Chaudhary, N., Westermann, S., Lamba, S., Shurpali, N., Sannel, A. B. K., Schurgers, G., ... & Smith, B. (2020). Modelling past and future peatland carbon dynamics across the pan-

Arctic. Global change biology, 26(7), 4119-4133.

Chen, H., Zhang, W., Gurmesa, G. A., Zhu, X., Li, D., & Mo, J. (2017). Phosphorus addition affects soil nitrogen dynamics in a nitrogen-saturated and two nitrogen-limited forests. European Journal of Soil Science, 68(4), 472-479.

Chen, J., Seven, J., Zilla, T., Dippold, M. A., Blagodatskaya, E., & Kuzyakov, Y. (2019). Microbial C: N: P stoichiometry and turnover depend on nutrients availability in soil: A ^{14}C, ^{15}N and ^{33}P triple labelling study. Soil Biology and Biochemistry, 131, 206-216.

Chen, J., van Groenigen, K. J., Hungate, B. A., Terrer, C., van Groenigen, J. W., Maestre, F. T., ... & Elsgaard, L. (2020). Long-term nitrogen loading alleviates phosphorus limitation in terrestrial ecosystems. Global change biology, 26(9), 5077-5086.

Chiapusio, G., Jassey, V. E., Bellvert, F., Comte, G., Weston, L. A., Delarue, F., ... & Binet, P. (2018). Sphagnum species modulate their phenolic profiles and mycorrhizal colonization of surrounding andromeda polifolia along peatland microhabitats. Journal of chemical ecology, 44(12), 1146-1157.

Chong, M., Humphreys, E., & Moore, T. R. (2012). Microclimatic response to increasing shrub cover and its effect on Sphagnum CO_2 exchange in a bog. Ecoscience, 19(1), 89-97.

Churchill, A. C., Turetsky, M. R., McGuire, A. D., & Hollingsworth, T. N. (2015). Response of plant community structure and primary productivity to experimental drought and flooding in an Alaskan fen. Canadian Journal of Forest Research, 45(2), 185-193.

Ciais, P., Sabine, C., Bala, G., Bopp, L., Brovkin, V., Canadell, J., ... & Thornton, P. (2014). Carbon and other biogeochemical cycles. In Climate change 2013: the physical science basis. Contribution of Working Group I to the Fifth Assessment Report of the Intergovernmental Panel on Climate Change (pp. 465-570). Cambridge University Press.

Clemmensen, K. E., Bahr, A., Ovaskainen, O., Dahlberg, A., Ekblad, A., Wallander, H., ... & Lindahl, B. D. (2013). Roots and associated fungi drive long-term carbon sequestration in boreal forest. Science, 339(6127), 1615-1618.

Clemmensen, K. E., Durling, M. B., Michelsen, A., Hallin, S., Finlay, R. D., & Lindahl, B. D. (2021). A tipping point in carbon storage when forest expands into tundra is related to mycorrhizal recycling of nitrogen. Ecology Letters.

Clemmensen, K. E., Finlay, R. D., Dahlberg, A., Stenlid, J., Wardle, D. A., & Lindahl, B. D. (2015). Carbon sequestration is related to mycorrhizal fungal community shifts during long-term succession in boreal forests. New Phytologist, 205(4), 1525-1536.

Clymo, R. S. (1984). The limits to peat bog growth. Philosophical Transactions of the Royal Society of London. B, Biological Sciences, 303(1117), 605-654.

Conant, R. T., Ryan, M. G., Ågren, G. I., Birge, H. E., Davidson, E. A., Eliasson, P. E., ... & Bradford, M. A. (2011). Temperature and soil organic matter decomposition rates–synthesis of current knowledge and a way forward. Global Change Biology, 17(11), 3392-3404.

Cornelissen, J. H., Quested, H. M., Van Logtestijn, R. S. P., Pérez-Harguindeguy, N., Gwynn-Jones, D., Díaz, S., ... & Aerts, R. (2006). Foliar pH as a new plant trait: can it explain variation in foliar chemistry and carbon cycling processes among subarctic plant species and types?. Oecologia, 147(2), 315-326.

Corrêa, A., Gurevitch, J., Martins-Loução, M. A., & Cruz, C. (2012). C allocation to the fungus is not a cost to the plant in ectomycorrhizae. Oikos, 121(3), 449-463.

Cotrufo, M. F., Wallenstein, M. D., Boot, C. M., Denef, K., & Paul, E. (2013). The M icrobial E fficiency-M atrix S tabilization (MEMS) framework integrates plant litter decomposition with soil organic matter stabilization: do labile plant inputs form stable soil organic matter?. Global change biology, 19(4), 988-995.

Crowther, T. W., Van den Hoogen, J., Wan, J., Mayes, M. A., Keiser, A. D., Mo, L., ... & Maynard, D. S. (2019). The global soil community and its influence on biogeochemistry. Science, 365(6455).

Cui, J., Zhu, Z., Xu, X., Liu, S., Jones, D. L., Kuzyakov, Y., ... & Ge, T. (2020). Carbon and nitrogen recycling from microbial necromass to cope with C: N stoichiometric imbalance by priming. Soil Biology and Biochemistry, 142, 107720.

Currey, P. M., Johnson, D., Dawson, L. A., Van der Wal, R., Thornton, B., Sheppard, L. J., ... & Artz, R. R. (2011). Five years of simulated atmospheric nitrogen deposition have only subtle effects on the fate of newly synthesized carbon in Calluna vulgaris and Eriophorum vaginatum. Soil Biology and Biochemistry, 43(3), 495-502.

Currey, P. M., Johnson, D., Sheppard, L. J., Leith, I. D., Toberman, H., Van Der WAL, R. E. N. É., ...

& Artz, R. R. (2010). Turnover of labile and recalcitrant soil carbon differ in response to nitrate and ammonium deposition in an ombrotrophic peatland. Global Change Biology, 16(8), 2307-2321.

Damman, A. W. H. (1978). Distribution and movement of elements in ombrotrophic peat bogs. Oikos, 480-495.

Dargie, G. C., Lewis, S. L., Lawson, I. T., Mitchard, E. T., Page, S. E., Bocko, Y. E., & Ifo, S. A. (2017). Age, extent and carbon storage of the central Congo Basin peatland complex. Nature, 542(7639), 86-90.

Davidson, E. A., & Janssens, I. A. (2006). Temperature sensitivity of soil carbon decomposition and feedbacks to climate change. Nature, 440(7081), 165-173.

Defrenne, C. E., Childs, J., Fernandez, C. W., Taggart, M., Nettles, W. R., Allen, M. F., ... & Iversen, C. M. (2020). High-resolution minirhizotrons advance our understanding of root-fungal dynamics in an experimentally warmed peatland. Plants, People, Planet.

Dentener, F., Drevet, J., Lamarque, J. F., Bey, I., Eickhout, B., Fiore, A. M., ... & Wild, O. (2006). Nitrogen and sulfur deposition on regional and global scales: A multimodel evaluation. Global biogeochemical cycles, 20(4).

Devêvre, O. C., & Horwáth, W. R. (2000). Decomposition of rice straw and microbial carbon use efficiency under different soil temperatures and moistures. Soil Biology and Biochemistry, 32(11-12), 1773-1785.

Dieleman, C. M., Branfireun, B. A., McLaughlin, J. W., & Lindo, Z. (2015). Climate change drives a shift in peatland ecosystem plant community: implications for ecosystem function and stability. Global change biology, 21(1), 388-395.

Dieleman, C. M., Branfireun, B. A., McLaughlin, J. W., & Lindo, Z. (2016). Enhanced carbon release under future climate conditions in a peatland mesocosm experiment: the role of phenolic compounds. Plant and Soil, 400(1), 81-91.

Dietze, M. C., Sala, A., Carbone, M. S., Czimczik, C. I., Mantooth, J. A., Richardson, A. D., & Vargas, R. (2014). Nonstructural carbon in woody plants. Annual review of plant biology, 65, 667-687.

Dijkstra, P., Thomas, S. C., Heinrich, P. L., Koch, G. W., Schwartz, E., & Hungate, B. A. (2011).

Effect of temperature on metabolic activity of intact microbial communities: evidence for altered metabolic pathway activity but not for increased maintenance respiration and reduced carbon use efficiency. Soil Biology and Biochemistry, 43(10), 2023-2031.

Dimitrov, D. D., Grant, R. F., Lafleur, P. M., & Humphreys, E. R. (2010). Modeling the effects of hydrology on ecosystem respiration at Mer Bleue bog. Journal of Geophysical Research: Biogeosciences, 115(G4).

Dise, N. B. (2009). Peatland response to global change. Science, 326(5954), 810-811.

Dorrepaal, E., Toet, S., Van Logtestijn, R. S., Swart, E., Van De Weg, M. J., Callaghan, T. V., & Aerts, R. (2009). Carbon respiration from subsurface peat accelerated by climate warming in the subarctic. Nature, 460(7255), 616-619.

Drake, J. E., Darby, B. A., Giasson, M. A., Kramer, M. A., Phillips, R. P., & Finzi, A. C. (2013). Stoichiometry constrains microbial response to root exudation-insights from a model and a field experiment in a temperate forest. Biogeosciences, 10(2), 821-838.

Dunleavy, H. R., & Mack, M. C. (2021). Long-term experimental warming and fertilization have opposing effects on ectomycorrhizal root enzyme activity and fungal community composition in Arctic tundra. Soil Biology and Biochemistry, 154, 108151.

Eastman, B. A., Adams, M. B., Brzostek, E. R., Burnham, M. B., Carrara, J. E., Kelly, C., ... & Peterjohn, W. T. (2021). Altered plant carbon partitioning enhanced forest ecosystem carbon storage after 25 years of nitrogen additions. New Phytologist, 230(4), 1435-1448.

Edwards, N. T., Tschaplinski, T. J., & Norby, R. J. (2002). Stem respiration increases in CO_2-enriched sweetgum trees. New Phytologist, 155(2), 239-248.

Elser, J. J., Bracken, M. E., Cleland, E. E., Gruner, D. S., Harpole, W. S., Hillebrand, H., ... & Smith, J. E. (2007). Global analysis of nitrogen and phosphorus limitation of primary producers in freshwater, marine and terrestrial ecosystems. Ecology letters, 10(12), 1135-1142.

Etminan, M., Myhre, G., Highwood, E. J., & Shine, K. P. (2016). Radiative forcing of carbon dioxide, methane, and nitrous oxide: A significant revision of the methane radiative forcing. Geophysical Research Letters, 43(24), 12-614.

Evans, M. R. (2012). Modelling ecological systems in a changing world. Philosophical Transactions of the Royal Society B: Biological Sciences, 367(1586), 181-190.

Falloon, P. D., & Smith, P. (2000). Modelling refractory soil organic matter. Biology and fertility of soils, 30(5), 388-398.

Fatichi, S., Manzoni, S., Or, D., & Paschalis, A. (2019). A mechanistic model of microbially mediated soil biogeochemical processes: a reality check. Global Biogeochemical Cycles, 33(6), 620-648.

Fellbaum, C. R., Gachomo, E. W., Beesetty, Y., Choudhari, S., Strahan, G. D., Pfeffer, P. E., ... & Bücking, H. (2012). Carbon availability triggers fungal nitrogen uptake and transport in arbuscular mycorrhizal symbiosis. Proceedings of the National Academy of Sciences, 109(7), 2666-2671.

Fellbaum, C. R., Mensah, J. A., Cloos, A. J., Strahan, G. E., Pfeffer, P. E., Kiers, E. T., & Bücking, H. (2014). Fungal nutrient allocation in common mycorrhizal networks is regulated by the carbon source strength of individual host plants. New Phytologist, 203(2), 646-656.

Fenner, N., & Freeman, C. (2011). Drought-induced carbon loss in peatlands. Nature geoscience, 4(12), 895-900.

Fenner, N., Freeman, C., Lock, M. A., Harmens, H., Reynolds, B., & Sparks, T. (2007). Interactions between elevated CO_2 and warming could amplify DOC exports from peatland catchments. Environmental science & technology, 41(9), 3146-3152.

Fernandez, C. W., & Kennedy, P. G. (2016). Revisiting the 'Gadgil effect': do interguild fungal interactions control carbon cycling in forest soils?. New phytologist, 209(4), 1382-1394.

Fernandez, C. W., Heckman, K., Kolka, R., & Kennedy, P. G. (2019). Melanin mitigates the accelerated decay of mycorrhizal necromass with peatland warming. Ecology Letters, 22(3), 498-505.

Fisher, J. B., Sitch, S., Malhi, Y., Fisher, R. A., Huntingford, C., & Tan, S. Y. (2010). Carbon cost of plant nitrogen acquisition: A mechanistic, globally applicable model of plant nitrogen uptake, retranslocation, and fixation. Global Biogeochemical Cycles, 24(1).

Flato, G., Marotzke, J., Abiodun, B., Braconnot, P., Chou, S. C., Collins, W., ... & Rummukainen, M. (2014). Evaluation of climate models. In Climate change 2013: the physical science basis. Contribution of Working Group I to the Fifth Assessment Report of the Intergovernmental Panel on Climate Change (pp. 741-866). Cambridge University Press.

Fortuniak, K., Pawlak, W., Siedlecki, M., Chambers, S., & Bednorz, L. (2021). Temperate mire fluctuations from carbon sink to carbon source following changes in water table. Science of The Total Environment, 756, 144071.

Franklin, O., Näsholm, T., Högberg, P., & Högberg, M. N. (2014). Forests trapped in nitrogen limitation–an ecological market perspective on ectomycorrhizal symbiosis. New Phytologist, 203(2), 657-666.

Fraser, C. J. D., Roulet, N. T., & Moore, T. R. (2001). Hydrology and dissolved organic carbon biogeochemistry in an ombrotrophic bog. Hydrological Processes, 15(16), 3151-3166.

Freeman, C., Evans, C. D., Monteith, D. T., Reynolds, B., & Fenner, N. (2001b). Export of organic carbon from peat soils. Nature, 412(6849), 785-785.

Freeman, C., Fenner, N., Ostle, N. J., Kang, H., Dowrick, D. J., Reynolds, B., ... & Hudson, J. (2004). Export of dissolved organic carbon from peatlands under elevated carbon dioxide levels. Nature, 430(6996), 195-198.

Freeman, C., Ostle, N., & Kang, H. (2001a). An enzymic 'latch' on a global carbon store. Nature, 409(6817), 149-149.

Frey, S. D. (2019). Mycorrhizal fungi as mediators of soil organic matter dynamics. Annual review of ecology, evolution, and systematics, 50, 237-259.

Frey, S. D., Lee, J., Melillo, J. M., & Six, J. (2013). The temperature response of soil microbial efficiency and its feedback to climate. Nature Climate Change, 3(4), 395-398.

Fritz, C., Van Dijk, G., Smolders, A. J. P., Pancotto, V. A., Elzenga, T. J. T. M., Roelofs, J. G. M., & Grootjans, A. P. (2012). Nutrient additions in pristine Patagonian Sphagnum bog vegetation: can phosphorus addition alleviate (the effects of) increased nitrogen loads. Plant Biology, 14(3), 491-499.

Frolking, S., & Roulet, N. T. (2007). Holocene radiative forcing impact of northern peatland carbon accumulation and methane emissions. Global Change Biology, 13(5), 1079-1088.

Frolking, S., Roulet, N. T., Moore, T. R., Lafleur, P. M., Bubier, J. L., & Crill, P. M. (2002). Modeling seasonal to annual carbon balance of Mer Bleue Bog, Ontario, Canada. Global Biogeochemical Cycles, 16(3), 4-1.

Frolking, S., Roulet, N. T., Moore, T. R., Richard, P. J., Lavoie, M., & Muller, S. D. (2001).

Modeling northern peatland decomposition and peat accumulation. Ecosystems, 4(5), 479-498.

Frolking, S., Roulet, N. T., Tuittila, E., Bubier, J. L., Quillet, A., Talbot, J., & Richard, P. J. H. (2010). A new model of Holocene peatland net primary production, decomposition, water balance, and peat accumulation. Earth System Dynamics, 1(1), 1-21.

Frolking, S., Talbot, J., Jones, M. C., Treat, C. C., Kauffman, J. B., Tuittila, E. S., & Roulet, N. (2011). Peatlands in the Earth's 21st century climate system. Environmental Reviews, 19(NA), 371-396.

Furze, M. E. (2018). Seasonal patterns of nonstructural carbohydrate reserves in four woody boreal species1. The Journal of the Torrey Botanical Society, 145(4), 332-339.

Gadgil, R. L., & Gadgil, P. D. (1971). Mycorrhiza and litter decomposition. Nature, 233(5315), 133-133.

Gale, M. R., & Grigal, D. F. (1987). Vertical root distributions of northern tree species in relation to successional status. Canadian Journal of Forest Research, 17(8), 829-834.

Gallego-Sala, A. V., Charman, D. J., Brewer, S., Page, S. E., Prentice, I. C., Friedlingstein, P., ... & Zhao, Y. (2018). Latitudinal limits to the predicted increase of the peatland carbon sink with warming. Nature climate change, 8(10), 907-913.

Galloway, J. N., Dentener, F. J., Capone, D. G., Boyer, E. W., Howarth, R. W., Seitzinger, S. P., ... & Vöosmarty, C. J. (2004). Nitrogen cycles: past, present, and future. Biogeochemistry, 70(2), 153-226.

Gavazov, K., Albrecht, R., Buttler, A., Dorrepaal, E., Garnett, M. H., Gogo, S., ... & Bragazza, L. (2018). Vascular plant-mediated controls on atmospheric carbon assimilation and peat carbon decomposition under climate change. Global change biology, 24(9), 3911-3921.

Gavazov, K., Hagedorn, F., Buttler, A., Siegwolf, R., & Bragazza, L. (2016). Environmental drivers of carbon and nitrogen isotopic signatures in peatland vascular plants along an altitude gradient. Oecologia, 180(1), 257-264.

Genre, A., Lanfranco, L., Perotto, S., & Bonfante, P. (2020). Unique and common traits in mycorrhizal symbioses. Nature Reviews Microbiology, 18(11), 649-660.

Georgiou, K., Abramoff, R. Z., Harte, J., Riley, W. J., & Torn, M. S. (2017). Microbial community-

level regulation explains soil carbon responses to long-term litter manipulations. Nature Communications, 8(1), 1-10.

Ghimire, B., Riley, W. J., Koven, C. D., Mu, M., & Randerson, J. T. (2016). Representing leaf and root physiological traits in CLM improves global carbon and nitrogen cycling predictions. Journal of Advances in Modeling Earth Systems, 8(2), 598-613.

Gill, A. L., & Finzi, A. C. (2016). Belowground carbon flux links biogeochemical cycles and resource-use efficiency at the global scale. Ecology Letters, 19(12), 1419-1428.

Gill, A. L., Giasson, M. A., Yu, R., & Finzi, A. C. (2017). Deep peat warming increases surface methane and carbon dioxide emissions in a black spruce-dominated ombrotrophic bog. Global change biology, 23(12), 5398-5411.

Glassman, S. I., Weihe, C., Li, J., Albright, M. B., Looby, C. I., Martiny, A. C., ... & Martiny, J. B. (2018). Decomposition responses to climate depend on microbial community composition. Proceedings of the National Academy of Sciences, 115(47), 11994-11999.

Goll, D. S., Vuichard, N., Maignan, F., Jornet-Puig, A., Sardans, J., Violette, A., ... & Ciais, P. (2017). A representation of the phosphorus cycle for ORCHIDEE (revision 4520). Geoscientific Model Development, 10(10), 3745-3770.

Gong, Y., Wu, J., & Le, T. B. (2021a). Counteractions between biotic and abiotic factors on methane dynamics in a boreal peatland: Vegetation composition change vs warming and nitrogen deposition. Geoderma, 395, 115074.

Gong, Y., Wu, J., Sey, A. A., & Le, T. B. (2021b). Nitrogen addition (NH_4NO_3) mitigates the positive effect of warming on methane fluxes in a coastal bog. Catena, 203, 105356.

Gong, Y., Wu, J., Vogt, J., & Le, T. B. (2019). Warming reduces the increase in N_2O emission under nitrogen fertilization in a boreal peatland. Science of the Total Environment, 664, 72-78.

Gong, Y., Wu, J., Vogt, J., & Ma, W. (2020). Greenhouse gas emissions from peatlands under manipulated warming, nitrogen addition, and vegetation composition change: a review and data synthesis. Environmental Reviews, 28(4), 428-437.

Gorham, E. (1991). Northern peatlands: role in the carbon cycle and probable responses to climatic warming. Ecological applications, 1(2), 182-195.

Gorham, E. (1995). The biogeochemistry of northern peatlands and its possible responses to global warming. Biotic feedbacks in the global climatic system: will the warming feed the warming, 169-187.

Goud, E. M., Moore, T. R., & Roulet, N. T. (2017). Predicting peatland carbon fluxes from non-destructive plant traits. Functional Ecology, 31(9), 1824-1833.

Hagenbo, A., Hadden, D., Clemmensen, K. E., Grelle, A., Manzoni, S., Mölder, M., ... & Fransson, P. (2019). Carbon use efficiency of mycorrhizal fungal mycelium increases during the growing season but decreases with forest age across a Pinus sylvestris chronosequence. Journal of Ecology, 107(6), 2808-2822.

Hagerty, S. B., Allison, S. D., & Schimel, J. P. (2018). Evaluating soil microbial carbon use efficiency explicitly as a function of cellular processes: implications for measurements and models. Biogeochemistry, 140(3), 269-283.

Hagerty, S. B., Van Groenigen, K. J., Allison, S. D., Hungate, B. A., Schwartz, E., Koch, G. W., ... & Dijkstra, P. (2014). Accelerated microbial turnover but constant growth efficiency with warming in soil. Nature Climate Change, 4(10), 903-906.

Hájek, T., Ballance, S., Limpens, J., Zijlstra, M., & Verhoeven, J. T. (2011). Cell-wall polysaccharides play an important role in decay resistance of Sphagnum and actively depressed decomposition in vitro. Biogeochemistry, 103(1), 45-57.

Hammer, E. C., Pallon, J., Wallander, H., & Olsson, P. A. (2011). Tit for tat? A mycorrhizal fungus accumulates phosphorus under low plant carbon availability. FEMS microbiology ecology, 76(2), 236-244.

Hanson, P. J., Griffiths, N. A., Iversen, C. M., Norby, R. J., Sebestyen, S. D., Phillips, J. R., ... & Ricciuto, D. M. (2020). Rapid net carbon loss from a whole-ecosystem warmed Peatland. AGU Advances, 1(3), e2020AV000163.

Hararuk, O., Allison, S. D., & Sayer, E. J. (2019, December). Identifying mechanisms of soil carbon dynamics at a tropical site: a data-model fusion approach. In AGU Fall Meeting Abstracts (Vol. 2019, pp. B31C-04).

Hargreaves, K. J., Milne, R., & Cannell, M. G. R. (2003). Carbon balance of afforested peatland in Scotland. Forestry, 76(3), 299-317.

He, H., Jansson, P. E., & Gärdenäs, A. I. (2021). CoupModel (v6. 0): an ecosystem model for coupled phosphorus, nitrogen, and carbon dynamics–evaluated against empirical data from a climatic and fertility gradient in Sweden. Geoscientific Model Development, 14(2), 735-761.

He, H., Jansson, P. E., Svensson, M., Björklund, J., Tarvainen, L., Klemedtsson, L., & Kasimir, Å. (2016). Forests on drained agricultural peatland are potentially large sources of greenhouse gases–insights from a full rotation period simulation. Biogeosciences, 13(8), 2305-2318.

He, H., Meyer, A., Jansson, P. E., Svensson, M., Rütting, T., & Klemedtsson, L. (2018). Simulating ectomycorrhiza in boreal forests: implementing ectomycorrhizal fungi model MYCOFON in CoupModel (v5). Geoscientific Model Development, 11(2), 725-751.

He, Y., Yang, J., Zhuang, Q., Harden, J. W., McGuire, A. D., Liu, Y., ... & Gu, L. (2015). Incorporating microbial dormancy dynamics into soil decomposition models to improve quantification of soil carbon dynamics of northern temperate forests. Journal of Geophysical Research: Biogeosciences, 120(12), 2596-2611.

Hedwall, P. O., Brunet, J., & Rydin, H. (2017). Peatland plant communities under global change: negative feedback loops counteract shifts in species composition. Ecology, 98(1), 150-161.

Heijmans, M. M., Berendse, F., Arp, W. J., Masselink, A. K., Klees, H., De Visser, W., & Van Breemen, N. (2001). Effects of elevated carbon dioxide and increased nitrogen deposition on bog vegetation in the Netherlands. Journal of ecology, 89(2), 268-279.

Heijmans, M. M., Mauquoy, D., Van Geel, B., & Berendse, F. (2008). Long-term effects of climate change on vegetation and carbon dynamics in peat bogs. Journal of Vegetation Science, 19(3), 307-320.

Heinemeyer, A., Tortorella, D., Petrovičová, B., & Gelsomino, A. (2012). Partitioning of soil CO_2 flux components in a temperate grassland ecosystem. European Journal of Soil Science, 63(2), 249-260.

Helbig, M., Humphreys, E. R., & Todd, A. (2019). Contrasting temperature sensitivity of CO_2 exchange in peatlands of the Hudson Bay Lowlands, Canada. Journal of Geophysical

Research: Biogeosciences, 124(7), 2126-2143.

Henriksson, N., Franklin, O., Tarvainen, L., Marshall, J., Lundberg-Felten, J., Eilertsen, L., & Näsholm, T. (2021). The mycorrhizal tragedy of the commons. Ecology Letters.

Herndon, E. M., Kinsman-Costello, L., Duroe, K. A., Mills, J., Kane, E. S., Sebestyen, S. D., ... & Wullschleger, S. D. (2019). Iron (oxyhydr) oxides serve as phosphate traps in tundra and boreal peat soils. Journal of Geophysical Research: Biogeosciences, 124(2), 227-246.

Hill, B. H., Elonen, C. M., Jicha, T. M., Kolka, R. K., Lehto, L. L., Sebestyen, S. D., & Seifert-Monson, L. R. (2014). Ecoenzymatic stoichiometry and microbial processing of organic matter in northern bogs and fens reveals a common P-limitation between peatland types. Biogeochemistry, 120(1), 203-224.

Hintze, J. L., & Nelson, R. D. (1998). Violin plots: a box plot-density trace synergism. The American Statistician, 52(2), 181-184.

Hobbie, E. A. (2006). Carbon allocation to ectomycorrhizal fungi correlates with belowground allocation in culture studies. Ecology, 87(3), 563-569.

Hobbie, E. A., & Högberg, P. (2012). Nitrogen isotopes link mycorrhizal fungi and plants to nitrogen dynamics. New phytologist, 196(2), 367-382.

Hobbie, S. E. (2008). Nitrogen effects on decomposition: A five-year experiment in eight temperate sites. Ecology, 89(9), 2633-2644.

Hodgkins, S. B., Richardson, C. J., Dommain, R., Wang, H., Glaser, P. H., Verbeke, B., ... & Chanton, J. P. (2018). Tropical peatland carbon storage linked to global latitudinal trends in peat recalcitrance. Nature communications, 9(1), 1-13.

Högberg, P., Johannisson, C., & Högberg, M. N. (2014). Is the high ^{15}N natural abundance of trees in N-loaded forests caused by an internal ecosystem N isotope redistribution or a change in the ecosystem N isotope mass balance?. Biogeochemistry, 117(2), 351-358.

Högberg, P., Näsholm, T., Franklin, O., & Högberg, M. N. (2017). Tamm Review: On the nature of the nitrogen limitation to plant growth in Fennoscandian boreal forests. Forest Ecology and Management, 403, 161-185.

Hoosbeek, M. R., Van Breemen, N., Berendse, F., Grosvernier, P., Vasander, H., & Wallén, B. (2001). Limited effect of increased atmospheric CO_2 concentration on ombrotrophic bog

vegetation. New Phytologist, 150(2), 459-463.

Hopple, A. M., Wilson, R. M., Kolton, M., Zalman, C. A., Chanton, J. P., Kostka, J., ... & Bridgham, S. D. (2020). Massive peatland carbon banks vulnerable to rising temperatures. Nature communications, 11(1), 1-7.

Houlton, B. Z., Wang, Y. P., Vitousek, P. M., & Field, C. B. (2008). A unifying framework for dinitrogen fixation in the terrestrial biosphere. Nature, 454(7202), 327-330.

Huang, Y., Guenet, B., Ciais, P., Janssens, I. A., Soong, J. L., Wang, Y., ... & Huang, Y. (2018). ORCHIMIC (v1. 0), a microbe-mediated model for soil organic matter decomposition. Geoscientific Model Development, 11(6), 2111-2138.

Hugelius, G., Loisel, J., Chadburn, S., Jackson, R. B., Jones, M., MacDonald, G., ... & Yu, Z. (2020). Large stocks of peatland carbon and nitrogen are vulnerable to permafrost thaw. Proceedings of the National Academy of Sciences, 117(34), 20438-20446.

Intergovernmental Panel on Climate Change. (2018). Global warming of 1.5° C: an IPCC special report on the impacts of global warming of 1.5° C above pre-industrial levels and related global greenhouse gas emission pathways, in the context of strengthening the global response to the threat of climate change, sustainable development, and efforts to eradicate poverty. Intergovernmental Panel on Climate Change.

Ise, T., Dunn, A. L., Wofsy, S. C., & Moorcroft, P. R. (2008). High sensitivity of peat decomposition to climate change through water-table feedback. Nature Geoscience, 1(11), 763-766.

Jach-Smith, L. C., & Jackson, R. D. (2020). Inorganic N addition replaces N supplied to switchgrass (Panicum virgatum) by arbuscular mycorrhizal fungi. Ecological Applications, 30(2), e02047.

Jackson, R. B., Canadell, J., Ehleringer, J. R., Mooney, H. A., Sala, O. E., & Schulze, E. D. (1996). A global analysis of root distributions for terrestrial biomes. Oecologia, 108(3), 389-411.

Janssens, I. A., Dieleman, W., Luyssaert, S., Subke, J. A., Reichstein, M., Ceulemans, R., ... & Law, B. E. (2010). Reduction of forest soil respiration in response to nitrogen deposition. Nature geoscience, 3(5), 315-322.

Järveoja, J., Nilsson, M. B., Gažovič, M., Crill, P. M., & Peichl, M. (2018). Partitioning of the net

CO_2 exchange using an automated chamber system reveals plant phenology as key control of production and respiration fluxes in a boreal peatland. Global Change Biology, 24(8), 3436-3451.

Jassey, V. E., & Signarbieux, C. (2019). Effects of climate warming on Sphagnum photosynthesis in peatlands depend on peat moisture and species-specific anatomical traits. Global change biology, 25(11), 3859-3870.

Jassey, V. E., Reczuga, M. K., Zielińska, M., Słowińska, S., Robroek, B. J., Mariotte, P., ... & Buttler, A. (2018). Tipping point in plant–fungal interactions under severe drought causes abrupt rise in peatland ecosystem respiration. Global Change Biology, 24(3), 972-986.

Jauhiainen, J., Wallén, B., & Malmer, N. (1998). Potential NH^{4+} and NO^{3-} uptake in seven Sphagnum species. The New Phytologist, 138(2), 287-293.

Jiang, L., Song, Y., Sun, L., Song, C., Wang, X., Ma, X., ... & Gao, J. (2020). Effects of warming on carbon emission and microbial abundances across different soil depths of a peatland in the permafrost region under anaerobic condition. Applied Soil Ecology, 156, 103712.

Jiang, S., Liu, Y., Luo, J., Qin, M., Johnson, N. C., Öpik, M., ... & Feng, H. (2018). Dynamics of arbuscular mycorrhizal fungal community structure and functioning along a nitrogen enrichment gradient in an alpine meadow ecosystem. New Phytologist, 220(4), 1222-1235.

Johansson, M. (2000). The influence of ammonium nitrate on the root growth and ericoid mycorrhizal colonization of Calluna vulgaris (L.) Hull from a Danish heathland. Oecologia, 123(3), 418-424.

Johnson, C. P., Pypker, T. G., Hribljan, J. A., & Chimner, R. A. (2013). Open top chambers and infrared lamps: A comparison of heating efficacy and CO_2/CH_4 dynamics in a northern Michigan peatland. Ecosystems, 16(5), 736-748.

Johnson, N. C., Graham, J. H., & Smith, F. A. (1997). Functioning of mycorrhizal associations along the mutualism–parasitism continuum. The New Phytologist, 135(4), 575-585.

Johnson, N. C., Wilson, G. W., Bowker, M. A., Wilson, J. A., & Miller, R. M. (2010). Resource limitation is a driver of local adaptation in mycorrhizal symbioses. Proceedings of the National Academy of Sciences, 107(5), 2093-2098.

Joosten, H. A. N. S. (2004). The IMCG global peatland database. Hans Joosten (Greifswald University, Germany).

Juan-Ovejero, R., Briones, M. J. I., & Öpik, M. (2020). Fungal diversity in peatlands and its contribution to carbon cycling. Applied Soil Ecology, 146, 103393.

Juutinen, S., Bubier, J. L., & Moore, T. R. (2010). Responses of vegetation and ecosystem CO_2 exchange to 9 years of nutrient addition at Mer Bleue bog. Ecosystems, 13(6), 874-887.

Juutinen, S., Moore, T. R., Laine, A. M., Bubier, J. L., Tuittila, E. S., De Young, A., & Chong, M. (2016). Responses of the mosses Sphagnum capillifolium and Polytrichum strictum to nitrogen deposition in a bog: growth, ground cover, and CO_2 exchange. Botany, 94(2), 127-138.

Kaiser, C., Franklin, O., Dieckmann, U., & Richter, A. (2014). Microbial community dynamics alleviate stoichiometric constraints during litter decay. Ecology letters, 17(6), 680-690.

Kattge, J., Knorr, W., Raddatz, T., & Wirth, C. (2009). Quantifying photosynthetic capacity and its relationship to leaf nitrogen content for global-scale terrestrial biosphere models. Global Change Biology, 15(4), 976-991.

Kavka, M., & Polle, A. (2017). Dissecting nutrient-related co-expression networks in phosphate starved poplars. PLoS One, 12(2), e0171958.

Keiluweit, M., Nico, P. S., Kleber, M., & Fendorf, S. (2016). Are oxygen limitations under recognized regulators of organic carbon turnover in upland soils?. Biogeochemistry, 127(2), 157-171.

Kennedy, P. G., Mielke, L. A., & Nguyen, N. H. (2018). Ecological responses to forest age, habitat, and host vary by mycorrhizal type in boreal peatlands. Mycorrhiza, 28(3), 315-328.

Keuper, F., van Bodegom, P. M., Dorrepaal, E., Weedon, J. T., van Hal, J., van Logtestijn, R. S., & Aerts, R. (2012). A frozen feast: Thawing permafrost increases plant-available nitrogen in subarctic peatlands. Global Change Biology, 18(6), 1998-2007.

Kiers, E. T., Duhamel, M., Beesetty, Y., Mensah, J. A., Franken, O., Verbruggen, E., ... & Bücking, H. (2011). Reciprocal rewards stabilize cooperation in the mycorrhizal symbiosis. science, 333(6044), 880-882.

Kiheri, H., Velmala, S., Pennanen, T., Timonen, S., Sietiö, O. M., Fritze, H., ... & Larmola, T.

(2020). Fungal colonization patterns and enzymatic activities of peatland ericaceous plants following long-term nutrient addition. Soil Biology and Biochemistry, 147, 107833.

Kilham, P. (1982). The biogeochemistry of bog ecosystems and the chemical ecology of Sphagnum [Musci]. Michigan Botanist.

Kivimäki, S. K., Sheppard, L. J., Leith, I. D., & Grace, J. (2013). Long-term enhanced nitrogen deposition increases ecosystem respiration and carbon loss from a Sphagnum bog in the Scottish Borders. Environmental and Experimental Botany, 90, 53-61.

Knorr, W., Prentice, I. C., House, J. I., & Holland, E. A. (2005). Long-term sensitivity of soil carbon turnover to warming. Nature, 433(7023), 298-301.

Kohout, P. (2017). Biogeography of ericoid mycorrhiza. In Biogeography of mycorrhizal symbiosis (pp. 179-193). Springer, Cham.

Kozlowski, T. T. (1997). Responses of woody plants to flooding and salinity. Tree physiology, 17(7), 490-490.

Kuzyakov, Y., & Xu, X. (2013). Competition between roots and microorganisms for nitrogen: mechanisms and ecological relevance. New Phytologist, 198(3), 656-669.

Kyaschenko, J., Clemmensen, K. E., Hagenbo, A., Karltun, E., & Lindahl, B. D. (2017). Shift in fungal communities and associated enzyme activities along an age gradient of managed Pinus sylvestris stands. The ISME journal, 11(4), 863-874.

Lafleur, P. M., Roulet, N. T., Bubier, J. L., Frolking, S., & Moore, T. R. (2003). Interannual variability in the peatland-atmosphere carbon dioxide exchange at an ombrotrophic bog. Global Biogeochemical Cycles, 17(2).

Laiho, R. (2006). Decomposition in peatlands: Reconciling seemingly contrasting results on the impacts of lowered water levels. Soil Biology and Biochemistry, 38(8), 2011-2024.

Laine, A. M., Mäkiranta, P., Laiho, R., Mehtätalo, L., Penttilä, T., Korrensalo, A., ... & Tuittila, E. S. (2019). Warming impacts on boreal fen CO_2 exchange under wet and dry conditions. Global change biology, 25(6), 1995-2008.

Lappalainen, E. (1996). Global peat resources.

Larmola, T., Bubier, J. L., Kobyljanec, C., Basiliko, N., Juutinen, S., Humphreys, E., ... & Moore, T. R. (2013). Vegetation feedbacks of nutrient addition lead to a weaker carbon sink in an

ombrotrophic bog. Global Change Biology, 19(12), 3729-3739.

Lawrence, D. M., Oleson, K. W., Flanner, M. G., Thornton, P. E., Swenson, S. C., Lawrence, P. J., ... & Slater, A. G. (2011). Parameterization improvements and functional and structural advances in version 4 of the Community Land Model. Journal of Advances in Modeling Earth Systems, 3(1).

Leroy, F., Gogo, S., Guimbaud, C., Bernard-Jannin, L., Hu, Z., & Laggoun-Défarge, F. (2017). Vegetation composition controls temperature sensitivity of CO_2 and CH_4 emissions and DOC concentration in peatlands. Soil Biology and Biochemistry, 107, 164-167.

Letts, M. G., Roulet, N. T., Comer, N. T., Skarupa, M. R., & Verseghy, D. L. (2000). Parametrization of peatland hydraulic properties for the Canadian Land Surface Scheme. Atmosphere-Ocean, 38(1), 141-160.

Levy, P., van Dijk, N., Gray, A., Sutton, M., Jones, M., Leeson, S., ... & Sheppard, L. (2019). Response of a peat bog vegetation community to long-term experimental addition of nitrogen. Journal of Ecology, 107(3), 1167-1186.

Li, J., Wang, G., Allison, S. D., Mayes, M. A., & Luo, Y. (2014). Soil carbon sensitivity to temperature and carbon use efficiency compared across microbial-ecosystem models of varying complexity. Biogeochemistry, 119(1), 67-84.

Li, J., Wang, G., Mayes, M. A., Allison, S. D., Frey, S. D., Shi, Z., ... & Melillo, J. M. (2019). Reduced carbon use efficiency and increased microbial turnover with soil warming. Global change biology, 25(3), 900-910.

Li, Q., Gogo, S., Leroy, F., Guimbaud, C., & Laggoun-Défarge, F. (2021). Response of peatland CO_2 and CH_4 fluxes to experimental warming and the carbon balance. Frontiers in Earth Science, 9, 471.

Li, T. T., Lei, Y., Dai, C., Yang, L. F., Li, Z. Q., & Wang, Z. X. (2018). Effects of both substrate and nitrogen and phosphorus fertilizer on Sphagnum palustre growth in subtropical high-mountain regions and implications for peatland recovery. Wetlands Ecology and Management, 26(4), 651-663.

Lilleskov, E. A., Kuyper, T. W., Bidartondo, M. I., & Hobbie, E. A. (2019). Atmospheric nitrogen deposition impacts on the structure and function of forest mycorrhizal communities: a

review. Environmental Pollution, 246, 148-162.

Limpens, J., Berendse, F., & Klees, H. (2004). How phosphorus availability affects the impact of nitrogen deposition on Sphagnum and vascular plants in bogs. Ecosystems, 7(8), 793-804.

Limpens, J., Berendse, F., Blodau, C., Canadell, J. G., Freeman, C., Holden, J., ... & Schaepman-Strub, G. (2008). Peatlands and the carbon cycle: from local processes to global implications–a synthesis. Biogeosciences, 5(5), 1475-1491.

Limpens, J., Granath, G., Gunnarsson, U., Aerts, R., Bayley, S., Bragazza, L., ... & Xu, B. (2011). Climatic modifiers of the response to nitrogen deposition in peat-forming Sphagnum mosses: a meta-analysis. New Phytologist, 191(2), 496-507.

Lin, X., Tfaily, M. M., Steinweg, J. M., Chanton, P., Esson, K., Yang, Z. K., ... & Kostka, J. E. (2014). Microbial community stratification linked to utilization of carbohydrates and phosphorus limitation in a boreal peatland at Marcell Experimental Forest, Minnesota, USA. Applied and environmental microbiology, 80(11), 3518-3530.

Lindahl, B. D., Kyaschenko, J., Varenius, K., Clemmensen, K. E., Dahlberg, A., Karltun, E., & Stendahl, J. (2021). A group of ectomycorrhizal fungi restricts organic matter accumulation in boreal forest. Ecology Letters, 24(7), 1341-1351.

Lindo, Z., Nilsson, M. C., & Gundale, M. J. (2013). Bryophyte-cyanobacteria associations as regulators of the northern latitude carbon balance in response to global change. Global change biology, 19(7), 2022-2035.

Litton, C. M., Raich, J. W., & Ryan, M. G. (2007). Carbon allocation in forest ecosystems. Global Change Biology, 13(10), 2089-2109.

Liu, L., Chen, H., Jiang, L., Zhan, W., Hu, J., He, Y., ... & Yang, G. (2019). Response of anaerobic mineralization of different depths peat carbon to warming on Zoige plateau. Geoderma, 337, 1218-1226.

Loisel, J., Yu, Z., Beilman, D. W., Camill, P., Alm, J., Amesbury, M. J., ... & Zhou, W. (2014). A database and synthesis of northern peatland soil properties and Holocene carbon and nitrogen accumulation. the Holocene, 24(9), 1028-1042.

Lovett, G. M., & Goodale, C. L. (2011). A new conceptual model of nitrogen saturation based

on experimental nitrogen addition to an oak forest. Ecosystems, 14(4), 615-631.

Luan, J., Wu, J., Liu, S., Roulet, N., & Wang, M. (2019). Soil nitrogen determines greenhouse gas emissions from northern peatlands under concurrent warming and vegetation shifting. Communications biology, 2(1), 1-10.

Lund, M., Bjerke, J. W., Drake, B. G., Engelsen, O., Hansen, G. H., Parmentier, F. J. W., ... & Rasse, D. P. (2015). Low impact of dry conditions on the CO_2 exchange of a Northern-Norwegian blanket bog. Environmental Research Letters, 10(2), 025004.

Mack, M. C., Schuur, E. A., Bret-Harte, M. S., Shaver, G. R., & Chapin, F. S. (2004). Ecosystem carbon storage in arctic tundra reduced by long-term nutrient fertilization. Nature, 431(7007), 440-443.

Macrae, M. L., Devito, K. J., Strack, M., & Waddington, J. M. (2013). Effect of water table drawdown on peatland nutrient dynamics: implications for climate change. Biogeochemistry, 112(1), 661-676.

Malik, A. A., Martiny, J. B., Brodie, E. L., Martiny, A. C., Treseder, K. K., & Allison, S. D. (2020). Defining trait-based microbial strategies with consequences for soil carbon cycling under climate change. The ISME journal, 14(1), 1-9.

Malik, A. A., Puissant, J., Buckeridge, K. M., Goodall, T., Jehmlich, N., Chowdhury, S., ... & Griffiths, R. I. (2018). Land use driven change in soil pH affects microbial carbon cycling processes. Nature communications, 9(1), 1-10.

Malmer, N., Albinsson, C., Svensson, B. M., & Wallén, B. (2003). Interferences between Sphagnum and vascular plants: effects on plant community structure and peat formation. Oikos, 100(3), 469-482.

Malmer, N., Svensson, B. M., & Wallén, B. (1994). Interactions between Sphagnum mosses and field layer vascular plants in the development of peat-forming systems. Folia Geobotanica et Phytotaxonomica, 29(4), 483-496.

Manzoni, S., Čapek, P., Mooshammer, M., Lindahl, B. D., Richter, A., & Šantrůčková, H. (2017). Optimal metabolic regulation along resource stoichiometry gradients. Ecology letters, 20(9), 1182-1191.

Manzoni, S., Čapek, P., Porada, P., Thurner, M., Winterdahl, M., Beer, C., ... & Way, D. (2018).

Reviews and syntheses: Carbon use efficiency from organisms to ecosystems–definitions, theories, and empirical evidence. Biogeosciences, 15(19), 5929-5949.

Manzoni, S., Taylor, P., Richter, A., Porporato, A., & Ågren, G. I. (2012). Environmental and stoichiometric controls on microbial carbon-use efficiency in soils. New Phytologist, 196(1), 79-91.

Marklein, A. R., & Houlton, B. Z. (2012). Nitrogen inputs accelerate phosphorus cycling rates across a wide variety of terrestrial ecosystems. New Phytologist, 193(3), 696-704.

Martino, E., Morin, E., Grelet, G. A., Kuo, A., Kohler, A., Daghino, S., ... & Perotto, S. (2018). Comparative genomics and transcriptomics depict ericoid mycorrhizal fungi as versatile saprotrophs and plant mutualists. New Phytologist, 217(3), 1213-1229.

Marttila, Hannu, et al. "Elevated nutrient concentrations in headwaters affected by drained peatland." Science of the total environment 643 (2018): 1304-1313.

McDowell, R. W., Worth, W., & Carrick, S. (2021). Evidence for the leaching of dissolved organic phosphorus to depth. Science of the Total Environment, 755, 142392.

McGill, W. B., & Cole, C. V. (1981). Comparative aspects of cycling of organic C, N, S and P through soil organic matter. Geoderma, 26(4), 267-286.

McGuire, A. D., Christensen, T. R., Hayes, D., Heroult, A., Euskirchen, E., Kimball, J. S., ... & Yi, Y. (2012). An assessment of the carbon balance of Arctic tundra: comparisons among observations, process models, and atmospheric inversions. Biogeosciences, 9(8), 3185-3204.

McPartland, M. Y., Kane, E. S., Falkowski, M. J., Kolka, R., Turetsky, M. R., Palik, B., & Montgomery, R. A. (2019). The response of boreal peatland community composition and NDVI to hydrologic change, warming, and elevated carbon dioxide. Global change biology, 25(1), 93-107.

McPartland, M. Y., Montgomery, R. A., Hanson, P. J., Phillips, J. R., Kolka, R., & Palik, B. (2020). Vascular plant species response to warming and elevated carbon dioxide in a boreal peatland. Environmental Research Letters, 15(12), 124066.

Melillo, J. M., Butler, S., Johnson, J., Mohan, J., Steudler, P., Lux, H., ... & Tang, J. (2011). Soil warming, carbon–nitrogen interactions, and forest carbon budgets. Proceedings of the

National Academy of Sciences, 108(23), 9508-9512.

Mettrop, I. S., Rutte, M. D., Kooijman, A. M., & Lamers, L. P. (2015). The ecological effects of water level fluctuation and phosphate enrichment in mesotrophic peatlands are strongly mediated by soil chemistry. Ecological Engineering, 85, 226-236.

Metzger, C., Jansson, P. E., Lohila, A., Aurela, M., Eickenscheidt, T., Belelli-Marchesini, L., ... & Drösler, M. (2015). CO_2 fluxes and ecosystem dynamics at five European treeless peatlands–merging data and process oriented modelling. Biogeosciences Discussions, 11(1), 9249-9297.

Meyer, A., Grote, R., & Butterbach-Bahl, K. (2012). Integrating mycorrhiza in a complex model system: effects on ecosystem C and N fluxes. European Journal of Forest Research, 131(6), 1809-1831.

Meyerholt, J., Zaehle, S., & Smith, M. J. (2016). Variability of projected terrestrial biosphere responses to elevated levels of atmospheric CO 2 due to uncertainty in biological nitrogen fixation. Biogeosciences, 13(5), 1491-1518.

Minkkinen, K., Ojanen, P., Koskinen, M., & Penttilä, T. (2020). Nitrous oxide emissions of undrained, forestry-drained, and rewetted boreal peatlands. Forest Ecology and Management, 478, 118494.

Minkkinen, K., Ojanen, P., Penttilä, T., Aurela, M., Laurila, T., Tuovinen, J. P., & Lohila, A. (2018). Persistent carbon sink at a boreal drained bog forest. Biogeosciences, 15(11), 3603-3624.

Mitchell, E. A., Gilbert, D., Buttler, A., Amblard, C., Grosvernier, P., & Gobat, J. M. (2003). Structure of microbial communities in Sphagnum peatlands and effect of atmospheric carbon dioxide enrichment. Microbial ecology, 46(2), 187-199.

Mokany, K., Raison, R. J., & Prokushkin, A. S. (2006). Critical analysis of root: shoot ratios in terrestrial biomes. Global change biology, 12(1), 84-96.

Moore Jr, A., & Reddy, K. R. (1994). Role of Eh and pH on phosphorus geochemistry in sediments of Lake Okeechobee, Florida (Vol. 23, No. 5, pp. 955-964). American Society of Agronomy, Crop Science Society of America, and Soil Science Society of America.

Moore, T. R. (2004). Nitrogen deposition and increased carbon accumulation in ombrotrophic peatlands in eastern Canada.

Moore, T. R. (2009). Dissolved organic carbon production and transport in Canadian peatlands. Geophysical monograph, 184, 229-236.

Moore, T. R., & Bubier, J. L. (2020). Plant and soil nitrogen in an ombrotrophic peatland, southern Canada. Ecosystems, 23(1), 98-110.

Moore, T. R., Bubier, J. L., & Bledzki, L. (2007). Litter decomposition in temperate peatland ecosystems: the effect of substrate and site. Ecosystems, 10(6), 949-963.

Moore, T. R., Bubier, J. L., Frolking, S. E., Lafleur, P. M., & Roulet, N. T. (2002). Plant biomass and production and CO_2 exchange in an ombrotrophic bog. Journal of ecology, 90(1), 25-36.

Moore, T. R., Knorr, K. H., Thompson, L., Roy, C., & Bubier, J. L. (2019). The effect of long-term fertilization on peat in an ombrotrophic bog. Geoderma, 343, 176-186.

Moore, T. R., Roulet, N. T., & Waddington, J. M. (1998). Uncertainty in predicting the effect of climatic change on the carbon cycling of Canadian peatlands. Climatic change, 40(2), 229-245.

Moore, T., Blodau, C., Turunen, J., Roulet, N., & Richard, P. J. (2005). Patterns of nitrogen and sulfur accumulation and retention in ombrotrophic bogs, eastern Canada. Global Change Biology, 11(2), 356-367.

Moorhead, D. L., & Weintraub, M. N. (2018). The evolution and application of the reverse Michaelis-Menten equation. Soil Biology and Biochemistry, 125, 261-262.

Moorhead, D. L., Lashermes, G., & Sinsabaugh, R. L. (2012). A theoretical model of C-and N-acquiring exoenzyme activities, which balances microbial demands during decomposition. Soil Biology and Biochemistry, 53, 133-141.

Morison, M. Q., Macrae, M. L., Petrone, R. M., & Fishback, L. (2018). Climate-induced changes in nutrient transformations across landscape units in a thermokarst subarctic peatland. Arctic, Antarctic, and Alpine Research, 50(1), e1519366.

Mpamah, P. A., Taipale, S., Rissanen, A. J., Biasi, C., & Nykänen, H. K. (2017). The impact of long-term water level draw-down on microbial biomass: a comparative study from two peatland sites with different nutrient status. European Journal of Soil Biology, 80, 59-68.

Müller, J., & Joos, F. (2021). Global peatlands under future climate–seamless model

projections from the Last Glacial Maximum. Biogeosciences Discussions, 1-45.

Munir, T. M., Khadka, B., Xu, B., & Strack, M. (2017). Mineral nitrogen and phosphorus pools affected by water table lowering and warming in a boreal forested peatland. Ecohydrology, 10(8), e1893.

Munir, T. M., Perkins, M., Kaing, E., & Strack, M. (2015). Carbon dioxide flux and net primary production of a boreal treed bog: Responses to warming and water-table-lowering simulations of climate change. Biogeosciences, 12(4), 1091-1111.

Munir, T. M., Xu, B., Perkins, M., & Strack, M. (2014). Responses of carbon dioxide flux and plant biomass to water table drawdown in a treed peatland in northern Alberta: a climate change perspective. Biogeosciences, 11(3), 807-820.

Murphy, M. T., & Moore, T. R. (2010). Linking root production to aboveground plant characteristics and water table in a temperate bog. Plant and soil, 336(1), 219-231.

Murphy, M. T., McKinley, A., & Moore, T. R. (2009). Variations in above-and below-ground vascular plant biomass and water table on a temperate ombrotrophic peatland. Botany, 87(9), 845-853.

Näsholm, T., Högberg, P., Franklin, O., Metcalfe, D., Keel, S. G., Campbell, C., ... & Högberg, M. N. (2013). Are ectomycorrhizal fungi alleviating or aggravating nitrogen limitation of tree growth in boreal forests?. New Phytologist, 198(1), 214-221.

Neff, J. C., Townsend, A. R., Gleixner, G., Lehman, S. J., Turnbull, J., & Bowman, W. D. (2002). Variable effects of nitrogen additions on the stability and turnover of soil carbon. Nature, 419(6910), 915-917.

Neumann, J., & Matzner, E. (2014). Contribution of newly grown extramatrical ectomycorrhizal mycelium and fine roots to soil respiration in a young Norway spruce site. Plant and soil, 378(1), 73-82.

Newman, E. I. (1995). Phosphorus inputs to terrestrial ecosystems. Journal of Ecology, 713-726.

Nichols, J. E., & Peteet, D. M. (2019). Rapid expansion of northern peatlands and doubled estimate of carbon storage. Nature Geoscience, 12(11), 917-921.

Norby, R. J., Childs, J., Hanson, P. J., & Warren, J. M. (2019). Rapid loss of an ecosystem

engineer: Sphagnum decline in an experimentally warmed bog. Ecology and Evolution, 9(22), 12571-12585.

Olid, C., Nilsson, M. B., Eriksson, T., & Klaminder, J. (2014). The effects of temperature and nitrogen and sulfur additions on carbon accumulation in a nutrient-poor boreal mire: Decadal effects assessed using 210Pb peat chronologies. Journal of Geophysical Research: Biogeosciences, 119(3), 392-403.

Olsrud, M., Carlsson, B. Å., Svensson, B. M., Michelsen, A., & Melillo, J. M. (2010). Responses of fungal root colonization, plant cover and leaf nutrients to long-term exposure to elevated atmospheric CO_2 and warming in a subarctic birch forest understory. Global Change Biology, 16(6), 1820-1829.

Olsrud, M., Melillo, J. M., Christensen, T. R., Michelsen, A., Wallander, H., & Olsson, P. A. (2004). Response of ericoid mycorrhizal colonization and functioning to global change factors. New Phytologist, 162(2), 459-469.

Parton, W. J., Hanson, P. J., Swanston, C., Torn, M., Trumbore, S. E., Riley, W., & Kelly, R. (2010). ForCent model development and testing using the Enriched Background Isotope Study experiment. Journal of Geophysical Research: Biogeosciences, 115(G4).

Parvin, S., Blagodatskaya, E., Becker, J. N., Kuzyakov, Y., Uddin, S., & Dorodnikov, M. (2018). Depth rather than microrelief controls microbial biomass and kinetics of C-, N-, P-and S-cycle enzymes in peatland. Geoderma, 324, 67-76.

Pellitier, P. T., Zak, D. R., Argiroff, W. A., & Upchurch, R. A. (2021). Coupled Shifts in Ectomycorrhizal Communities and Plant Uptake of Organic Nitrogen Along a Soil Gradient: An Isotopic Perspective. Ecosystems, 1-15.

Peltoniemi, K., Adamczyk, S., Fritze, H., Minkkinen, K., Pennanen, T., Penttilä, T., ... & Laiho, R. (2021). Site fertility and soil water-table level affect fungal biomass production and community composition in boreal peatland forests. Environmental Microbiology.

Peltoniemi, K., Straková, P., Fritze, H., Iráizoz, P. A., Pennanen, T., & Laiho, R. (2012). How water-level drawdown modifies litter-decomposing fungal and actinobacterial communities in boreal peatlands. Soil biology and biochemistry, 51, 20-34.

Perotto, S., Daghino, S., & Martino, E. (2018). Ericoid mycorrhizal fungi and their genomes:

another side to the mycorrhizal symbiosis?. New Phytologist, 220(4), 1141-1147.

Phaiboun, A., Zhang, Y., Park, B., & Kim, M. (2015). Survival kinetics of starving bacteria is biphasic and density-dependent. PLoS computational biology, 11(4), e1004198.

Phillips, R. P., Brzostek, E., & Midgley, M. G. (2013). The mycorrhizal-associated nutrient economy: a new framework for predicting carbon–nutrient couplings in temperate forests. New Phytologist, 199(1), 41-51.

Pinceloup, N., Poulin, M., Brice, M. H., & Pellerin, S. (2020). Vegetation changes in temperate ombrotrophic peatlands over a 35 year period. PloS one, 15(2), e0229146.

Pinsonneault, A. J., Moore, T. R., & Roulet, N. T. (2016a). Effects of long-term fertilization on peat stoichiometry and associated microbial enzyme activity in an ombrotrophic bog. Biogeochemistry, 129(1), 149-164.

Pinsonneault, A. J., Moore, T. R., & Roulet, N. T. (2016b). Temperature the dominant control on the enzyme-latch across a range of temperate peatland types. Soil Biology and Biochemistry, 97, 121-130.

Potvin, L. R., Kane, E. S., Chimner, R. A., Kolka, R. K., & Lilleskov, E. A. (2015). Effects of water table position and plant functional group on plant community, aboveground production, and peat properties in a peatland mesocosm experiment (PEATcosm). Plant and soil, 387(1), 277-294.

Pouliot, R., Rochefort, L., Karofeld, E., & Mercier, C. (2011). Initiation of Sphagnum moss hummocks in bogs and the presence of vascular plants: Is there a link?. Acta Oecologica, 37(4), 346-354.

Prescott, C. E. (2010). Litter decomposition: what controls it and how can we alter it to sequester more carbon in forest soils?. Biogeochemistry, 101(1), 133-149.

Prescott, C. E., Grayston, S. J., Helmisaari, H. S., Kaštovská, E., Körner, C., Lambers, H., ... & Ostonen, I. (2020). Surplus carbon drives allocation and plant–soil interactions. Trends in ecology & evolution.

Preston, M. D., Smemo, K. A., McLaughlin, J. W., & Basiliko, N. (2012). Peatland microbial communities and decomposition processes in the James Bay Lowlands, Canada. Frontiers in microbiology, 3, 70.

Qiu, C., Zhu, D., Ciais, P., Guenet, B., & Peng, S. (2020). The role of northern peatlands in the global carbon cycle for the 21st century. Global Ecology and Biogeography, 29(5), 956-973.

Qiu, C., Zhu, D., Ciais, P., Guenet, B., Krinner, G., Peng, S., ... & Ziemblinska, K. (2018). ORCHIDEE-PEAT (revision 4596), a model for northern peatland CO 2, water, and energy fluxes on daily to annual scales. Geoscientific Model Development, 11(2), 497-519.

Qiu, C., Zhu, D., Ciais, P., Guenet, B., Peng, S., Krinner, G., ... & Hastie, A. (2019). Modelling northern peatland area and carbon dynamics since the Holocene with the ORCHIDEE-PEAT land surface model (SVN r5488). Geoscientific Model Development, 12(7), 2961-2982.

Radu, D. D., & Duval, T. P. (2018). Precipitation frequency alters peatland ecosystem structure and CO_2 exchange: contrasting effects on moss, sedge, and shrub communities. Global change biology, 24(5), 2051-2065.

Rains, K. C., & Bledsoe, C. S. (2007). Rapid uptake of ^{15}N-ammonium and glycine-^{13}C, ^{15}N by arbuscular and ericoid mycorrhizal plants native to a Northern California coastal pygmy forest. Soil Biology and Biochemistry, 39(5), 1078-1086.

Ratcliffe, J. L., Campbell, D. I., Clarkson, B. R., Wall, A. M., & Schipper, L. A. (2019). Water table fluctuations control CO_2 exchange in wet and dry bogs through different mechanisms. Science of the Total Environment, 655, 1037-1046.

Ratcliffe, J. L., Lowe, D. J., Schipper, L. A., Gehrels, M. J., French, A. D., & Campbell, D. I. (2020). Rapid carbon accumulation in a peatland following Late Holocene tephra deposition, New Zealand. Quaternary Science Reviews, 246, 106505.

Rattle, J. (2006). Dissolved nitrogen dynamics in an ombrotrophic bog (Doctoral dissertation, McGill University).

Read, D. J., Leake, J. R., & Perez-Moreno, J. (2004). Mycorrhizal fungi as drivers of ecosystem processes in heathland and boreal forest biomes. Canadian Journal of Botany, 82(8), 1243-1263.

Ritson, J. P., Alderson, D. M., Robinson, C. H., Burkitt, A. E., Heinemeyer, A., Stimson, A. G., ... & Evans, M. G. (2021). Towards a microbial process-based understanding of the resilience

of peatland ecosystem service provisioning–a research agenda. Science of the Total Environment, 759, 143467.

Riutta, T., Laine, J., & Tuittila, E. S. (2007). Sensitivity of CO_2 exchange of fen ecosystem components to water level variation. Ecosystems, 10(5), 718-733.

Robroek, B. J., Jassey, V. E., Kox, M. A., Berendsen, R. L., Mills, R. T., Cécillon, L., ... & Bodelier, P. L. (2015). Peatland vascular plant functional types affect methane dynamics by altering microbial community structure. Journal of Ecology, 103(4), 925-934.

Rosinger, C., Sandén, H., & Godbold, D. L. (2020). Non-structural carbohydrate concentrations of Fagus sylvatica and Pinus sylvestris fine roots are linked to ectomycorrhizal enzymatic activity during spring reactivation. Mycorrhiza, 30(2), 197.

Roulet, N. T., Lafleur, P. M., Richard, P. J., Moore, T. R., Humphreys, E. R., & Bubier, J. I. L. L. (2007). Contemporary carbon balance and late Holocene carbon accumulation in a northern peatland. Global Change Biology, 13(2), 397-411.

Rydin, H., & Clymo, R. S. (1989). Transport of carbon and phosphorus compounds about Sphagnum. Proceedings of the Royal Society of London. B. Biological Sciences, 237(1286), 63-84.

Rydin, H., Jeglum, J. K., & Bennett, K. D. (2013). The biology of peatlands, 2e. Oxford university press.

Salazar, A., Sulman, B. N., & Dukes, J. S. (2018). Microbial dormancy promotes microbial biomass and respiration across pulses of drying-wetting stress. Soil Biology and Biochemistry, 116, 237-244.

Salimi, S., & Scholz, M. (2021). Impact of future climate scenarios on peatland and constructed wetland water quality: A mesocosm experiment within climate chambers. Journal of Environmental Management, 289, 112459.

Salmon, V. G., Brice, D. J., Bridgham, S., Childs, J., Graham, J., Griffiths, N. A., ... & Hanson, P. J. (2021). Nitrogen and phosphorus cycling in an ombrotrophic peatland: a benchmark for assessing change. Plant and Soil, 1-26.

Šantrůčková, H., Picek, T., Tykva, R., Šimek, M., & Pavlů, B. (2004). Short-term partitioning of 14 C-[U]-glucose in the soil microbial pool under varied aeration status. Biology and

fertility of soils, 40(6), 386-392.

Savage, K., Davidson, E. A., & Tang, J. (2013). Diel patterns of autotrophic and heterotrophic respiration among phenological stages. Global Change Biology, 19(4), 1151-1159.

Scharlemann, J. P., Tanner, E. V., Hiederer, R., & Kapos, V. (2014). Global soil carbon: understanding and managing the largest terrestrial carbon pool. Carbon Management, 5(1), 81-91.

Schiestl-Aalto, P., Ryhti, K., Mäkelä, A., Peltoniemi, M., Bäck, J., & Kulmala, L. (2019). Analysis of the NSC storage dynamics in tree organs reveals the allocation to belowground symbionts in the framework of whole tree carbon balance. Frontiers in Forests and Global Change, 2, 17.

Schimel, J., Balser, T. C., & Wallenstein, M. (2007). Microbial stress-response physiology and its implications for ecosystem function. Ecology, 88(6), 1386-1394.

Schmidt, M. W., Torn, M. S., Abiven, S., Dittmar, T., Guggenberger, G., Janssens, I. A., ... & Trumbore, S. E. (2011). Persistence of soil organic matter as an ecosystem property. Nature, 478(7367), 49-56.

Shao, S., Roulet, N., Wu. J., He, H. (2021). Integrating McGill Wetland Model (MWM) with Cohort Development and Microbial Controls, Manuscript under review.

Shao, S., Roulet, N., Wu. J., He, H., Moore, T., Bubier, J., Larmola, T. (2021). A Mycorrhiza-mediated Carbon, Nitrogen and Phosphorus Cycling Model to Simulate Peatland's Response to Nutrient Fertilization, Manuscript in preparation.

Shaver, G. R., & Laundre, J. (1997). Exsertion, elongation, and senescence of leaves of Eriophorum vaginatum and Carex bigelowii in Northern Alaska. Global Change Biology, 3(S1), 146-157.

Sheppard, L. J., Leith, I. D., Leeson, S. R., Dijk, N. V., Field, C., & Levy, P. (2013). Fate of N in a peatland, Whim bog: immobilisation in the vegetation and peat, leakage into pore water and losses as N_2O depend on the form of N. Biogeosciences, 10(1), 149-160.

Sheppard, L. J., Leith, I. D., Mizunuma, T., Leeson, S., Kivimaki, S., Neil Cape, J., ... & Smart, S. (2014). Inertia in an ombrotrophic bog ecosystem in response to 9 years' realistic perturbation by wet deposition of nitrogen, separated by form. Global change

biology, 20(2), 566-580.

Shi, M., Fisher, J. B., Brzostek, E. R., & Phillips, R. P. (2016). Carbon cost of plant nitrogen acquisition: global carbon cycle impact from an improved plant nitrogen cycle in the Community Land Model. Global change biology, 22(3), 1299-1314.

Shi, X., Ricciuto, D. M., Thornton, P. E., Xu, X., Yuan, F., Norby, R. J., ... & Griffiths, N. A. (2021). Extending a land-surface model with Sphagnum moss to simulate responses of a northern temperate bog to whole ecosystem warming and elevated CO_2. Biogeosciences, 18(2), 467-486.

Shi, X., Thornton, P. E., Ricciuto, D. M., Hanson, P. J., Mao, J., Sebestyen, S. D., ... & Bisht, G. (2015). Representing northern peatland microtopography and hydrology within the Community Land Model. Biogeosciences, 12(21), 6463-6477.

Shinozaki, K., Yoda, K., Hozumi, K., & Kira, T. (1964). A quantitative analysis of plant form-the pipe model theory: I. Basic analyses. Japanese Journal of ecology, 14(3), 97-105.

Siegel, D. I., & Glaser, P. H. (1987). Groundwater flow in a bog-fen complex, Lost River Peatland, northern Minnesota. The Journal of Ecology, 743-754.

Sihi, D., Gerber, S., Inglett, P. W., & Inglett, K. S. (2016). Comparing models of microbial–substrate interactions and their response to warming. Biogeosciences, 13(6), 1733-1752.

Sihi, D., Inglett, P. W., Gerber, S., & Inglett, K. S. (2018). Rate of warming affects temperature sensitivity of anaerobic peat decomposition and greenhouse gas production. Global change biology, 24(1), e259-e274.

Sinsabaugh, R. L., Manzoni, S., Moorhead, D. L., & Richter, A. (2013). Carbon use efficiency of microbial communities: stoichiometry, methodology and modelling. Ecology letters, 16(7), 930-939.

Sinsabaugh, R. L., Turner, B. L., Talbot, J. M., Waring, B. G., Powers, J. S., Kuske, C. R., ... & Follstad Shah, J. J. (2016). Stoichiometry of microbial carbon use efficiency in soils. Ecological Monographs, 86(2), 172-189.

Sitch, S., Smith, B., Prentice, I. C., Arneth, A., Bondeau, A., Cramer, W., ... & Venevsky, S. (2003). Evaluation of ecosystem dynamics, plant geography and terrestrial carbon cycling in the LPJ dynamic global vegetation model. Global change biology, 9(2), 161-185.

Smith, L. C., Sheng, Y., & MacDonald, G. M. (2007). A first pan-Arctic assessment of the influence of glaciation, permafrost, topography and peatlands on northern hemisphere lake distribution. Permafrost and Periglacial Processes, 18(2), 201-208.

Smith, S. E., & Read, D. J. (2010). Mycorrhizal symbiosis. Academic press.

Soares, M., & Rousk, J. (2019). Microbial growth and carbon use efficiency in soil: links to fungal-bacterial dominance, SOC-quality and stoichiometry. Soil Biology and Biochemistry, 131, 195-205.

Song, Y., Song, C., Hou, A., Ren, J., Wang, X., Cui, Q., & Wang, M. (2018). Effects of temperature and root additions on soil carbon and nitrogen mineralization in a predominantly permafrost peatland. Catena, 165, 381-389.

Spahni, R., Joos, F., Stocker, B. D., Steinacher, M., & Yu, Z. C. (2013). Transient simulations of the carbon and nitrogen dynamics in northern peatlands: From the Last Glacial Maximum to the 21st century. Climate of the Past, 9(3), 1287-1308.

Spohn, M., & Widdig, M. (2017). Turnover of carbon and phosphorus in the microbial biomass depending on phosphorus availability. Soil Biology and Biochemistry, 113, 53-59.

Spohn, M., Klaus, K., Wanek, W., & Richter, A. (2016a). Microbial carbon use efficiency and biomass turnover times depending on soil depth–Implications for carbon cycling. Soil Biology and Biochemistry, 96, 74-81.

Spohn, M., Pötsch, E. M., Eichorst, S. A., Woebken, D., Wanek, W., & Richter, A. (2016b). Soil microbial carbon use efficiency and biomass turnover in a long-term fertilization experiment in a temperate grassland. Soil Biology and Biochemistry, 97, 168-175.

Steinweg, J. M., Plante, A. F., Conant, R. T., Paul, E. A., & Tanaka, D. L. (2008). Patterns of substrate utilization during long-term incubations at different temperatures. Soil biology and biochemistry, 40(11), 2722-2728.

Sterner, R. W., & Elser, J. J. (2017). Ecological stoichiometry. Princeton university press.

St-Hilaire, F., Wu, J., Roulet, N. T., Frolking, S., Lafleur, P. M., Humphreys, E. R., & Arora, V. (2010). McGill wetland model: evaluation of a peatland carbon simulator developed for global assessments. Biogeosciences, 7(11), 3517-3530.

Strack, M., & Waddington, J. M. (2007). Response of peatland carbon dioxide and methane

fluxes to a water table drawdown experiment. Global biogeochemical cycles, 21(1).

Strack, M., Munir, T. M., & Khadka, B. (2019). Shrub abundance contributes to shifts in dissolved organic carbon concentration and chemistry in a continental bog exposed to drainage and warming. Ecohydrology, 12(5), e2100.

Strack, M., Waddington, J. M., Rochefort, L., & Tuittila, E. S. (2006). Response of vegetation and net ecosystem carbon dioxide exchange at different peatland microforms following water table drawdown. Journal of Geophysical Research: Biogeosciences, 111(G2).

Straková, P., Penttilä, T., Laine, J., & Laiho, R. (2012). Disentangling direct and indirect effects of water table drawdown on above-and belowground plant litter decomposition: consequences for accumulation of organic matter in boreal peatlands. Global Change Biology, 18(1), 322-335.

Sulman, B. N., Brzostek, E. R., Medici, C., Shevliakova, E., Menge, D. N., & Phillips, R. P. (2017). Feedbacks between plant N demand and rhizosphere priming depend on type of mycorrhizal association. Ecology letters, 20(8), 1043-1053.

Sulman, B. N., Desai, A. R., Cook, B. D., Saliendra, N., & Mackay, D. S. (2009). Contrasting carbon dioxide fluxes between a drying shrub wetland in Northern Wisconsin, USA, and nearby forests. Biogeosciences, 6(6), 1115-1126.

Sulman, B. N., Desai, A. R., Saliendra, N. Z., Lafleur, P. M., Flanagan, L. B., Sonnentag, O., ... & van der Kamp, G. (2010). CO_2 fluxes at northern fens and bogs have opposite responses to inter-annual fluctuations in water table. Geophysical Research Letters, 37(19).

Sulman, B. N., Desai, A. R., Schroeder, N. M., Ricciuto, D., Barr, A., Richardson, A. D., ... & Weng, E. (2012). Impact of hydrological variations on modeling of peatland CO_2 fluxes: Results from the North American Carbon Program site synthesis. Journal of Geophysical Research: Biogeosciences, 117(G1).

Sulman, B. N., Shevliakova, E., Brzostek, E. R., Kivlin, S. N., Malyshev, S., Menge, D. N., & Zhang, X. (2019). Diverse mycorrhizal associations enhance terrestrial C storage in a global model. Global Biogeochemical Cycles, 33(4), 501-523.

Takriti, M., Wild, B., Schnecker, J., Mooshammer, M., Knoltsch, A., Lashchinskiy, N., ... & Richter, A. (2018). Soil organic matter quality exerts a stronger control than stoichiometry on

microbial substrate use efficiency along a latitudinal transect. Soil Biology and Biochemistry, 121, 212-220.

Talbot, J., Roulet, N. T., Sonnentag, O., & Moore, T. R. (2014). Increases in aboveground biomass and leaf area 85 years after drainage in a bog. Botany, 92(10), 713-721.

Tarnocai, C. (2006). The effect of climate change on carbon in Canadian peatlands. Global and planetary Change, 53(4), 222-232.

Taylor, A. F., & Alexander, I. A. N. (2005). The ectomycorrhizal symbiosis: life in the real world. Mycologist, 19(3), 102-112.

Terrer, C., Phillips, R. P., Hungate, B. A., Rosende, J., Pett-Ridge, J., Craig, M. E., ... & Jackson, R. B. (2021). A trade-off between plant and soil carbon storage under elevated CO_2. Nature, 591(7851), 599-603.

Thormann, M. N. (2006). Diversity and function of fungi in peatlands: a carbon cycling perspective. Canadian journal of soil science, 86(Special Issue), 281-293.

Thormann, M. N., & Bayley, S. E. (1997). Aboveground plant production and nutrient content of the vegetation in six peatlands in Alberta, Canada. Plant Ecology, 131(1), 1-16.

Thormann, M. N., & Rice, A. V. (2007). Fungi from peatlands. Fungal diversity, 24(2415), 299.

Thormann, M. N., Bayley, S. E., & Currah, R. S. (2004). Microcosm tests of the effects of temperature and microbial species number on the decomposition of Carex aquatilis and Sphagnum fuscum litter from southern boreal peatlands. Canadian journal of microbiology, 50(10), 793-802.

Thornton, P. E., Lamarque, J. F., Rosenbloom, N. A., & Mahowald, N. M. (2007). Influence of carbon-nitrogen cycle coupling on land model response to CO_2 fertilization and climate variability. Global biogeochemical cycles, 21(4).

Thum, T., Caldararu, S., Engel, J., Kern, M., Pallandt, M., Schnur, R., ... & Zaehle, S. (2019). A new model of the coupled carbon, nitrogen, and phosphorus cycles in the terrestrial biosphere (QUINCY v1. 0; revision 1996). Geoscientific Model Development, 12(11), 4781-4802.

Tian, J., Branfireun, B. A., & Lindo, Z. (2020). Global change alters peatland carbon cycling through plant biomass allocation. Plant and Soil, 455(1), 53-64.

Tiemann, L. K., & Billings, S. A. (2011). Changes in variability of soil moisture alter microbial community C and N resource use. Soil Biology and Biochemistry, 43(9), 1837-1847.

Tipping, E., Benham, S., Boyle, J. F., Crow, P., Davies, J., Fischer, U., ... & Toberman, H. (2014). Atmospheric deposition of phosphorus to land and freshwater. Environmental Science: Processes & Impacts, 16(7), 1608-1617.

Toberman, H., Tipping, E., Boyle, J. F., Helliwell, R. C., Lilly, A., & Henrys, P. A. (2015). Dependence of ombrotrophic peat nitrogen on phosphorus and climate. Biogeochemistry, 125(1), 11-20.

Treseder, K. K. (2004). A meta-analysis of mycorrhizal responses to nitrogen, phosphorus, and atmospheric CO_2 in field studies. New phytologist, 164(2), 347-355.

Trivedi, P., Leach, J. E., Tringe, S. G., Sa, T., & Singh, B. K. (2020). Plant–microbiome interactions: from community assembly to plant health. Nature reviews microbiology, 18(11), 607-621.

Tucker, C. L., Bell, J., Pendall, E., & Ogle, K. (2013). Does declining carbon-use efficiency explain thermal acclimation of soil respiration with warming?. Global Change Biology, 19(1), 252-263.

Turunen, J., Roulet, N. T., Moore, T. R., & Richard, P. J. (2004). Nitrogen deposition and increased carbon accumulation in ombrotrophic peatlands in eastern Canada. Global Biogeochemical Cycles, 18(3).

Turunen, J., Tomppo, E., Tolonen, K., & Reinikainen, A. (2002). Estimating carbon accumulation rates of undrained mires in Finland–application to boreal and subarctic regions. The Holocene, 12(1), 69-80.

Tveit, A., Schwacke, R., Svenning, M. M., & Urich, T. (2013). Organic carbon transformations in high-Arctic peat soils: key functions and microorganisms. The ISME journal, 7(2), 299-311.

Utstøl-Klein, S., Halvorsen, R., & Ohlson, M. (2015). Increase in carbon accumulation in a boreal peatland following a period of wetter climate and long-term decrease in nitrogen deposition. New Phytologist, 206(4), 1238-1246.

Van Breemen, N. (1995). How Sphagnum bogs down other plants. Trends in ecology & evolution, 10(7), 270-275.

van der Linde, S., Suz, L. M., Orme, C. D. L., Cox, F., Andreae, H., Asi, E., ... & Bidartondo, M. I.

(2018). Environment and host as large-scale controls of ectomycorrhizal fungi. Nature, 558(7709), 243-248.

Van Geel, M., Jacquemyn, H., Peeters, G., van Acker, K., Honnay, O., & Ceulemans, T. (2020). Diversity and community structure of ericoid mycorrhizal fungi in European bogs and heathlands across a gradient of nitrogen deposition. New Phytologist, 228(5), 1640-1651.

van't Padje, A., Galvez, L. O., Klein, M., Hink, M. A., Postma, M., Shimizu, T., & Kiers, E. T. (2021a). Temporal tracking of quantum-dot apatite across in vitro mycorrhizal networks shows how host demand can influence fungal nutrient transfer strategies. The ISME journal, 15(2), 435-449.

van't Padje, A., Werner, G. D., & Kiers, E. T. (2021b). Mycorrhizal fungi control phosphorus value in trade symbiosis with host roots when exposed to abrupt 'crashes' and 'booms' of resource availability. New Phytologist, 229(5), 2933-2944.

Vesala, R., Kiheri, H., Hobbie, E. A., van Dijk, N., Dise, N., & Larmola, T. (2021). Atmospheric nitrogen enrichment changes nutrient stoichiometry and reduces fungal N supply to peatland ericoid mycorrhizal shrubs. Science of The Total Environment, 148737.

Vicca, S., Luyssaert, S., Peñuelas, J., Campioli, M., Chapin III, F. S., Ciais, P., ... & Janssens, I. A. (2012). Fertile forests produce biomass more efficiently. Ecology letters, 15(6), 520-526.

Vitt, D. H. (2006). Functional characteristics and indicators of boreal peatlands. In Boreal peatland ecosystems (pp. 9-24). Springer, Berlin, Heidelberg.

Vitt, D. H., Halsey, L. A., Bauer, I. E., & Campbell, C. (2000). Spatial and temporal trends in carbon storage of peatlands of continental western Canada through the Holocene. Canadian Journal of Earth Sciences, 37(5), 683-693.

Vowles, T., & Björk, R. G. (2019). Implications of evergreen shrub expansion in the Arctic. Journal of Ecology, 107(2), 650-655.

Walbridge, M. R., & Navaratnam, J. A. (2006). Phosphorous in boreal peatlands. In Boreal peatland ecosystems (pp. 231-258). Springer, Berlin, Heidelberg.

Walker, T. N., Garnett, M. H., Ward, S. E., Oakley, S., Bardgett, R. D., & Ostle, N. J. (2016). Vascular plants promote ancient peatland carbon loss with climate warming. Global Change Biology, 22(5), 1880-1889.

Walker, T. W., Kaiser, C., Strasser, F., Herbold, C. W., Leblans, N. I., Woebken, D., ... & Richter, A. (2018). Microbial temperature sensitivity and biomass change explain soil carbon loss with warming. Nature climate change, 8(10), 885-889.

Wang, G., Post, W. M., & Mayes, M. A. (2013). Development of microbial-enzyme-mediated decomposition model parameters through steady-state and dynamic analyses. Ecological Applications, 23(1), 255-272.

Wang, K., Peng, C., Zhu, Q., Zhou, X., Wang, M., Zhang, K., & Wang, G. (2017). Modeling global soil carbon and soil microbial carbon by integrating microbial processes into the ecosystem process model TRIPLEX-GHG. Journal of Advances in Modeling Earth Systems, 9(6), 2368-2384.

Wang, M., & Moore, T. R. (2014). Carbon, nitrogen, phosphorus, and potassium stoichiometry in an ombrotrophic peatland reflects plant functional type. Ecosystems, 17(4), 673-684.

Wang, M., Larmola, T., Murphy, M. T., Moore, T. R., & Bubier, J. L. (2016). Stoichiometric response of shrubs and mosses to long-term nutrient (N, P and K) addition in an ombrotrophic peatland. Plant and Soil, 400(1-2), 403-416.

Wang, M., Moore, T. R., Talbot, J., & Richard, P. J. (2014). The cascade of C: N: P stoichiometry in an ombrotrophic peatland: from plants to peat. Environmental Research Letters, 9(2), 024003.

Wang, M., Moore, T. R., Talbot, J., & Riley, J. L. (2015). The stoichiometry of carbon and nutrients in peat formation. Global Biogeochemical Cycles, 29(2), 113-121.

Wang, M., Murphy, M. T., & Moore, T. R. (2014). Nutrient resorption of two evergreen shrubs in response to long-term fertilization in a bog. Oecologia, 174(2), 365-377.

Wang, M., Talbot, J., & Moore, T. R. (2018). Drainage and fertilization effects on nutrient availability in an ombrotrophic peatland. Science of The Total Environment, 621, 1255-1263.

Wang, S., Zhuang, Q., Yu, Z., Bridgham, S., & Keller, J. K. (2016). Quantifying peat carbon accumulation in Alaska using a process-based biogeochemistry model. Journal of Geophysical Research: Biogeosciences, 121(8), 2172-2185.

Wang, Y. P., Jiang, J., Chen-Charpentier, B., Agusto, F. B., Hastings, A., Hoffman, F., ... & Luo, Y.

Q. (2016). Responses of two nonlinear microbial models to warming and increased carbon input. Biogeosciences, 13(4), 887-902.

Wania, R., Ross, I., & Prentice, I. C. (2009a). Integrating peatlands and permafrost into a dynamic global vegetation model: 1. Evaluation and sensitivity of physical land surface processes. Global Biogeochemical Cycles, 23(3).

Wania, R., Ross, I., & Prentice, I. C. (2009b). Integrating peatlands and permafrost into a dynamic global vegetation model: 2. Evaluation and sensitivity of vegetation and carbon cycle processes. Global Biogeochemical Cycles, 23(3).

Ward, E. B., Duguid, M. C., Kuebbing, S. E., Lendemer, J. C., Warren, R. J., & Bradford, M. A. (2021). Ericoid mycorrhizal shrubs alter the relationship between tree mycorrhizal dominance and soil carbon and nitrogen. Journal of Ecology.

Ward, E. J., Warren, J. M., McLennan, D. A., Dusenge, M. E., Way, D. A., Wullschleger, S. D., & Hanson, P. J. (2019). Photosynthetic and respiratory responses of two bog shrub species to whole ecosystem warming and elevated CO_2 at the boreal-temperate ecotone. Frontiers in Forests and Global Change, 2, 54.

Ward, S. E., Ostle, N. J., Oakley, S., Quirk, H., Henrys, P. A., & Bardgett, R. D. (2013). Warming effects on greenhouse gas fluxes in peatlands are modulated by vegetation composition. Ecology letters, 16(10), 1285-1293.

Weedon, J. T., A. Kowalchuk, G., Aerts, R., van Hal, J., van Logtestijn, R., Taş, N., ... & M. van Bodegom, P. (2012). Summer warming accelerates sub-arctic peatland nitrogen cycling without changing enzyme pools or microbial community structure. Global Change Biology, 18(1), 138-150.

Weedon, J. T., Aerts, R., Kowalchuk, G. A., van Logtestijn, R., Andringa, D., & van Bodegom, P. M. (2013). Temperature sensitivity of peatland C and N cycling: does substrate supply play a role?. Soil Biology and Biochemistry, 61, 109-120.

Weltzin, J. F., Bridgham, S. D., Pastor, J., Chen, J., & Harth, C. (2003). Potential effects of warming and drying on peatland plant community composition. Global Change Biology, 9(2), 141-151.

Weltzin, J. F., Pastor, J., Harth, C., Bridgham, S. D., Updegraff, K., & Chapin, C. T. (2000).

Response of bog and fen plant communities to warming and water-table manipulations. Ecology, 81(12), 3464-3478.

Wen, Y., Zang, H., Freeman, B., Musarika, S., Evans, C. D., Chadwick, D. R., & Jones, D. L. (2019). Microbial utilization of low molecular weight organic carbon substrates in cultivated peats in response to warming and soil degradation. Soil Biology and Biochemistry, 139, 107629.

Werner, G. D., Strassmann, J. E., Ivens, A. B., Engelmoer, D. J., Verbruggen, E., Queller, D. C., ... & Kiers, E. T. (2014). Evolution of microbial markets. Proceedings of the National Academy of Sciences, 111(4), 1237-1244.

Whitehead, S. J., Caporn, S. J. M., & Press, M. C. (1997). Effects of elevated CO_2, nitrogen and phosphorus on the growth and photosynthesis of two upland perennials: Calluna vulgaris and Pteridium aquilinum. The New Phytologist, 135(2), 201-211.

Wieder, R. K., Vitt, D. H., Vile, M. A., Graham, J. A., Hartsock, J. A., Fillingim, H., ... & McMillen, K. J. (2019). Experimental nitrogen addition alters structure and function of a boreal bog: critical load and thresholds revealed. Ecological Monographs, 89(3), e01371.

Wieder, W. R., Bonan, G. B., & Allison, S. D. (2013). Global soil carbon projections are improved by modelling microbial processes. Nature Climate Change, 3(10), 909-912.

Wieder, W. R., Cleveland, C. C., Smith, W. K., & Todd-Brown, K. (2015). Future productivity and carbon storage limited by terrestrial nutrient availability. Nature Geoscience, 8(6), 441-444.

Wiedermann, M. M., Kane, E. S., Potvin, L. R., & Lilleskov, E. A. (2017). Interactive plant functional group and water table effects on decomposition and extracellular enzyme activity in Sphagnum peatlands. Soil Biology and Biochemistry, 108, 1-8.

Williams, C. J., Shingara, E. A., & Yavitt, J. B. (2000). Phenol oxidase activity in peatlands in New York State: response to summer drought and peat type. Wetlands, 20(2), 416-421.

Willmott, C. J. (1982). Some comments on the evaluation of model performance. Bulletin of the American Meteorological Society, 63(11), 1309-1313.

Wilson, R. M., Hopple, A. M., Tfaily, M. M., Sebestyen, S. D., Schadt, C. W., Pfeifer-Meister, L., ... & Hanson, P. J. (2016). Stability of peatland carbon to rising temperatures. Nature

Communications, 7(1), 1-10.

Wilson, R. M., Tfaily, M. M., Kolton, M., Johnston, E. R., Petro, C., Zalman, C. A., ... & Kostka, J. E. (2021). Soil metabolome response to whole-ecosystem warming at the Spruce and Peatland Responses under Changing Environments experiment. Proceedings of the National Academy of Sciences, 118(25).

Wisser, D., Marchenko, S., Talbot, J., Treat, C., & Frolking, S. (2011). Soil temperature response to 21st century global warming: the role of and some implications for peat carbon in thawing permafrost soils in North America. Earth System Dynamics, 2(1), 121-138.

Worrall, F., Moody, C. S., Clay, G. D., Burt, T. P., & Rose, R. (2016). The total phosphorus budget of a peat-covered catchment. Journal of Geophysical Research: Biogeosciences, 121(7), 1814-1828.

Wu, J., & Roulet, N. T. (2014). Climate change reduces the capacity of northern peatlands to absorb the atmospheric carbon dioxide: The different responses of bogs and fens. Global Biogeochemical Cycles, 28(10), 1005-1024.

Wu, J., Roulet, N. T., Nilsson, M., Lafleur, P., & Humphreys, E. (2012). Simulating the carbon cycling of northern peatlands using a land surface scheme coupled to a wetland carbon model (CLASS3W-MWM). Atmosphere-ocean, 50(4), 487-506.

Wu, Y., & Blodau, C. (2013). PEATBOG: a biogeochemical model for analyzing coupled carbon and nitrogen dynamics in northern peatlands. Geoscientific Model Development, 6(4), 1173-1207.

Wu, Y., Blodau, C., Moore, T. R., Bubier, J., Juutinen, S., & Larmola, T. (2015). Effects of experimental nitrogen deposition on peatland carbon pools and fluxes: a modelling analysis. Biogeosciences, 12(1), 79-101.

Wu, Y., Kwak, J. H., Karst, J., Ni, M., Yan, Y., Lv, X., ... & Chang, S. X. (2021). Long-term nitrogen and sulfur deposition increased root-associated pathogen diversity and changed mutualistic fungal diversity in a boreal forest. Soil Biology and Biochemistry, 155, 108163.

Wu, Y., Verseghy, D. L., & Melton, J. R. (2016). Integrating peatlands into the coupled Canadian Land Surface Scheme (CLASS) v3. 6 and the Canadian Terrestrial Ecosystem Model (CTEM) v2. 0. Geoscientific Model Development, 9(8), 2639-2663.

Wutzler, T., & Reichstein, M. (2008). Colimitation of decomposition by substrate and decomposers–a comparison of model formulations. Biogeosciences, 5(3), 749-759.

Xiao, W., Chen, X., Jing, X., & Zhu, B. (2018). A meta-analysis of soil extracellular enzyme activities in response to global change. Soil Biology and Biochemistry, 123, 21-32.

Xing, Y., Bubier, J., Moore, T., Murphy, M., Basiliko, N., Wendel, S., & Blodau, C. (2011). The fate of 15 N-nitrate in a northern peatland impacted by long term experimental nitrogen, phosphorus and potassium fertilization. Biogeochemistry, 103(1), 281-296.

Xu, J., Morris, P. J., Liu, J., & Holden, J. (2018). PEATMAP: Refining estimates of global peatland distribution based on a meta-analysis. Catena, 160, 134-140.

Xu, X., Schimel, J. P., Thornton, P. E., Song, X., Yuan, F., & Goswami, S. (2014). Substrate and environmental controls on microbial assimilation of soil organic carbon: a framework for Earth system models. Ecology letters, 17(5), 547-555.

Xu, X., Thornton, P. E., & Post, W. M. (2013). A global analysis of soil microbial biomass carbon, nitrogen and phosphorus in terrestrial ecosystems. Global Ecology and Biogeography, 22(6), 737-749.

Yang, X., Thornton, P. E., Ricciuto, D. M., & Post, W. M. (2014). The role of phosphorus dynamics in tropical forests–a modeling study using CLM-CNP. Biogeosciences, 11(6), 1667-1681.

Ye, J. S., Bradford, M. A., Dacal, M., Maestre, F. T., & García-Palacios, P. (2019). Increasing microbial carbon use efficiency with warming predicts soil heterotrophic respiration globally. Global Change Biology, 25(10), 3354-3364.

Young, D. M., Baird, A. J., Morris, P. J., & Holden, J. (2017). Simulating the long-term impacts of drainage and restoration on the ecohydrology of peatlands. Water Resources Research, 53(8), 6510-6522.

Yu, L., Ahrens, B., Wutzler, T., Schrumpf, M., & Zaehle, S. (2020). Jena Soil Model (JSM v1. 0; revision 1934): a microbial soil organic carbon model integrated with nitrogen and phosphorus processes. Geoscientific Model Development, 13(2), 783-803.

Yu, Z. C. (2012). Northern peatland carbon stocks and dynamics: a review. Biogeosciences, 9(10), 4071-4085.

Zackrisson, O., Nilsson, M. C., Dahlberg, A., & Jäderlund, A. (1997). Interference mechanisms in conifer-Ericaceae-feathermoss communities. Oikos, 209-220.

Zaehle, S. (2013). Terrestrial nitrogen–carbon cycle interactions at the global scale. Philosophical Transactions of the Royal Society B: Biological Sciences, 368(1621), 20130125.

Zaehle, S., Friend, A. D., Friedlingstein, P., Dentener, F., Peylin, P., & Schulz, M. (2010). Carbon and nitrogen cycle dynamics in the O-CN land surface model: 2. Role of the nitrogen cycle in the historical terrestrial carbon balance. Global Biogeochemical Cycles, 24(1).

Zak, D. R., Pellitier, P. T., Argiroff, W., Castillo, B., James, T. Y., Nave, L. E., ... & Tunlid, A. (2019). Exploring the role of ectomycorrhizal fungi in soil carbon dynamics. New Phytologist, 223(1), 33-39.

Zhang, H., Väliranta, M., Piilo, S., Amesbury, M. J., Aquino-López, M. A., Roland, T. P., ... & Tuittila, E. S. (2020). Decreased carbon accumulation feedback driven by climate-induced drying of two southern boreal bogs over recent centuries. Global change biology, 26(4), 2435-2448.

Zhang, Y., Li, C., Trettin, C. C., Li, H., & Sun, G. (2002). An integrated model of soil, hydrology, and vegetation for carbon dynamics in wetland ecosystems. Global Biogeochemical Cycles, 16(4), 9-1.

Zhao, G., Bryan, B. A., King, D., Luo, Z., Wang, E., Song, X., & Yu, Q. (2013). Impact of agricultural management practices on soil organic carbon: simulation of A ustralian wheat systems. Global change biology, 19(5), 1585-1597.

Zheng, Q., Hu, Y., Zhang, S., Noll, L., Böckle, T., Richter, A., & Wanek, W. (2019). Growth explains microbial carbon use efficiency across soils differing in land use and geology. Soil Biology and Biochemistry, 128, 45-55.

Živković, T. (2019). Biological nitrogen fixation in ombrotrophic peatlands (Doctoral dissertation, McGill University).